Hungarian University of Agriculture and Life Sciences

Doctoral School of Biological Sciences

Ph.D. Dissertation

Removal of micro-pollutants from wastewater by bioremediation

By

Eszter Rápó

DOI: 10.54598/003110

Gödöllő, Hungary

2022

Title: Removal of micro-pollutants from wastewater by bioremediation

Discipline: Biological Sciences

Name of Doctoral School: Doctoral School of Biological Sciences

Head: Prof. Dr. Zoltán Nagy
Professor, DSc.
Hungarian University of Agriculture and Life Sciences, Faculty of Agricultural and Environmental Sciences,
Institute of Biological Sciences

Supervisors: Dr. habil. Tonk Szende-Ágnes
Associate professor
Sapientia Hungarian University of Transylvania, Faculty of Science and Arts Cluj-Napoca
Department of Environmental Science

Prof. Dr. Posta Katalin
Professor, DSc.
Hungarian University of Agriculture and Life Sciences, Faculty of Agricultural and Environmental Sciences
Institute of Biological Sciences
Department of Genetics, Microbiology and Biotechnology

....
Approval of Head of Doctoral School Approval of Supervisor

TABLE OF CONTENTS

"Water is life's matter and matrix,
mother and medium.
There is no life without water."
Albert Szent-Györgyi

1. INTRODUCTION

Water is a vital natural resource, as it is a prerequisite for life, and its properties make it a key basic component of production in various industrial sectors. Water in sufficient quality and quantity is an important raw material and as such its production is an important task.

In global scale it is estimated that 80% of wastewater is released to the environment without adequate treatment (UNESCO, 2017). Moreover, The United Nations' (UN) World Water Report 2017 highlights new and rapidly expanding pollutants that represent a clear knowledge and research gap. Such pollutants include the family of organic (pharmaceutical residues, pesticides, paints) and inorganic (heavy metals, cyanides) micropollutants.

Micropollutants are pollutants that are found in the environment at very low concentrations (μg/l, ng/l). The long-term effects of micropollutants on humans and the environment are not yet known and proven. It is therefore essential to carry out research that will help us understand the dynamics of these pollutants, their impact on the environment and on the organism, and to develop methods to remove them from wastewater. As there is a lack of regulation of new pollutants, appropriate studies need to be carried out in order to set up regulations (Afsane Chavoshani et al., 2020).

Humanity has used materials since ancient times that are capable of staining other materials, initially working with natural colors of animal and vegetable origin. However, nowadays the modern textile industry uses synthetic dyes to color their products producing wastewater containing organic matter with strong color (Salleh et al., 2011). It is reported that over 50,000 tons of dye, containing hazardous, carcinogenic mutagenic substances that can damage life (aquatic, human and vegetal), are discharged via effluent into the environment annually (Tan et al., 2008). Textile industries wastewaters have complex composition, their exposure to nature in large quantities involve complicated cleaning technologies, especially if the contaminants are at low concentrations, generally these treatments are associated with high costs, therefore their practical application impossible.

Inorganic micropollutants include heavy metals. In recent years, there have been growing ecological and global public health concerns about metal pollution in the environment. Cadmium, perhaps one of the most toxic heavy metals, is a major concern due to its high mobility, bioaccumulation and high solubility, which makes it crucial to remove from the industrial

wastewaters (Bashir et al., 2018). They accumulate and persist in nature and cannot biodegrade, causing serious damage to the water system and then posing a threat to living organisms through the food chain (Z. Zhang et al., 2021).

The main problem is that wastewater treatment plants cannot fully remove these substances with the technology currently used, so they can leach into surface water and end up in drinking water, which is then returned to the body. Adequate removal requires very expensive investments. At the same time, the situation is complicated by the fact that certain treatment technologies can lead to the formation of even more hazardous substances (metabolites) than the original ones.

1.1. Objectives

This dissertation is based on six research (one of which is under review) and one review paper of internationally accepted scientific articles with impact factor, as well as a university note. The main idea and topic of all these papers is the removal of organic, synthetically produced dyes and cadmium micropollutants from water by environmentally friendly bioremediation techniques. In our research, adsorption techniques were used to remove emerging contaminants. Household and industrial waste and, in the case of cadmium, cosmetic clay were used as adsorbents.

The first **aim** of this thesis was to develop an alternative remediation method for the removal of inorganic and organic micropollutants and to determinate the optimal dye removal conditions.

In order to achieve these goals, the following objectives were conducted:

- We have chosen adsorption as a simple and inexpensive water cleaning process. The technique requires no special parameters for efficient operation, it is an effective method for the removal of several pollutants, organic matter and a wide range of possible adsorbents are available.
- Nowadays many alternative adsorbents are analyzed to replace the commonly used activated carbon. In the 2. *Literature overview* section, we will present possible adsorbent materials, moreover, the requirements for the efficient adsorbents are also listed. Based on these criteria we used using various adsorbent materials, for the removal of organic dyes powdered, calcined and alginate embedded eggshell, brewery's yeast, while, for the removal of Cd^{2+} Aslavital cosmetic clay.
- Several model contaminants indicator and textile model dyes and Cd^{2+} micropollutants were selected which may represent the major categories of water polluter types.
- In order to achieve the optimal experimental conditions, the effect of several influential parameters were studied.

- Moreover, we provide up-to-date information on the adsorption of dyes from aqueous solutions, while we summarize and compare our results with articles from the last five years (2017–2021).
- Based on our findings and reviewed articles, general trends were drawn regarding the effects of initial dye concentration, pH, adsorbent dosage, particle size and temperature.

Another focal aim of the thesis is the characterization of adsorbents (eggshell, brewery's yeast, Aslavital cosmetic clay) and contaminants using known and practical analytical methods.

- For the determination of contaminants concentration determination UV-Vis spectrophotometer (dye concentrations) and flame atomic absorption spectrophotometer (Cd^{2+} concentration) were used.
- The morphology and elemental composition of the adsorbent materials and dyes were also analyzed.
- The structure of the eggshell thin section was studied using a wide range of microscopes: stereomicroscope, polarization microscope, scanning electron microscope and EDS measurements were also performed on each layer.
- Scanning electron microscopy (SEM) images of eggshell (thin section, powdered, calcined), ACC clay and brewery's yeast was made before and after adsorption together with elemental distribution EDS analyses.
- The determination of functional groups, surface chemistry was done for powdered/calcined eggshell and RBV-5R dye, moreover Aslavital cosmetic clay and Cd^{2+} removal. For this purpose, Raman microspectroscopic and Fourier transform infrared spectroscopy data were analyzed in OriginPro 8.5 software.
- The thermal stability and textural property of powdered eggshell was carried out using a DTA-TG differential heat analyzer. Moreover, total surface area (St), pore volume (Vp) and pore radius (Rm) of eggshell were also determined.
- Aslavital cosmetic clay crystalline structure was investigated with X-ray powder diffraction (XRD).

Analytical instrumental studies help in the knowledge of the adsorption mechanism, as the measurements provide insight into the chemical, physical and surface properties of the adsorbent and the contaminant. To further understand the adsorption mechanisms, beside the large-scale instrumental results, mathematical models were carried out.

- With the help of equilibrium data, the specific parameters of isotherm models were calculated.

- In case of dye removal process the linearized Langmuir, Freundlich, Dubinin-Radushkevich and Temkin models were used. On the other hand, in case of Cd^{2+} adsorption, beside the linear versions, non-linear regression analyses of the two-parameter Langmuir, Freundlich and Temkin as well as the three-parameter Toth, Khan, Liu Redlich-Peterson and Radke-Prausnitz isotherm models were analyzed using OriginPro 8.5 software.
- Pseudo first- and second order kinetic models were calculated from equilibrium data and the linear regression coefficients were compared.
- As diffusion can take part during the contaminant removal process from wastewaters, intra-particle and film diffusion were determined.

1.2. Memory structure

The present study consists of five big chapters: introduction, literature overview, materials and methods, results and discussions, and lastly conclusions. Moreover, the new scientific results are highlighted at the end of the thesis (Figure 1).

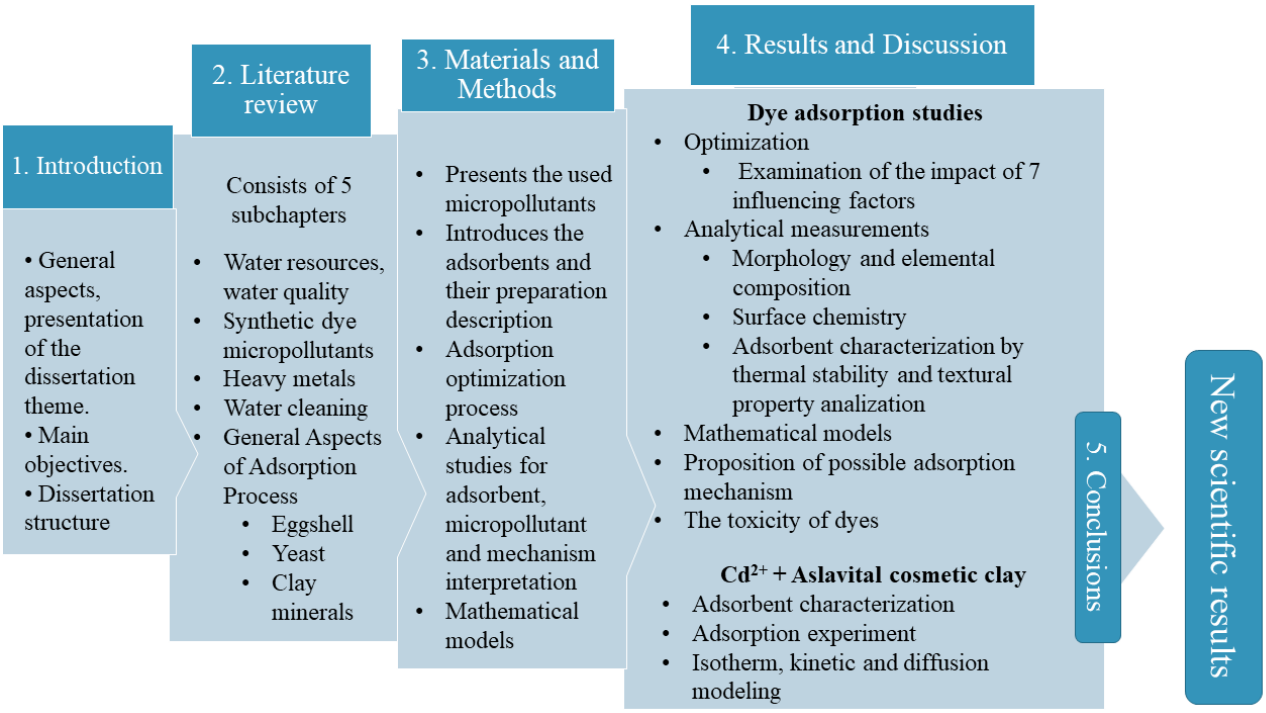

Figure 1. Memory structure of the thesis.

2. LITERATURE OVERVIEW

2.1. Water resources, water quality

Over the centuries, human ambition and the desire for comfort have brought with them the degradation of the natural environment. This has led to a deterioration in air quality, over-exploitation of soils and their barrenness through inappropriate management, and left our natural waters heavily polluted—a problem that needs to be solved (Tiyasha et al., 2020, pp. 2000–2020). Between 2000 and 2020, the global population increased from 6.1 billion to 7.8 billion people. During this period, 2 billion people gained access to safely managed drinking water services, and the number of people lacking safely managed services decreased by 342 million (© World Health Organization (WHO) and the United Nations Children's Fund (UNICEF) 2021, 2021). The rapid population growth is leading to agricultural and industrial overproduction, with a concomitant decline in water quality and a reduction in quantity as well. According to the 2015 World Water Development Report, the demand for water around the world will increase by 55% over the next 15 years, indicating that the Earth's current water supplies can cover only 60% of our future needs by 2030 (Alice Park, 2015).

One of the causes of the freshwater crisis, which is slowly unfolding worldwide, is the presence of various natural or man-made contaminants (Dutta et al., 2021). As a result of the development of human civilization, the pollution caused by the release and/or use of a wide range of chemicals has reached serious proportions. Global anthropogenic pollution has led to the accumulation of a wide range of organic xenobiotic compounds that have adverse effects on human health and intact ecosystems. Xenobiotics are compounds that do not exist as natural products or may contain structural elements that cannot be synthesized biochemically (de Oliveira et al., 2020). Pesticides, pharmaceuticals, heavy metals, oils, detergents, industrial chemicals and dyes can reduce the water quality.

Water pollution occurs when harmful substances - often chemicals or micro-organisms - contaminate a stream, river, lake, ocean, aquifer or other body of water, degrading the water quality and making it toxic to human consumption, natural life processes or the environment.

Water is uniquely vulnerable to pollution because it is known as a "universal solvent" and can dissolve more substances than any other process on earth; thus, water is potentially hazardous if unnatural substances are introduced into it. Toxic substances from farms, cities and factories can easily dissolve and mix with it, causing water pollution. It can be considered a dilute solution, a suspension containing dissolved gases, salts, colloidal or macroscopic suspended pollutants, micro-organisms or sediments. In our natural waters, contaminants often occur as a result of

various natural and anthropogenic activities. The concept of water quality can be interpreted in several ways: from a legal and scientific point of view, it is understood as the property or capacity of the water body to possess all the properties that allow it to be used beneficially.

2.2. Synthetic dye micropollutants

2.2.1. Definition of Dyestuff

Dyestuffs are hydro or oil-soluble, colored organic chemical compounds that are usually dissolved in water and bound to surfaces or fabrics to impart color to textiles. The majority of dyes are complex organic molecules that are designed to bind strongly to the polymer molecules that make up the textile fiber, and must be able to withstand a wide range of external effects (Benkhaya et al., 2020; Chequer et al., 2013; Mazharul Islam Kiron, 2021).

In his book “Synthetic dyes”, Gurdeep R. Chatwal (Gurdeep R. Chatwal, 2009) defines dyes as colored organic compounds or mixtures used to color paper, cloth, plastics and leather. The dye substrate must be resistant to washing and stable to light. It is important to note that not all colored materials are dyes, as a dye must be fixed to the material to give it a permanent color (Gurdeep R. Chatwal, 2009).

According to the internationally accepted convention of Colour Index International, dyes are defined as intensely colored or fluorescent organic substances that impart color to a substrate by selective light absorption. These substances dissolve and/or undergo a process that destroys, if not permanently, the crystal structure by adsorption, mechanical action, ionic or chemical bonding (© Society of Dyers and Colourists & AATCC, 2018).

Dyes are usually large aromatic molecules, often with many rings linked together. An aromatic ring structure linked to a side chain in the dye molecule structure is necessary for resonance and hence for the transfer of color (IARC Working Group on the Evaluation of Carcinogenic Risk to Humans, 2010). The resonance structures responsible for color are those that cause the shifting or appearance of absorption bands in the visible spectrum of light. In the synthesis of a dye, the correlation of chemical structure and color is achieved by a chromogen-chromophore-auxochrome combination. Three essential groups can be found in a dye molecule: the chromophore, auxochrome and matrix (Benkhaya et al., 2020). Thus, dyes are organic colorants that contain at least one unsaturated compound (chromophores) and one functional group (auxochromes). The chromophore present in the structure may be an aromatic structure containing benzene, naphthalene, or anthracene rings. The chromophore group responsible for the color formation is represented by the following radicals: azo (-N=N-); carbonyl (=C=O); carbon (=C=C=C=); carbon-nitrogen (>C=NH or -CH=N-); nitroso (-NO or N-OH); nitro (-NO or =NO-OH); and

sulfur (>C=S, and other carbon-sulfur groups). These, in combination with a chromogen, form the basis for the chemical classification of dyes. Since the chromogen-chromophore structure is often insufficient to provide adequate solubility and thus the dye cannot adhere to the fiber of the material, auxochromes are required. Auxochromes enhance the color of the dye. Auxochromes, also known as binding affinity groups, can be amine ($-NHX_2$), hydroxyl (-OH), carboxyl groups (-COOH), aldehydes (-CHO), sulfonic acid ($-SO_3H$) or their derivatives (Berradi et al., 2019; El-Sikaily et al., 2012; Gürses et al., 2016; Mahapatra, 2016).

2.2.2. Brief History of Dye Usage

The word dye is from Middle English "deie" and from Old English "dag" and "dah". The first known use of the word dye was before the 12th century (Letha Malan Oelz, 2018).

Human eyes can see more than one million colors, all of which can be found in our natural habitats. These wonderful and unique colors attract humans' attention from the surroundings, and everyday tools were made to mimic these colors. Archeological excavations prove that the art of dying can be dated back to the appearance of human civilization. Figure 2 contains a timeline, based on the detailed historical overview of Susan C. Druding (unfortunately, the literature data has been lost, so its references are missing), where some important historical milestones regarding dyestuffs are represented (Druding, 1982; Nawab et al., 2016).

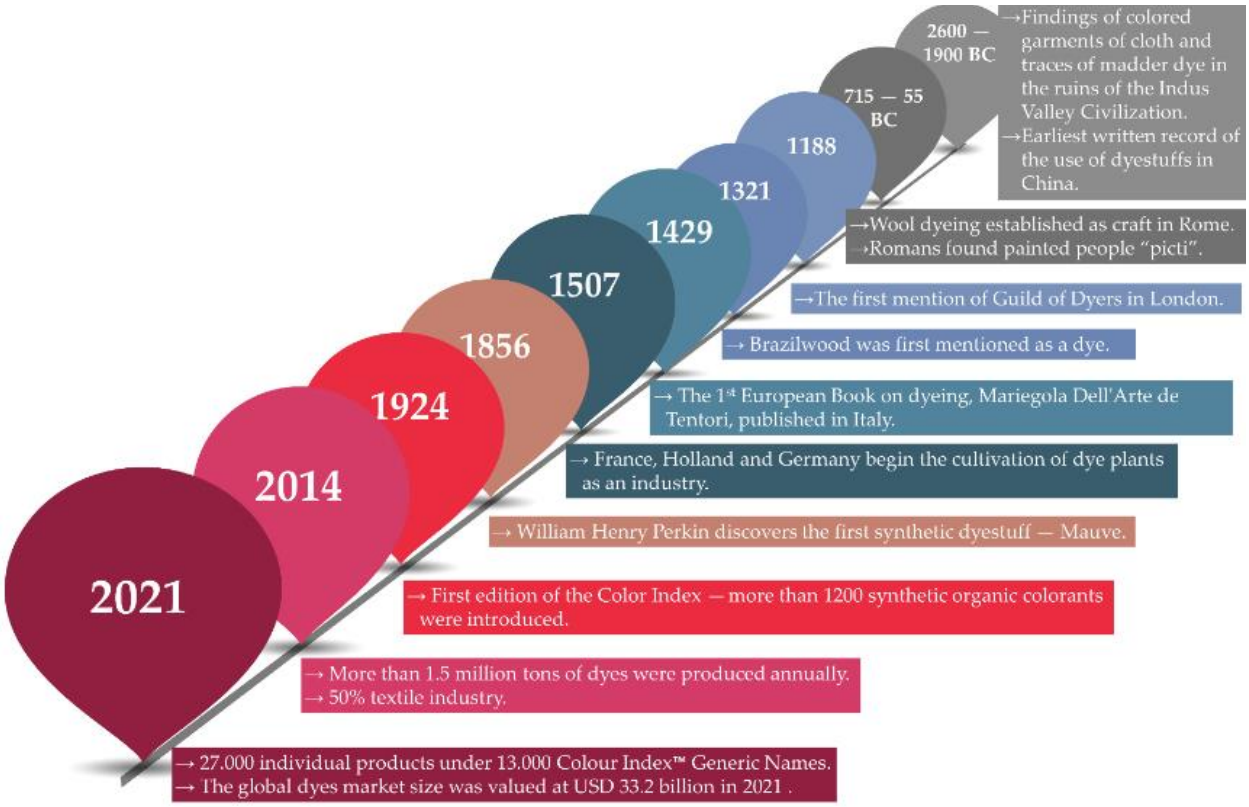

Figure 2. Historical timeline of dye usage, invention and interesting facts.

Without wishing to be exhaustive, we would like to mention a few interesting facts, as a detailed list can be found in the literature. According to these data, colored garments of cloth and traces of madder dye were found in the ruins of the Indus Valley Civilization dated between 2,600 and 1,900 BC. Moreover, the first written record about dyestuff usage was found in China during this period (Mansour, 2013). Another interesting investigation showed that the cave paintings of "El Castillo" in Spain were painted about 40,000 years ago. Probably the oldest colored flax fiber dated around 34,000 BC was found in the Republic of Georgia (in a prehistoric cave) (Md. Imran Hossain, 2021). Several mentions are made between 715 and 55 BC, from the Roman Empire, where wool dyeing appeared as a craft, and purple has been used for dyeing their clothing, like robes. After the conquest of Susa in 333 BC (the capital of Persia), Alexander the Great mentions that he found purple cloths in the royal treasury (dating from 541 BC) (Druding, 1982; Letha Malan Oelz, 2018; Nawab et al., 2016). The 5,000 talents of purple cloth colored with mucus (yellowish material from sea snail's tiny gland near its neck) today is worth about $68 million (Kassinger, 2003).

Jumping ahead in time, the 12th century saw the establishment of several painters' guilds in Europe's major cities (e.g., London in 1188). In Florence, in the middle of the century, there were more than 200 registered painters, clothiers and tailors. Several rulers took measures to protect merchants and quality (Druding, 1982).

At the beginning of the 15th century, Cennino Cennini (Padua, Italy) published his treatise, the Method of Painting Cloths by Means of Moulds, in which he described the method of printing cloth. The first European book on painting, Mariegola Dell'Arte de Tentori, was published in Italy in 1429. From 1507 onwards, several European countries (France, the Netherlands and Germany) began to grow dye plants on an industrial scale (Druding, 1982).

Prior to the industrial revolution, to the middle of the 19th century, all dyestuff was made from natural sources: plants, animals, and minerals. The small quantities of the main components of dyes, the long distances involved, and the weather conditions were the economic disadvantages of using natural dyes. For this reason, there was a need to be able to produce commonly used dyes quickly and easily by synthetic means in any region, thus making the product cheaper, and transport and trade more reliable. Literature records suggest that the substitution and thus production of naturally occurring indigo and madder dyes posed difficulties for chemists of the time (Kassinger, 2003).

The root of the *Rubia tinctorum* plant, most commonly cultivated in Turkey, was used to extract cadherin, whose coloring principle is alizarin. In a complicated process, it was mixed with aluminum to form an insoluble red metal complex, bright red in color, with cellulose fibers.

Indigo, also a plant dye (*Indigofera tinctoria*), was the most important natural blue dye. In ancient times, the flowering indigo plant was cut and fermented in wooden vats underwater for 10–15 h. A yellow solution was obtained, from which the raw indigo was released as blue flakes in the air. The leaves of the plant are rich in indoxyl, and after fermentation, free indoxyl is released, which is rapidly oxidized in air to the desired color, and is insoluble in water (Kassinger, 2003).

Therefore, the discovery and development of synthetic dyes are closely intertwined with the development of organic chemistry and the industrial, economic, and social demands of the 19th century. There were a lot of attempts to produce synthetic dyes; however, these were not successful due to their poor lightfastness. The discoverer and pioneer of synthetic dyes is said to be William Henry Perkin. On Easter 1856, while studying the production of artificial quinine for the treatment of malaria (oxidized dichromate), he isolated a small amount of purple dye. He named the dye 'mauve', which soon became a favorite of the royal family, and a new industry was launched (Hunger, 2002). Until the beginning of the twentieth century, the dye industry continued to flourish, with many different types of dyes being produced, making it essential to classify, record and catalogue them. In 1924, the first edition of the Color Index was published, listing over 1200 organic and synthetic dyes.

It was reported that in 2014, more than 1.5 million tons of dyes were produced worldwide, out of which 50% were used by the textile industry (Elkady et al., 2011; Forgács et al., 2004). According to an article published in 2016, over 50,000 tons of different synthetic dyes were annually produced and approximately up to 10% were mixed with water bodies (Asif Tahir et al., 2016).

Up to date statistics show that the global dyes market size was valued at USD 33.2 billion in 2021. The Colour Index™ contains 27,000 individual products under 13,000 generic names and properties ("Global Dyes & Pigments Market Size Report, 2021-2028," 2021, pp. 2021–2028; Market Data Forecast ltd, 2021). It is projected that the revenue generated by the manufacture of dyes and pigments in Romania will amount to approximately $65.1 million by 2023 (Statista Research Department, 2019).

2.2.3. Classification of Dyes

As the quantity and variety of dyes has increased throughout history, it has become essential to classify them. There are several different classifications, based on their structure, source, color, solubility and application methods. Basically, the most common classification is based on their chemical structure and application (Bhardwaj and Bharadvaja, 2021). Figure S1. combines the grouping by ionic nature (particle charge upon dissolution in aqueous medium) with the application. Accordingly, we can speak of non-ionic and ionic dyes; the latter being cationic and

anionic in nature. They are classified according to the method of application as reactive, direct and acid (anionic dyes), basic (cationic dyes), or disperse and vat (non-ionic dyes) (Gürses et al., 2016; Yagub et al., 2014).

2.2.3.1. Reactive Dyes

Reactive dyes make it possible to obtain a high wet strength compared to the less expensive direct dyes. However, their use is not always possible because of the difficulty in obtaining good unison. Another characteristic is that the chlorine-fastness is slightly lower than that of vat dyes, as is its light fastness under extreme conditions (Benkhaya et al., 2017). It has been reported that the reactive dyes are the only textile colorants that form a covalent bond with the substrate/textile fiber, usually cotton, during the application process under the influence of alkaline pH and heat (Demirbas, 2009; Farouk and Gaffer, 2013; Katheresan et al., 2018). Reactive dyes contain reactive groups such as vinyl-sulfone, chlorotriazine, trichloro pyrimidine, and difluoro-chloro pyrimidine, that covalently bond with the fiber during the dyeing process (Labanda et al., 2009; Prol, 2019). Adsorption results show that since reactive dyes are soluble in aqueous medium and have a greater negative charge density, the adsorption process was related to electrical attraction between anionic dyes and positively charged surfaces of adsorbent (Prol, 2019; Rachakornkij et al., 2004). Initially, these dyes were designed for cellulose fibers, but nowadays they are used for cotton, wool and poly-amide fabrics; moreover some fiber-reactive dyes for protein and polyamide fibers are also commercially available (Raval et al., 2017). With about 1150 entries in Color Index and ever rising volumes, the importance of reactive dyes in the global coloration business cannot be overemphasized. An equally well-known entrenched position is enjoyed by the chlorotriazines and vinyl-sulphones in the reactive system space, despite the introduction of at least one new reactive group every year from 1956 until 1971, except 1969 (Bhate et al., 2017; Paul Rys and Heinrich Zollinger, 1989). It is estimated that losses of 1–2% occur during the manufacturing process of dyes, while up to 1–10% of dyes are released back into the environment during use. For reactive dyes, the estimated loss is around 4%. (Forgács et al., 2004; Li et al., 2019). According to other sources after the colorization process, approximately 10–50% of the initial dye load remains unused (Easton, 1995; Vijayaraghavan et al., 2009; Rápó et al., 2020a). Reactive dyes are said to be the most problematic among other dyes, as they tend to pass through conventional treatment systems unaffected, therefore their removal is a difficult task (Lazaridis et al., 2003; Rachakornkij et al., 2004).

2.2.3.2. Direct Dyes

Direct dye is still the most widely applied in the dying and printing processes of the textile industry (Hassaan et al., 2017). Direct dyes are water-soluble and anionic in nature, and they contribute 17% share in the textile industry, having wide utility in printing and dyeing cotton, viscose, silk, wool and leather (Garg et al., 2019; Horng and Huang, 1993; Irshad et al., 2021). Although these dyes are water-soluble anionic dyes, they cannot be classified as acid dyes because the acid groups are not the means of attachment to the fiber. Since these dyes do not require any kind of fixing, they are called direct dyes (Raval et al., 2017). The major chromophore types are as follows: azo, stilbene, phthalocyanine, dioxazine, formazan, anthraquinone, quinolone and thiazole. Direct dyes are known to be easy to use, with a wide range of colors and shades, but have a low resistance to washing; this is what drives them out of the market compared to reactive dyes (Benkhaya et al., 2017; Burkinshaw, 1995; Burkinshaw and Salihu, 2019).

2.2.3.3. Acid Dyes

Acid dyes, as their name implies, contain one or more acidic functions (SO_3H and COOH) in their molecules (Benkhaya et al., 2020). They have excellent chemical and photochemical stability, which is why their industrial effluents have a complex composition, poor biodegradability and high tinctorial value (Patil et al., 2011; Wu et al., 2020; Yao et al., 2018). This makes them difficult to remove by conventional methods. Their degradation products or metabolites can be potentially mutagenic or carcinogenic and can damage aquatic ecosystems. The use of water-soluble acid dyes, in particular sulphonic acid dyes, is very widespread due to their bright color and high solubility (Benkhaya et al., 2020; Dai et al., 2018; Wu et al., 2020). Acid dyes account for about 30% to 40% of total dye consumption. They are used in textiles, printing and dyeing, paper, leather, food, cosmetics, pharmaceutical and other industries for dyeing, e.g., nylon, wool, silk and modified acrylic (Benkhaya et al., 2020). The dye molecules are structurally very different and often contain some metal complexes. The defining characteristic of the group is the presence of sulphonated groups, which ensure water solubility, and azo-chromophore systems (the most important group), anthraquinone, triphenylmethane or copper phthalocyanine (Benkhaya et al., 2017; Prol, 2019; Raval et al., 2017).

2.2.3.4. Cationic-Basic Dyes

Basic dyes belong to the group of cationic dyes because they form a colored cationic salt in aqueous solution. Later, these cationic salts react with the anionic surface of the substrate (acrylic, paper and nylon). The resulting cations are electrostatically attracted to the negatively charged substrates (Kyzas et al., 2013).

The cationic functional groups (-NR^{3+} or =NR^{2+}) are usually acid-soluble amino and substituted amino compounds. They would bind to the fiber by forming ionic bonds with its anionic groups (Raval et al., 2017).

In a literature study, it is recorded that this class of dyes is readily visible even at very low concentrations. This property contributes to the reduced efficiency of natural biological self-cleansing by blocking the penetration of sunlight, thus reducing photosynthetic activity. Basic dyes are highly resistant to degradation due to the number of aromatic rings associated with their resonance capacity, and their complex and large structure, which makes them durable and stable in the environment (Bayram and Ayranci, 2010, p. 7; Benvenuti et al., 2019; Morais da Silva et al., 2020; Vikrant et al., 2018).

2.2.3.5. Disperse Dyes

Disperse dyes are water-insoluble dyes; their structure is small and non-ionic with attached polar functional groups, such as -NO_2 and -CN. They are applied to hydrophobic fibers from an aqueous dispersion (Raval et al., 2017). They are mainly used for the dyeing of polyesters because they can interact with the polyester chains by forming dispersed particles. Disperse dyes are employed on cellulose acetate, nylon, acrylic fibers and cellulose fibers. The main classes are benzodifuranone, nitro, styryl, azo and anthraquinone groups (Kausar et al., 2018). Disperse dyes have a low solubility in water, therefore they must be applied with a dispersing aid, and are mainly used for acetate or polyester fiber (Liu et al., 2019, pp. 3-). From a chemical point of view, more than 50% of disperse dyes are simple azo compounds, about 25% are anthraquinones, and the rest are methine, nitro or naphthoquinone dyes (Chavan, 2011). Disperse dyes are also described as "sublimation" inks, as the ink molecules "sublimate" or change directly from solid to gas due to the application of heat, skipping any liquid state entirely (Cie, 2015). The majority of disperse dyes are based on azo structures; however, violet and blue colors are often obtained from anthraquinone derivatives (Benkhaya et al., 2020; Clark, 2011; Shamey, 2009). Disperse dye particles, due to their nano size, can keep better stability, especially in high temperature dyeing processes (Y. Qin et al., 2020).

2.2.3.6. Vat Dyes

Vat dyes are the main sources of pollution in the wastewater of textile and other industrial effluents, and they are widely used in dyeing cellulosic cotton fabrics (Qayyum et al., 2020). These types of dyes are water-insoluble. Their main application is for cellulosic fiber, notably cotton dying (Prol, 2019). Vat dyes are characterized by excellent color fastness, washability and chlorine-bleachable colored fibers (Benkhaya et al., 2020; Božič and Kokol, 2008). The

disadvantage of their application is that, as they are practically insoluble in water and thus have no affinity for cellulosic fibers, they are difficult to use (reduction and oxidation mechanisms) (Zhang et al., 2000). In conventional tank dyeing processes, the dye is reduced in alkaline medium with strong reducing agents, from which the most important is sodium dithionite ($Na_2S_2O_4$) (Balan and Monteiro, 2001; Chaari et al., 2021).

Nirav P. Raval et al. (Raval et al., 2017) made a detailed classification in their article, where the dyes are grouped based on:

- source of materials/origin (natural–substantive and adjective–synthetic);
- method of application to the substrate (acid, basic, direct, mordant, reactive, disperse, solvent, sulfur);
- their chemical structure (azo, nitro, indigoid, cyanine, xanthene, quinione-imine, acridine, oxazine, anthraquinone, phthalein, triphenylmethane, nitroso, diarylmethane); and
- the electronic origins of color (donor–acceptor chromogens, polyene chromogens, $n \rightarrow \pi^2$ chromogens, cyanine type chromogens) (Benkhaya et al., 2020; Prol, 2019; Raval et al., 2017).

2.3. Heavy metals

As a result of anthropogenic (industrial, agricultural) activities (mining, extracting, use of fertilizers) and (partly) geochemical natural processes (volcanic eruptions), pollution with heavy metals has increased in natural water bodies (Mikhailenko et al., 2020). Heavy metal sources from natural and anthropogenic activities are shown in Figure S2.

Cadmium is a naturally occurring element of the heavy metal family that is present in the Earth's crust at concentrations of approximately 0–11 mg/kg as a natural constituent of rocks (Zhao et al., 2020). Research has estimated that soils that are not directly contaminated by cadmium contamination may contain cadmium at concentrations of 0.06–1.1 mg/kg (Zhao et al., 2020).

Cadmium pollution is known to be of great concern because of its high bioaccumulation and non-biodegrading properties (Long et al., 2021). Cadmium in drinking water should not exceed the limit value of 0.003 mg/L as recommended by the World Health Organization (World Health Organization, 2019). Moreover, from industrial, mining, and other activities, the discharged concentration should be lower than 2 mg/L (Basu et al., 2017). Exceeding these values poses severe health effects by causing cadmium poisoning and itai-itai disease with bone degradation, which can negatively affect blood pressure and even cause cancer (Peng et al., 2020). Cadmium also has a negative effect on plant development, reducing seed germination, growth and plant

biomass, affecting photosynthetic activity, evapotranspiration rate, stomatal conductance, electrolyte leakage and relative water content (El Rasafi et al., 2020; S. Qin et al., 2020).

Romania has a long history of mining and non-ferrous metallurgy (Emil Cardos et al., 2007). As a result, heavy metals can accumulate in many areas, contaminating water and soil. It is estimated that 18% of Romanian population is at risk of serious pollution (Bora et al., 2020). A study has investigated heavy metal soil contamination in 34 counties of Romania (near schools and kindergartens). Their results showed that cadmium levels in the soil were 0–0.86 mg/kg (Moldoveanu, 2014). The cadmium content of Romanian soils and water bodies, as well as of various crop plants and fungi, has been studied in recent years (Calmuc et al., 2021; Iordache et al., 2016; Radu and Lacatusu, 2008; Tóth et al., 2016; Triebskorn et al., 2008; Zugravu et al., 2009).

A survey was carried out near the Baia Mare mining and metallurgical complex, where soil samples and grapes (*Vitis vinifera L.*) were collected, and their concentrations of heavy metals determined. Cadmium in soil was detected in two areas, with an average of 15.84 mg/kg Cd in the Baia Mare area and 26.84 mg/kg Cd in the Baia Sprie area. Examining the Cd content of different vine species in these areas, it was found that the roots of *Feteasca regala* from Baia Mare and *Feteasca alba* from Baia Sprie contained the highest levels of cadmium (7.09 ± 0.83 mg/kg and 3.07 ± 0.12 mg/kg, respectively). The cadmium content of the wine samples analyzed (0.02–0.06 mg/L Cd) exceeds the permitted limit (0.01 mg/L) (Bora et al., 2020).

Heavy metal pollution in water, sediment and fish meat was studied in Natura 2000 site “Buhuşi-Bacău-Bereşti”. The maximum concentration for water samples approved by the World Health Organization was exceeded in all studied areas with the measured cadmium concentration, 0.0521 mg/L, exceeding 10.42 times the permitted maximum value. In the case of fish samples, the Cd concentration in gills was 0.911 mg/kg and in the muscle reached 0.522 mg/kg, however, the maximum accepted concentration in the EU is 0.05 mg/kg (Bontas et al., 2020).

In addition to the study of the cadmium content of certain plant foods and waters, it is essential to investigate the Cd removal from soil and water.

2.4. Water cleaning

As one of the most important environmental challenges of our time is to ensure that the Earth's population has access to sufficient water of appropriate quality and quantity. The supply of drinking water is a major social and economic problem. The task of industrial waterworks is to convert raw water from the environment (surface water and groundwater) into drinking water and to produce it in compliance with the required standards. Since raw water may contain large

quantities of inorganic ions, dissolved organic matter, agricultural and industrial waste, it is not suitable for direct consumption. The quality of the water, both at the point of production and at the point of delivery to the consumer, and in particular the latter, must meet the quality standards laid down by the authorities. In the course of water treatment and purification, raw water extracted from nature is subjected to a series of technologies to make it fit for consumption. The principle of the technology is that successive operations gradually remove coarse sediments and impurities of a smaller particle size, which are then dissolved in the water.

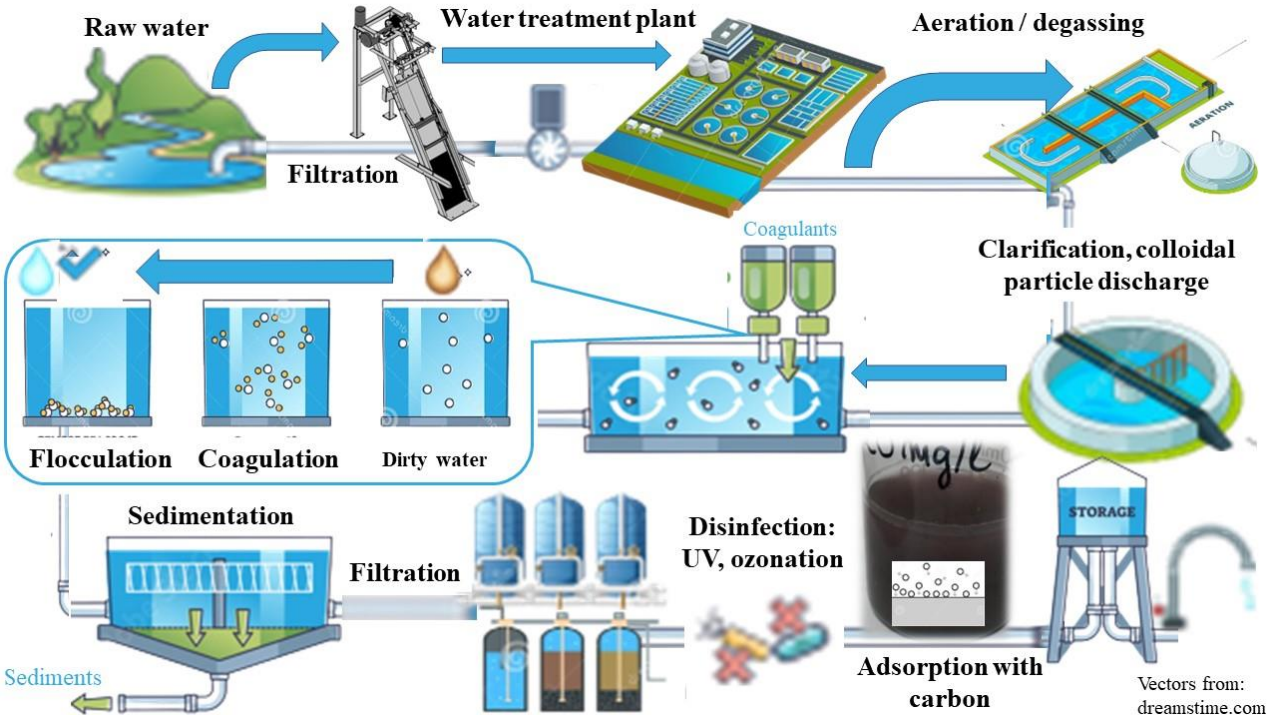

Figure 3. The process of drinking water production (Vectors for the flow chart are from dreamstime.com)

The general structure of drinking water production follows the steps:

- coarse filtration using grids to remove larger impurities,
- aeration to remove oxygen, manganese, iron and methane,
- separation to remove colloidal particles and precipitation of volatile substances,
- filtration using various filter media to remove suspended solids,
- disinfection using different methods (e.g. chlorination, ozonation),
- adsorption, most often using activated carbon,
- disinfection.

A close look at the schematic scheme of drinking water production shows that adsorption plays a very important role in the process, where unpleasant tastes, colors, odors, toxic organic compounds, heavy metals can be easily removed.

2.4.1. Dye Removing Methods, Technologies

The sources of dye contaminants in freshwater can be the textile, pharmaceutical, food leather, paint and varnishing industry effluents. Other sources are households, and moreover the untreated or partially treated effluents from wastewater treatment plants (Dutta et al., 2021). According to the literature, five major industries are known to be responsible for the presence of dye effluents in the environment: the textile industry (54%), the dyeing industry (21%), paper and pulp industry (10%), tannery and paint industry (8%), and the dye manufacturing industry (7%) (De Gisi et al., 2016; Katheresan et al., 2018).

After the dyeing process of textiles, the resulting dye-concentrated wastewater is often discharged into nature at high pH and temperatures without any treatment. The oxygen transfer mechanism and the self-purification process of environmental water bodies will get disturbed by this phenomenon (Bouabidi et al., 2018; Kant, 2011; Katheresan et al., 2018). Wastewater from the paint industry is a difficult effluent to treat, not only because of its high biological and chemical oxygen demand, high suspended solids content and other hazardous substances, but also because of the aesthetic harm it causes to the visual appearance (Ishak et al., 2020; Peck Kah Yeow et al., 2020). These substances are often of synthetic origin and have a complex aromatic molecular structure, which increases their chemical and microbiological stability, hence their difficult removal from water. The introduction of dyes into the water system causes a number of health and environmental problems:

- Dyes increases the water turbidity;
- Dyes have a major impact on the photosynthetic activity of the aquatic environment because they block the penetration of light into the water, thus inhibiting the growth of algae, which are not only important for oxygen production but are a pillar of the food chain;
- Most of the dyes are carcinogenic (bladder, kidney, liver), mutagenic and toxic to living organisms;
- They can cause allergic reactions: skin, eye, mucous membrane irritation, dermatitis, respiratory problems; and
- They cause harm to aquatic environment, and may be toxic to aquatic organisms due to their aromatic, heavy metal and chlorine content (Dutta et al., 2021; Jadhav and Jadhav, 2021; Sachidhanandham and Periyasamy, 2020).

The presence of dyes in natural waters has not received attention in the last 30 years and has only recently become part of environmental legislation. As per this law, dye utilizing industries have to ensure wastewater released from their factories abide by the International Dye Industry Wastewater Discharge Quality Standards that were adopted from the Zero Discharge of Hazardous

Chemicals Programme (ZDHC) (Katheresan et al., 2018; ZDHC: Zero Discharge of Hazardous Chemicals, 2016).

Dye removal methods have been summarized in review articles by many authors (Beulah and Muthukumaran, 2020; Bhatia et al., 2017; Donkadokula et al., 2020; Hessel et al., 2007; Ihsanullah et al., 2020; Katheresan et al., 2018; Madhav et al., 2018; Mashkoor and Nasar, 2021; Pavithra et al., 2019; Samsami et al., 2020; Selvaraj et al., 2021; Singh and Singh, 2017; Slama et al., 2021; Yaseen and Scholz, 2019; Zhou et al., 2019). The importance of removing dyes is driven by a number of factors; they are harmful to health, often mutagenic and carcinogenic, inhibit photosynthetic activity in the aqueous medium, and even at very low levels (< 1 ppm) are highly visible and undesirable in water bodies, with color being the most obvious parameter affecting water quality (Chikri et al., 2020; Crini, 2006). Hessel C. et al. described the percentage of non-fixed dye that may be discharged in the effluent as a function of dye classes from EPA and OECD legislation (Katheresan et al., 2018).

Throughout recent years, numerous investigations have been made to find the ideal technology for dye wastewater purification. Even though a high range of methods have been studied in the past 30 years, only several are truly being implemented by the concerning industries these days due to the limitations they possess (Katheresan et al., 2018).

As it appears in the review articles referred to above, dye remediation technologies can be divided into three main categories: physical, chemical, and biological methods. As a summary, Figure 4 contains some of the used methods, and their advantages and disadvantages (Samsami et al., 2020).

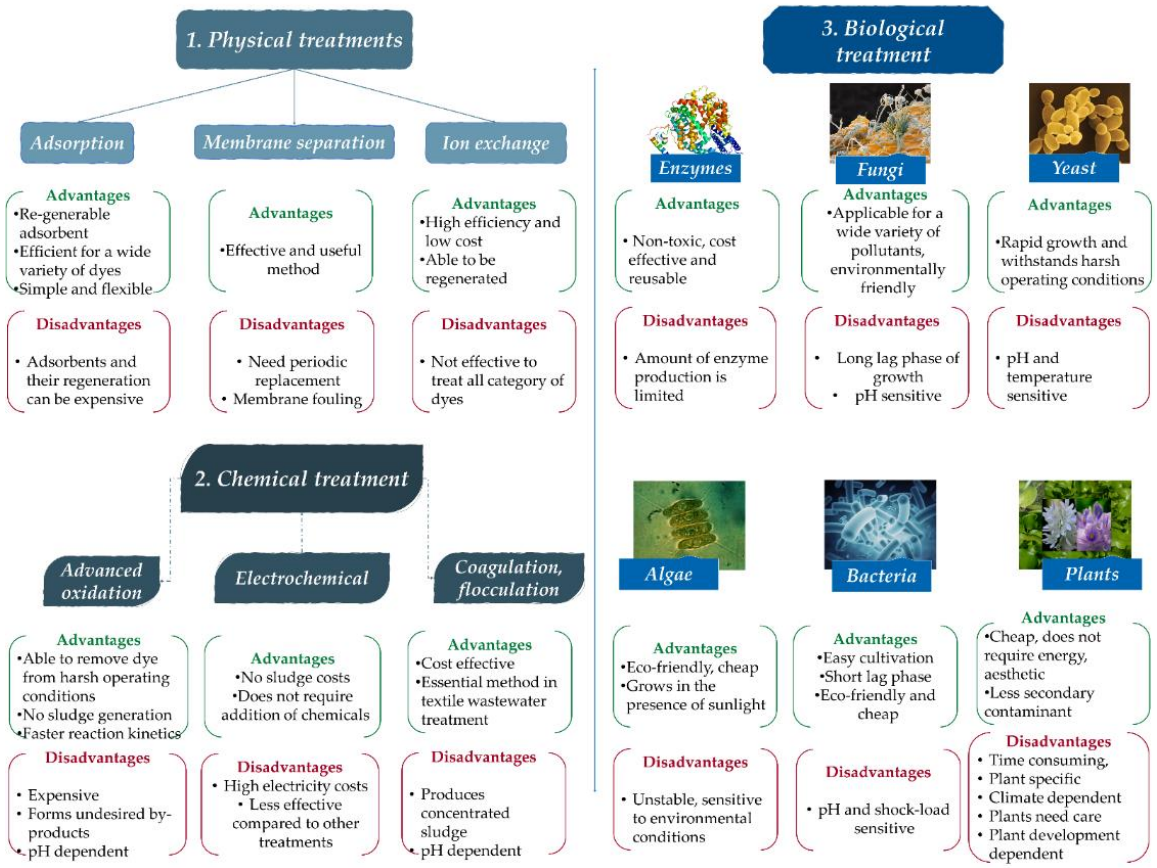

Figure 4. Dye removing methods and their advantages/disadvantages (Samsami et al., 2020).

Review articles exclusively analyze and compare paint removal methods. Often, published studies are used to illustrate the effectiveness of the methods presented. In these studies, several methods are classified into the three main categories of paint removal (Beulah and Muthukumaran, 2020; Bhatia et al., 2017; Katheresan et al., 2018; Madhav et al., 2018; Samsami et al., 2020). Physical dye removing techniques can be: adsorption, membrane separation, reverse osmosis, ion exchange, ultrasonic mineralization, nano-remediation and photo-Fenton processes. Chemical methods are: catalytic reduction, coagulation/flocculation, electrochemical reduction, photolysis/photochemical reduction, advance oxidation processes, ultraviolet irradiation ozonation, clay minerals and zeolites. Biological methods can be divided to phytoremediation and microbial remediation (bacterial, algae, fungi, mycoremediation, enzyme degradation and phycoremediation) (Bhardwaj and Bharadvaja, 2021; Katheresan et al., 2018; Semeraro et al., 2017).

2.4.2. Cadmium Removing Methods

In addition to the study of the cadmium content of certain plant foods and waters, it is essential to investigate the Cd removal from soil and water. Many physical and chemical methods have been used to remove heavy metals from soils and wastewaters (Gul et al., 2021; Haider et al., 2021; Hamid et al., 2020; Hou et al., 2020; Riaz et al., 2021; Rosca et al., 2021; Y. Zhang et al., 2021;

X. Zhao et al., 2021). A comprehensive and critical review as its title suggests was written by Naef A.A. Qasem et al., where the authors enlisted a high range of heavy metal removal techniques from wastewaters (Qasem et al., 2021). They classify the discussed methods into five types: adsorption-, membrane-, chemical-, electric- and photocatalytic-based remediation treatments (Figure 5).

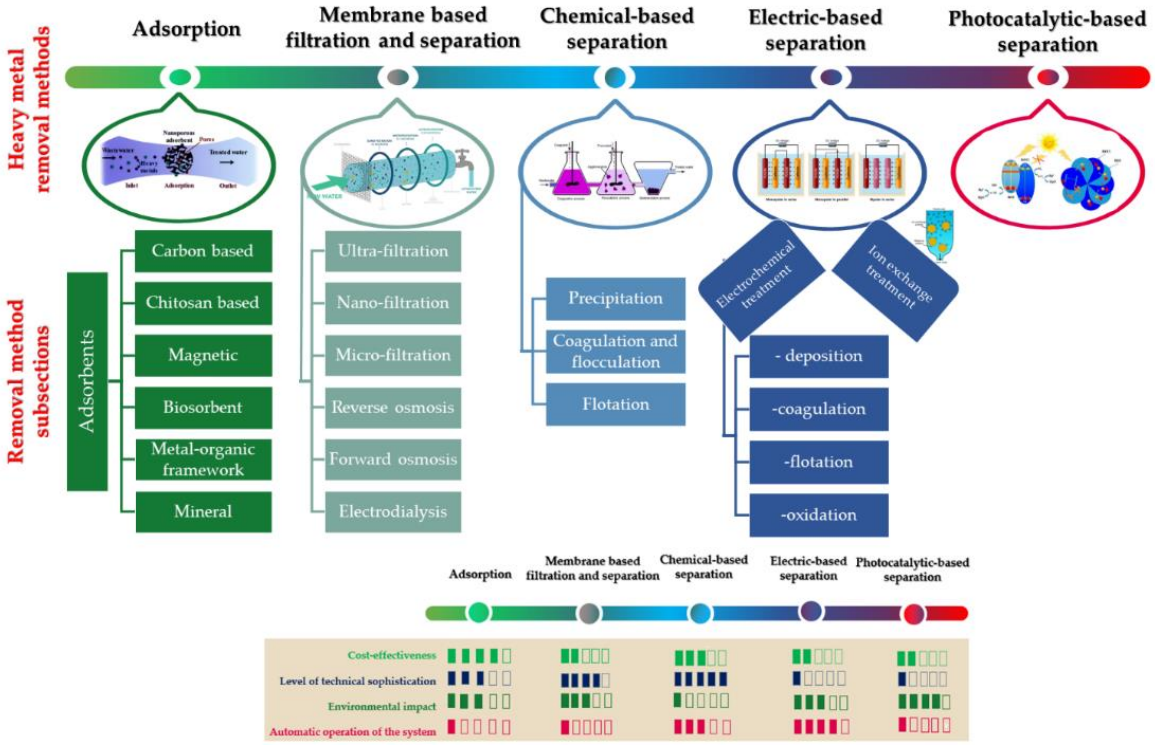

Figure 5. Heavy metal removal techniques from wastewaters (Edited and adapted based on (Crystal Quest© Water Filters, 2021; Gao and Meng, 2021; Qasem et al., 2021; Zaimee et al., 2021)).

2.5. General Aspects of Adsorption Process

2.5.1. Definition and used terms

The term adsorption was first used in 1881 by the German physicist Heinrich Kayser (M and Choudhary, 2017). The past decade has seen a boom in environmental adsorption studies on the adsorptive removal of pollutants from the aqueous phase. It is preferred over other methods because of its relatively simple design, operation, cost effectiveness, and energy efficiency (Tan and Hameed, 2017).

It is a mass transfer process in which a substance (adsorbate) moves from a gas or liquid phase to form a surface monomolecular layer on a solid or liquid condensed phase (substrate, the adsorbent). It usually involves the molecules, atoms or even ions of a gas, liquid or solid in a dissolved state that are attached to the surface. In practice, adsorption is performed as an operation,

either in batch or continuous mode, in a column packed with porous sorbents (Abebe et al., 2018). Figure 6 (adapted without any change from (Tran et al., 2017)) contains the most important, basic terms regarding the adsorption process that are often wrongly used in the literature.

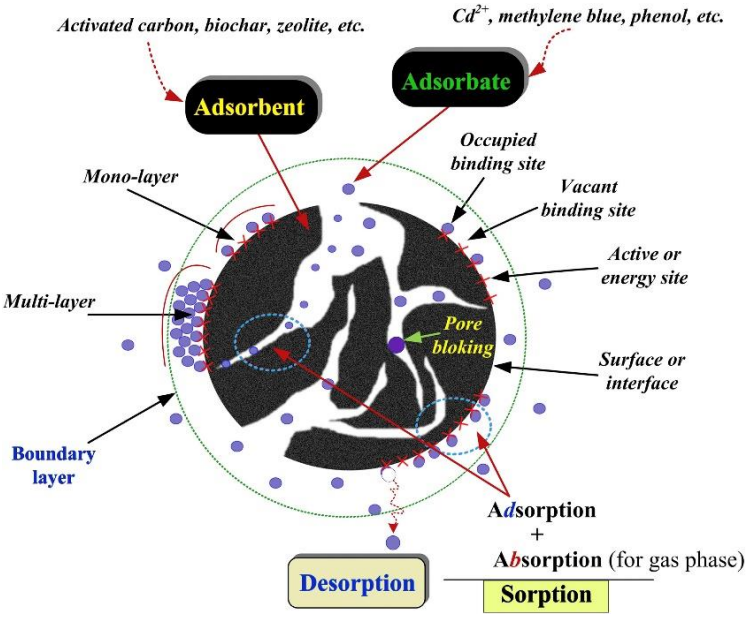

Figure 6. Some basic terms used in adsorption technology (Figure from (Tran et al., 2017).

Adsorption is often confused by the term absorption. The difference between absorption and adsorption is that in absorption the molecules penetrate a three-dimensional matrix, while in adsorption the molecules attach to a two-dimensional matrix (Al-Ghouti and Da'ana, 2020; Qi et al., 2017; Sims et al., 2019). The process is usually reversible (the reverse process is called desorption), so that sorption is responsible not only for the extraction of substances but also for their release.

2.5.3. Types of adsorption

Adsorption can occur due to physical forces or chemical bonds, primarily as a result of surface energy. In general, partially exposed surface particles tend to attract other particles into position. There are several ways of classifying adsorption, and Figure 7 provides a classification based on the nature of the bond (physical or chemical bonds) formed between the adsorbent and the pollutant, describing its characteristics (Kamaya Parashar, 2015; Ruthven, 1984; Terry and Noble, 2004).

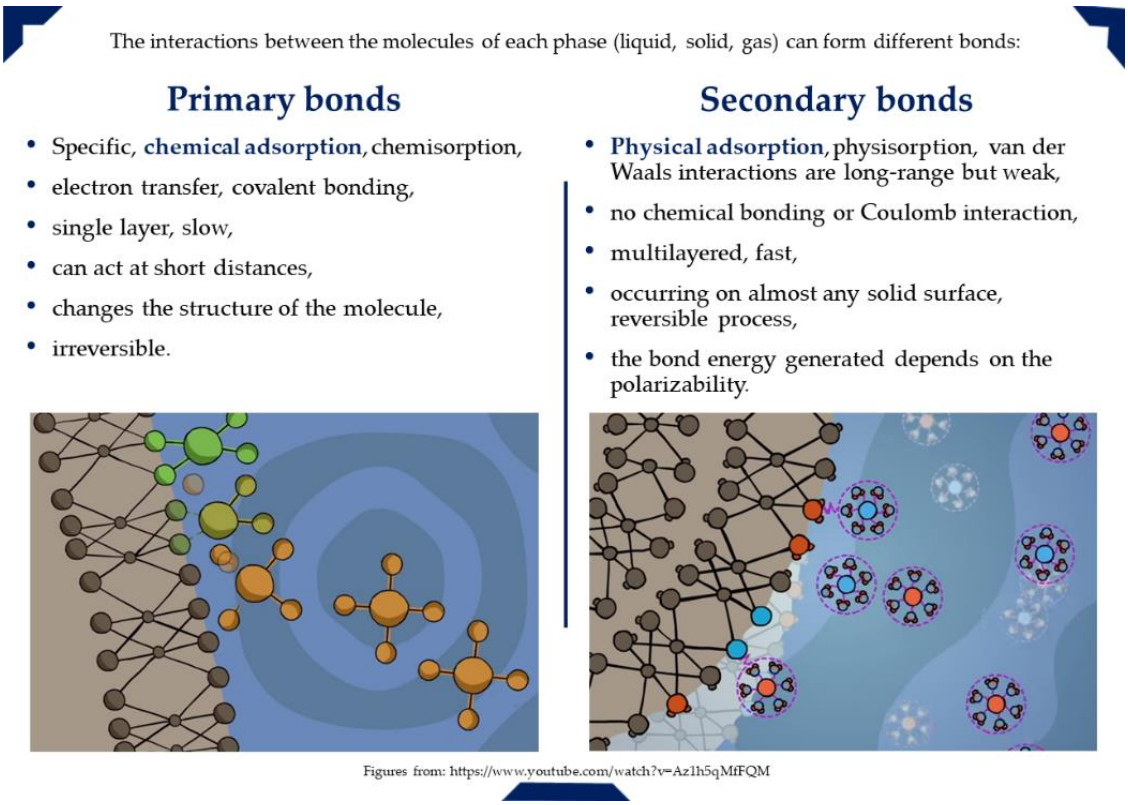

Figure 7. Types of adsorption bonds and nature of adsorption.

Since adsorption phenomena occur in many natural, biological, physical and chemical systems, people tend to apply it in industrial processes and take advantage of its benefits. It is increasingly used for purification or separation purposes; it is also a wastewater treatment technique for the removal of a wide range of compounds from industrial wastewater due its low cost and easy operation (Al-Ghouti and Da'ana, 2020; Guo and Wang, 2019). Adsorption is most commonly performed to remove low concentrations of non-degradable organic compounds from groundwater, drinking water production, process water, or as tertiary treatment, for example after biological water purification (EMIS, 2020).

In summary, adsorption, surface enrichment, refers to the binding of atoms, ions and molecules on the active centers of a solid surface (surface binding).

In most cases, the method does not require unnecessary energy input; the removal rate often depends on the kinetic equilibrium and is determined by the surface characteristics and composition of the adsorbent. The progress of adsorption depends largely on the affinity of the adsorbent, its ability to react with the pollutant and the adsorption mechanism between the sorbent and the functional groups of the pollutant. The end point of the adsorption process is considered to be the concentration value at which equilibrium stability between the solid and liquid phase volumes is reached (Tonk Szende and Rápó Eszter, 2020).

2.5.4. Possible Adsorbents

A wide range of review articles (Afroze and Sen, 2018; Aruna et al., 2021; Bulgariu et al., 2019; Homaeigohar, 2020; Hynes et al., 2020; Kyzas et al., 2018, 2017; Lai et al., 2019; Mashkoor and Nasar, 2021; Mok et al., 2020; Nasar and Mashkoor, 2019; Nayeri and Mousavi, 2020; Pai et al., 2021) discuss the use, classification, effectiveness and properties of different adsorbents as they are some of the key influencing factors of the process. The characteristics through the advantages and limitations of most adsorbents are also reviewed. This is due to the fact that in recent years, researchers have focused their attention on the use of new, alternative, cost-effective, environmentally friendly, green adsorbents to replace the commonly used activated carbon (Zhou et al., 2019). Since adsorption processes are required to have high removal efficiency even at trace levels, it is crucial to investigate and develop new adsorbents with better properties, i.e., low cost and easily accessible. The adsorbents may be collected from agricultural or animal waste, or industrial by-products. All adsorbents, by their intrinsic nature, have functional groups that play the key role in adsorption; therefore, the type of the adsorbent is a key factor in the waste removal process (Chakraborty et al., 2020). Each adsorbent has its own characteristics, such as porosity, pore structure, adsorbent surface area, and structural specificity (Pourhakkak et al., 2021).

A high range of adsorbents have been studied to remediate dye contaminated waters: clays (Brião et al., 2018; Ngulube et al., 2017; Wang et al., 2019), chitosan (Lipatova et al., 2018; Murcia-Salvador et al., 2019), cyclodextrin (Pellicer et al., 2017, 2019; Vahedi et al., 2017), eggshell (Rápó et al., 2018, 2019, 2020a, 2020c), orange peel (Ahmed et al., 2020), fluorene-based covalent triazine framework (Mokhtari et al., 2020), cellulose (Maleš et al., 2020), wool (Khamis et al., 2020), shrimp (Doan et al., 2020), rice bran hydrogel beads (Hong et al., 2021), coccine (Pham et al., 2021), seeds (Alghamdi and El Mannoubi, 2021; Mansouri et al., 2021).

Up until now, different materials have been used for the removal of Cd^{2+}, such as brewery yeast (Tonk et al., 2015), barley husks (Osasona et al., 2018), brewed tea waste (Çelebi et al., 2020), nanocomposites (He et al., 2020; Zhao et al., 2019), eggshell (Tonk et al., 2017; Zadeh et al., 2018), sunflower (Jain et al., 2013), peanut shell (Villar da Gama et al., 2018), sugarcane bagasse (Harripersadth et al., 2020), different clay materials (Cornelia et al., 2009; Es-sahbany et al., 2021; Ghorbel-Abid et al., 2010; Rao and Kashifuddin, 2016; Samad et al., 2020; Zhou et al., 2020), and minerals like montmorillonite, kaolinite, illite, zeolite, diatomite, vermiculite (Y. Zhao et al., 2021).

With the increase in the number of adsorbents used, their classification and sorting has become indispensable. The different types of adsorbents can be classified in several ways; however, the most common ones are listed below (Crini et al., 2019):

- natural materials: sawdust, wood, fuller's earth or bauxite;
- natural materials treated to develop their structures and properties: activated carbons, activated alumina or silica gel;
- manufactured materials: polymeric resins, zeolites or alumino-silicates;
- agricultural solid wastes and industrial by-products: date pits, fly ash or red mud;
- biosorbents: chitosan, fungi or bacterial biomass.

Another classification is based on their origin:

- *Natural adsorbents* include carbon, clays, clays minerals, zeolites and ores. These natural materials are often relatively inexpensive, abundant, plentiful and readily available;
- *Synthetic adsorbents* are adsorbents produced from agricultural products and wastes, household wastes, industrial wastes, sewage sludges and polymer adsorbents.

We can distinguish five main categories of novel adsorbents (Zhou et al., 2019): (i) clay/zeolites and composites; (ii) biosorbents; (iii) agricultural solid wastes; (iv) industrial by-products and their composites; (v) miscellaneous adsorbents. Biosorbents further include chitosan, cyclodextrin, biomass and their composites. Agricultural solid wastes, as adsorbents, include sawdust, bark and other materials like cotton fiber, coffee/tea residues, rice husk, different vegetable and fruit peels and their composites. The industrial by-products include metal hydroxide sludge, fly ash and red mud. Nanomaterials and metal organic frameworks are examples of miscellaneous adsorbents.

Requirements for sorbents (Mok et al., 2020):

- Ability to work under several wastewater parameters;
- Cost effectiveness;
- Removal capability of diverse contaminants;
- High adsorption capacity;
- High selectivity for various concentrations;
- High porosity and specific surface area;
- High durability;
- Reusability of adsorbent, ease of regeneration;
- Fast kinetics; and
- Being present in large quantities.

2.5.5. Eggshell

Eggs represent a major ingredient in a large variety of food products such as cakes, salad dressings and fast foods, the production of which results in several daily tons of eggshell waste

and incur considerable disposal costs in the world (Arabhosseini, 2018). Therefore, eggshell waste is available in huge quantities from the food processing, egg breaking, and hatching industries. About 250,000 tons of eggshell waste is produced annually worldwide by the food processing industry only (Nitin Verma et al., n.d.). Around 40% of egg production originates in the developing countries, with only 20% produced in the developed world. Global egg production in 2010 was around 69 million tons (Gomes and Pasquini, 2018). The problem is that this huge amount of waste is highly hazardous and is hard to get rid of. When disposing it to landfill, eggshell, rich in protein, attracts rats, bugs and bacteria that can infect the soil. The messy holding containers in which eggshell waste is stored can have an unpleasant odor due to the rotting proteins, which can affect the neighborhood, causing air pollution.

Due to their porous structure, eggshells have large specific surface areas; therefore, they are excellent biosorbents (De Angelis et al., 2017; Mashangwa et al., 2017; Rápó et al., 2019, 2018; Tonk et al., 2017). Moreover, its efficiency can be intensified by carcinization when exposed to heat, resulting a completely changed main structure.The eggshell structure is uneven and granulated. One eggshell, which consists of 95–97% calcite ($CaCO_3$) crystals, contains approximately 17,000 pores (Guru and Dash, 2014; Tsai et al., 2006). The complex structure of chicken eggshell contains various organic molecules and mineralized components such as calcite (mainly in palisade and mammillary layers), which are combined in several layers. Instead of the simple $CaCO_3$ crystal layers, the shell consists of very complex mineral formations in a protein matrix. Five different organic and calcite layers build up chicken eggshell. The eggshell thickness is between 280 and 400 µm (Becking, 1975; Dauphin et al., 2006; Hamilton, 1986; Tyler and Geake, 1953) and is composed of the inner and outer membrane (70 µm), mammillary layer (100 µm), palisade layer (200 µm), prismatic layer (8 µm) and thin cuticle (10 µm).

2.5.6. Yeast

Beer is considered the third most consumed liquid after water and tea. With the up to 75 liters of clean water required to make a pint of beer and with an annual production of 1.91 billion hectoliters the beer industry is extremely dependent on one of the most endangered resources on the planet (Conway, 2020; smarter business, 2020). Its by-product is brewer's yeast, which is generated during fermentation processes and remains in large quantities as a waste. Although some of the yeast can be used several times in brewing technology, the rate of dead cells is constantly increasing during re-use, so it is inevitable to remove the entire amount of yeast after a few fermentation cycles.

In biosorption technology these yeast cells can be alternatives. The yeasts have many advantages compared to bacteria and filamentous fungi. Yeasts are a better raw biosorbent material for the

removal of reactive dye due to their unicellular nature and high growth rate (Mahmoud, 2016). According to studies, *Saccharomyces cerevisiae* is the most studied yeast strain as biosorbent (Ulas and Ergun, 2019). It is not only easily cultivated at large scale, it can be obtained from various industries as a by-product, but most of all it is considered safe, therefore it is widely acceptable by the public and can be used in practice. Moreover, it is an ideal model organism which can help in the mechanism identification (Wang and Chen, 2006).

2.5.7. Clay minerals

Clay materials, having a particle size of less than 2 μm, have a high specific surface area. The naturally occurring materials are mainly composed of silica, alumina, and water. Furthermore, the surface of clay minerals can contain many exchangeable cations and anions (Srinivasan, 2011), but in most cases the surface of the clay is negatively charged. The clay surface can contain Ca^{2+}, Mg^{2+}, H^{+}, K^{+}, NH^{4+}, Na^{+}, SO_4^{2-}, Cl^{-}, PO_4^{3-}, and NO^{3-}. According to Rajani Srinivasan, these ions can be easily exchanged with other ions while the mineral structure of clay is not affected (Srinivasan, 2011). This property also contributes to being an excellent adsorbent for removing metal cations from water (Obaje et al., 2013). Compared to other adsorbents, its advantage is that its surface is very porous, resulting in a high attractive force and many active binding sites (Uddin, 2017). Hence, its binding performance is also higher (Churchman et al., 2006; Srinivasan, 2011; Uddin, 2017; Velde, 1995).

Clay minerals can be classified in various ways; however, these four types can also be divided: layer and chain silicates, sesquioxides, and other inorganic minerals. Layered silicates are the primary constituents of soils (Shainberg and Levy, 2005). It consists of a planar octahedral layer, structurally the octahedral layer is attached to a tetrahedral layer both above and below. It is arranged in repeating intervals between the t-o-t layers (Arabmofrad et al., 2020). Typical representatives include kaolinite (1:1 layered silicate) and illite (2:1 layered silicate) (Kumari and Mohan, 2021).

Both kaolinite and illite belong to the group of layered silicates. Layer silicates are the primary constituents of the earth's crust and have good impermeability.

Kaolinite is a 1:1 type of layered silicate, i.e., it contains a tetrahedral layer of silicon and an octahedral layer of aluminum, which are bonded together by oxygen. Hence, the layers have a triclinic symmetry, where a tetrahedral (SiO_4) and an octahedral (AlO_6) sheet alternate (Srinivasan, 2011). It is electrostatically neutral in its properties. It contains hydrogen bonding between the oxygen atoms and hydroxyl ions of the paired layers. The weak hydrogen bonding between the layers can result in frequent random movements. This results in kaolinite minerals of lower

crystallinity as opposed to triclinic kaolinite. Kaolinite, with its ideal structure, is free of charges. Since the kaolinite mineral structure is fixed by hydrogen bonds, in aqueous media the layers do not expand and the shrink-swell capacity is low (Kumari and Mohan, 2021; Miranda-Trevino and Coles, 2003; Uddin, 2017). Due to its highly compacted structure, kaolinite gains are difficult to break down and kaolinite layers cannot be easily separated. the adsorption itself takes place on the surface and edges of the kaolinite, so this is the place, where the impurities, contaminants can be trapped (Miranda-Trevino and Coles, 2003). The literature data suggest a low specific surface area (5–40 m^2/g) compared to other clay minerals. Due to its low isomorphic substitution, kaolinite has a low ion adsorption capacity. Cation exchange capacity at pH 7, 3–15 mEq/100 g (Kumari and Mohan, 2021).

In a study reported by Jorge C. Miranda-Trevino, the kaolinite samples contained some illite and that resulted in the increase in cation exchange capacity to 17.8 mEq/100 g (at pH = 7) (Miranda-Trevino and Coles, 2003). In the meantime, the surface area was measured to be 16.41 m^2/g.

The illite is also a layered silicate, but of the 2:1 type. This means that an octahedral sheet is enclosed by a tetrahedral sheet at the bottom and a tetrahedral sheet at the top (Figure 10). The tetrahedral sheet contains 20% aluminum atoms instead of silicon atoms, which have significant ion (isomorphic) substitution. The adsorption capacity, swelling and shrinkage capacity are lower than montmorillonite and vermiculite, but higher than kaolinite, in which interlayered sheets are present. Illite shows a higher cation exchange capacity than kaolinite, typically 10–40 mEq/100 g (pH = 7), while the specific surface area 10–100 m^2/g (Kumari and Mohan, 2021; Uddin, 2017).

3. MATERIALS AND METHODS

3.1. Studied micropollutants

3.1.1. Indicators and textile dyes used in adsorption

Methylene Blue (MB) and Malachite Green (MG) cationic dyes were purchased from Loch-Ner.s.r.o., Czech Republic and Loba Chemie, Wien-Fischamend, Austria, respectively and were used without any further purification treatment. Anionic indicators Congo Red (CR) and Bromphenol Blue (BPB) were purchased from Merck KGaA, Germanz and Loba Chemie Wien-Fischamend respectively (Figure 8).

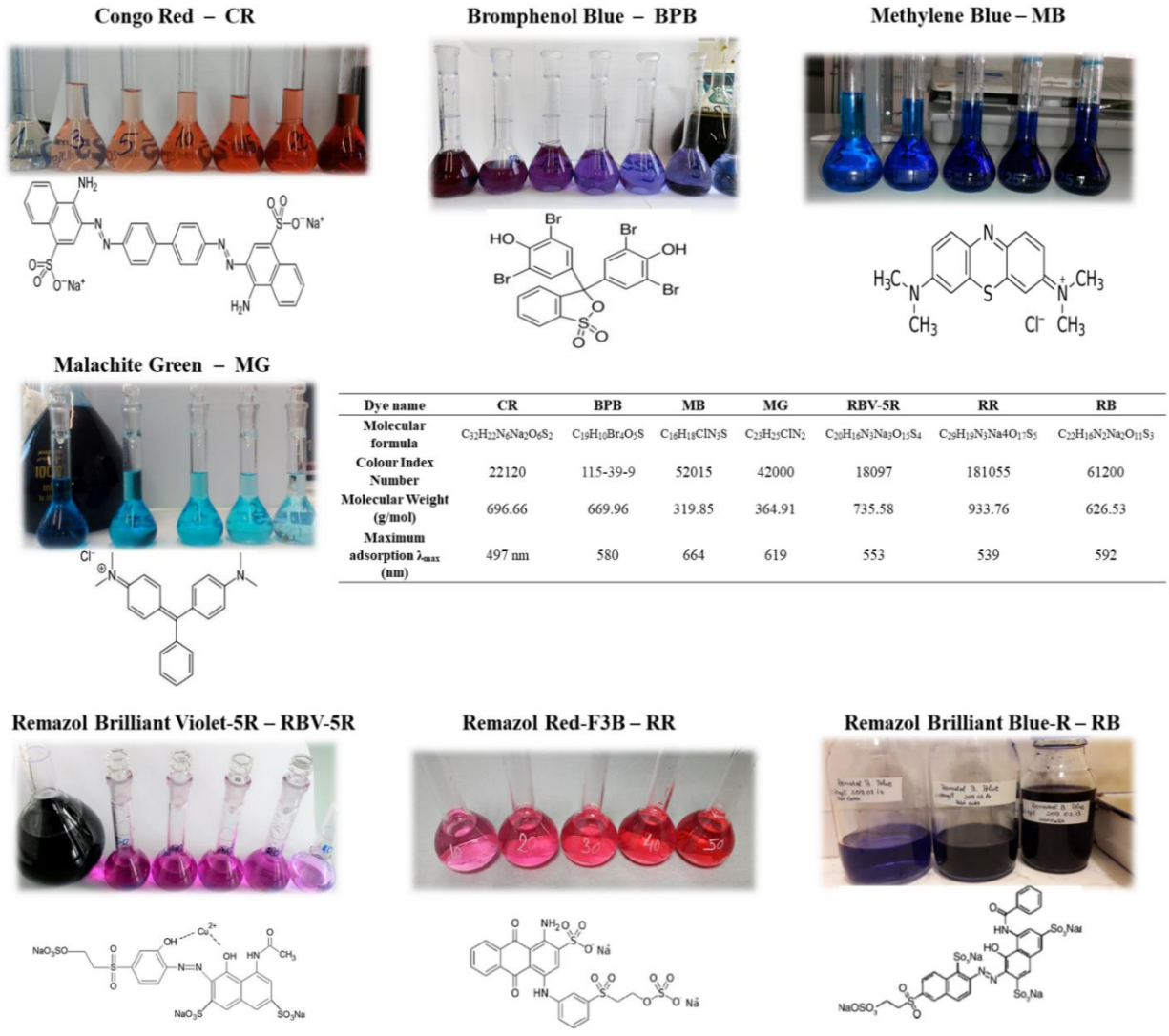

Dye name	CR	BPB	MB	MG	RBV-5R	RR	RB
Molecular formula	$C_{32}H_{22}N_6Na_2O_6S_2$	$C_{19}H_{10}Br_4O_5S$	$C_{16}H_{18}ClN_3S$	$C_{23}H_{25}ClN_2$	$C_{20}H_{16}N_3Na_3O_{15}S_4$	$C_{26}H_{19}N_3Na_4O_{17}S_5$	$C_{22}H_{16}N_2Na_2O_{11}S_3$
Colour Index Number	22120	115-39-9	52015	42000	18097	181055	61200
Molecular Weight (g/mol)	696.66	669.96	319.85	364.91	735.58	933.76	626.53
Maximum adsorption λ_{max} (nm)	497 nm	580	664	619	553	539	592

Figure 8. The characteristics of studied indicator and textile dyes.

Stock solutions of dyes were prepared by dissolving 1 g of each dye in 1 L deionized water. During the adsorption experiments, 1 g/L stock solution was diluted to obtain the needed concentration.

Analytical grade Remazol Brilliant Violet 5R (RBV-5R), Remazol Brilliant Red F3B (RR) and Remazol Brilliant Blue R (RB) textile dyes were bought from DyeStar Singapore Pte. Ltd.,

Singapore and were used without any further purification. A stock solution of 2 g/L was diluted when needed for experiments.

3.1.2. Cd^{2+} metal solution preparation

The synthetic wastewater with different initial concentrations was diluted from 1 g/L stock solutions of the reagent cadmium nitrate tetrahydrate [$Cd(NO_3)_2 * 4H_2O$] of analytical grade.

3.2. Adsorbent preparations

3.2.1. Adsorbent preparation for dye removal

This thesis investigates the adsorbent characteristics, adsorption capacity, dye removal properties and optimization of two wastes, eggshell and brewer's yeast.

Eggshells were collected from kitchen waste. To prevent decomposition and to remove dirt particles, the samples were washed several times with tap water, subsequently with deionized water (MilliQ), and finally dried in a drying cabinet (Memmert UN75 PLUS) at 80°C until mass equilibrium was reached. The samples were kept in an airtight box until later use.

The dried eggshells were used in four forms for different reasons: (1) approximately 0.5 cm diameter eggshell units for the structure study; (2) powdered; (3) calcined and (4) alginate embedded for adsorption study.

(1) To study the chicken eggshell structure before and after dye adsorption, thin sections were made. The eggshells were fixed in plastic cups with superglue on the edges, then cast in a two-component epoxy (Buehler EpoThinTM2) resin, held under vacuum (Buehler Cast N'Vac castable Vacuum System) for 10 min to remove the bubbles generated. The resin was allowed to set for two days, the sample was then cut to shape and polished on 40, 10, 2 μm diamond powders in sequence at 300 rpm using a Buehler Beta Grinder-Polisher instrument. After grinding, the sample surface was polished with 1 μm Al_2O_3 powder, followed by 0.5 μm diamond powder. The specimen was bonded to a slide, which had also been previously polished with standard 500 powder (SiC carbide) in order to increase the adhesive surface area where the adhesive could easily embed. The surface of the glass has lost its perfect smoothness and has become matt (Figure 9).

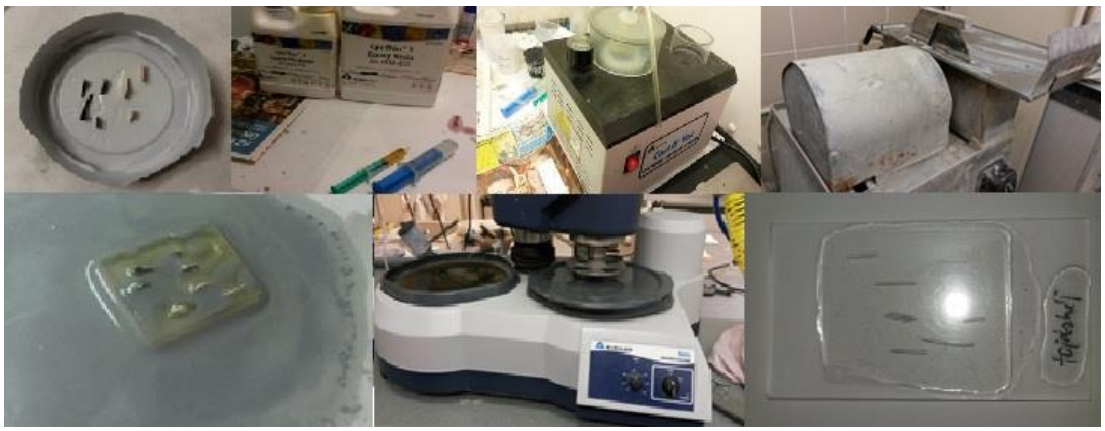

Figure 9. Preparation of eggshell thin section.

(2) The dried eggshells were crushed in a mortar, shredded using Bosch TSM6A013B electric grinder, and then adjusted to different particle sizes (treatment <=160 µm, 160 – 315 µm) using a geological sieve. The eggshell powder was used as an adsorbent without any physical or chemical pre-treatment (Figure 10).

Figure 10. Preparation of eggshell powder.

(3) The 160 µm particle sized powdered eggshell was calcined at 1,000^{o}C for 4 hours with a Nabertherm 30 – 3,000^{o}C oven.

$$CaCO_3 \rightarrow CaO + CO_2$$

(4) In our study, the adsorption capacity of eggshell in immobilized form was also studied by dropping 1.5 g of eggshell in a mixture of 30 mL of deionized water, 1 g of sodium alginate, 2 mL of ET-OH into 200 mL of 0.2 M $CaCl_2$ solution using a hypodermic needle to form small beads (Figure 11).

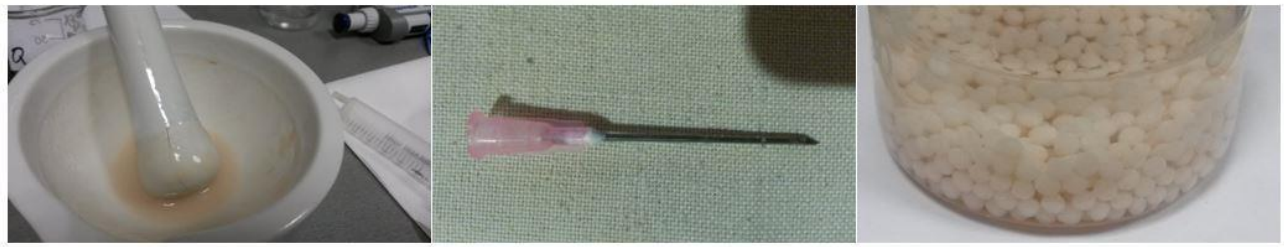

Figure 11. Preparation of alginate embedded eggshell.

Saccharomyces cerevisiae yeast (BY) was supplied from a brewery factory in Romania and was used as a biosorbent after preparation. In the brewing process, after a few fermentation cycles, the brewer's yeast by-product was lyophilised. For lyophilization of yeast in aqueous solution, we used the Telstar Cryodos 50 lyophilization system, which operates at -30°C and $4x10^{-2}$ mbar pressure. The yeast solution was placed in 50 mL centrifuge tubes and frozen at -80°C, and then mounted on the distribution tubes of the lyophilisation system. The lyophilisation was carried out until the samples were completely dry (24 hours).

3.2.2. Details about the Aslavital cosmetic clay adsorbent and experimental design

The sorbent (ACC) used in this research is a particular Aslavital Diatomaceous earth (100% natural diatomaceous clay) manufactured and marketed by the Farmec S.A. It comes from the Pădurea Craiului Mountains, therefore, has a well-defined chemical and mineral composition. Moreover, it is not chemically treated. Deposits of Jurassic fire clays are well known within the Pădurea Craiului Mountains. Their compositions are dominated by kaolinite, with minor amounts of illite and quartz. In the adsorption experiments ACC was used without any physical or chemical alteration.

According to patent 118259/2003 "Composition of a clay-based product and the method of treatment that can be carried out with it", the mineral composition of the clay is 40–60% kaolinite, 22–30% illite, 4–10% quartz, 1–4% limonite. The chemical composition of the clay is 21–33% Al_2O_3, 52–59% SiO_2, 2–3.8%, Fe_2O_3, 0.4–1.3% TiO_2, 0.4–0.8% CaO, 0.1–1% MgO, 1.7–4% K_2O + Na_2O.

Adsorption of Cd^{2+} on Aslavital cosmetic clay (ACC) was carried out by the batch equilibrium method. One gram of adsorbent was added to the 100 mL artificial cadmium wastewater of desired concentration in 250 mL Erlenmeyer flasks. The solutions were stirred on a rotary shaker at 300 rpm until equilibrium was reached. The Cd^{2+} concentration was investigated with the help of flame atomic absorption spectrophotometer. The effect of time on the adsorption of ACC and Cd^{2+} was determined by analyzing the residual metal ion concentration in the liquid after contact periods of 0, 5, 10, 15, 20, 30, 40, 50, 60, 75, 90, 105, 120, 135, 150, 175 and 190 min.

3.3. Influencing parameters

The efficiency of liquid phase adsorption, and therefore the optimal operation of the water treatment process, depends on several parameters. The sorption performance, as illustrated in Figure12, is influenced by physico-chemical factors, the type of pollutant (in this study, the dyes) and its chemical structure, and the properties of the adsorbent used.

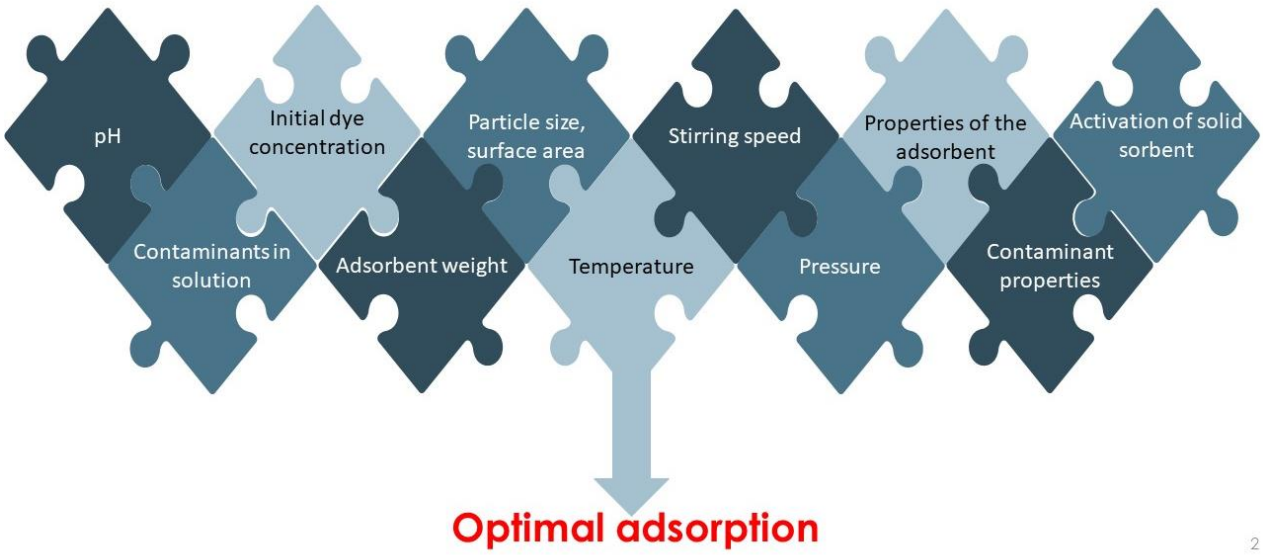

Figure 12. Factors affecting adsorption process.

Such physicochemical parameters are the adsorbent/adsorptive interaction, the surface chemistry and pore structure of the adsorbent, particle size, nature of the adsorbent, presence of other ions in the aqueous solution, pH, temperature, pressure, and contact time. The properties of the adsorbate, its molecular weight, molecular structure, molecular size and polarity should also be taken into account (Razi et al., 2017; Yagub et al., 2014). The effects of all these parameters should be taken into account when designing an adsorption process. Optimization of such conditions will greatly aid the development of industrial-scale dye removal technology. The most studied influencing factors (initial dye concentration, aqueous solution pH, adsorbent volume and particle size, and temperature) will be presented through our results from dye (indicators and textile dyes) and Cd^{2+} adsorption with different adsorbents (eggshell, yeast and ACC) in the results and discussion part. Moreover, our result will be compared with the results of research over the last five years (2017-2021). General trends will be formulated based on the results obtained, considering the effects of the factors.

In water treatment systems, the efficiency of dye removal (E) and the maximum amount of micropollutant bound in equilibrium (q) are the two most important metrics and quantitative parameters to characterize the outcome of the adsorption process (Terangpi and Chakraborty, 2017; Yagub et al., 2014).

$$E(\%) = \frac{C_i - C_f}{C_i} \cdot 100 \quad (1)$$

$$q = \frac{(C_i - C_f) \cdot V}{m} \quad (2)$$

where: E (%)—efficiency; q (mg/g)—amount of dye bound in equilibrium; C_i (mg/L)—initial dye concentration; C_f (mg/L)—final dye concentration; m (g)—amount of adsorbent; and V (L)—volume of aqueous solution.

The adsorption of indicators, textile dyes and Cd^{2+} on different adsorbent's surface was studied in aqueous solutions using 250 mL Erlenmeyer flasks, where 100 mL micropollutant solutions were constantly mixed with VARIOMAG Electronisher MULTIPOINT HP multi-magnetic shaker. To determine adsorption, batch equilibrium technique was used, whereby the suspension of micropollutants and adsorbents was stirred until equilibrium was reached and the concentration of the pollutant was monitored at predetermined intervals. Samples taken at each time interval were placed in eppendorf centrifuge tubes and centrifuged at 10,000 rotation/minute for 5 min (Hettick Zentrifugen Mikro 20). The supernatant was placed in a cuvette using an eppendorf micropipette and the concentration of the solution was determined by spectrophotometry. In each case, three parallel experiments were executed, and results are the means and standard deviations of a total 9 measurements.

3.3.1. The effect of initial micropollutant concentration

The initial micropollutant (indicators, textile dyes and Cd^{2+}) concentration is perhaps one of the most important factors that influences the adsorption process. It indirectly affects the efficiency of pollutant removal by reducing or increasing the availability of binding sites on the adsorbent surface.

In order to investigate the effect of concentration on adsorption the following experimental designs were build in the different published studies:

- 100 mL of **CR** (pH = 8.05), **BPB** (pH = 2.7), **MB** (pH = 3.95), **MG** (pH = 2.76) solutions were mixed at 700 rpm, 20 ^{o}C, with 3 g of **powdered eggshell** at different initial concentrations between 10-50 mg/L;
- 100 mL **RBV-5R** solutions at C_i = 20–100 mg/L were mixed with 1 **g powdered eggshell**. The constant parameters are as follows: particle size of 160 µm, room temperature of 20 °C, 700 rpm agitation speed, and initial pH of 6;
- adsorption with **calcined eggshell** (160 µm particle size) was studied using constantly rotating (700 rpm) 1.5 g calcined eggshell in a 100 mL aqueous solution of **RBV-5R** azo-dye between 20-100 mg/L concentrations at 20 ^{o}C without pH adjustment (pH=6);

- 1.5 g **calcined eggshell** (160 µm particle size) was added to C_i = 20-100 mg/L **RR, RB** pH = 7, T = 20±0.5 ºC, 700 rpm;
- The effect of initial **RR** dye concentration and contact time was studied at 5-1,000 mg/L concentrations. Constant experimental parameters: 1.5/100 g/mL **yeast**, 20 ºC, 700 rpm agitation speed, pH: 6;
- The effect of initial **Cd^{2+}** concentration was tested by varying the Cd^{2+} concentration in the range of 10-160 mg/L, 0.1 g/L ACC using a magnetic stirrer at room temperature (T = 20 °C) and fixed pH of 7.

3.3.2. The effect of solution pH

According to several papers, the key parameter in almost all adsorption processes is the pH of the dye solution. This factor affects the capacity of the adsorbent and the efficiency of the process.

In each case 1M HCl and NaOH was used as pH adjuster Hanna HI4521 pH/mV/ISE/temperature Bench Meter with dual channel electrode. Firstly, the dye solutions were prepared, then the Berzelius flask containing the solution was put on a magnetic stirrer, and the wished pH was adjusted. The experimental designs for the study of solution pH as influencing factor are:

- CR, BRP, MB, MG + powdered eggshell: pH = 2-10, C_i = 30 mg/L, 3 g of 160 µm particle sized biomass, 750 rpm, T = 20±2 ºC;
- RBV-5R + powdered eggshell: pH = 2-11, C_i = 20 mg/L, 1.5 g of 160 µm, 750 rpm, T = 20±2 ºC;
- RBV-5R + calcined eggshell: pH = 2-11, C_i = 20 mg/L, 1.5 g of 160 µm, 750 rpm, T = 20±2 ºC;
- RR, RV + calcined eggshell: pH = 3-9, C_i = 20 mg/L, 1.5 g of 160 µm, 700 rpm, T = 20±2 ºC;
- RR + yeast: pH = 3-11, C_i = 20 mg/L, 1.5 g of 160 µm, 700 rpm, T = 20±2 ºC.

3.3.3. The effect of adsorbent dosage

The amount of adsorbent is an important parameter that influences the adsorption process, through the quantitative ratio of adsorbent to adsorbent. Since the adsorbent determines the adsorbent capacity for a given initial concentration, the dosage of the adsorbent is an important parameter (Şentürk and Alzein, 2020).

The effect of adsorbent dosage was investigated for textile dyes RBV-5R (both for powdered and calcined eggshell), RR (calcined eggshell and brewery's yeast) and RB (calcined eggshell):

- RBV-5R + powdered eggshell: m = 0.5-1.5 g of 160 µm, C_i = 20 mg/L, 750 rpm, T = 20±2 ºC;
- RBV-5R + calcined eggshell: m = 0.5-2 g of 160 µm, C_i = 20 mg/L, 750 rpm, T = 20±2 ºC;

- RR, RV + calcined eggshell: m = 0.5-2 g of 160 µm, C_i = 20 mg/L, 700 rpm, T = 20±2 ºC;
- RR + yeast: m = 0.5-2.5 g, C_i = 20 mg/L, 700 rpm, T = 20±2 ºC.

3.3.4. The effect of adsorbent particle size

Although not regularly investigated in biosorption studies, particle size can be an important factor in heterogeneous chemical reactions and adsorption (Stjepanović et al., 2021). The small particle sizes result in a higher specific surface area. Specific surface area (SSA), defined as the total surface area of a solid material per unit of mass, is an important feature for sorption processes. SSA is dependent on the size of the particles, as well as on the structure and porosity of the material (Šljivić-Ivanović and Smičiklas, 2020). The most common unit of measurement is m^2/g.

The relationship of adsorption capacity to particle size depends on two criteria (Aljeboree et al., 2017; Iqbal et al., 2011):

- the chemical structure of the dye molecule (its ionic charge) and its chemistry (its ability to form hydrolyzed species); and
- the intrinsic characteristic of the adsorbent (its crystallinity, porosity and rigidity of the polymeric chains).

To study the effect of the particle size of eggshells, 100 mL RBV-5R dye solution (20 mg/L concentration) was prepared. Then, 1.5 g eggshell with different particle sizes (<=160 µm, 160-315 µm, unsorted particle size range) was added to the solution and agitated at constant agitation speed (700 rpm) without temperature or pH adjustment.

3.3.5. The effect of adsorption shaking speed

In a batch process, the mixing speed of the aqueous suspension may affect the time required to remove the contaminant.

The effect of mixing speed was studied for the removal of RBV-5R dye with powdered eggshell at 350 and 700 rpm. Constant parameters were: C_i=20 mg/l, 1,5 g adsorbent, 160 µm, pH=6,0±0,2, T=20±1 ºC.

3.3.6. The effect of solution temperature

The effect of temperature is also a significant physico-chemical factor as it affects the treatment process by shifting the nature of the reaction from endothermic to exothermic, or vice versa (Peck Kah Yeow et al., 2020). Moreover, it has a strong effect on the adsorption as it can increase or decrease the amount of adsorption (Badawy et al., 2020).

In the present work, the influence of temperature is presented trough the results of RBV-5R textile dye adsorption both with powdered and calcined eggshells, moreover, with RR textile dye removal

with brewery's yeast. Experiments were carried out with the help of IKA C-MAG HS7 magnetic shaker. The effect of temperature (20, 30, 40 °C) on adsorption was investigated, where the 1.5 g adsorbents (160 µm particle sized powdered or calcined eggshell, yeast) was stirred constantly at 700 rpm and the samples contained 100 mL 20 mg/L RBV-5R or 5 mg/L RR dye solutions.

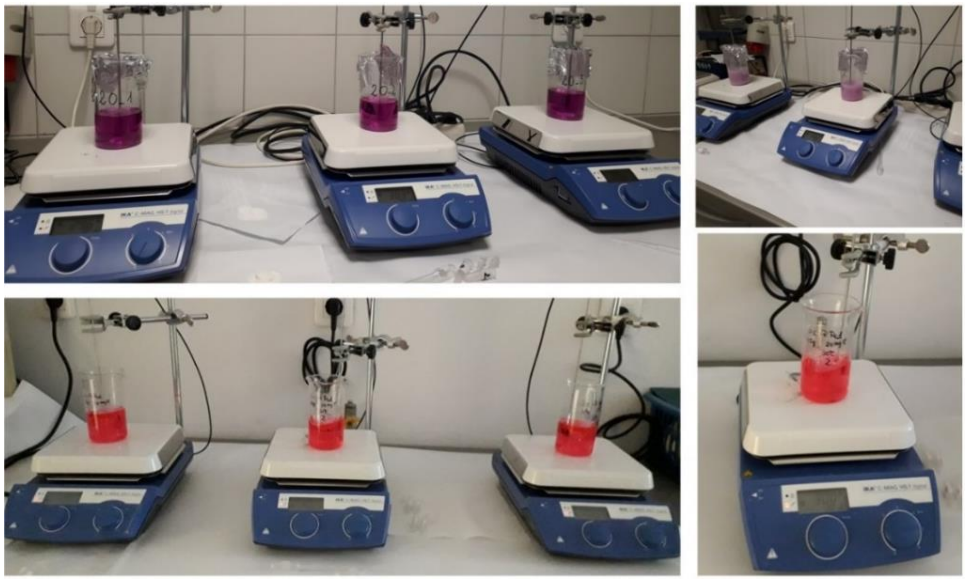

Figure 13. The study of temperature dependence.

3.4. Analytical measurements

A wide range of analytical techniques are used to study the biosorption process, to characterize the contaminants and adsorbents, and to study the adsorption mechanism between the adsorbent and the micropollutant. Figure 14 represents all the techniques used in this thesis.

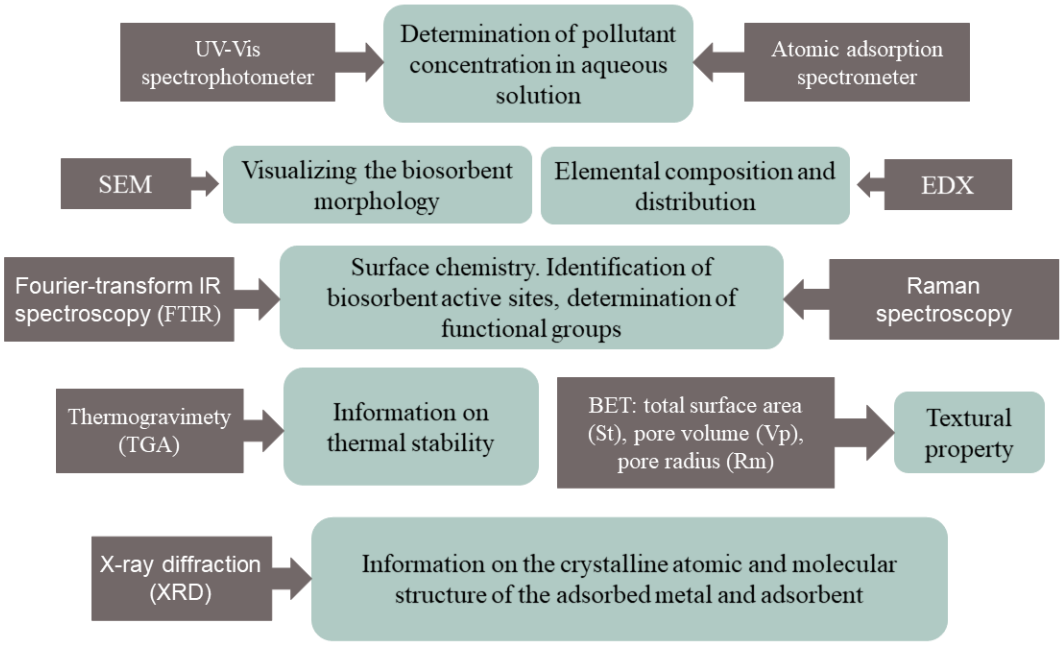

Figure 14. Instrumental tools used in the adsorption process (Adapted from (Fomina and Gadd, 2014).

3.4.1. Concentration determination

Agilent Cary 60 UV-Vis spectrophotometer was used to periodically measure dye concentrations:

- λ_{max} = 497, 580, 664, 619 nm, respectively for CR, BPB, MB, MG indicators,
- λ_{max} = 553, 539, 592 nm, respectively for RBV-5R, RR and RB textile dyes.

The concentrations were calculated by using calibration curve quantitative measuring technique. Results listed below are the means and standard deviations from 9 different measurements.

The Cd^{2+} concentration was investigated with the help of flame atomic absorption spectrophotometer. For this measurement we used SensAA Dual GBS Scientific Equipment, Australia. The unknown solution's Cd^{2+} ion concentration was determined by calibration with a standard cadmium solution in the concentration range 0 – 2.5 mg/L, λ = 228.8 nm.

Figure 15. The used UV-Vis and flame atomic absorption spectrophotometer.

3.4.2. Morphology and elemental composition

The structure of the thin sectioned eggshell was studied using stereomicroscope (Nikon SMZ1000 and Nikon D5000), polarization microscope (Nikon Eclipse LV100 POL), scanning electron microscope – SEM (FEI Quanta 3D), and EDS (Hitachi TM4000 Plus SEM equipped with Quantax 75 SDD EDS system) measurements were also performed on each layer.

Scanning electron microscopy (SEM) is one of the most important tools for analyzing the surface and morphology of adsorbents. The primary advantage of the SEM is the high resolution that can be achieved during the examination, making it an important instrument for materials analysis. SEM provides magnified images of the size, shape, composition, and other physical and chemical properties of the sample (10.1515/geo-2020-0145). Therefore, SEM images of eggshell (thin section, powdered, calcined), ACC clay and brewery's yeast was made before and after adsorption together with EDS analyses.

The SEM images were performed using 15 kV high voltage and 18 - 150 pA beam current under low vacuum chamber pressure (80-100 Pa water steam environment). Spot EDS measurements were carried out using 20 kV high voltage and 4 nA beam current.

In order to visualize the distribution of different elements within eggshell profiles (Ca, Mg, S, P) EDS elemental maps were carried out using 15 kV high voltage and 2.4 nA beam current. Analyzes were taken in the Research and Instrument Core Facility of the Faculty of Science, Eötvös Loránd University, Budapest.

Figure 16. Instruments used for morphology study.

The powdered and calcined eggshell, ACC and yeast surface was studied by scanning electron microscopy (JEOL (USA) JSM 5510 LV SEM) at various magnifications before and after adsorption. During the tests, eggshell particle sizes of 160 μm (control, 2 g/L indicator and textile dye solution); moreover, ACC (control and 2 g/L Cd^{2+} adsorbed ACC) were used. In case of the yeast, 3 g of yeast was kept in 2 g/L RR dye solution for 24 hours. To improve the quality of the images and to increase the electrical conductivity of the surface, the surface of the samples was covered with a thin layer (10nm) of 1.33×10^{-6} mBar vacuum.

Scanning Jeol JEM 5510 JV and Oxford Instruments EDS Analysis System Inca 300 (UK) were used to examine the elemental composition of the adsorbents on the control and the dye/Cd^{2+} adsorbed samples (2 g/L micropollutant). Elemental distribution was studied, and enrichment factors were calculated. The value obtained gives the percentage of elements in the „contaminated" sample relative to the control sample.

$$\delta = \frac{R_{sample} - R_{control}}{R_{control}} \cdot 100 \qquad (3)$$

Where: δ- enrichment factor, R_{sample}- the EDS results for adsorbent in the 2 g/L solution, $R_{control}$- the amount of elements in the control adsorbent obtained during EDS measurement.

3.4.3. Determination of functional groups, surface chemistry

Raman microspectroscopic measurements were carried out at the Research and Instrument Core Facility of the Faculty of Science, Eötvös Loránd University, Budapest. To study the eggshell powder (dye treated and control) and dye powder, we used a confocal HORIBA Labram HR (high-resolution) spectrometer with Nd:YAG laser (λ=532 nm) excitation and 1,800 grooves/mm optical grating. The laser power was 130 mW, and the laser spot diameter was ~1.5 μm (Berkesi et al., 2017).

Fourier transform infrared spectroscopy data were obtained using a JASCO 615 FTIR spectrophotometer in the wavelength range of 500–4,000 cm^{-1}, and the observed bands were analyzed by using ORIGIN PRO 8.5 software. These studies were carried out at National Institute for Research and Development of Isotopic and Molecular Technologies, INCDTIM Cluj-Napoca, Romania.

3.4.4. Thermal stability and textural property

For the characterization of powdered, calcined eggshell, thermal analysis was carried out using a DTA-TG differential heat analyzer, Model: STA 449 F5 Jupiter, Manufacturer: Netzsch GmbH, Germany, with graphite furnace, with a possibility of analysis of up to 1,600 °C. The heat treatment temperature of the samples was 1,200 °C at a heating rate of 10 K/min under a nitrogen atmosphere.

Total surface area (St), pore volume (Vp) and pore radius (Rm) of eggshell were obtained from N_2 adsorption–desorption isotherms (measured at -196 °C) using the BET model for St determination and the Dollimore–Heal method for Vp and Rm.

The isotherms were recorded using a Sorptomatic 1990 apparatus (Thermo Electron Corporation). Prior to determination, the samples were degassed at 150 °C under vacuum (approximately 1 Pa) for 3 hours to remove the physically adsorbed impurities from the surface. No pressure variation was observed during 1 hour at the end of sample degassing (N. Tangboriboon et al., 2012; Ramesh et al., 2018; Wang and Jehng, 2011). The eggshell density was determined with ethanol using a pycnometer (Nagy et al., 2013a).

3.4.5. Crystalline structure

The X-ray powder diffraction (XRD) patterns of ACC were obtained with a Bruker D8 Advance diffractometer using CuKα1 monochromatic radiation (λ = 1.5405980Å) obtained with

a germanium (1:1:1) monochromator. The diffractometer is equipped with a LINXEYE detector and X-ray tube operates at 40 kV and 40 mA. DIFFRAC plus XRD Commander Program was used for data acquisition employing a scan rate of 0.05°/s in the angular domain 2θ = 5–85°.

3.5. Mathematical models

3.5.1. Adsorption isotherms

In biosorption studies, the rate of adsorption can be greatly influenced by the ratio of adsorbate to adsorbent. According to the Kroeker correlation described in the literature, the amount of material adsorbed per species increases with decreasing amount (mass) of adsorbent in aqueous solution of a given volume and concentration. It is calculated from the equilibrium value of the adsorption process at constant temperature in isotherm models. The isotherm model expresses the amount of adsorbed substance as a function of the concentration of the solution.

The four, most widely used (Langmuir, Freundlich, Temkin, Dubinin-Radushkevich) two-parameter isotherm models in linear form were used in all of the six articles that this thesis is built on. Figure 17 contains the linear forms of these isotherm models, their graphical representation and the method their specific parameters were calculated.

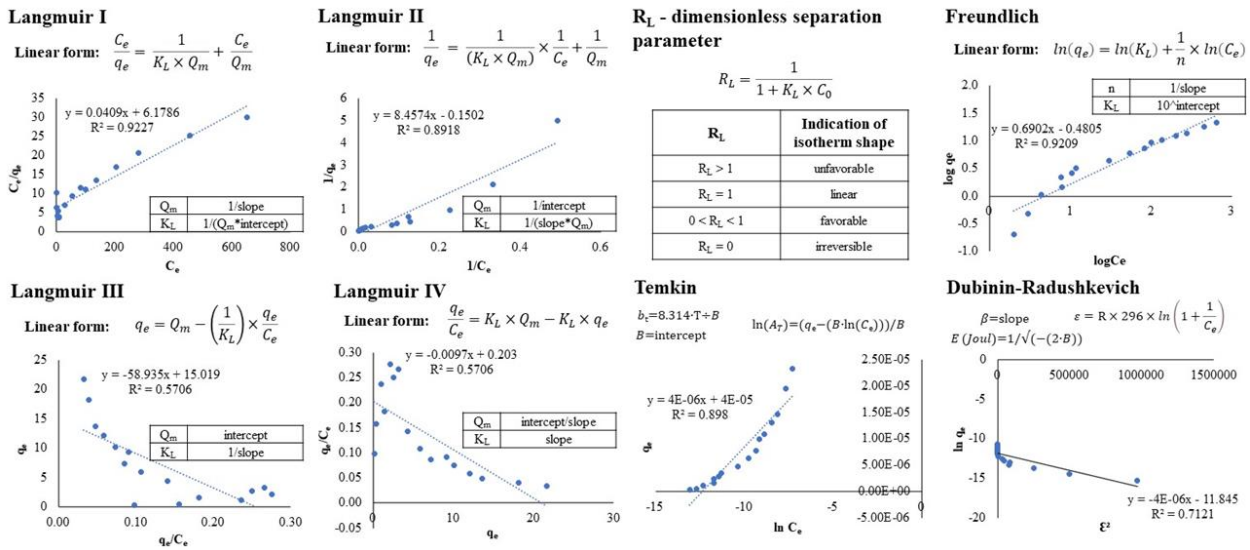

Figure 17. Linear forms of isotherm models and the calculation of their parameters.

Statistical biases can arise when the isothermal equations are linearized, as the linear fit depends on the method chosen, the data available and the errors of the experiment performed. During the evaluation of experimental data, the linear transformation changes the distribution of the error (either in the positive or negative direction). Data overestimation, data clumping or overweighing can occur during the transformation if the system is sensitive to extreme (too high

or too low) experimental values. Often, regardless of the resulting high linear regression coefficient (R^2) values, the model is not representative of the adsorption experimental behavior (González-López et al., 2021; López-Luna et al., 2019). To avoid these limitations, the development of computer programs has made modelling and error analysis possible. Non-linear regression analyses of the two-parameter Langmuir, Freundlich and Temkin as well as the three-parameter Toth (Tóth, 1981), Khan (Khan et al., 1997), Liu (Liu et al., 2003), Redlich-Peterson (Redlich and Peterson, 1959) and Radke-Prausnitz (Radke and Prausnitz, 1972) isotherm models were analyzed using OriginPro 8.5 software. In order to further explore the feasibility of (RR + yeast) adsorption, beside the four (Langmuir, Freundlich, Temkin, Dubinin-Radushkevich) linear, two-parameter isotherm models, the non-linear versions of the Langmuir, Freundlich, Temkin, Dubinin-Radushkevich two-parameter and Liu, Toth, Kahn, Sips, Redlich-Peterson and Radke-Prausnitz three-parameter isotherm models were investigated. The models were calculated for adsorption experiments where 1.5 g/100 mL yeast was constantly stirred (700 rpm) in batch mode with 5–1,000 mg/L RR dye for 330 minutes, pH = 6, T = 20±1 °C.

In case of Cd^{2+} and clay adsorption the non-linear versions of the Langmuir, Freundlich, Temkin two-parameter and Liu, Toth and Kahn three-parameter isotherm models were studied.

The performance of these model predictions and the robustness of the results obtained were validated using statistical measures (the linear regression coefficient (R^2), chi-square error (χ^2), root mean square error (RMSE), and hybrid fractional error (HYBRID)). The equations (Figure 18) for these error analyses are given below (Ayawei et al., 2017; Hossain et al., 2013; Suwannahong et al., 2021).

$$R^2 = 1 - \frac{\sum_{n=1}^{n}(q_{e,exp.} - q_{e,calc.})^2}{\sum_{n=1}^{n}(q_{e,exp.} - \overline{q_{e,calc.}})^2} \qquad \chi^2 = \sum_{i=1}^{n}\frac{(q_{e,calc.} - q_{e,exp.})^2}{q_{e,exp.}}$$

$$RMSE = \sqrt{\frac{\sum_{n=1}^{n}(q_{e,exp.} - q_{e,calc.})^2}{n - p}} \qquad HYBRID = \frac{100}{n - p} \times \sum_{i=1}^{n}\left(\frac{q_{e,exp.} - q_{e,calc.}}{q_{e,exp.}}\right)$$

Figure 18. Equations of statistical measures, where n—the number of experiments performed; $q_{e,exp.}$ (mg/g)—the value of the maximum amount of substance bound in the equilibrium obtained in practice; $q_{e,calc.}$ (mg/g)—the calculated value of quantity equilibrium; $q_{e,calc.}$ (mg/g)—average of the calculated quantity equilibrium; p (polynomial model)—the number of parameters included in the isotherm models tested.

Figure 19 contains the linear and non-linear equations of these isotherm models together with the theories, assumptions and boundaries of these models.

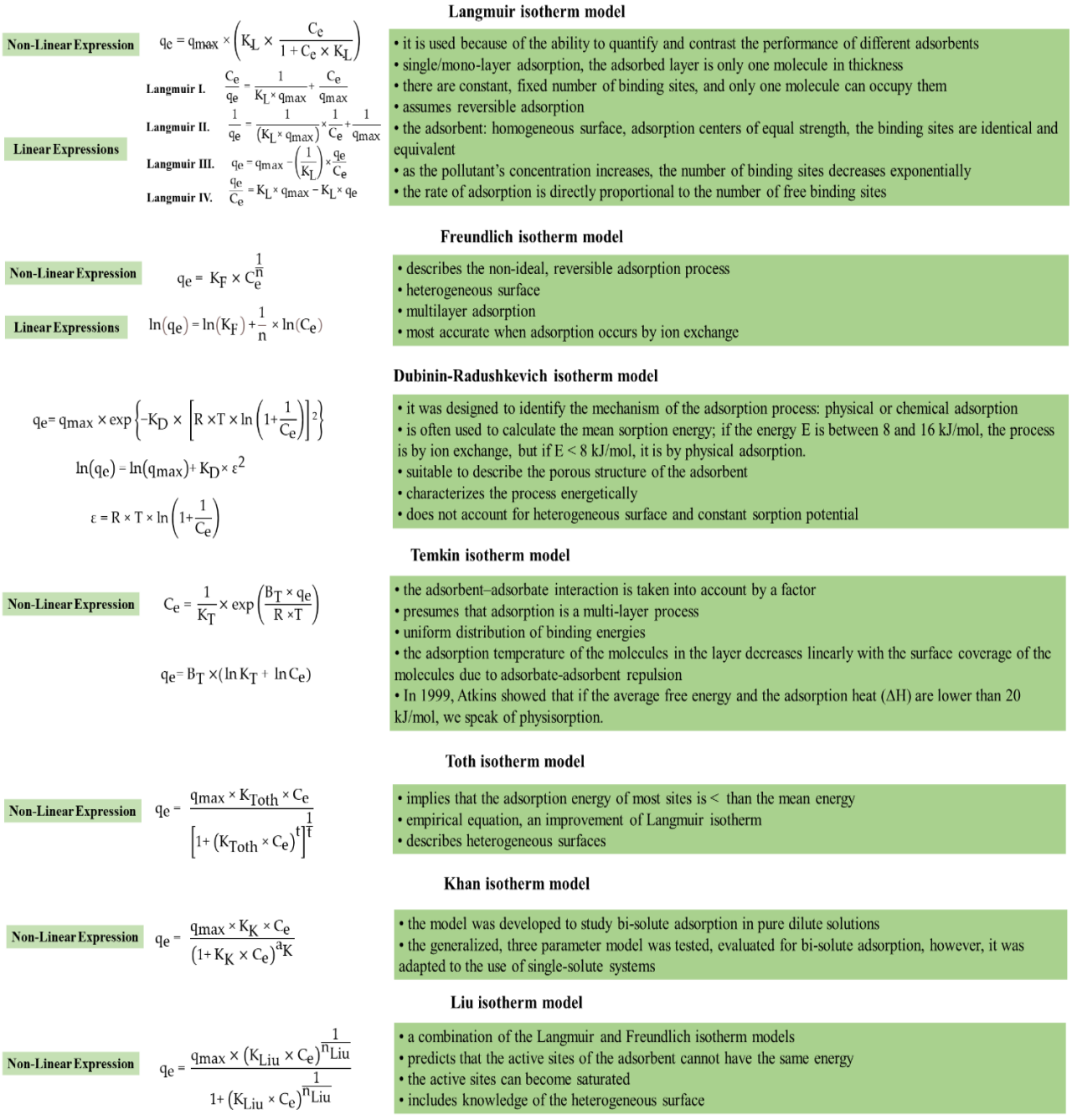

Figure 19. Equations, theories, assumptions, and boundaries of adsorption isotherm models, where q_e—the concentration of solid phase adsorbent at equilibrium (mg/g); q_{max}—single layer maximum adsorption or saturation capacity (mg/g); C_e—concentration of the contaminant solution at equilibrium (mg/L); b—adsorption equilibrium constant specific to the test substance; $K_{L,F,D,T,Toth,Liu,Khan}$—are the concentration-dependent partition coefficients for the respective isotherms providing information on the adsorption capacity of the biosorbent; n—Freundlich and Liu constants, adsorption intensity; A_T—Temkin's isotherm equilibrium constant (L/g); b_T—Temkin constant; B—constant (J/mol); R—ideal gas constant (8.314 mol/K); T—absolute temperature (K); ε—Dubinin–Radushkevich constant (mol^2/J^2); t—Liu constant; a_K—Khan constant (Foo and Hameed, 2010; Khan et al., 1997; Wang and Guo, 2020).

3.5.2. Adsorption kinetic and diffusion models

Kinetic models have been studied to describe the mechanism of the biosorption process. In particular, we used the pseudo-first- and second-order kinetic models, which are very frequently reported in the literature. In practice, we compare the linear regression coefficients of each kinetic model in order to find the best fitting model. The reaction rate describes the kinetics of chemical reactions; it is closely related to the time variation of the concentration of a given adsorbate. The model can be used to calculate the rate constant (k) of the process and the theoretical value of the maximum amount of solute bound at equilibrium (q_e). In many cases, the pseudo-superscript (Lagergren) equation cannot be used for the whole experimental time because it describes the initial period of the sorption process more accurately. Similarly, the pseudo-second-order model (Ho and McKay) is applied to the solid biosorption of the solid phase, but this is based on the total accurately characterizes adsorption over the full-time interval (Ho and McKay, 1999; Kőnigné Péter, 2012; Lagergren S., 1898). The equations describing the kinetic and diffusion models are given in Table 1.

Table 1. Summary of kinetic and diffusion model equations.

Kinetic/Diffusion Models	**Equations Describing the Models Non-Linear Form**	**Parameters**
Pseudo I-order kinetic model	$\frac{dq_t}{dt} = k_1(q_e - q_t)$	• q_t—amount of Cd adsorbed during a given time interval (mg/g) • q_e—equilibrium pollutant adsorption value (mg/g) • k_1—equilibrium constant, first order adsorption rate constant (g/mg/min) • k_2—equilibrium constant, constant of the second order adsorption rate (g/mg/min)
Pseudo II-order kinetic model	$\frac{dq_t}{dt} = k_2(q_e - q_t)^2$	
Linear forms		
Pseudo II. Type I.	**Pseudo II. Type II.**	**Pseudo II. Type III.**
$\frac{t}{q_t} = \frac{1}{k_{2,I} \times q_e^2} + \frac{1}{q_e} \times t$	$\frac{1}{t} = k_{2,II} \times q_e^2 \times \left(\frac{1}{q_t}\right) - k_{2,II} \times \frac{1}{q_e}$	$\frac{1}{q_t} = \left(\frac{1}{k_{2,III} \times q_e^2}\right) \times \frac{1}{t} + \frac{1}{q_e}$
Pseudo II. Type IV.	**Pseudo II. Type V.**	**Pseudo II. Type VI.**
$\frac{1}{q_e - q_t} = \frac{1}{q_e} + k_{2,IV} \times t$	$\frac{q_t}{t} = -k_{2;V} \times q_e \times q_t + k_{2;V} \times q_e^2$	$q_t = q_e - \left(\frac{1}{k_{2,VI} \times q_e}\right) \times \frac{q_t}{t}$
Equation describing diffusion	$q_t = x_i + K\sqrt{t}$	• K—rate constant • x_i—boundary layer thickness • q_t—amount of Cd adsorbed on the ACC at time t

Diffusion is the mixing of one substance with another, by heat or by some driving force, it is an important concept in both chemistry and physics. Possible driving forces can be the concentration and the tension difference. In effect, the random thermal movement of particles of matter by thermal heat. In addition to the kinetic models, the mechanism of adsorption can be also described by diffusion, which is determined by the adsorption phenomena. Four steps are distinguished

during adsorption on the surface of a porous adsorbent, which describe the transport process (Figure 20):

1. bulk transport, the transport in the solution phase, a fast process;
2. film diffusion, a slow stage where the contaminant molecules (in our case dyes and Cd2+) are transported to the outer surface of the adsorbent (eggshell, yeast, ACC) through a hydrodynamic boundary layer or film layer;
3. intra-particle diffusion, also a slow process whereby contaminant molecules diffuse into the pores of the adsorbent, along the surface of the pore wall, or both;
4. adsorption bond formation (physical or chemical), also a rapid process (Tran et al., 2017).

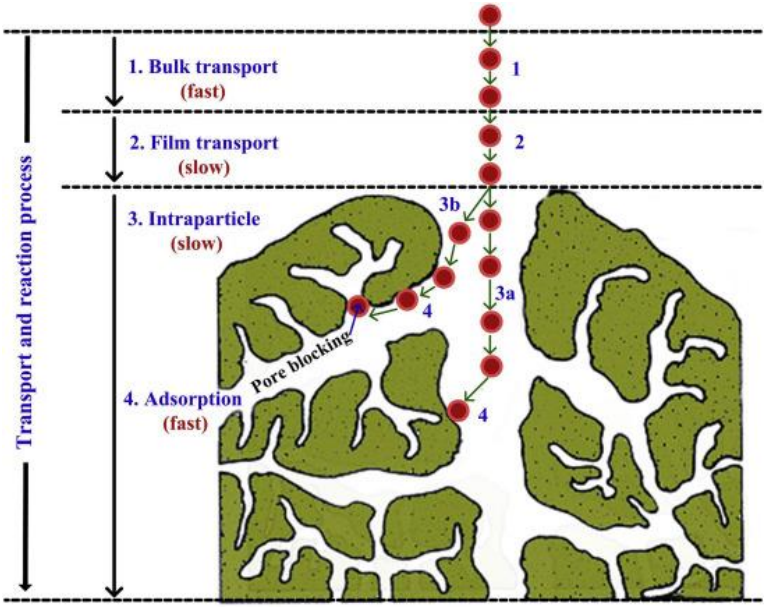

Figure 20. Transport processes during adsorption by a porous adsorbent (Tran et al., 2017).

3.5.3. Artificial neural network (ANN)

An artificial neural network (ANN) is a statistical modelling method (functioning as a black box) that helps to understand the behaviour of a system by knowing input data and predicting output results. Six input parameters (i.e., initial concentration, biomass weight, particle size, pH, temperature, contact time) were given to the EasyNN software program package, thereby resulting in a 6:7:1 network structure (Hassani et al., 2014; Indolean et al., 2017; Török, 2015).

4. RESULTS AND DISCUSSION

4.1. The influence of initial parameter changes in dye adsorption

4.1.1. The effect of initial micropollutant concentration

The effect of initial dye concentration relies on the immediate relation between the dye concentration and the available binding sites on the adsorbent surface (Ta Wee Seow and Chi Kim Lim, 2016). Initial concentration provides an important driving force to overcome all mass transfer resistances of the dye between the aqueous and solid phases, therefore higher concentration can increase the adsorption (Aksu and Dönmez, 2003).

During our research the effect of CR, BPB anionic and MB, MG cationic indicators uptake by chicken eggshell household waste was examined using different initial dye concentrations between 10-50 mg/L. Figure 21a-d. shows the efficiency and quantity in equilibrium of various dyes at different initial concentration, where 3 g eggshell powder of 160 µm particle size was constantly shaken at 750rpm with 100 mL solution at room temperature (T=20±2 ºC) without pH adjustment (pH_{CR}=8.05, pH_{BPB}=2.7, pH_{MB}=3.95, pH_{MG}=2.76). With the increase of initial dye concentration in case of CR, MB and MG, the adsorption capacity also increased, whereas in case of BPB there was no such trend.

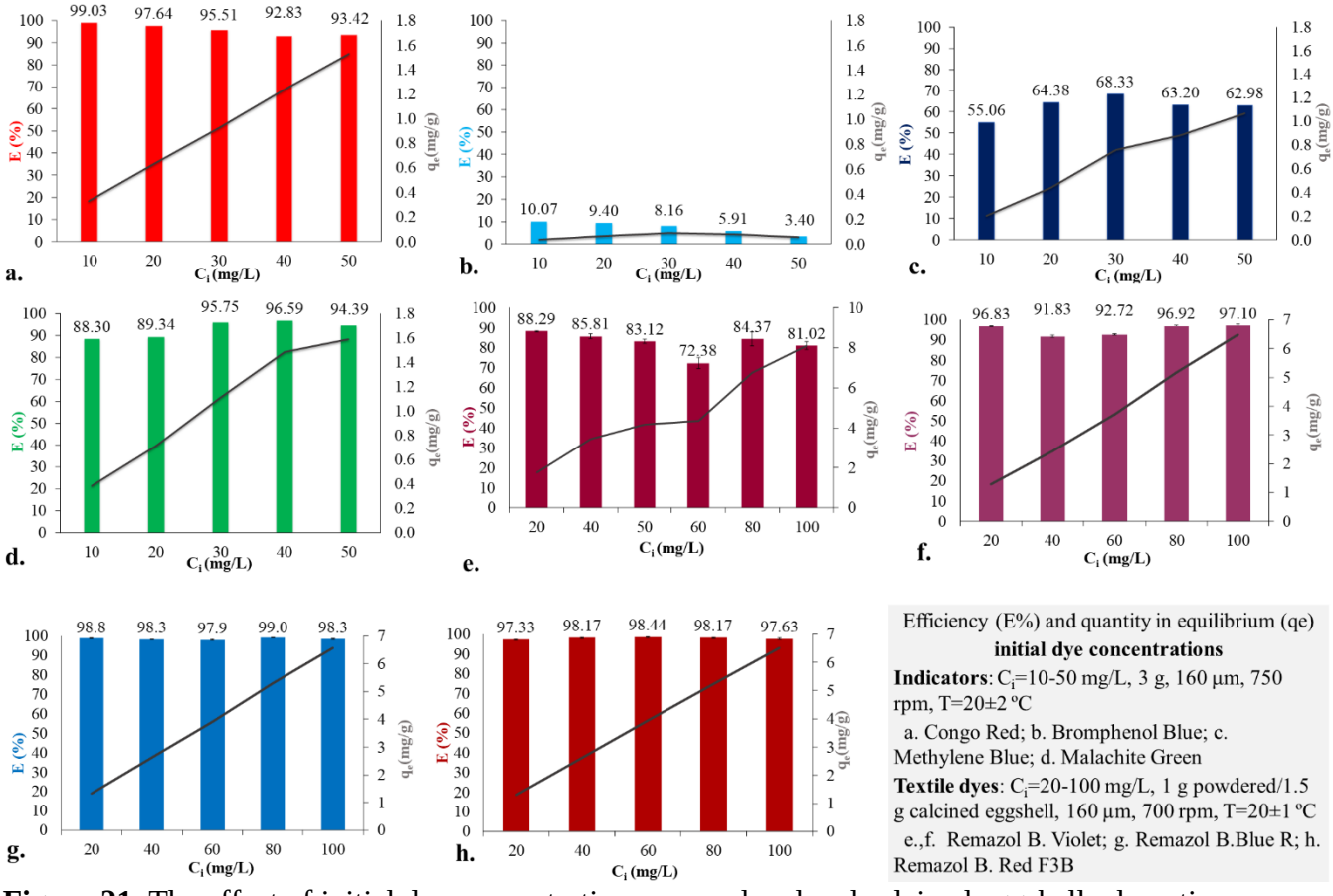

Efficiency (E%) and quantity in equilibrium (qe)
initial dye concentrations

Indicators: C_i=10-50 mg/L, 3 g, 160 µm, 750 rpm, T=20±2 ºC

a. Congo Red; b. Bromphenol Blue; c. Methylene Blue; d. Malachite Green

Textile dyes: C_i=20-100 mg/L, 1 g powdered/1.5 g calcined eggshell, 160 µm, 700 rpm, T=20±1 ºC

e.,f. Remazol B. Violet; g. Remazol B.Blue R; h. Remazol B. Red F3B

Figure 21. The effect of initial dye concentration on powdered and calcined eggshell adsorption.

The effect of the initial dye concentration on the uptake of RBV-5R dye by our eggshell waste was studied using dye concentrations ranging between 20 and 100 mg/L. With increasing initial concentration, the adsorption capacity also increased, whereas the efficiency decreased (Figure 20e.).

Five different studies (C_i = 20-100 mg/L) were made for the adsorption process of RBV-5R removal with calcined eggshell at a constant 700 rpm at room temperature, 1.5 g of biomass (1,000 °C calcined eggshell) without adjusting the pH of the aqueous medium. The equilibrium values obtained at the end of the adsorption were used to calculate the efficiency of the biosorption and the maximum amount of material in equilibrium. Figure 20f. graphically illustrates the calculated values. Here we can observe that the efficiency achieved is in all cases greater than 90%. Compared to our previous study (untreated eggshell adsorption), no clear trend was observed regarding the increase in concentration. But for subsequent comparison, studies were performed on the 20 mg/L solution.

In order to study the effect of RR and RB dye concentration on calcined eggshell surface, experiments were carried out using a fixed amount of adsorbent (1.5 g), a stirring rate of 700 rpm without pH adjustment, but varying the initial dye concentration between 20-100 mg/L, as shown in Figure 21g-h. All values are the means and standard errors of nine parallel results. Both for RR and RB we achieved an efficiency that was higher than 97%, regardless of dye concentration. However, adsorption equilibrium was reached in 90 minutes. A similar trend was observed in the case of Remazol Brilliant Violet-5R dye, under same initial conditions with calcined eggshell (E=90%). The adsorption capacity increased with the increase of dye concentration, which can be explained with the high driving force for mass transfer at a high initial dye concentration (Bulut and Aydın, 2006).

In the present study, we investigated the effect of RR concentration on the adsorption of brewery's yeast on a broader range (Figure 22). 16 different initial concentration values were used in the experiments, ranging from 5 to 1,000 mg/L. We observed an initial increase in dye removal efficiency, reaching a maximum of 80.6% at a concentration of 40 mg/L. The increase in efficiency can be explained by the fact that at lower concentrations more active binding sites were available for the binding of dye molecules. At concentrations of 40, 50 and 60 mg/L, the E was almost constant, as the active sites were saturated. After saturation, the number of binding sites were limited. The values of quantity in equilibrium (q_e) were also studied. The q_e increased with increasing concentration ($q_{e;5\ mg/L}$= 0.2 mg/g; $q_{e;1000\ mg/L}$= 21.7 mg/g).

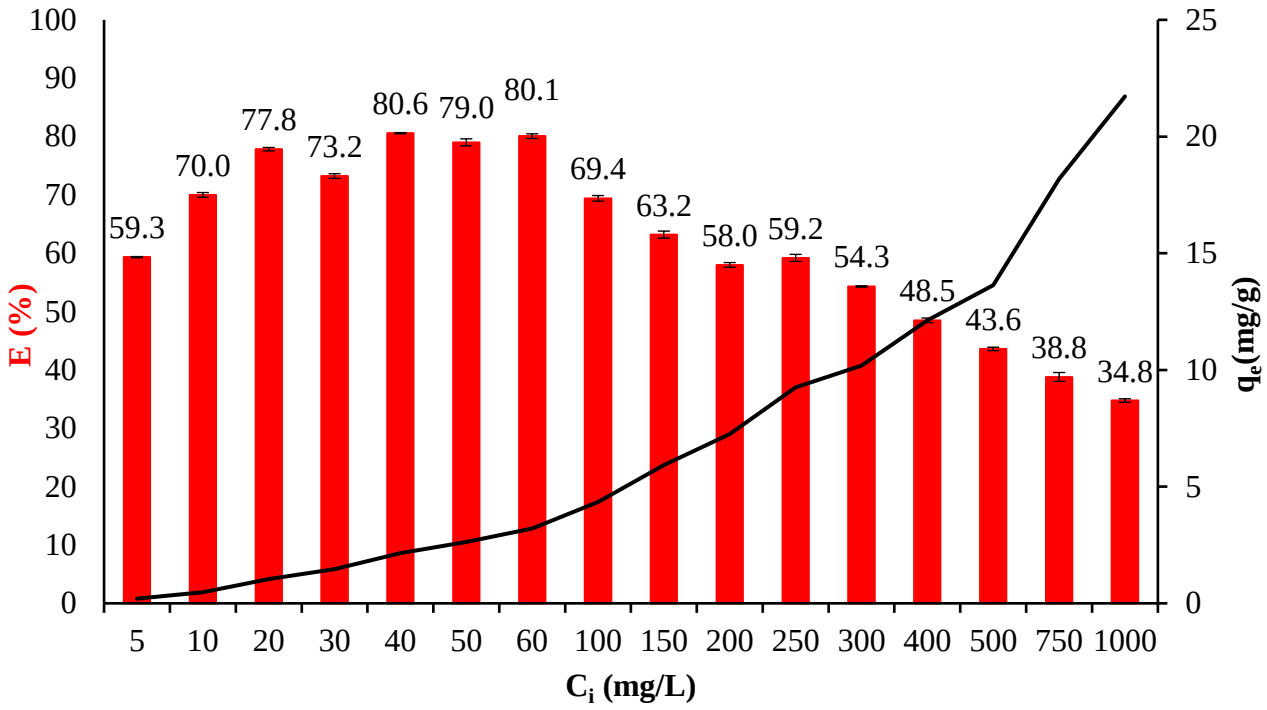

Figure 22. The effect of initial RR concentration on yeast adsorption, C_i = 5–1,000 mg/L, 1.5 g yeast, 700 rpm, pH = 6.0 ± 0.2, T = 20 ± 1 °C. Result are the means and standard deviations of 9 experiments.

By examining the effect of initial dye concentration through our results and exemplified by the results in Table S1., three trends can be observed:

- the removal efficiency decreases as the initial concentration increases;
- removal efficiency increases as the initial concentration increases; and
- no significant change in removal efficiency.

Most often, the percentage of dye removal decreases with increasing initial paint concentration. This phenomenon can be explained by the saturation of adsorption sites on the adsorbent surface. In this case, as the initial concentration increases, so does the capacity of the adsorbent, which is due to the high mass transfer driving force at high initial dye concentrations. The initial concentration of solute acts as a driving force for the adsorption process, favoring diffusion and mass transfer processes from the solution (with a higher amount of dye) to the free surface of the adsorbent (Al-Ghouti and Al-Absi, 2020; Seow and Lim, 2016).

If the concentration of the solution increases, and with it, the amount of bound material shows a similar trend, then at low initial solution concentration the surface area of the adsorbent and thus the number of adsorption binding sites is high, so the contaminant ions or molecules (in our case dye molecules) can easily bind to the adsorbent surface. At higher initial solution concentrations, the total available adsorption sites are limited, which may result in a reduction in the percentage

removal of contaminants. The increase at higher initial concentrations may be attributed to increased driving forces (Mondal and Kar, 2018; Tejada-Tovar et al., 2021).

At low concentrations, the ratio of active sites to dye molecules can be high, allowing all molecules to interact with the adsorbent and be removed from solution almost instantaneously (Silva et al., 2020).

Arellano G. Rodríguez et al. (Rodríguez-Arellano et al., 2021) reported that a negative linear effect between removal efficiency, amount of bound material and initial concentration occurred when removing CR with cocoa bean shells (Rodríguez-Arellano et al., 2021). Accordingly, as the initial dye concentration increased, the adsorption capacity of the biosorbent decreased. Referring to other similar studies with CR, it was explained that the equilibrium adsorption capacity increases with increasing initial dye concentration, a process controlled by the mechanism of resistance to removal of CR (Rodríguez-Arellano et al., 2021).

Even though it is a driving force, a clear, generalizable influence of the initial concentration as a parameter is not possible since several experimental conditions act in combination on the specific contaminant and the adsorbent under study.

4.1.2. The effect of solution pH

The pH affects the solution chemistry of contaminants, the activity of functional groups in the adsorbent, the competition with coexisting ions in the solution, and the surface charge of the adsorbent. The pH of the aqueous medium can also influence the properties of the adsorbent, the adsorption mechanism, and the dissociation of dye molecules. Not only the adsorbent but also the chemical structure of the dye can be altered by the pH of the solution. The pH changes the surface charge and the degree of ionization of the adsorbed ion (Brito et al., 2018; Gamoudi and Srasra, 2019; Kanwal et al., 2017; Khasri et al., 2021; Rápó et al., 2018; Yildirim, 2021). The pH of aqueous solution can highly affect the biosorbents' (eggshell) surface charge. In acidic media, the surface of the adsorbent is protonated, while in a basic medium its surface deprotonates. Dye biosorption is a pH-dependent process. The pH of the aqueous medium can influence the biosorption of the dyes: changes in sorbent properties, adsorption mechanism, dissociation of the dye molecules, and the chemical structure of the dye.

During our research, the adsorption processes were studied by varying the indicator dyes' aqueous solutions pH, ranging between 2-10. As seen in Figure 23. CR dyes' highest adsorption efficiency was obtained at pH=2, but in all cases, E was above 93%. BPB dyes' highest efficiency was also at pH=2 (E=67%). For MB the adsorption was most efficient at pH=10, achieving 75% efficiency, while the lowest was at pH=2 where E=14%. MG is similar to CR dye, with a high

percentage efficiency at all pHs. Thus, it can be said that BPB anionic dye preferred acidic medium, while MB cationic dye preferred the basic medium, whereas there was no significant change in case of CR and MG, because the efficiency was high at all pHs. Similar results were obtained by Zeroual et al., 2006; Iqbal and Ashiq, 2010; Salleh et al., 2011; Zulfikar and Setiyanto, 2013; Tiwari et al., 2015; El-Dars et al., 2015.

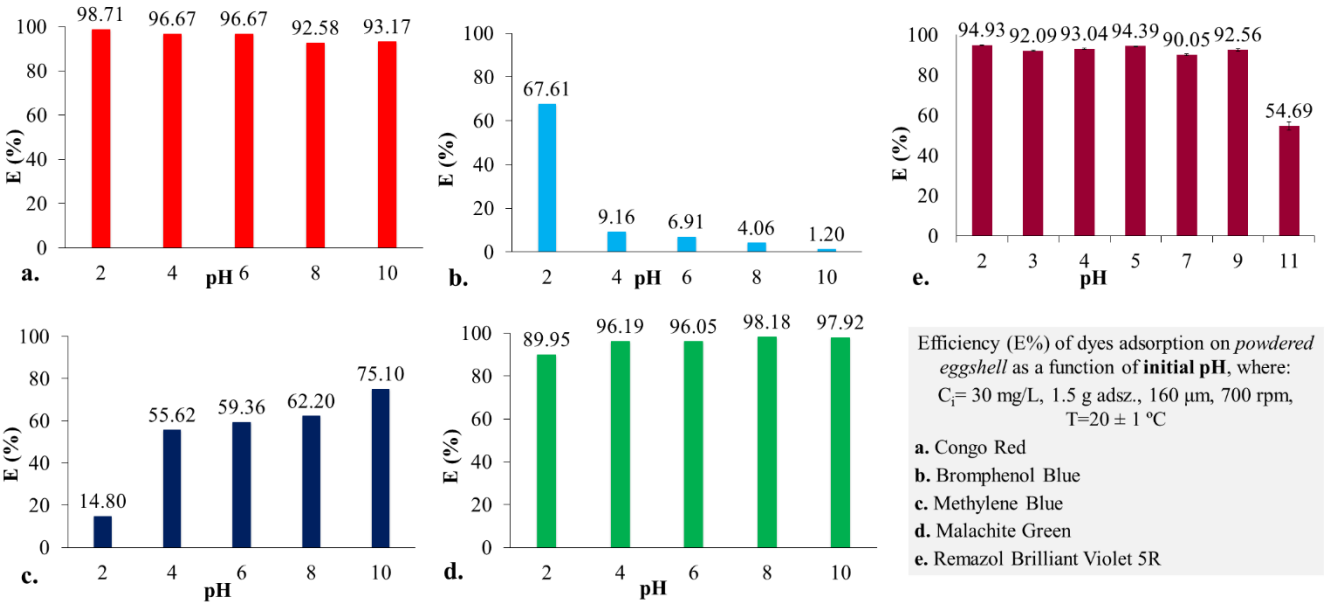

Figure 23. Efficiency (E%) of dyes adsorption on powdered eggshell as a function of initial pH.

Reactive dyes and thus RBV-5R, are anionic in nature. This property implies that the dye may be adsorbed in acidic medium with greater efficiency. Therefore, the initial pH of the solution can significantly influence not only the chemical structure of the dyes but also the eggshell surface charge. In case of adsorption on powdered eggshell surface (Figure 23e.), the dye adsorbed with highest efficiency in acidic medium (at pH = 2, the E>94%), on the other hand it was lowest at pH = 11 (E=54.69%). In contrast with powdered eggshell, in case of calcined eggshell (Figure 24a.) there was no significant change in E and q_e values. The calcined eggshell used in our research contains CaO, which is alkaline, highly influencing the pH of the aqueous medium. At the end of the adsorption experiments, the solutions were filtered, and the pH of the filtrate was checked. All solutions showed a pH of around 11.

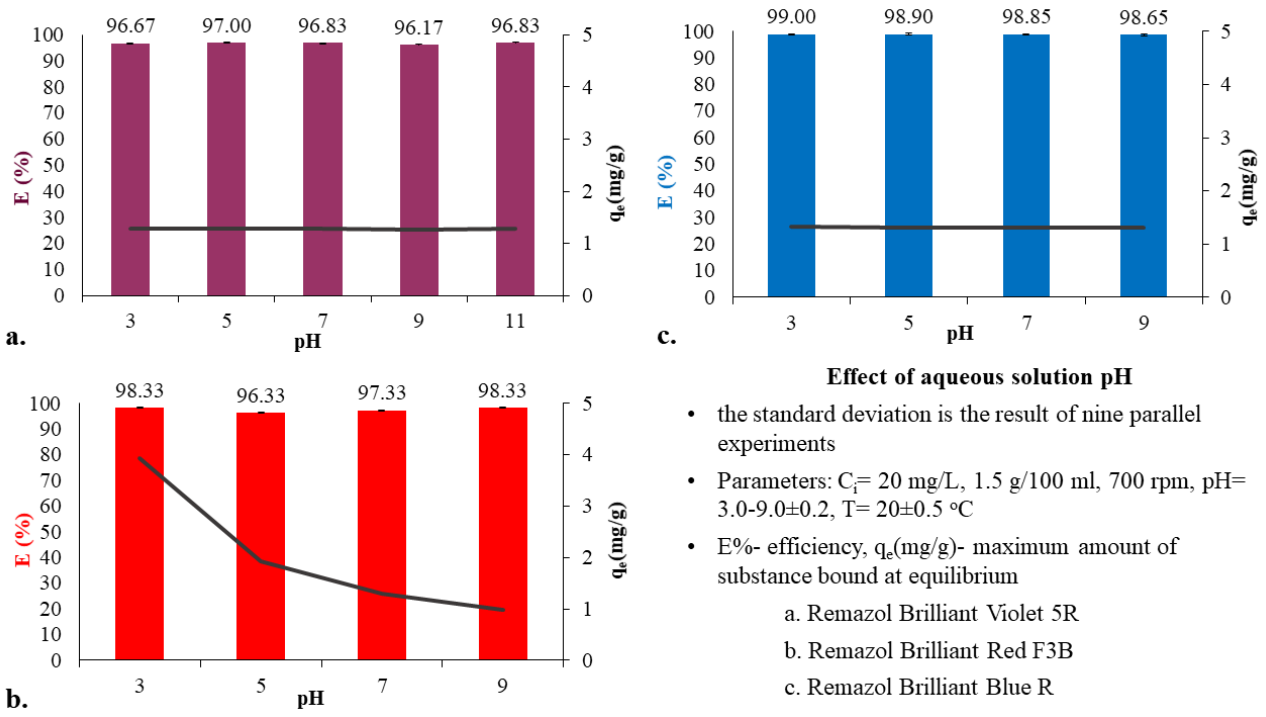

Figure 24. Efficiency (E%) of dyes adsorption on calcined eggshell as a function of initial pH.

RR and RB being reactive dyes, thus anionic, the adsorption is preferable in acidic conditions. The effect of pH was investigated on the adsorption of RR and RB dyes on the surface of calcined eggshell (Figure 24b-c.). For this study the pH of aqueous dye solution was adjusted with 0.1N NaOH and 0.1N HCl. In batch conditions, after the desired pH was reached, calcined eggshell was added to the solution. Calcined eggshell is the product of $CaCO_3$; therefore, it changed the pH to basic when it was added to the dye solution. Amarasinghe and Wanniarachchi (2019) reported that after calcination (in raw eggshell the $CaCO_3$ transformed to CaO) when exposed to the atmosphere CaO converted to $Ca(OH)_2$, dissolving it in water solution gives it a basic character (Achala Amarasinghe and Dakshika Wanniarachchi, 2019). This is the reason why the efficiency results in Figure 24b-c. are almost identical. Highest adsorption efficiency was achieved for both dyes at pH=3 (E_{RR}=98.33%; E_{RB}=99%).

RR dye, as reactive dyes, is also anionic in nature, therefore we expected it to adsorb on the yeast surface better in acidic medium. Our assumptions were proven, as the highest E (88.5%) was reached at pH=3, smallest at pH=11, where E=46.5%.

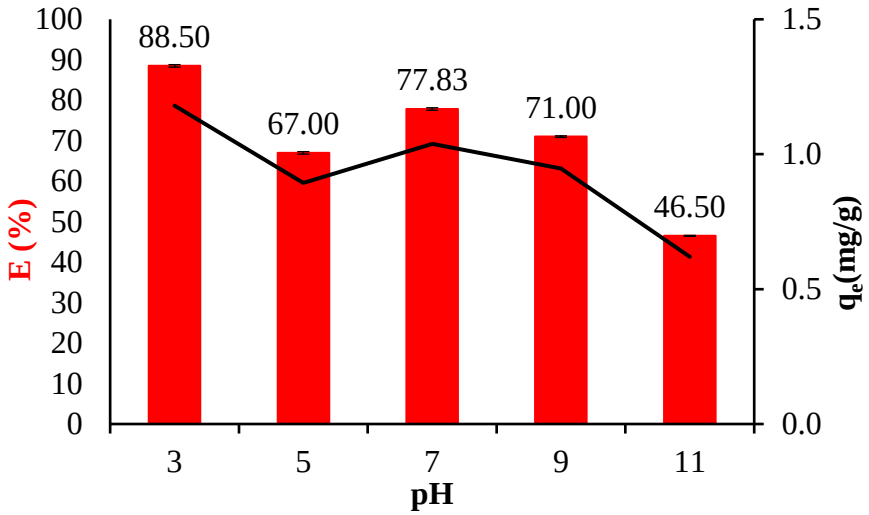

Figure 25. The effect of pH on the adsorption of RR dye on brewery's yeast (C_i = 20 mg/L, 1.5 g yeast, 700 rpm, T = 20 ± 1 °C).

Practical applications done through our experiments and literature results (Table S2.) demonstrate that anionic dyes bind more effectively to the adsorbent surface in acidic media, whereas cationic dyes bind more effectively in basic media. Usually, the pH of the aqueous dye solution is adjusted with HCl and NaOH. When HCl is added to the solution, the surface of the adsorbent in the solution is protonated, allowing the anionic dye to bind more efficiently on its surface, due to the electrostatic attraction. Conversely, in basic medium, the addition of NaOH deprotonates the biomass surface, resulting in a repulsive force between the anionic dye and the biomass. Thus, the reverse phenomenon is observed for cationic dyes.

4.1.3. The effect of adsorbent dosage

The amount of biomass is an important factor in the adsorption process. In theory, the higher the amount of adsorbent present in the aqueous medium, the more binding sites are available to the dye molecules. Nonetheless, after a while, the binding dye molecules are depleted in the solution. In our research (Figure 26.) we investigated the adsorption parameters of different initial amounts of powdered- (0.5; 1; 1.5; 2; 2.5 g), calcined eggshells (0.5; 1; 1.5; 2 g) and yeast (0.5; 1; 1.5; 2; 2.5 g).

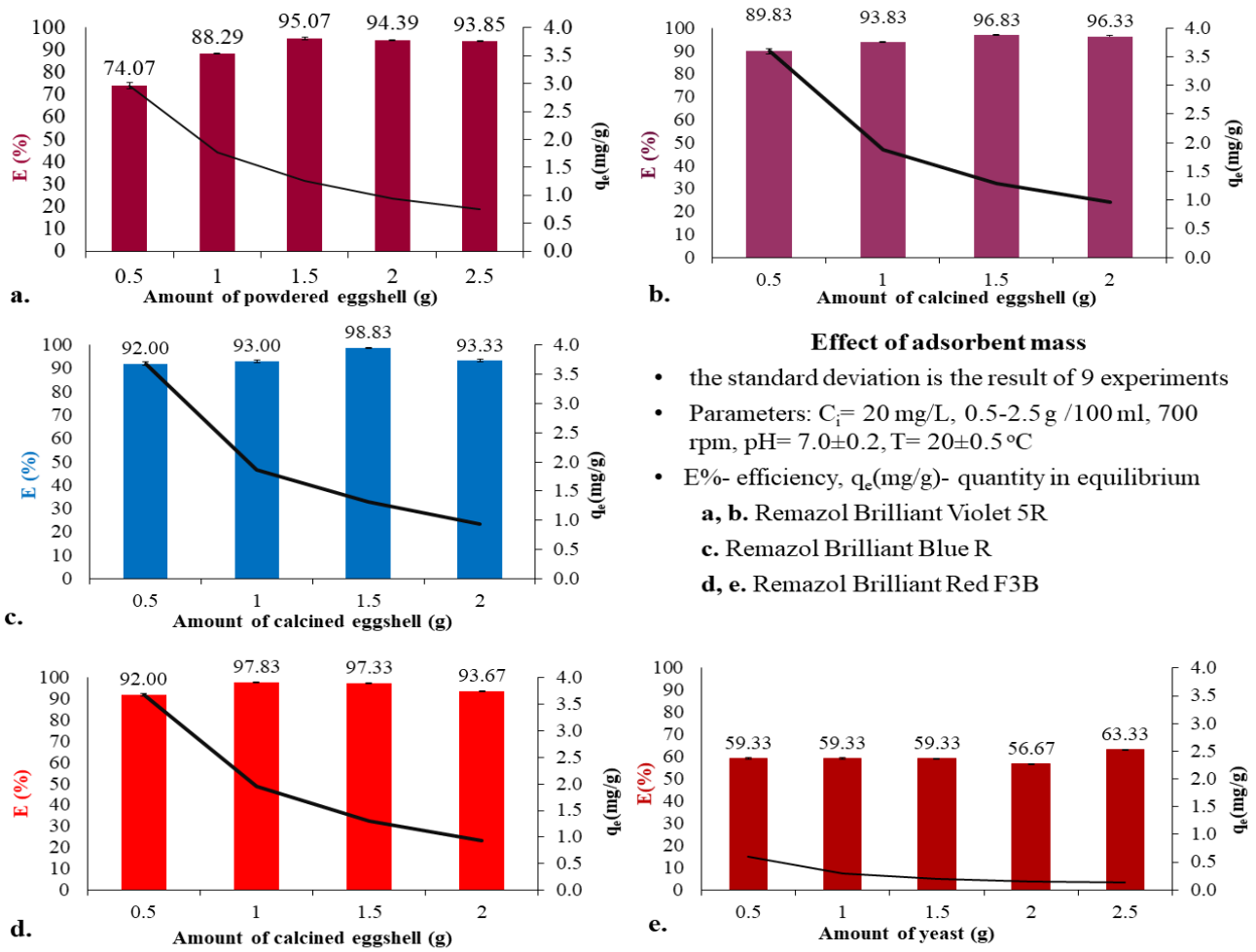

Figure 26. The effect of adsorbent dosage on the adsorption of dyes.

The effect of the amount of powdered eggshell on both the biosorption capacity and the percentage of RBV-5R dye removal was studied at five different adsorbent dosages (0.5-2.5 g). The figure shows that by increasing the adsorption dosage, the removal efficiency also increased until 1.5 g/100 mL, but after that, saturation was reached (Figure 26a.).

We studied the dye's adsorption on calcined eggshell increases, where the removal efficiency increases, but the quantity in equilibrium exhibits a decreasing tendency. Based on the results, the highest efficiency was obtained (E% = 96.83) for 1.5 g of calcined eggshell.

The effect of calcined eggshell dosage on RR and RB dye removal was evaluated using 0.5; 1; 1.5; 2 g of adsorbent with both textile dye, constant parameters being C_i=20 mg/L, 700 rpm, pH unadjusted, T=20±0.5 °C. From the results (Figure 26d.), it can be inferred that RR dye had the highest adsorption efficiency in case of 1g adsorbent, where E=97.83%, whereas in case of 1.5g adsorbent we got E=97.33%. We can see a trend of – mainly constant – decrease. On the other hand, RB dye adsorption was highest when adsorbed with 1.5 g calcined eggshell (E=98.83%),

smallest (E=92%), when 0.5 g calcined eggshell was added to dye solution. Due to increase in surface area when more adsorbent was added, higher efficiency was achieved, but after all pores were bounded by dye molecules, there was no need for further amount increase.

The amount of adsorbent (m; the yeast) is an important parameter because it affects the number of binding sites available. The efficiency of dye removal depends on the interaction between the adsorbent and the pollutant. Preliminary research has shown that in most cases, as m (g) increases, E also increases. In contrast, q_e is negatively correlated with the change in mass. In our study, the highest efficiency was obtained with the addition of 2.5 g yeast in a 5 mg/L RR solution suspension (Figure 26e.). On the other hand, q_e decreased from 0.59 mg/g to 0.13 mg/g as the mass increased.

According to Kroeker's rule, the specific adsorbed volume, for a constant initial concentration, decreases with increasing adsorbent mass (Pernyeszi et al., 2019). Thus, increasing the adsorbent dose is positively correlated with the efficiency and performance of dye removal. With increasing adsorbent dosage, at fixed contaminant concentrations, more active surface area is available for adsorption and more active adsorption sites are available (Ma et al., 2020).

As the concentration of biomass (the amount of adsorbent) increases, the efficiency of pollutant removal (E%) increases, but there is no direct proportionality between the amount of biomass and the amount of pollutant removed (q_e).

In contrast, as the concentration of biosorbent increases, the amount adsorbed per species (q_e) decreases. This can be since the shape of the sorption isotherm changes with increasing biosorbent concentration. The decrease in the specific adsorbed amount is probably due to the fact that some of the surface or surface groups may not be saturated in the more concentrated suspensions (Dehghani et al., 2021; Esmaeili et al., 2020; Neag et al., 2019; Salahshour et al., 2021).

During the dye removal process, the capacity may decrease for two reasons (Popa et al., 2021):

- adsorption sites remain unsaturated while the number of sites available for adsorption increases; or
- aggregation or agglomeration of adsorbent particles may occur, reducing the available surface area and increasing the diffusion path length.

Scientific studies in recent years have investigated the removal of different dyes with different amounts of broad-spectrum adsorbent. Some examples of these are listed in Table S3. to support the detected relationships between mass and adsorption. It is observed that at fixed pollutant concentrations, as the mass of the adsorbent increases, the efficiency increases, and the maximum amount of material bound decreases.

Several studies also report that this increase in efficiency lasts until a saturation state is reached and then steadily decreases, sometimes slightly. This can be explained by the fact that after a certain adsorbent dose, maximum adsorption is reached and the amount of ions bound to the adsorbent and the amount of free ions remains constant, even with the further addition of adsorbent (Hamza et al., 2018; Salahshour et al., 2021; Şentürk and Alzein, 2020).

4.1.4. The effect of adsorbent particle size

In adsorption by static batch methods, smaller particle sizes result in higher adsorption capacity and efficiency, since there are more active sites for binding (Nikam and Mandal, 2020).

We tested the effect of particle size on the biosorption process. The rate of paint removal shows a decreasing trend as the particle size increases. Both the biosorption capacity (1.26; 1.23; 1.21) and the efficiency (94.39; 92.09; 90.87) decrease with increasing eggshell powder particle size (160 µm; 315 µm; Unsorted). The highest efficiency (94%) was obtained with eggshells with a particle size of 160 µm (Figure 27).

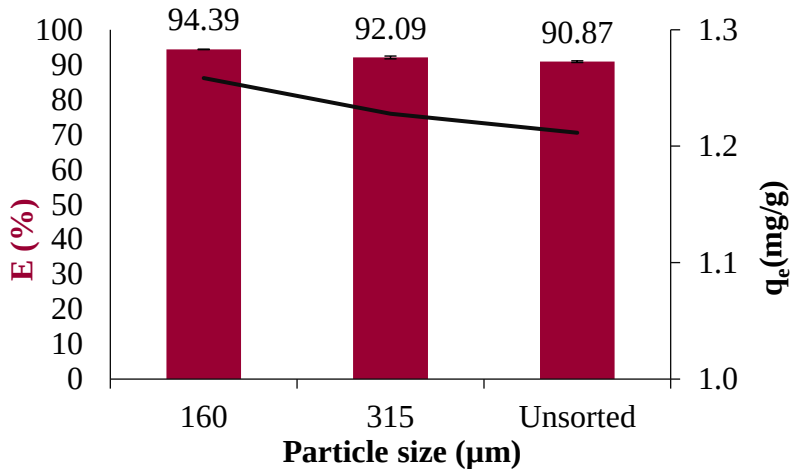

Figure 27. Effect of particle size C_i=20 mg/L, 1.5 g powdered eggshell, 700 rpm, pH=6.0±0.2, T=20±1 ºC.

Moreover, Table S4. represents results of studies where the effect of particle size was investigated, and a similar trend was observed. With the decrease of the particle size, the BET surface of the material increases.

If the particle size is too small, the adsorption capacity may be lower, depending on the type of adsorbent, as the lighter particles float and thus cannot contact the solution. The separation of these small particles from water after biosorption can be challenging (Stjepanović et al., 2021).

4.1.5. The effect of adsorption shaking speed

When a solid sample of known mass is exposed to a liquid phase of known composition, the concentration varies continuously until equilibrium is reached because of the multiplication. The

time required for this, which can be effectively reduced by shaking or stirring, is determined from preliminary kinetic measurements. The amount adsorbed can be calculated from the initial and equilibrium composition and the amount of the materials (solid mass and liquid volume). The rate is also experiment-dependent (adsorbent, contaminant, adsorption method). Increasing the rate will increase the biosorption removal rate of adsorbed impurities by minimizing mass transfer resistance, but may damage the physical structure of the biosorbent (Harrache et al., 2019; Hii, 2021; Intidhar Jabir Idan et al., 2017; Muinde et al., 2017; Munagapati et al., 2020; Yu et al., 2018). In our experiments with the adsorption of RBV-5R and powdered eggshell the rate of dye removal increased as the shaking speed increased (Figure 28).

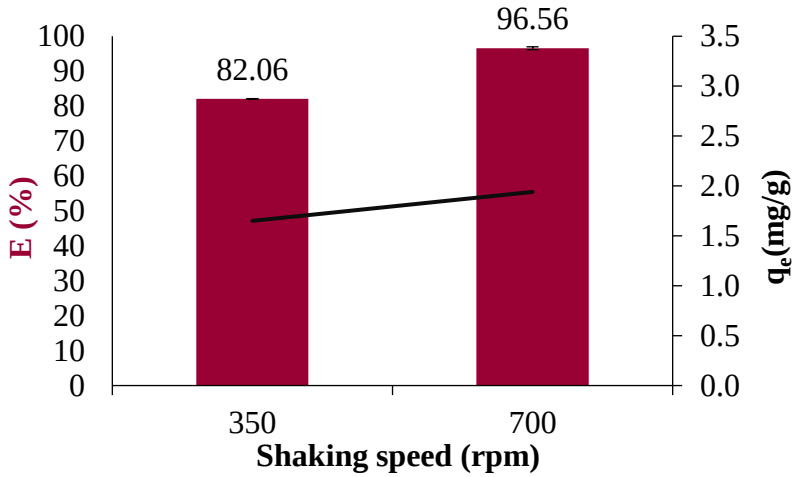

Figure 28. The effect of shaking speed C_i=20 mg/L, 1.5 g, 160 µm, pH=6.0±0.2, T=20±1 °C.

4.1.6. The effect of solution temperature

The temperature can affect the efficiency of the sorption differently depending on the adsorbent and the pollutant. In general, it enhances biosorption of adsorption impurities by increasing the surface activity and kinetic energy of the adsorbate, but it can also damage the physical structure of the biosorbent.

- As the temperature rises, the rate of chemical reaction also increases, so if the sorption process is chemisorption ($\Delta H_{chemisorption} \approx -200$ kJ/mol), then higher sorption efficiency will be seen at higher temperatures (this would eventually reach equilibrium).
- On the other hand, if the process is a physical adsorption ($\Delta H_{physisorption} \approx -20$ kJ/mol), then the higher temperature will negatively affect the adsorption. Temperature can chemically alter the adsorbent, its adsorption sites and activity (Tonk Szende and Rápó Eszter, 2020).

In our research, the adsorption properties of the powdered and calcined eggshell were studied by changing the temperatures (20, 30, 40 °C) of the RBV-5R dye solution (Figure 29).

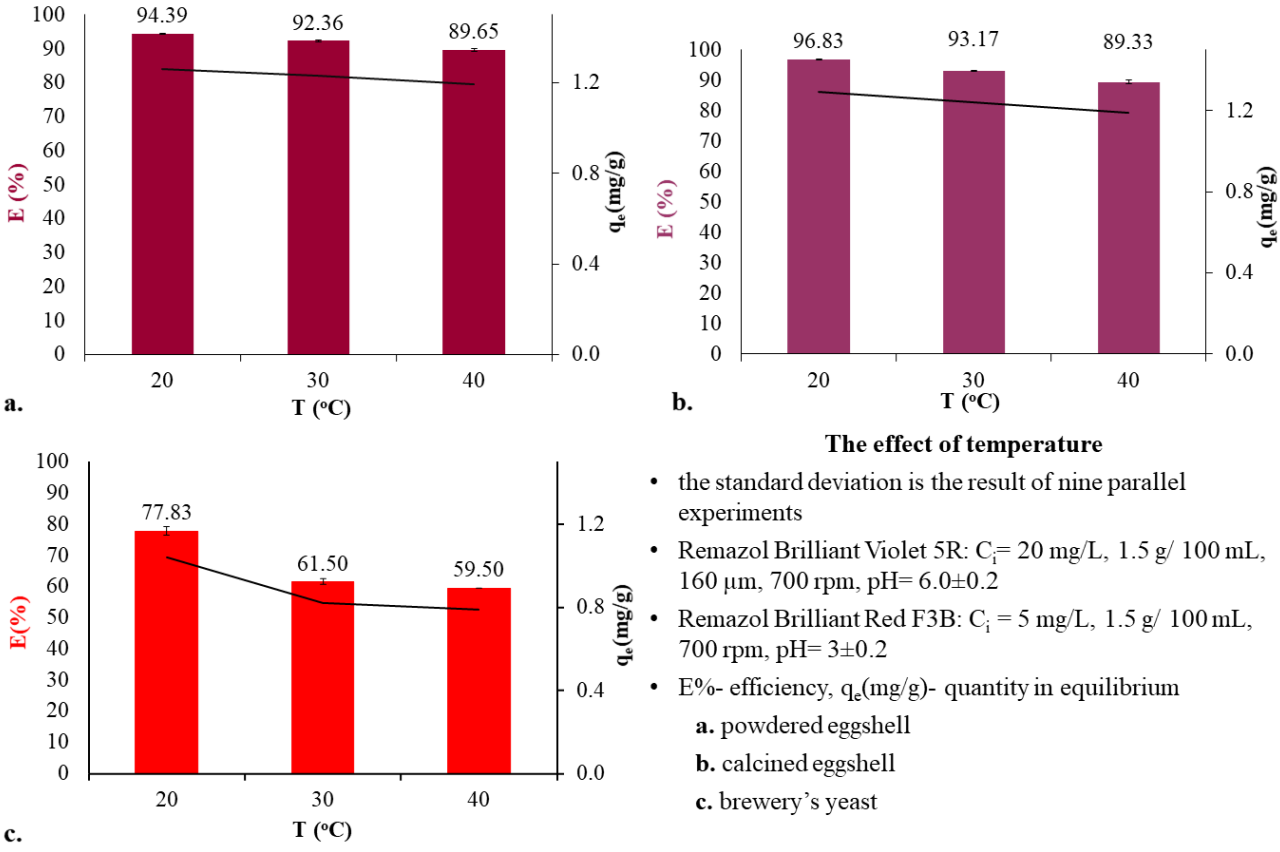

Figure 29. The effect of temperature on dye adsorption.

Our results show that the adsorption capacity and the percentage of RBV-5R biosorption on eggshell biomass is an exothermic process because the efficiency decreased with increasing temperature. The maximum efficiency was 94.4% at 20 °C, while 92.4% at 30 °C and 89.7% at 40 °C. A similar trend can be observed in the case of the adsorption capacity (Figure 29a).

Figure 29b. depicts the effect of temperature dependence on the efficiency and the quantity in equilibrium in case of calcined eggshell and RBV-R dye adsorption. It can be observed that the efficiency and the quantity in equilibrium decreases with the increase in the temperature of the aqueous medium. Similar results were obtained for calcined eggshells, but with lower efficiency (20 ºC: 96.83, 30 ºC: 93.17, 40 ºC: 89.33). This was anticipated because the molecules' thermal movement increases with the increase of temperature, and thus adsorption decreases.

In our study, with RR dye removal by brewery's waste, both the efficiency and q decreased with increasing temperature (Figure 29c). At 20 °C, the efficiency/ quantity in equilibrium was 94.4%/1.04 mg/g, while at 30 °C it was 92.4%/0.82 mg/g and at 40 °C it was 89.7%/0.79 mg/g. Results indicate that the sorption can be attributed to weak Van der Waals and dipole forces and bonds. As the temperature increases, the thermal motion of the molecules increases, so the adsorption decreases.

We can differentiate two types of processes: endothermic and exothermic (Table S5.).

- Exotherm: with the increase of temperature, the adsorption process (efficiency) decreases. It can be explained with the fact that the adsorptive powers among adsorbate and the active sites of the adsorbent become weak with the increase in temperature, and dye removal efficiency decreased (Abualnaja et al., 2021). Exothermic adsorption is usually used to control the diffusion process, as the mobility of the dye ions increases when heat is added to the system (Khalaf et al., 2021).
- Endotherm: with the increase of temperature, the adsorption process (efficiency) increases, due to more availability of active sites as a result of the activation of the adsorbent surface at higher temperatures (Sharma et al., 2021). Increasing the values of adsorption capacity by increasing the temperature may be attributed to an increase in the mobility of the large dye ions (El-Harby et al., 2017).

All in all, better adsorption at higher temperatures may indicate the endothermic nature of the process, while being exothermic at lower temperatures.

After studying the effect of initial temperature on adsorption, ***thermodynamic parameters*** are calculated. It is well known that the adsorption processes are strongly dependent on the working temperature, which is controlled by thermodynamic parameters including the standard enthalpy change (ΔH_0, J/mol), the standard entropy change (ΔS_0, J/mol) and the standard free Gibbs energy change (ΔG_0, J/mol) of the adsorption processes. These parameters are computed from the Gibbs–Helmholtz equation: $\Delta G = \Delta H - T\Delta S$ (Tran et al., 2020). Gibbs free energy, enthalpy and entropy are state functions, so ΔG, ΔH and ΔS depend on the final state and the initial state of the adsorption system. Gibbs free energy, enthalpy and entropy have extensive property, so attention must be paid to the amount of substance that these thermodynamic parameters correspond to (Chen et al., 2021).

During the adsorption of dye molecules, with the increase of temperature, the value of entropy (ΔS) and enthalpy (ΔH) can be increased or decreased.

Molecules before adsorption can move in three dimensions, but as they get adsorbed on the surface, the motion of them is restricted towards the surface, and their disorder decreases, resulting in the decline in entropy indicating an exothermic process. This may also be explained on the basis that the solubility of dyes increased at higher temperatures while adsorbate–adsorbent interactions decreased, resulting in decreased adsorption (Ali et al., 2020). The increase in entropy and enthalpy indicates an endothermic process (Abdel-Aziz et al., 2020; Miraboutalebi et al., 2020; Pradhan and Bajpai, 2020; Rios-Donato et al., 2017; Tran et al., 2020).

Thermodynamic parameters were calculated for C_i=20 mg/L RBV-5R dye solution, 1 g powdered eggshell, 160 μm, 700 rpm, and pH=6.0±0.2. From the results, we can see that the Gibbs free energy (ΔG) decreases with increasing temperature (T: 293 K=0.375 kJ/mol, T: 303 K=-0.480 kJ/mol, T: 313 K=-1.336 kJ/mol), indicating that adsorption is a spontaneous process. The calculated value of the enthalpy (ΔH=25.44 kJ/mol) is less than 85 kJ/mol, which proves that adsorption involves a physical process. The positive entropy value (ΔS=0.086 J/mol·K) suggests increased randomness at the solid/solution interface (Bello and Ahmad, 2011; Subramani S.E. and Thinakaran N., 2017).

In line with the results of powdered eggshell experiments, when we used calcined eggshell for the removal of RVB-5R, we received ΔH=49.6 KJ/mol, enthalpy, that is less than 84 kJ/mol but positive. According to literature data, it can be concluded that adsorption is an endothermic process and physical adsorption occurs (ΔH < 84 KJ/mole physical adsorption; ΔH 84- 420 kJ/mol of chemical adsorption). The positive value of ΔS=0.2 J/mol*K entropy indicates the randomness of the adsorption process. Gibbs' free energy is reduced by the effect of temperature (1.8; 0.2; -1.5). The lower the temperature, the higher the spontaneity of the process, so it is inversely proportional (Bello and Ahmad, 2011; Mohadi et al., 2016; Park et al., 2007; Witoon, 2011).

In summary, based on thermodynamic data, it can be said that RBV-5R dye biosorption on eggshell (powdered and calcined) surface is a spontaneous and endothermic process. Physical adsorption occurs between the dye molecules and the surface of the eggshell.

In case of RR dye adsorption on brewery's yeast the following experimental parameters were set to determine the thermodynamic parameters: C_i = 5 mg/L RR dye solution, 1.5 g yeast, 700 rpm stirring speed and pH = 6.0 ± 0.2. The calculated entropy, enthalpy, and Gibbs free energy values show that the Gibbs free energy (ΔG) value decreases with increasing temperature (-3.67, -4.96, -6.25 kJ/mol), indicating that the spontaneity of the process is inversely proportional to temperature. A positive value of ΔH enthalpy (34.14 kJ/mol) indicates the endothermic nature of the adsorption process. In our experiment, the enthalpy value is around 25 kJ/mol, as a result of which the adsorption is physical. A positive value of ΔS entropy (0.13 J/molK) indicates an increase in the randomness of the adsorption process at the solid / liquid interface. In summary, therefore, Gibbs' free energy values demonstrate that biosorption of RR dye and yeast is a thermodynamically possible and spontaneous process. Based on the enthalpy value obtained, the adsorption is an endothermic process and physical adsorption takes place between the yeast and the dye.

4.1.7. The effect adsorbent properties

The nature of the biosorbent is of major importance for the performance of adsorption: availability of binding sites, growth (in the case of living biomass) and treatment history, physical or chemical modification. Returning to experimental results with eggshells, we studied the rate and time effectiveness of removal in the presence of eggshells in three forms. We compared the efficiency and the maximum amount of material bound at equilibrium of powdered, calcined eggshells and eggshells embedded in alginate beads. It can be seen that the calcined eggshell binds the dye with the highest efficiency. It can also be said that, under the same experimental conditions, the adsorption equilibrium with the plain eggshell was around 300 min, while with the calcined eggshell it was 30 min, and for the eggshell embedded in alginate beads this time was 390 min. Taking all this into account, it is preferable to use eggshells in calcined form.

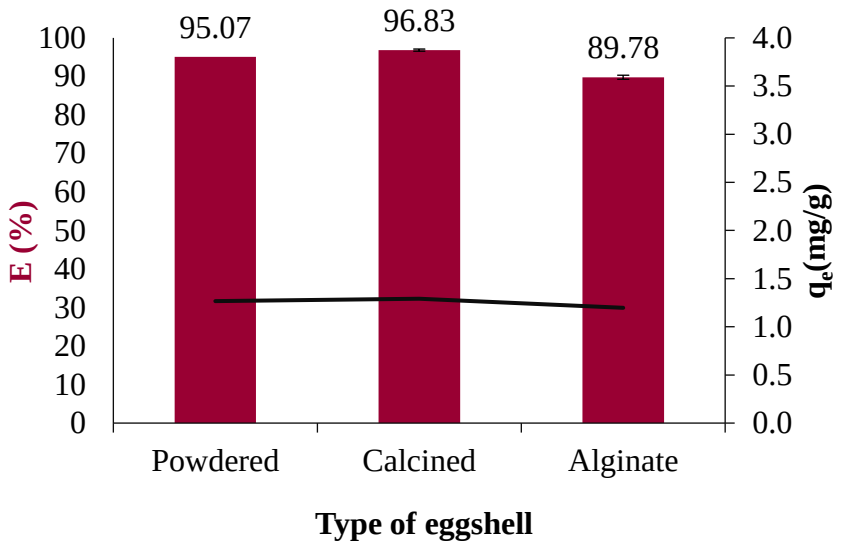

Figure 30. The effect of adsorbent material type.

To compare the adsorbents, using the RR model dye (representative of Remazol dyes), we examined the efficacy of calcined eggshell (the most effective form of eggshell used) and brewer's yeast. Under the same experimental conditions (C_i=20 mg/L, 1.5 g calcined eggshell/yeast, 160 µm, 700 rpm, T=20±1 ºC), the dye with calcined eggshell achieved 97.5% and the brewer's yeast 77.5% efficiency.

We can conclude that calcined eggshell is the most efficient adsorbent we have used.

4.2. Analytical measurements for dye adsorption

4.2.1. Morphology and elemental composition

4.2.1.1. Eggshell thin section

Different microscopic studies were carried out to examine the eggshell structure by comparing the untreated eggshell with that containing adsorbed RBV-5R dye to determine which layers are involved in dye diffusion. Figure 31b shows that the dye-adsorbed samples' cuticle, membrane and mammilla unit became purple due to adsorption.

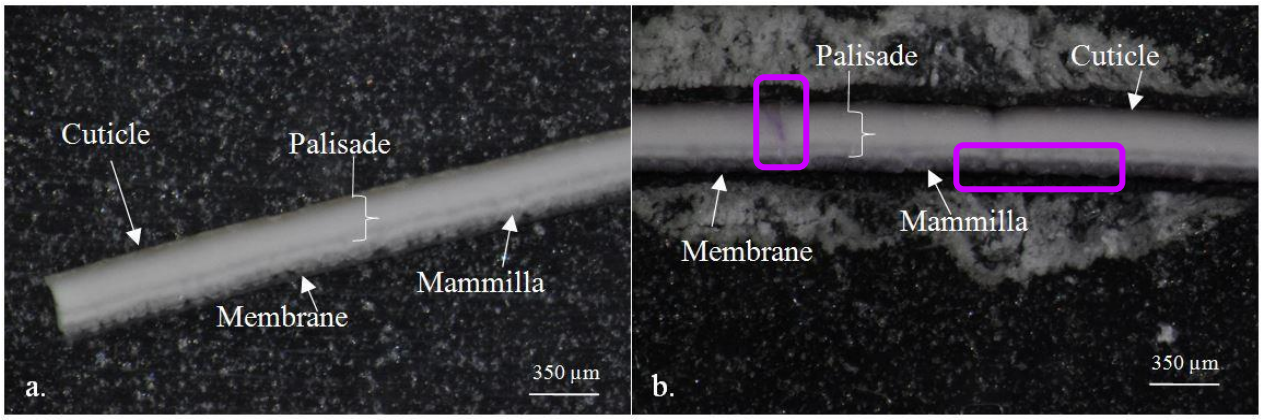

Figure 31. Stereomicroscopic images of thin sections from different structural units (cuticle, palisade, mammilla, membrane layer) of the (a) control eggshell and (b) eggshell with 2 g/L RBV-5R adsorbed.

The palisade layer is only purple if there is a crack on the eggshell surface. The same situation can be seen in the polarization microscope images with reflected light at increasing magnifications from the a-b couple (Figure 32).

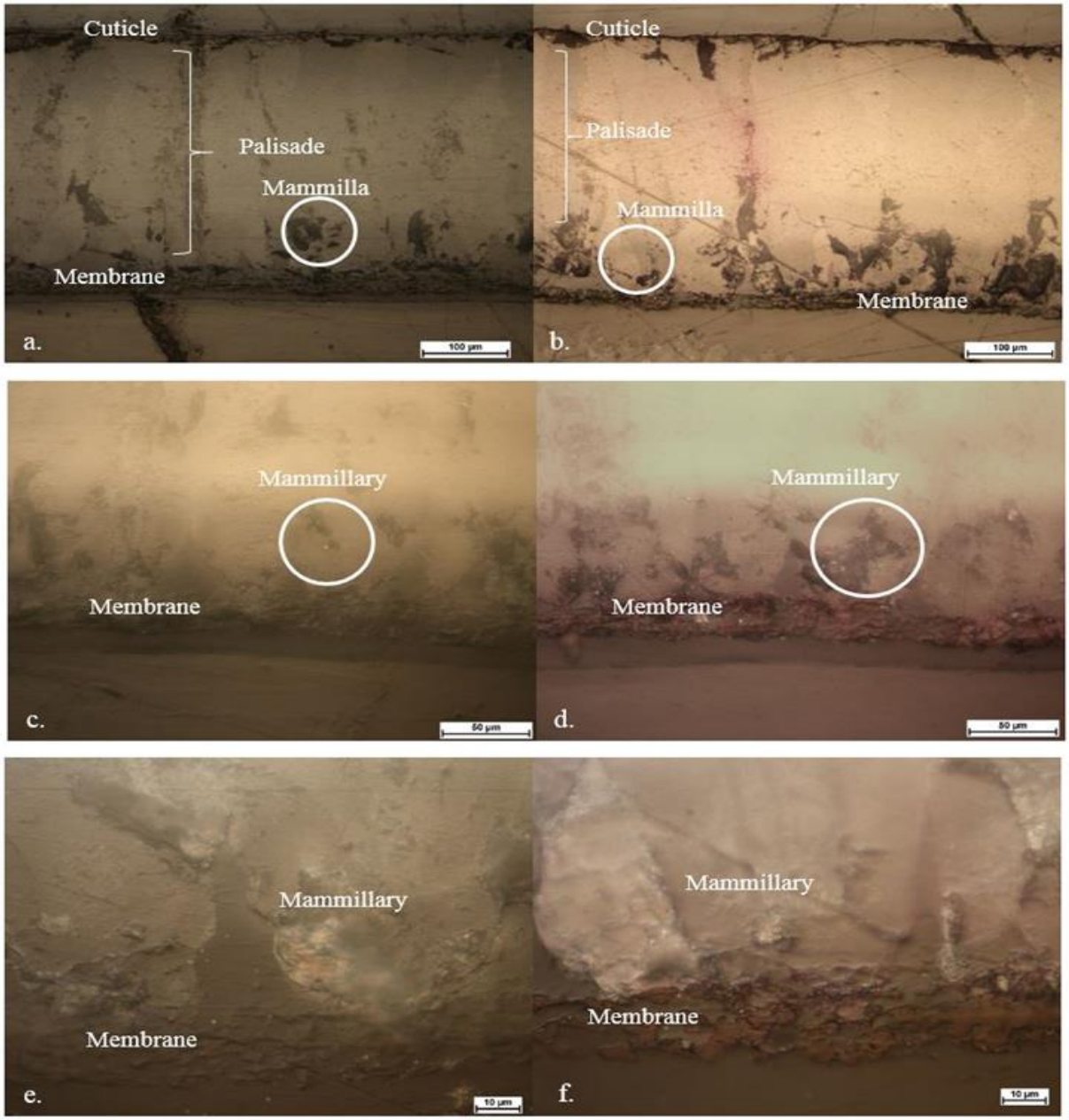

Figure 32. Polarization microscope images of thin sections from (a, c, e) the control eggshell and (b, d, f) eggshell with 2 g/L RBV-5R adsorbed.

Secondary electron microscopy images, obtained for the control eggshell and the eggshell in the textile-dye solution, display the surface morphology of the eggshell, but the polished surface with the characteristic eggshell layers (membrane, mammillary, palisade and cuticle) was also visualized. Figure 33 presents the elemental distribution of calcium, magnesium, sulphur and phosphorous in the eggshell section. Net intensity maps shed light on the difference in abundances between the minimum and maximum amount of each element. The intensity of the color is consistent with the concentration of the element in each area.

Mg is highly enriched in the cuticle, and the amount decreases abruptly until the mammillary layer, where it increases, on the other hand relatively homogenous Ca distribution was found in the whole thin sections. Therefore, it can be concluded that eggshell is made of Mg-bearing calcite. The concentration of P is the highest near the outside surface of the eggshell in the cuticle layer. In contrast with that of P, the amount of S is the highest in the inner part of the eggshell in the membrane layer. Since the dye contains sulphur, after adsorption, RBV-5R also appears in the cuticle layer. (Ribeiro et al., 2017; Shah et al., 2016; Török, 2015)

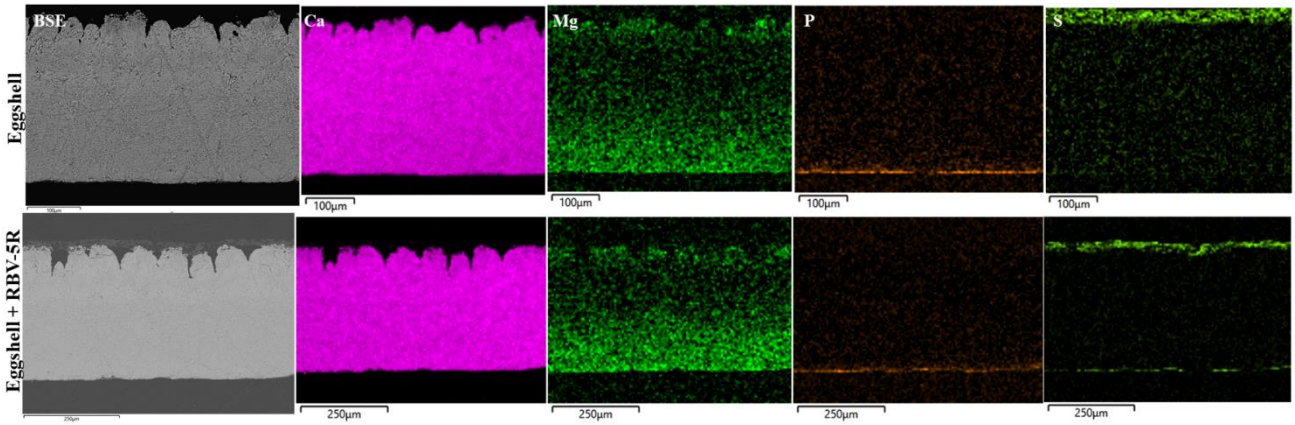

Figure 33. SEM images and EDS elemental maps of an eggshell thin section.

Each layer has a different composition. After adsorption, the membrane, mammillary and cuticle layers show the characteristic elements of the dye molecule, namely, N, S and Cu, proving the eggshell's adsorptive capability. The palisade, composed of columnar calcite crystals, contains Ca, O and C. After the adsorption experiment on the eggshells, the amount of magnesium increased, but the characteristic elements (Cu, S, N, O) of the dye could not be detected, which suggests that the dye did not reach the inner layers of the eggshell, even when a 2 g/L dye solution was used, presumably due to the structure and/or composition of the eggshell layer (Table 2).

Table 2. Representative elemental composition of each eggshell layer.

	Membrane wt (%)		**E. factor (%)**	**Mammillary wt (%)**		**E. factor (%)**	**Palisade wt (%)**		**E. factor (%)**	**Cuticle wt (%)**		**E. factor (%)**
	Control	**Dye**		**C.**	**D.**		**C.**	**D.**		**C.**	**D.**	
C	81.9	61.5	-24.9	18	15.7	-12.9	11.9	12.6	5.7	14.3	25.7	80.2
N	0	9.3	>	0	3.1	>	0	0	0	0	4.2	>
O	13.5	22.7	67.7	45.3	44.8	-1	47.5	47.6	0.2	47.7	41.7	-12.6
S	0	3.2	>	0.1	0.6	358.3	0	0	0	0	1	>
Ca	0	1.1	>	35.7	37.1	3.9	40.1	38.7	-3.4	35.6	28.1	-21.2
Cu	0	1	>	0	0	0	0	0	0	0	0.4	>

4.2.1.2. Eggshell powder

The surface characterization (morphology and texture) of the homogenous eggshell powder before and after adsorption was determined by scanning electron microscopy (SEM).

Figure 34 shows the SEM of the control sample (160 μm sized eggshell without adsorption) and four dye (CR, BPB, MB, MG) treated samples with 50 mg/L dye solutions. It can be seen that the porous, cross-linked structure of eggshell disappears in comparison to the control sample (Figure 34.a) in case of MB, MG, Congo Red; this is due to the fact that the eggshell has incorporated the color into its "caverns". On the other hand, in case of BPB (Figure 34.e) some of the cross-linked structure is saturated, in other parts smaller or larger aggregates have appeared, but the cross-linked structure, characteristic to eggshell structure, is still visible. This can be explained in the following way: when comparing the result with the amount of bounded material, we can see that BPB has the smallest value (c_i=50 mg/L, q_e=0.06 mg/g), so we can conclude that there are still free binders and the eggshells' crystal grid structure is still visible.

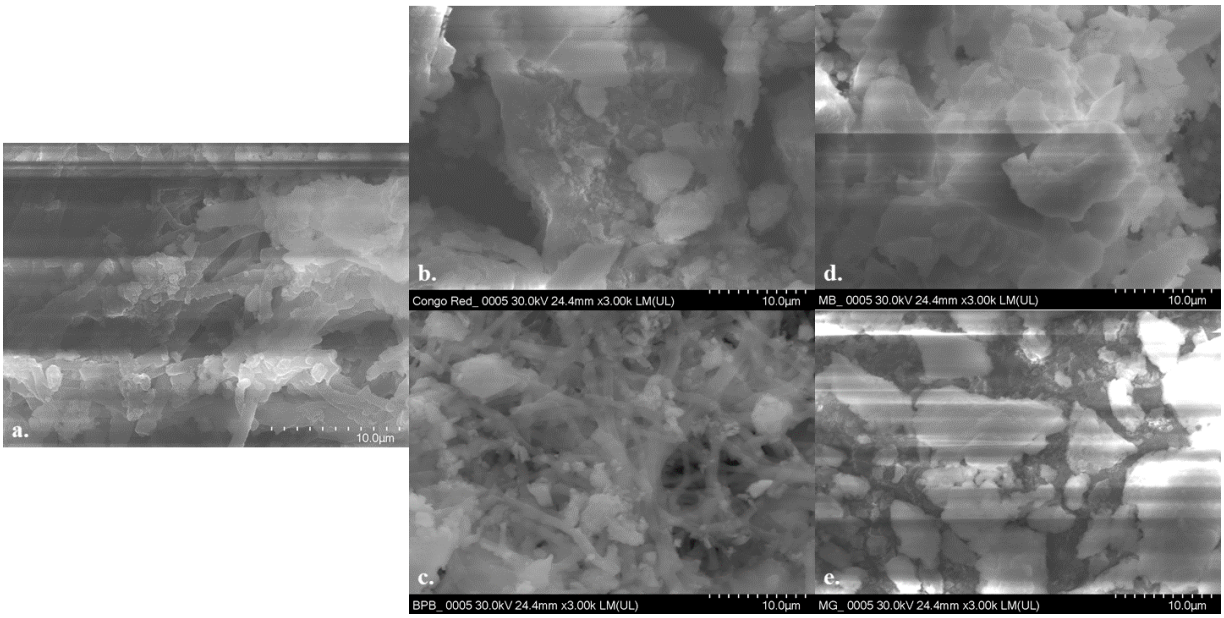

Figure 35. a. control, 50 mg/L **b.** CR, **c.** BPB, **d.** MB, **e.** MG adsorbed powdered eggshell.

In order to examine the elemental composition of the eggshell both for control and dye (CR, BPB, MB, MG) adsorbed samples X-ray spectroscopy (EDS) was carried out. From Table 3 we can see that eggshell contains mostly C, O, Ca. Samples contaminated with dye not only contain elements specific to eggshell but also elements gained from the dye they were adsorbed with, we can see that new elements appeared, some completely disappeared while others only decreased. The decrease of Mg while the increase of S can be seen. Furthermore, S (keystone of dyes) appears in each sample, while N is eliminated. In the case of BPB, the presence of Br proves the eggshells'

adsorption ability. Results obtained demonstrate that even in small concentrations (50 mg/L) the elemental composition of the eggshell can change when is used for dye adsorption.

Table 3. Eggshells' EDS, results are the means of 9 data (C_{dye}= 50 mg/L, 160 μm)

Elements	Wt(%) control eggshell	Wt(%) MB	Wt(%) MG	Wt(%) Congo Red	Wt(%) BPB
C	22.94 ± 9.14	25.17 ± 2.62	24.66 ± 6.02	23.50 ± 5.88	25.09 ± 6.61
N	0.31 ± 0.74	0	0	0	0
O	43.99 ± 10.78	46.11 ± 1.24	47.63 ± 6.55	45.06 ± 2.08	47.05 ± 8.35
Na	0.06 ± 0.11	0.05 ± 0.04	0.06± 0.07	0.1 ± 0.05	0.05 ± 0.08
F	0	0.87 ± 0.69	1.76 ± 1.69	2.39 ± 0.81	1.52 ± 1.73
Mg	0.45 ± 0.24	0.33 ± 0.04	0.31 ± 0.04	0.36 ± 0.03	0.19 ± 0.22
Si	0	0	0.01 ± 0.02	0.02 ± 0.04	0
P	0.08 ± 0.22	0.08 ± 0.05	0.11 ± 0.05	0.1 ± 0.03	0.09 ± 0.07
S	0.18 ± 0.33	0.24 ± 0.03	0.237 ± 0.22	0.24 ± 0.06	0.39 ± 0.2
Ca	29.25 ± 9.55	26.75 ± 1.27	28.77 ± 5.14	27.86 ± 3.34	28.97 ± 5.12
Cu	0	0.02 ± 0.02	0.02 ± 0.02	0.01 ± 0.02	0
K	0.02 ± 0.05	0	0	0	0
Br	0	0	0	0	0.13 ± 0.16

In case of RBV-5R dye adsorption on the surface of powdered eggshell images were taken at 2,000× magnification, where one can observe the macroporous structure and the rough and dense texture of the control sample of powdered eggshell (Figure 35). Moreover, the high porosity of the eggshell powder particles is also shown, which can be identified as gas exchange pores. This structure ensures the adsorption capacity of the eggshell, as it can accumulate dye in the pores. After contacting the dye (Figure 34b), the surface became smoother as if it had been polished, with apparently fewer and smaller pores.

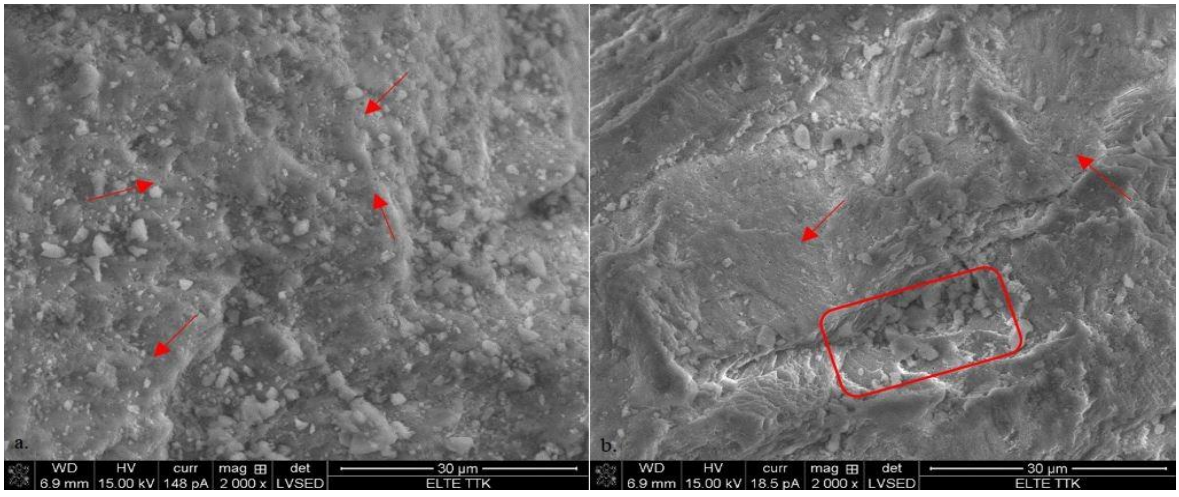

Figure 35. SEM micrographs of powdered eggshell **(a)** control and **(b)** eggshell with 100 mg/L RBV-5R adsorbed.

EDS measurements on powdered eggshell were performed before and after adsorption of RBV-5R dye. The results obtained are the means and standard deviations of 17 analyses (C_{RBV-5R}=100 mg/L, 160 μm). The control sample contains a high proportion of carbon (23±9 wt%), oxygen

(44±1 wt%) and calcium (29±10 wt%). The RBV-5R dye consists of carbon (33.5±2 wt%), oxygen (38±11 wt%), nitrogen (2.4± 5 wt%), sulphur (0.6±0.8 wt%) and in traces copper (0.08±0.15 wt%), which appear in the eggshell composition after biosorption. The appearance of S and Cu and the increased amount of N clearly demonstrate the ability of the eggshell to adsorb RBV-5R.

4.2.1.3. Calcined eggshell

The morphological properties and texture of the surface of the calcined eggshell used during the adsorption were also studied by SEM, both for the control and RBV-5R, RR, RB dyes adsorbed calcined eggshells. Figure 36 shows the captured images at 5,000x and 15,000x magnifications. In the figures (Figures 36a and 36b), the porous structure of the calcined eggshell is observed between the irregular shaped structures. Moreover, on the surface some small crystals of about 300 nm can be found. Following the adsorption (Figures 36c and 36d), this porous and irregular structure disappears, with the molecules of the dye filling the "gaps".

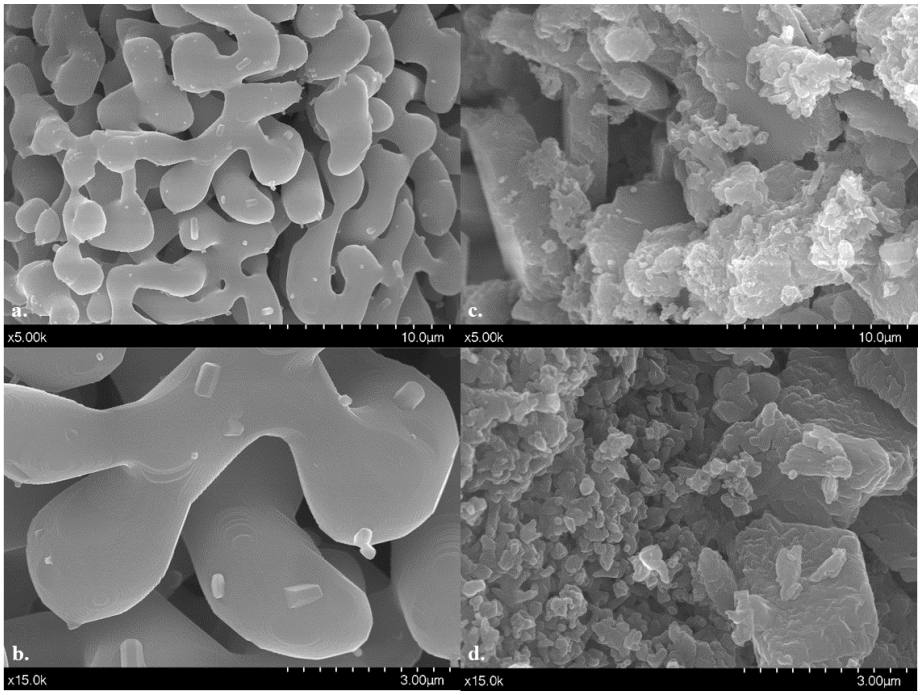

Figure 36. SEM (a, b) control and (c, d) 2 g/L RBV-5R dye adsorbed calcined eggshell.

As seen in Figure 37a, calcined eggshell has a heterogenous, irregularly shaped, porous structure. After adsorption (Figure 37b, c) the interaction between calcined eggshell and the dyes resulted in the disappearance of irregularly shaped forms, dye saturated pores, the appearance of aggregates in surface, therefore the whole structure, surface of calcined eggshell changed due to biosorption.

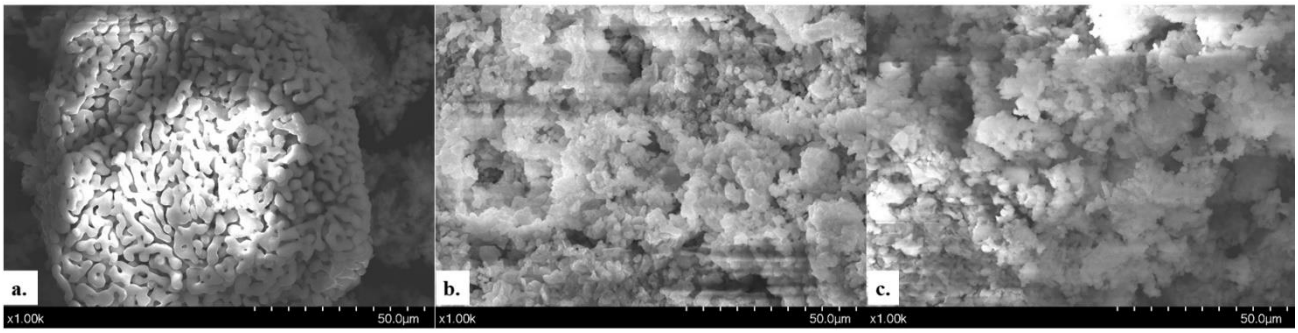

Figure 37. SEM photographs of (a) control (b) RR and (c) RB adsorbed calcined eggshell waste

To determine the elemental composition of calcined eggshell (control and dye adsorbed), energy-dispersive X-ray spectroscopy (EDS) was performed where the dye-adsorbed biomass was in a 2 g/L solution (Table 4). The adsorbent contains mostly Ca (59%) and O (36%), it was expected due to calcination process, where $CaCO_3$ becomes CaO and CO_2 when exposed to heat (1,000 ^oC 4 h).

Table 4. Results of EDS analyses, means and standard deviations of 10 measurements

Elements	Wt(%) Control	Wt(%) RBV-5R dye	Wt(%) RBV-5R + calcined eggshell	Wt(%) RR dye	Wt(%) RR + calcined eggshell	Wt(%) RB dye	Wt(%) RB + calcined eggshell
Ca	59.63 ± 14.81	0.01±0.01	51.29±19.27	0.02 ± 0.01	31.79 ± 4.39	0.06± 0.02	42.26 ± 5.78
O	35.97 ± 14.16	28.70±6.77	36.04±11.28	31.12 ± 2.41	52.10 ± 2.06	36.36 ± 7.82	47.52 ± 1.76
C	3.33 ± 1.94	39.80 ± 9.70	9.897 ± 6.573	49.89 ± 4.54	15.27 ± 3.41	29.19 ± 7.58	9.31 ± 4.69
Mg	0.76 ± 0.27	0	0.670 ± 0.217	0.02 ± 0.02	0.39 ± 0.21	0.03 ± 0.01	0.50 ± 0.04
N	0.32 ± 0.37	0.20±0.43	2.093 ± 1.627	0.07 ±0.16	0	0.89 ± 0.40	0
Na	0	17.18 ±8.07	0	8.43 ± 1.95	0.13 ± 0.06	14.27 ± 3.38	0.07 ± 0.03
Al	0	0	0	0.04 ± 0.04	0.10 ± 0.02	0.30 ± 0.31	0.05 ± 0.07
Cu	0	2.4±1.98	0	0	0	0	0
S	0	0	0	8.67 ± 0.67	0.29 ± 0.07	9.19 ± 3.15	0.19 ± 0.03

However, small percentage of C, N and Mg remained in the samples (maybe from organic matter). Gold was also present but is not listed in the table because of its small value (it was attached to the specimen in vacuum to increase conductivity).

The structure of the dyes (Table 4) showed that O, C, Na, Cu and N are fundamental building blocks of RBV-5R dye; C, O, Na and S are the components of RR dye and O, C, Na, S and N are the main constituents of RB dye. In all cases we observe the decrease of Ca, the increase of C, O due to dissolution after dye adsorption. After RBV-5R adsorption, the amount of C and the amount of N increased by more than 500%, which is typically derived from the dye, being an azo dye. The appearance in small quantities of S (appears in the dye content respectively to RR, RB dyes) indicates the binding of dye molecules into calcined eggshell surface.

4.2.1.3. Brewery's yeast

The surface morphological properties of the yeast and RR dye used during adsorption were studied by ***scanning electron microscopy*** (SEM). Both the control and the dye-adsorbed yeast sample were recorded (Figure 38a.c). The spherical, cellular, special-shaped structure of the paint can be observed (Figure 38b). The spindle and pointed egg-shaped yeast, which are also reported in the literature, are also shown in the figure (Figure 38a). After adsorption, this porous structure disappears, which is seen in the composition of the peaks, the cells seem to have fused, a cellular morphology difference can be seen (Figure 38c). Presumably, the structure has changed because of the process and the "gaps" are saturated with the dye molecules.

The chemical composition of yeast, RR dye and yeast sample after RR adsorption was determined with ***energy diffusion spectroscopy*** (EDS). Comparative spectra can be seen in Figure 38.d and e. According to the spectra the C, O, P, S, K and Cu elementary peaks of dye adsorbed yeast showed a different intensity compared to the control sample. Results show that the dye contains S (0.16 ± 0.06) and Cu (0.56 ± 0.34 wt%) in traces, moreover, after adsorption due to dye uptake, the yeast sample contained Cu. Based on the result of the enrichment factors (Figure 38f), the amount of C and S increased in the sample.

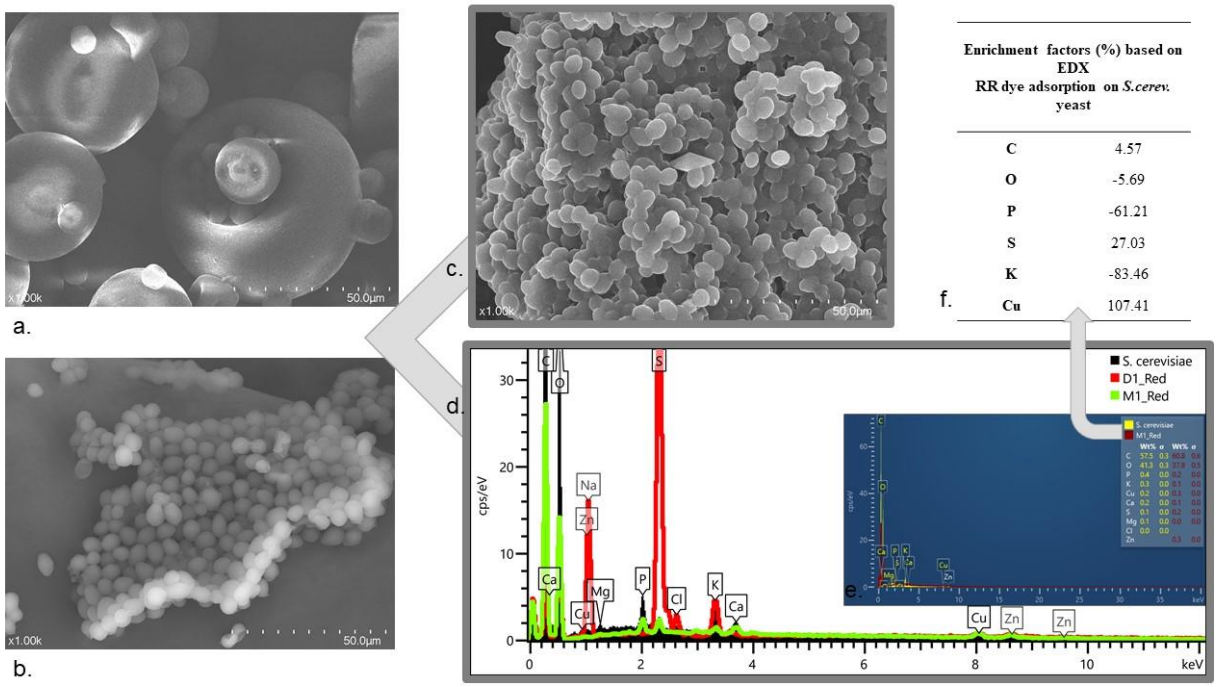

Enrichment factors (%) based on EDX RR dye adsorption on *S.cerev.* yeast	
C	4.57
O	-5.69
P	-61.21
S	27.03
K	-83.46
Cu	107.41

Figure 38. Adsorbent characterization, where SEM micrographs (a) RR dye, (b) control *S.cerev*. (c) 1 g/L RR adsorbed yeast; EDS spectra (d) comparison of *S.cerev.* (black), RR dye (red), yeast sample after RR adsorption (green), (e) comparison of *S.cerev*. (yellow), yeast sample after RR adsorption (red) with numerical values; (f) enrichment factor calculations based on EDS measurements.

4.2.2. Determination of functional groups, surface chemistry

4.2.2.1. Eggshell surface chemistry before and after RBV-5R adsorption

Firstly, the Raman spectroscopy of each eggshell layer was investigated. Eggshell has a complex composition of various organic molecules and mineralized components that are combined through the layers. According to previously published articles, the eggshell membrane contains 75-76% proteins, 4-5% carbohydrates and 20% water. The major protein component has disulphide crosslinks and lysine, while a smaller part is composed of collagen and glycoprotein (Leach, 1982). The Raman bands of the control and dye-adsorbed thin section eggshell are characteristic of S–S (507 cm^{-1}) bonds, amino acids such as tryptophan (758 cm^{-1}), tyrosine (860 cm^{-1}), and phenylalanine (1001 cm^{-1}), amide groups (1243 cm^{-1}), and C–H functional groups (1448 cm^{-1}). Raman shifts can also represent carbohydrates such as ribose and xylose at 507, 758, 1115, 1243, 1448 cm^{-1} (Rygula et al., 2013; Wiercigroch et al., 2017). During the daily production of eggs, approximately 6 g of mineral is deposited on a chicken eggshell (Hincke et al., 2012). The palisade layer is mostly composed of $CaCO_3$, and its Raman bands are located at 282, 712 and 1087 cm^{-1}. The spongy and organic cuticle covers the entire outer layer of the eggshell. Since the outer layer of the eggshell, which is attached to the lime shell, forms the top layer, gas is exchanged by osmosis, and there are no pore channels. The cuticle is composed of organic matter: 80-95% protein (water insoluble), 4-5% carbohydrates, 2.5-3.5% lipids and 3-3.5% ash (Becking, 1975; D'Alba et al., 2017; Dauphin et al., 2006; Leach, 1982). Raman shifts at 1115 and 1274 cm^{-1} in our samples certify the presence of neutral fats (Czamara et al., 2015) such as triacylglycerol, and bands at 860 and 1274 cm^{-1} indicate the presence of amide bonds (specific to albumen and collagen) and tyrosine amino acids. The presence of carbohydrates is proven by bands at 503, 606, 1115 (xylose), 633, 1115, and 1274 cm^{-1} (ribose) as well as 356 and 633 (lactose). After dye adsorption, new bands appear in each layer at 520, 580/581, 996, 1258/1261, 1304, 1332, 1403 and 1437 cm^{-1} that are specific to the C–H, C–S and N=N functional groups of the dye.

Functional groups present on eggshell powder before and after RBV-5R dye adsorption were also identified by FTIR spectroscopy. Figure 39a shows characteristic FTIR spectra, providing information on the binding nature of eggshell with the dye. Following adsorption, new bands appear, including at 1398 cm^{-1}, representing sulfonic groups characteristic of the dye; at 1648 cm^{-1}, indicating naphthalene; and between 1980 and 2281 cm^{-1}, representing the dye fingerprint zone. Stretching vibrations appear above 2967 cm^{-1}, specific to phenolic O–H, secondary amine N–H, and aromatic C–H bonds (Ribeiro et al., 2017; Shah et al., 2016; Török, 2015).

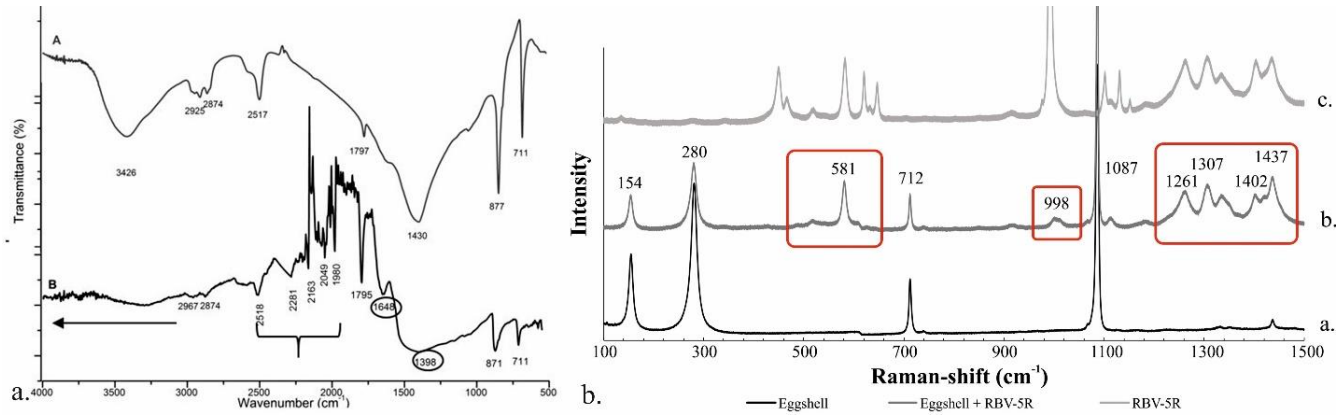

Figure 39. (a) FTIR spectra of the (a) control eggshell and (b) eggshell with 2 g/L RBV-5R adsorbed, (b) Raman spectra of the (a) control eggshell, (b) eggshell with 2 g/L RBV-5R adsorbed, and (c) dye.

To determine the material structure of eggshell powder before and after dye adsorption, vibrational Raman spectroscopic measurements were carried out. Information on the eggshell adsorbent and the spectra obtained in the Raman shift range of 100-1500 cm^{-1} are shown in Figure 39b; In the spectrum of the untreated and treated eggshell, the typical bands of calcite ($CaCO_3$) mentioned in the literature (Sharma, 2007; Thomas et al., 2015) are also found at 154-155, 280-281, 712, and 1087 cm^{-1}. The spectrum of dye-adsorbed eggshell contains some characteristic bands of the dye as well (with a smaller or greater intensity, namely, 520, 581-582, 992-998, 1261, 1307, 1334, 1402 and 1437 cm^{-1}). The newly emerging bands typically correspond to aliphatic C–S bonds and N=N bonds (HORIBA, 2018).

4.2.2.2. Calcined eggshell surface chemistry before and after RBV-5R adsorption

Functional groups of calcined eggshells before and after adsorption were determined using Fourier transformations infrared spectroscopy in a wavelength range of 500 and 4,000 cm^{-1} (Figure 40). Typical peaks of calcite and CaO are found at 874, 1442, 1795 cm^{-1} wavelengths, 713 and 1050 cm^{-1} typically exhibit peaks of R-SO_2, functional groups on 2923 and 2853 cm^{-1} represent CH (Ejikeme et al., 2014; Patel, 2011; Slimani et al., 2014; Subramani S.E. and Thinakaran N., 2017).

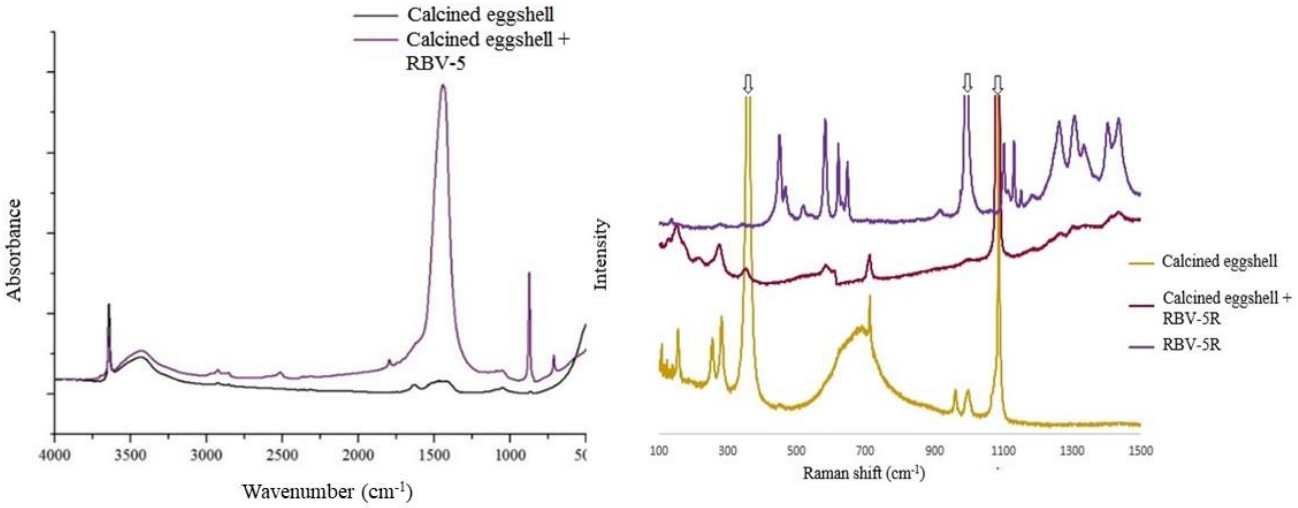

Figure 40. (a) FTIR and (b) Raman spectrum for control, 2 g/L RBV-5R dye adsorbed calcined eggshell and RBV-5R dye.

Figure 40b illustrates the spectra obtained in the Raman Shift interval between 100-1,500 cm^{-1}. The figure from top to bottom includes the calcined eggshell, RBV-5R dye adsorbed biomass and RBV-5R fabric dye spectra. Spectrums of the control and the dye adsorbed calcined eggshells contained peaks of calcite described in literature (Ho and McKay, 1999; P. Vinayan et al., 2016) at 150-154, 712-711, 1087-1086 cm^{-1}. Peaks at 281-274 and 3618 cm^{-1} represent $Ca(OH)_2$. We also observe the characteristic peaks of the dye on the dye-adsorbed biomass sample: 582, 1261-1262, 1307-1306, 1437-1435 cm^{-1}. Newly emerging peaks may be suitable for aliphatic C-S, N=N bonds (Ribeiro et al., 2017).

4.2.3. Thermal stability and textural property

Materials can change their physical and chemical properties due to heat, and thermal analyses can be used to test these properties. During the process, the eggshell biosorbent properties were investigated as a function of elapsed time or temperature variation. The most important ingredient of eggshell is calcite with a known decomposition temperature of 900 °C (Wang and Jehng, 2011). But at this temperature we found gray/black residues in the sample. Figure 40 made with Proteus software shows the TG-thermogravimetric curve and the DTA differential thermal analysis curve (which gives the heat flow at the temperature).

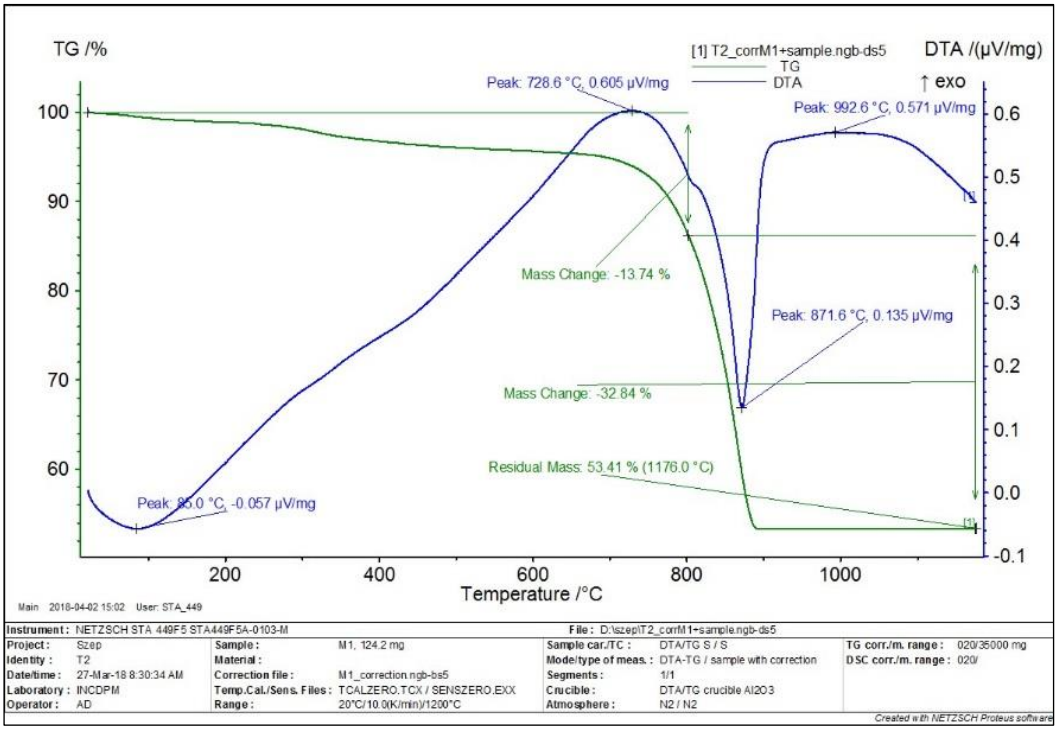

Figure 40. Thermogravimetric measurements (Created with NETZSCH Proteus software): TG - Thermogravimetry, DTA - Differential Thermoanalytics.

Based on the TG curve (green curve), there are two main mass losses owing to temperature, below 800 ºC and in the range 800-900 ºC. In the first case, mass loss can be explained with the disappearance of adsorbed water molecules and organic compounds. In the second case, the main weight loss corresponds to 32.84% by weight when the $CaCO_3$ phase is transformed into a CaO phase. Since the mass of the sample remained constant after 900 °C, we can assume that the transformation is complete (N. Tangboriboon et al., 2012; Ramesh et al., 2018). According to the DTA curve, decomposition occurs at 728.6 ºC, which is the maximum temperature at which endothermic phenomenon (heat is required for the process) or decomposition occurs.

Total surface area (St), pore volume (Vp) and pore radius (Rm) were calculated, and eggshell density was also determined with ethanol. The surface area of 160 µm pore size eggshell powder was 1.8 m^2/g, the pore volume was 0.01 cm^3/g and the density (ρ) was 1.3 g/cm^3. The pore radius presented a multimodal mesoporous-macroporous pore size distribution, with three different size regions: 20-30 Å, 60-80 Å and 200 Å. For eggshell powder with a 315 µm pore size, the surface area was below 1 m^2/g and could not be evaluated. Based on the values obtained in the BET surface and Dollimore–Heal method, listed in Table 5, it can be observed that after the adsorption the surface area (S_t) of the calcined eggshell decreased, thus dye molecules had become incorporated into the pores. Moreover, we can see that the pore volume (V_p) also decreased after dye adsorption.

Table 5. Eggshell surface area and pore volume

Sample	S_t (m^2/g)	Vp (cm^3/g)
Control calcined eggshell	3.0	0.015
Dye adsorbed calcined eggshell	1.7	0.012

The size distribution of the pore bars of the two samples is shown in Figure 41. Figure 41a shows the multimodal mesoporous and macroporous structure of untreated calcined eggshell having three main ranges for the pore radius: 21-20 Å, 110 Å and 280 Å. The first two are located in the mesoporous region and the last one is in the small macroporous region.

As for the sample after the adsorption, due to the small value of the surface, the pore size analysis is not very accurate, but there are two types of pores with radius of about 30 Å and 90 Å. For values above 150 °C, the pore radius cannot be calculated due to the nitrogen condensation between the material particles.

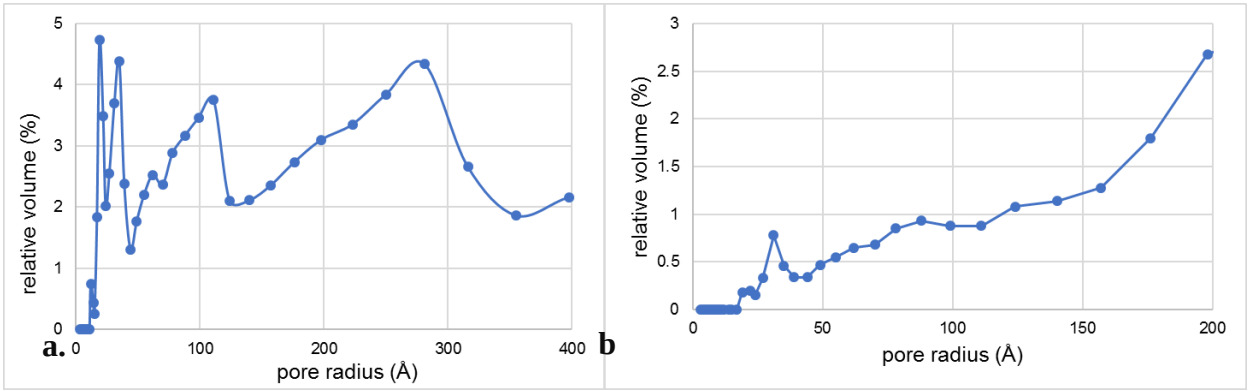

Figure 41. Pore size distribution (a) control (b) dye adsorbed calcined eggshell.

4.3. Mathematical models

4.3.1. Adsorption isotherms

The determination of the most appropriate adsorption equilibrium correlation, isotherm and kinetic model is essential to understand new biosorbents and to achieve the ideal adsorption system. The study of these mathematical models is crucial for reliable prediction of adsorption parameters and constants. Furthermore, these empirical models provide information on quantitative comparisons of adsorbent behavior, in case a comparison with other studies, adsorbent systems or research and experimental conditions is desired. Equilibrium relationships, commonly referred to as adsorption isotherms, describe in perspective how pollutants interact with adsorbents. They are critical for optimizing the adsorption mechanism pathways. Models must be studied to express the surface properties and capacities of adsorbents and to design adsorption systems efficiently (Suwannahong

et al., 2021; Wang and Guo, 2020). The knowledge of the adsorption equilibrium is one of the most important information, because it allows to know and understand an adsorption process. The adsorption isotherms can be used to know the type of adsorption (physical or chemical nature), the surface properties of the adsorbent (homogeneous or heterogeneous surface). The adsorption capacity can be calculated and compared with the results obtained experimentally. Finally, an equilibrium relationship between the adsorbent (powdered-, calcined eggshell and yeast) and the adsorbate (CR, BPB, MB, MG, RBV-5R, RR, RB dyes) can be established and identified. Consequently, the investigation of the isotherms and kinetics is a critical part of adsorption research, as their understanding and interpretation can provide insight into the adsorption mechanism, thus ensuring the optimization and efficient design of the system.

Recently, one of the most used methods is linear regression analysis, which reveals the best-fitting models. The linear regression method quantifies the distribution of adsorbed substances, analyses the adsorption system, and checks the consistency of the theoretical assumptions of the adsorption isotherm model (Ayawei et al., 2017). To calculate or predict the parameters of the four most frequently used isotherm models (Langmuir, Freundlich, Temkin, Dubinin-Radushkevich), the equations of each model were converted to linear form using the linear least squares method.

Table 6 contains the calculated parameters characteristic to each isotherm model. As shown in Table 5 MB fits the Dubinin-Radushkevich isotherm model more closely, which indicates that chemical adsorption also occurs, ion exchange happens, similar results were obtained using walnut as biosorbent for MB removal (Tang et al., 2017). In case of MG the liner regression coefficients are very near values but it aligned closer to Freundlich isotherm model, Santhi et al. got Freundlich isotherm as well by studying MG adsorption on prawn waste (Santhi et al., 2009). In case of BPB and Congo Red the adsorption process can be described by Langmuir isotherm model.

Based on the correlation coefficients calculated for RBV-5R and powdered eggshell adsorption (Langmuir: 0.945, Freundlich: 0.839, D-R.: 0.563 and Temkin: 0.709) obtained from plotting the linearized isotherms, the Langmuir isotherm model fits best, with high accuracy. The Langmuir isotherm model indicates that adsorption took place in the specific homogenous sites of the eggshell; it assumes that once an adsorbed molecule occupies the available eggshell adsorption sites, no more adsorptions can occur on the surface sites of the material. Furthermore, we reach maximum adsorption when a saturated monolayer appears on the eggshell surface. The model cannot provide a solid and clear depiction or understanding of the mechanical phenomena, but it gives the adsorption capacity value, which is 9.94 mg/g in this study (Abbas et al., 2018).

Table 6. Adsorption isotherm models calculated constants for dye adsorption onto eggshell

	Langmuir			Freundlich			Dubinin-Radushkevich			Temkin		
	K_L (L/mg)	q_{max} (mg/g)	R^2	n	K_f ($mg^{(1-1/n)}L^{1/n}/g$)	R^2	β ($mol^2 kJ^2$)	E (kJ/mol)	R^2	A_T (L/g)	B (J/mol)	R^2
Powdered eggshell												
MB	0.04	0.87	0.911	0.78	36.9	0.93	9×10^{-6}	0.24	0.99	2.36	2×10^{-5}	0.989
MG	0.33	2.13	0.856	2.09	1.46	0.965	3×10^{-7}	1.29	0.955	2.53	7×10^{-5}	0.961
CR	3.75	1.22	0.999	2.5	1.02	0.996	4×10^{-8}	3.54	0.854	2.66	2×10^{-6}	0.917
BPB	0.59	0.04	0.827	1.02	1.23	0.811	8×10^{-7}	2.89	0.755	2.13	2×10^{-7}	0.803
RBV-5R	0.093	9.935	0.945	1.589	1.09	0.839	2×10^{-6}	0.5	0.563	2.4	4×10^{-5}	0.709
Calcined eggshell												
RBV-5R	0.133	16.95	0.924	1.388	2.31	0.678	2×10^{-7}	1.58	0.833	2.4	3×10^{-5}	0.282
RR	0.71	10.87	0.88	0.987	3.251	0.879	3×10^{-13}	1291	0.988	2.4	3×10^{-5}	0.282
RB	0.86	8.92	0.928	1.43	4.16	0.83	2×10^{-12}	500	0.754	2.5	5×10^{-5}	0.71

Similar tendency was observed in case of RBV-5R and calcined eggshell adsorption (Langmuir: 0.924, Freundlich: 0.678, D-R.: 0.833 and Temkin: 0.282), assuming that the adsorption is reversible, monolayer. The surface of the adsorbent, in this case calcined eggshell, has a homogeneous, uniform strength with a constant number of binding centers that incorporate only one molecule into a binding site.

As shown in Table 3, the linear regression coefficient of RR is highest (R^2=0.988) in the case of the Dubinin-Radushkevich isotherm model. The D-R model is an empirical adsorption model, which presumes a multilayer character, where Van der Waal's forces occur between the adsorbent (calcined eggshell) and adsorbate (RR dye). It is applicable for physical adsorption processes and describes the adsorption on microporous adsorbents. On the other hand, in case of RB dye the Langmuir isotherm model shows better fitness, R^2 being 0.987.

In case of RR dye removal with brewery's yeast, the results were used to rank the best-fit models: Langmuir I. (R^2=0.923) > Freundlich (R^2 = 0.921) > Temkin (R^2 = 0.898) > Langmuir II. (R^2=0.892) > Dubinin-Radushkevich (R^2 = 0.712) > Langmuir III. (R^2=0.571) > Langmuir IV. (R^2=0.508). It is observed that under our experimental conditions, the Langmuir isotherm fits the equilibrium data with higher accuracy among the linear models. However, there was only a small difference compared to the Freundlich model. The Langmuir model assumes that the adsorption is monolayer, whereas the Freundlich model suggests that the active sites and the energy are exponentially distributed. For the Langmuir I. model, the separation parameter, R_L was calculated; the value of R_L indicates the type and favorability of the isotherms, i.e. irreversible if R_L = 0;

favorable, when $0 < R_L < 1$; linear, when $R_L = 0$; or unfavorable if $R_L > 1$. We found that R_L ranges from 0.13 to 0.97 (determined for 16 initial concentrations in the range 5 to 1,000 mg/L), indicating favorable adsorption. At high concentrations, the R_L values were close to the lower acceptable range, indicating a high degree of irreversibility. At higher concentrations, we obtained R_L values close to 1 $R_{L\text{-}5mg/L}$=0.97, $R_{L\text{-}10mg/L}$=0.94.

Another similar characteristic of all the experiments conducted is that B – Temkin constant is less than 20 kJ/mol and E – energy is less than 8 kJ/mol. We can therefore assume that the adsorption occurs by physisorption, forming weak van der Waals interactions in a single-layer adsorption surface with equivalent binding sites.

4.3.2. Adsorption kinetic and diffusion models

To better understand the mechanism of dye adsorption on eggshell and to find the best-fitting model to describe our obtained data, various kinetic models were applied. The kinetic adsorption models establish the effect of time on adsorption and determine the rate of dye removal. Experimental data were analyzed using pseudo-first-order (Lagergren) and pseudo-second-order (Ho & McKay) kinetic models. From Table 7 we can see that for all dye adsorption data, the constant values of McKay pseudo-second-order kinetic models showed the best fit.

Table 7. Kinetic data of dye adsorption on eggshell surface

CR		Pseudo-first-order			Pseudo-second-order			*MB*		Pseudo-first-order			Pseudo-second-order		
C (mg/L)	q_e (exp) (mg/g)	k_1 (1/t)	q_e (calc) (mg/g)	R^2	k_2 (g/mg×t)	q_e (calc) (mg/g)	R^2	C (mg/L)	q_e (exp) (mg/g)	k_1 (1/t)	q_e (calc) (mg/g)	R^2	k_2 (g/mg×t)	q_e (calc) (mg/g)	R^2
10	0.33	-0.06	0.36	0.604	0.71	0.99	0.996	10	0.2	-0.04	0.11	0.118	-5.59	0.61	0.997
20	0.63	-0.04	0.53	0.847	0.42	1.91	0.999	20	0.44	-0.03	0.09	0.159	0.42	1.91	0.999
30	0.92	-0.02	0.65	0.742	0.24	2.75	0.999	30	0.76	-0.12	0.61	0.714	0.24	2.75	0.999
40	1.24	-0.03	0.91	0.844	0.18	3.73	0.999	40	0.88	-0.08	0.33	0.292	0.18	3.73	0.999
50	1.53	-0.01	0.77	0.555	0.12	4.67	0.999	50	1.07	-0.07	0.29	0.144	0.12	4.67	0.999
BPB		Pseudo-first-order			Pseudo-second-order			*MG*		Pseudo-first-order			Pseudo-second-order		
C (mg/L)	q_e (exp) (mg/g)	k_1 (1/t)	q_e (calc) (mg/g)	R^2	k_2 (g/mg×t)	q_e (calc) (mg/g)	R^2	C (mg/L)	q_e (exp) (mg/g)	k_1 (1/t)	q_e (calc) (mg/g)	R^2	k_2 (g/mg×t)	q_e (calc) (mg/g)	R^2
10	0.04	-0.02	0.06	0.731	2.45	0.11	0.995	10	0.39	0.03	0.05	0.022	-5.92	1.07	0.999
20	0.07	-0.03	0.29	0.262	0.21	0.42	0.919	20	0.71	-0.02	0.12	0.137	-36.46	2.14	0.999
30	0.09	-0.07	0.55	0.935	0.25	0.68	0.991	30	1.11	-0.08	0.25	0.276	8.89	3.3	0.999
40	0.08	-0.03	0.61	0.946	0.11	0.73	0.997	40	1.48	-0.03	0.28	0.05	-18.53	4.31	0.999
50	0.06	-0.06	0.39	0.978	0.4	0.52	0.976	50	1.59	-0.05	0.18	0.073	-34.7	4.71	0.999
RBV-5R + powdered eggshell		Pseudo-first-order			Pseudo-second-order			*RBV-5R + calcined eggshell*		Pseudo-first-order			Pseudo-second-order		
C (mg/L)	q_e (exp) (mg/g)	k_1 (1/min)	q_e (calc) (mg/g)	R^2	k_2 (g/mg×min)	q_e (calc) (mg/g)	R^2	C (mg/L)	q_e (exp) (mg/g)	k_1 (1/min)	q_e (calc) (mg/g)	R^2	k_2 (g/mg×min)	q_e (calc) (mg/g)	R^2
20	2.34	1.04×10^{-2}	1.546	0.97	1.30×10^{-2}	1.988	0.98	20	1.29	0.534	1.43	0.839	6.842	1.946	0.9999
40	5.68	1.31×10^{-2}	3.136	0.987	1.46×10^{-2}	3.634	0.995	40	2.45	0.019	1.67	0.459	0.553	3.678	0.9997
60	16.57	0.97×10^{-2}	4.379	0.942	0.43×10^{-2}	4.715	0.981	60	3.71	0.014	2.12	0.521	0.174	5.571	0.9997
80	12.5	0.94×10^{-2}	4.802	0.96	0.62×10^{-2}	6.978	0.996	80	5.71	0.052	1.07	0.453	0.246	7.806	0.9999
100	18.98	1.14×10^{-2}	8.71	0.896	0.29×10^{-3}	8.666	0.987	100	6.47	0.022	1.64	0.519	0.133	9.728	0.9999
RR		Pseudo-first-order			Pseudo-second-order			*RB*		Pseudo-first-order			Pseudo-second-order		
C (mg/L)	q_e (exp) (mg/g)	k_1 (1/min)	q_e (calc) (mg/g)	R^2	k_2 (g/mg×min)	q_e (calc) (mg/g)	R^2	C (mg/L)	q_e (exp) (mg/g)	k_1 (1/min)	q_e (calc) (mg/g)	R^2	k_2 (g/mg×min)	q_e (calc) (mg/g)	R^2
20	1.3	0.04	1.05	0.373	6.88	1.3	1	20	1.32	0.35	0.37	0.808	9.7	1.32	1
40	2.62	0.13	0.6	0.526	5.58	2.62	1	40	2.62	0.14	0.36	0.578	3.66	2.62	1
60	3.94	0.11	0.36	0.41	0.47	0.95	0.984	60	3.92	0.46	-1.22	0.857	0.58	1.25	0.999
80	5.24	0.1	-0.28	0.435	1.39	5.26	1	80	5.28	0.04	-1.25	0.759	0.43	5.29	1
100	6.51	0.33	-0.71	0.566	1.8	6.54	0.999	100	6.56	0.13	-0.09	0.862	0.23	6.59	1

The quantity in equilibrium from experiments q_e(exp) in some cases is very close or similar to the quantity in equilibrium calculated q_e(calc) value from the, this shows the adequacy of experimental measurement data to pseudo-second-order kinetic model (Costa and Paranhos, 2019).

Intra-particle and liquid film diffusion rate constants and linear regression coefficients were calculated in case of RBV-5R dye adsorption on the surface of eggshell. Based on the literature data, three regions can be observed if we study intra-particle diffusion: (1) diffusion of RBV-5R molecules through the solution to the external surface of eggshell; (2) transport of RBV-5R molecules to the intra-particle active sites; and (3) adsorption of RBV-5R molecules to the eggshell intra-particle active sites. The obtained results (*D*-pore diffusion coefficient values ranging between 1.7×10^{-10} and 3.6×10^{-10} cm^2/s), as well as the fact that the intercept points do not pass through the origin, lead to the conclusion that the two diffusion models are not rate-determining steps, and only the biosorption process affects adsorption speed. Table 8 summarizes the calculated parameters for each diffusion model (intra-particular, liquid film), namely the linear regression coefficients, intersects, velocity values, and particle diffusion coefficient (D).

Similar trend was observed in case of RBV-5R dye adsorption on the surface of calcined eggshell. The pore diffusion coefficients range from 6.60×10^{-9} to 9.09×10^{-8} cm^2/s by varying the concentration. It can also be observed that none of the incisions pass through the origin of any diffusion model. It can be concluded that during the binding of the dye on the surface of the eggshell, the intra-particle section is not rate-determining, nor does the liquid film diffusion affect the adsorption process (Bello and Ahmad, 2011; Mohadi et al., 2016). In summary, the speed of the process is only determined by biosorption.

Table 8. Parameters of diffusion models

RBV-5R + powdered eggshell		**Intra-particle diffusion**			**Liquid film diffusion**		
C (mg/l)	**D (cm^2/s)**	**k_{ip} ($mg/g\cdot min^{1/2}$)**	**intercept**	**R^2_{ip}**	**k_{fd} (1/min)**	**intercept**	**R^2_{fd}**
20	1.77×10^{-10}	0.101	0.212	0.917	0.007	-0.29	0.904
40	3.63×10^{-10}	0.152	0.928	0.915	0.014	-0.31	0.988
50	2.21×10^{-10}	0.193	0.684	0.939	0.012	-0.07	0.89
60	1.38×10^{-10}	0.196	0.511	0.98	0.003	-0.25	0.959
80	2.94×10^{-10}	0.257	1.562	0.937	0.005	-0.45	0.949
100	1.70×10^{-10}	0.352	1.308	0.963	0.004	-0.33	0.959
RBV-5R + calcined eggshell		**Intra-particle diffusion**			**Liquid film diffusion**		
C (mg/l)	**D (cm^2/s)**	**k_{ip} ($mg/g\cdot min^{1/2}$)**	**Intercept**	**R^2_{ip}**	**k_{fd} (1/min)**	**Intercept**	**R^2_{fd}**
20	9.09×10^{-8}	0.06	1.088	0.746	0.399	-2.08	0.841
40	1.39×10^{-8}	0.012	2.287	0.218	0.018	-2.86	0.666
60	6.60×10^{-9}	0.028	3.326	0.334	0.001	-2.59	0.508
80	1.31×10^{-8}	0.151	3.776	0.375	0.059	-2.31	0.819
100	8.86×10^{-9}	0.169	4.579	0.418	0.019	-2.19	0.506

4.3.3. Artificial neural network (ANN)

Since OUTPUT=TARGET+0.0100 (received from the program and shown in Supplementary Fig. S2a), our network has a good performance, and it predicts with high precision. The network topologies of the input, middle and output components are shown in Figure S3. The network exhibited a significant weight distribution of negative values for the initial concentration and the pH and eventually the time; simultaneously, high positive input weights were observed for the initial concentrations, biomass weight and pH. Our results show a succession of sensitivity, which determines the network's main weights, giving a hierarchy of the most influential parameters: initial concentration → pH → biomass weight → contact time → particle size → temperature. Similar results were reached by (Hassani et al., 2014; Indolean et al., 2017; Török, 2015).

4.5. Possible mechanisms

4.5.1. RBV-5R dye adsorption on eggshell surface

Based on our current knowledge, no binding process or mechanism between the eggshell and the dye has been described explicitly in any research article. Relying on our results and the little information found in the literature, we formulate our ideas about possible processes. The mechanism of RBV-5R dye, as with any dyestuff's adsorption on eggshell or different adsorbent surfaces, highly depends on the physical and chemical characteristics of the adsorbent and dye. Therefore, a high range of parameter changes and analytical measurements were carried out, as discussed in the previous sections.

The initial pH of the solution is an important factor for adsorption processes. The pH can alter the chemical balance of the ions present both in the RBV-5R dye and eggshell adsorbent; thus, the pH influences the electrostatic interactions between the dye and sorbent. The organic matter of eggshell comprises various functional groups, such as hydroxyl, amine, and carbonyl groups. When the eggshell powder was mixed with the dye solution, calcium salts may partially dissolve and release Ca^{2+}, HCO_3^-, CO_3^{2-} and OH^- ions, which can form a negatively surfaced charge (Abdel-Khalek et al., 2017; Parvin et al., 2019). In acidic media (HCl), the eggshell surface exhibits a positive charge, so there is a high electrostatic attraction between the eggshell powder and the anionic, negatively charged dye (this dye contains aromatic rings such as phenolic OH and sulfonate SO_3^- groups that ionize in aqueous solution and form coloured anions (Ribeiro et al., 2017)). By adding NaOH, the number of negatively charged sites of eggshell increases, resulting in electrostatic repulsion.

The adsorption mechanism was studied by isotherm, kinetic and diffusion models. Since in our experimental conditions the Langmuir isotherm showed a better fit, adsorption takes place on a

homogenous surface, and monolayer adsorption occurs. In this case, we can calculate the R_L separation parameter (Parvin et al., 2019); the R_L value indicates the type and favorability of the isotherm to be irreversible (R_L=0), favorable (0<R_L<1), linear (R_L=0) or unfavorable (R_L>1). We found that 0.1<R<0.35, which suggested favorable adsorption; however, R_L values close to the lower acceptable range suggest high irreversibility. Constant calculations from the Temkin and Dubinin-Radushkevich models, as mentioned before, suggest the appearance of physisorption where weak van der Waals interactions are formed in a single-layer adsorption surface with equivalent binding sites. The physical nature and spontaneous and random characteristics of adsorption are suggested by the calculated thermodynamic parameters.

FTIR and Raman analyses (both for powdered eggshell and for different layers of eggshell) proved the presence of specific functional groups from organic and inorganic compounds such as $^{-}$OH, C=O, $=CH_2$, aromatic, –SH and –COOH groups. All these surface functional groups indicate that eggshell exhibits a moisture adsorption capability, which makes this material a potential adsorbent by participating in adsorption. FTIR spectra of RBV-5R showed bands that correspond to phenolic O–H, aromatic C–H, amide N–H, aliphatic C–H_n, amide C=O, C=C, N=N, R–SO_3^- and C–S functional groups (Ribeiro et al., 2017).

The results obtained from the pH studies and FTIR/Raman analyses indicate that adsorption occurred mostly via electrostatic attraction, where the protonated eggshell surface attracted the anionic dye sulfonate group. Considering two previous articles (Chatterjee et al., 2007; Ribeiro et al., 2017), three possible interactions can be between the dye and adsorbent: hydrogen bonding between hydroxyl groups of eggshell and electronegative residues of RBV-5R; ionic interactions at pH values where surface charge is neutral and physisorption occurs; and π-electron resonance.

4.5.2. RR dye adsorption on yeast

In our research, we used yeast (lyophilized) residues from the production of a brewery in Romania to remove organic dye from water. After the fermentation cycle, the available biomass can contain both living and dead cells. Live yeast cells can perform the stain removal in two different ways. The dye is adsorbed on the cell wall of the yeast, penetrates the cell wall, accumulates inside the cell or biodegradation can occur by various enzymes (oxidases and reductases). Irrespective of the nature of the yeast cell (living or dead), biosorption occurs between the contaminant (RR dye) and the yeast cell wall, which can be by electrostatic interaction, complexation, chelation and microprecipitation, ion exchange or physical and chemical adsorption, depending on a number of factors (Danouche et al., 2021).

The mechanism of dye biosorption on yeast is complex and not fully understood, is a sophisticated and multi-faceted process, and may involve more than one mechanism (Castro et al., 2017). The

biosorption capacity of yeast cells and the mechanism of dye removal may be influenced by the nature of the biomass (living or dead yeast cell), the functional groups on the cell wall, the number of reactive binding sites and their availability, and the affinity (i.e. binding strength) between the sites and the dye. The nature of the dye molecule (anionic or cationic), the physico-chemical conditions of the adsorption treatment (contact time, impurity concentration, amount of yeast, pH, temperature) (Sahoo and Prelot, 2020). In recent years, early biosorption studies have mostly used living cells, but it has been found that dead yeast cells may have the same or even higher binding capacity (Wang and Chen, 2006).

Some studies have described the structure and components of the *S. cerevisiae* yeast cell and the functional groups that occur on its surface. Its composition includes proteins, amino acids, polysaccharides and lipids. Accordingly, carboxyl, hydroxyl, amide, amino, phosphate and other charged groups have been identified, which show strong binding forces with the dye molecules. It has been shown that the biosorption process can also be achieved by chelation and the formation of ionic bridges between the dye molecules and the functional groups.

Depending on the type of interaction between the adsorbent surface and the contaminant, the biosorption process can be divided into two types: (i) chemical adsorption, an irreversible process resulting in the formation of strong chemical bonds; and (ii) physical adsorption, which is reversible, in most cases characterized by weak van der Waals forces, H-bonds, polarity and dipole-dipole H-bonding interactions. Furthermore, FTIR studies have demonstrated that Yoshida H-bonding, dipole-dipole H-bonding, π-π and n-π interactions can occur upon adsorption of dye molecules on yeast cells (Figure 42 shows a possible general mechanism) (Danouche et al., 2021).

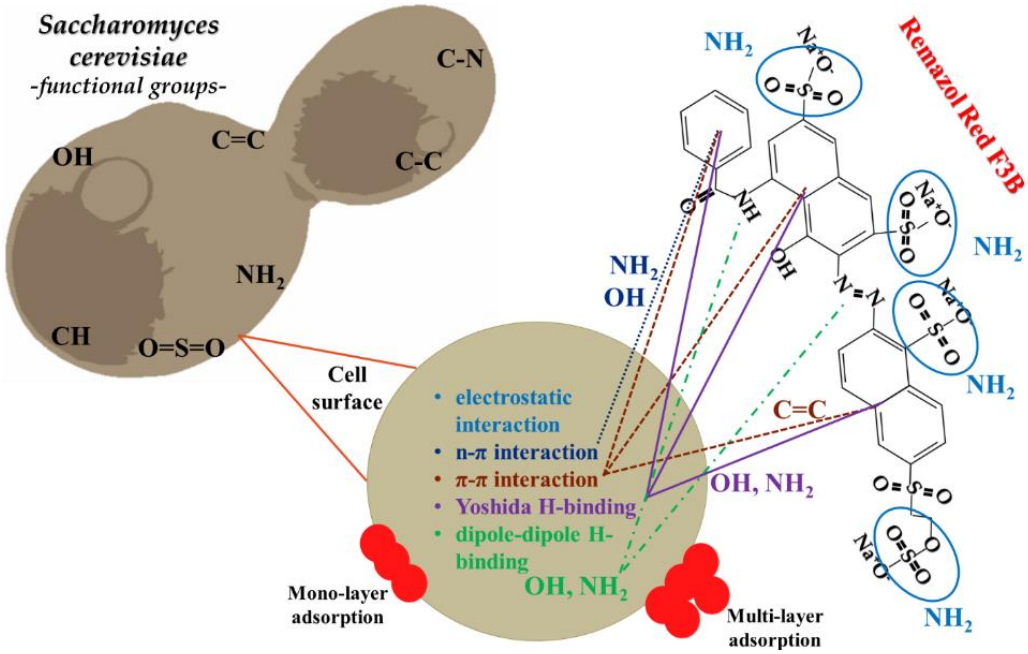

Figure 42. Proposed interaction of RR dye with *Saccharomyces cerevisiae* brewery's yest.

4.5.3. Eggshell as an adsorbent – advantages and disadvantages

Eggshell as waste contributes to pollution (Abdulrahman et al., 2014) when disposed of in landfills due to its rich protein content because it serves a source for biocontamination. The messy holding containers in which eggshell waste is stored can have an unpleasant odour, which can affect nearby neighbourhoods, causing air pollution.

The eggshell adsorbent employed was used without any physical or chemical treatment, avoiding special sophisticated methods, instruments, or controlled conditions (pH, temperature). In case of RBV-5R adsorption on powdered eggshell, the material was efficient even for high dye concentration elimination (E=81% in case of C_i=100 mg/L), where the adsorption capacity was 8.1 mg/g. Particle size was the most significant influencing parameter regarding the efficacy of the adsorbent.

A comparison is almost impossible due to the different base materials of the adsorbents as well as different contaminants and processing conditions. On the other hand, we investigated the adsorption of this same dye (RBV-5R) with calcined eggshell under the same conditions (C_i=20 mg/L, 1.5 g/100 mL biomass, 160 μm, 700 rpm, pH =6.0±0.2, T=20±2 °C), which exhibited an adsorption efficiency of 96.83% and adsorption capacity of 1.29 mg/g, reaching equilibrium within 30 minutes.

Overall, in addition to the disadvantages, the use of eggshells as an adsorbent will not only reduce the pollution effect of the waste but also help in the water cleaning process as a new value-added product. The practice of using untreated eggshell waste as a low-cost adsorbent for wastewater treatment could contribute to a more sustainable and successful management of this biowaste.

4.7. Effectiveness and Characterization of Novel Mineral Clay in Cd^{2+} Adsorption

4.7.1. Characterization of Cosmetic Clay

4.7.1.1. SEM and EDS

Scanning electron microscopy was used to investigate the micromorphology and structural peculiarities of ACC. Figure 43 shows the ACC adsorbent before (Figure 43a–c) and after (Figure 43d–f) adsorption with Cd^{2+}. The porous structure of ACC can be seen in Figure 43a, moreover, it shows that the surface of the adsorbent is filled with 10–300 μm holes. On the other hand, the SEM image of the sample that adsorbed Cd^{2+} shows slightly distinct morphology. The porous structure of ACC disappeared after adsorption, the surface is smoother, and some aggregates appear on the surface.

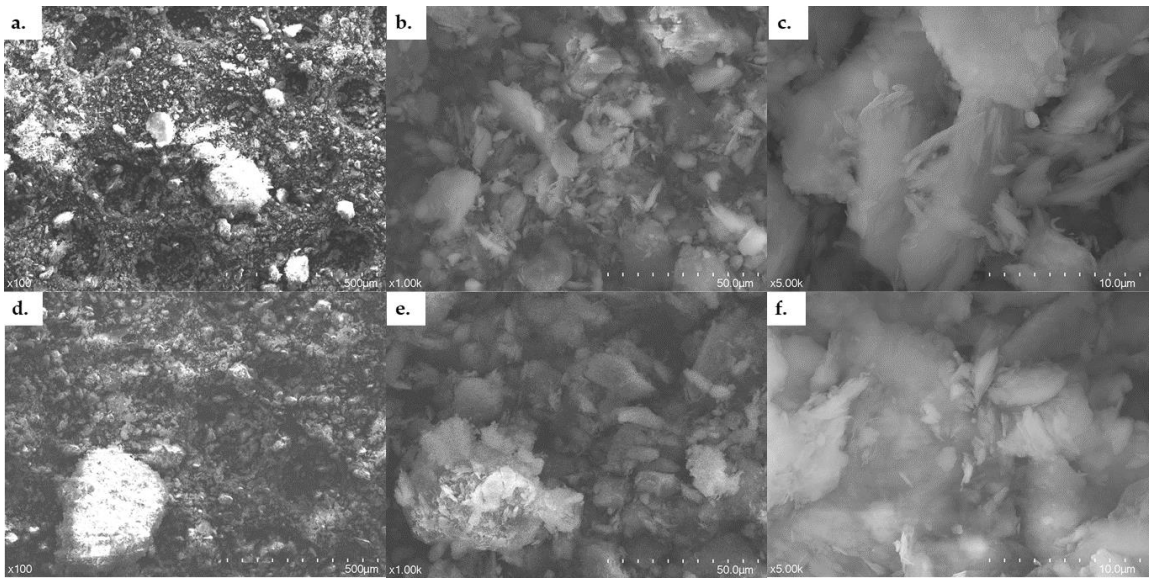

Figure 43. SEM (**a**–c) control and (**d**–**f**) 2 g/L Cd^{2+} adsorbed ACC.

From EDS results, we can conclude that ACC contains a relatively high percentage of Al (W_t(%) = 11.4 ± 0.9) and Si (W_t(%) = 13.7 ± 1.4), moreover Mg (W_t(%) = 0.2 ± 0.01), K (W_t(%) = 1.5 ± 0.2), Ti (W_t(%) = 0.4 ± 0.03), and Fe (W_t(%) = 0.6 ± 0.1), in small quantities. Therefore, it can be affirmed that ACC is an alumina-silicate mineral. This result corresponds to the elemental composition described on the product packaging and in the patent. After the adsorption process: Al (W_t(%) = 12.0 ± 0.4) and Si (W_t(%) = 14.4 ± 0.7), moreover Mg (W_t(%) = 0.2 ± 0.01), K (W_t(%) = 1.5 ± 0.1), Ti (W_t(%) = 0.5 ± 0.03), and Fe (W_t(%) = 0.6 ± 0.1), the clay adsorbed the Cd^{2+} ions from the polluted water. This can be seen from the EDS results, where Cd^{2+} appears in the sample (W_t(%) = 0.2 ± 0.01).

An example from another study, where H. Es-sahbany et al. studied the removal of Ni with the help of clay taken from the Ain Dorrij—Ouezzane region of Morocco. The results of elemental composition of the clay material contained Ca (20.65 ± 0.08%), Si (12.7 ± 1.9%), Al (8.3 ± 0.3%), Ti (0.34 ± 0.01%) and Fe (4.83 ± 0.02%). The used clay mainly consisted of kaolinite, chlorite phase and slight amount of quartz (Es-sahbany et al., 2021).

4.7.1.2. Surface characteristics - FTIR

FTIR spectrum of ACC presenting the peculiar bands is shown in Figure 44 between the range of 1800 cm^{-1} to 400 cm^{-1}. The investigation of cosmetic clay as a suspension in deionized water presents many characteristic bands. First of all, two broad bands not represented on the figure were seen around 3697 and 3620 cm^{-1} attributed to hydroxyl stretching. However, spectral bands at 1105, 1031, and 1008 cm^{-1} according to (José Eduardo Ferreira da Costa Gardolinski, 2005) were

assigned to Si-O-Si and Si-O stretching, and most of the silicate minerals contain them. Our study's result is also in correspondence regarding the bond at 912 cm^{-1} with the literature, being assigned the deformation of the Al-OH bonds. At a lower spectral range, the bands are more complicated to define. Usually, the remaining bonds correspond to the vibration of the Si-O bond (Kostin et al., 2015). Bonds at 796 cm^{-1} could be assigned to a hydroxyl translation mode, while 754, 696, and 537 cm^{-1} could be ascribed to Si-O stretching and Al-O-H deformations and Si-O-Al translation mode. At the lower range, 472 and 420 cm^{-1} bands to ν6 (e) and ν3 (a1) modes of the SiO_4 tetrahedra. Moreover, the band at 430 cm^{-1} could be attributed to O-Al-O bending with a minor contribution of O-Si-O bending (Frost et al., 1997, 1993; Frost and Vassallo, 1996; Johansson et al., 1998). After the adsorption with Cd^{2+} solution made from $Cd(NO_3)_2 * 4H_2O$ salt, a particularly strong vibration was observed at 1384 cm^{-1} that can be attributed to NO_3 asymmetric stretching (Chen et al., 2014; José Eduardo Ferreira da Costa Gardolinski, 2005; Nekhlaoui et al., 2021; Niño et al., 2013).

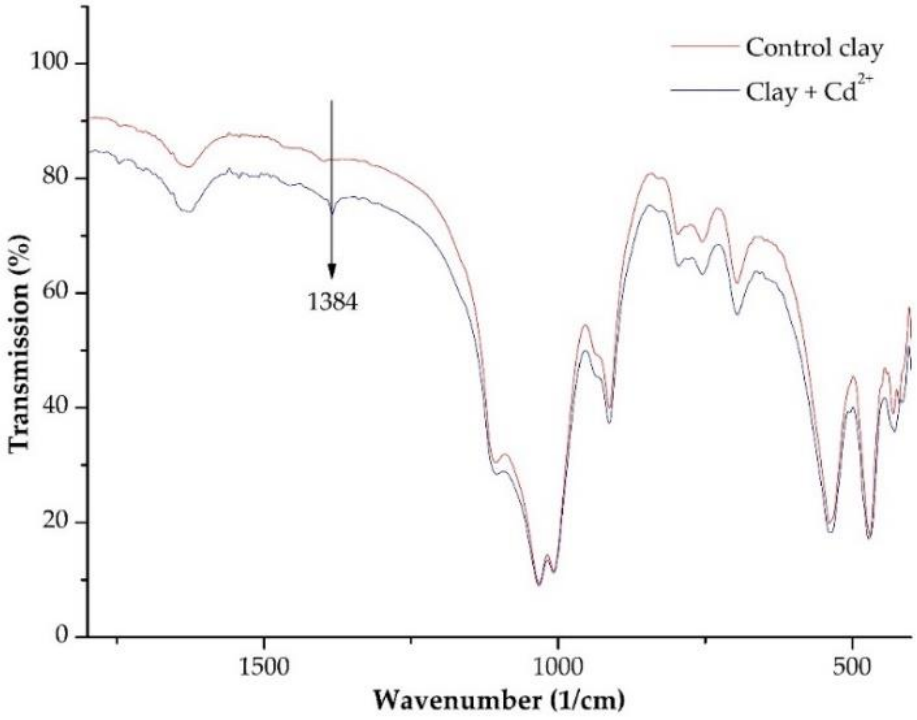

Figure 44. FTIR control and 2 g/L Cd^{2+} adsorbed ASLAVITAL clay.

4.7.1.3. Crystalline structure - XRD

Since soil, rocks, dust and clay samples contain various highly crystalline components, the XRD is a proper analysis that can be used to highlight the mineral composition of the studied ACC. Comparing the two patterns, namely Clay + Cd^{2+} and Control clay (Figure 45a) shows a high similarity, with both samples having high crystallinity.

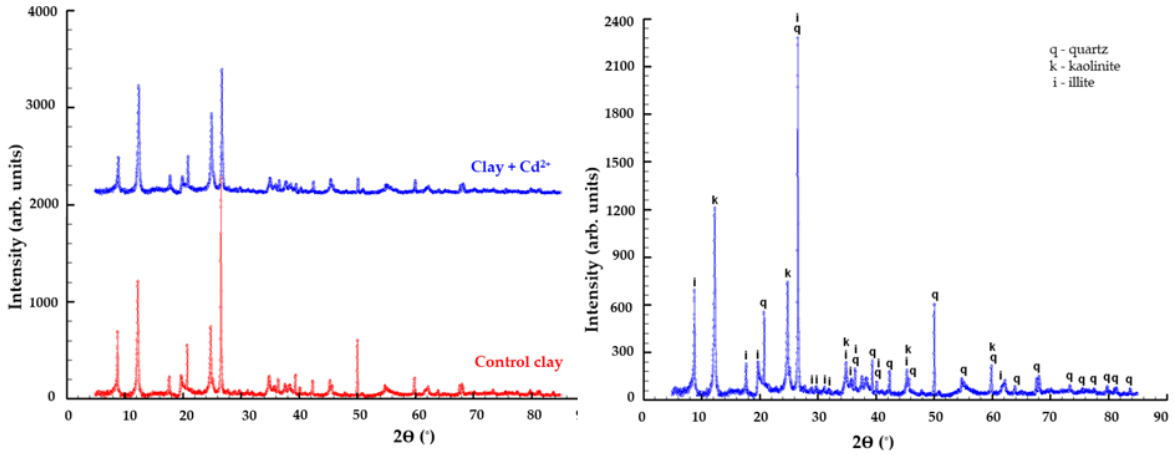

Figure 45. (a) X-ray powder diffraction comparison of the two samples (b) Diffraction pattern of ACC showing the crystalline phases (q-quartz, i-illite and k-kaolinite).

In order to highlight the existence of different crystalline phases contained in the samples (Figure 45), the diffraction patterns were investigated using the Match software, which has its incorporated database. In this sense, the analysis of Control clay revealed that the sample contains three major components. As expected, the sample being clay contains silicon oxide-SiO_2 (in the form of quartz). The other two identified components are phyllosilicate minerals, based on silicate groups. One phase is Potassium Aluminium Silicate Hydroxide-$(KH_3O)Al_2Si_3AlO_{10}(OH)_2$, known as a form of illite and Aluminium silicate hydroxide-$Al_2Si_2O_5(OH)_4$ known as kaolinite. Figure 45 (for Control clay sample) specified each diffraction line to which of the three phases it belongs by the following notations: q-quartz, i-illite and k stands for kaolinite. The following database reference codes were used in the actual identification: 99-201-2847 for quartz, 99-200-3858 for kaolinite and 00-026-0911 for illite.

4.7.1.4. Surface characteristics - Raman Spectroscopy

In the control sample (Figure 46), the most intense Raman band was detected around 146 cm^{-1}. Weaker Raman bands were identified at around 130, 200, 260, 333, 398, 426, 467, 511, 634, 702, 792 and 909 cm^{-1}. In the OH-region, Raman bands at ~3624, 3659, and 3702 cm^{-1} were detected.

The Raman spectra of the Cd-treated samples were identical to the control samples. The most intense Raman band was detected around 146 cm^{-1}. Several weak bands were also recognized at around 130, 198, 259, 334, 398, 426, 467, 511, 638, 705, 791 and 910 cm^{-1}. Additionally, at high frequencies, bands at 3624, 3658, and 3698 cm^{-1} were also identified. Rarely crystals with intense bands around 126, 200, 464 cm^{-1}, with weaker bands at 262, 365 cm^{-1} were also detected in both samples.

Based on the Raman spectra of the control and Cd-treated ACC powders, the following phases could be identified. The most intense Raman bands (~146, 200, 398, 511 and 638 cm^{-1}) are

characteristic of anatase (TiO_2), which is a typical phase detected in kaolinite-bearing clays (Murad, 1997). The weak Raman signals of kaolinite can be attributed to the observed bands at around 130, 259, 333, 426, 464, 704 m 791 and 910 cm^{-1} (Michaelian, 2011). The characteristic bands of hydroxyl groups found in kaolinite could also be detected near 3624, 3658 and 3700 cm^{-1} (Frost and Gaast, 1997). Rare crystals of quartz with intense bands at 126, 200 and 464 cm^{-1} could also be detected. Illite could not be directly detected with Raman spectrometry since it has overlapping peaks (Liu, 2001) with both quartz (~464 cm^{-1}) and kaolinite (~464 and ~705 cm^{-1}). Raman band, which can be associated with the absorption band of NO_3 (Cd solution was made from $Cd(NO_3)_2 * 4H_2O$ salt) on the FTIR could not be detected.

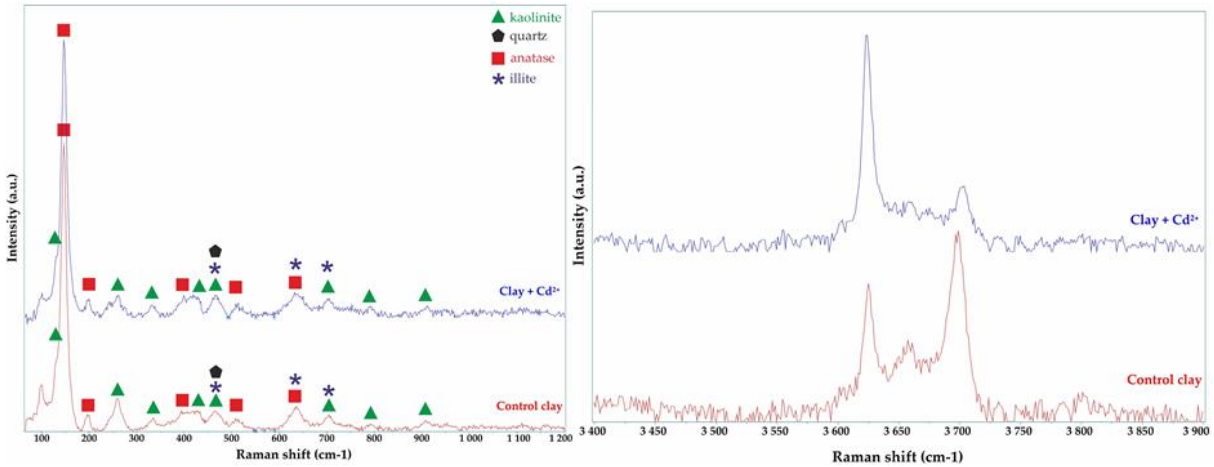

Figure 46. Representative Raman spectra of the control and 2 g/L Cd^{2+} adsorbed ACC.

4.7.2. Adsorption Experiments of Cd^{2+} and clay

Usually, the optimum of the operational parameters for an adsorption process is affected by many factors. However, one of the most important factors controlling adsorption performance could be the time when the Cd^{2+} ions are in contact with ACC adsorbent. Figure 47 shows the evolution in time of the Cd^{2+} removal from aqueous solution with the help of ASLAVITAL cosmetic clay. It can be observed that the initial concentration of contaminants decreases with time. All five concentrations exhibited a more rapid decrease rate initially, and then the adsorption rates tended to be flat. According to the literature, it is due to the rich number of active binding sites on the surface of the adsorbent (Lei et al., 2019; Tonk et al., 2017).

For equilibrium and then kinetic studies, batch adsorption measurements were carried out. We can see that Cd^{2+} ions gradually occupied the porous, vacant sites of ACC surface. However, no significant variation in the residual Cd^{2+} was observed and equilibrium was reached as time passed.

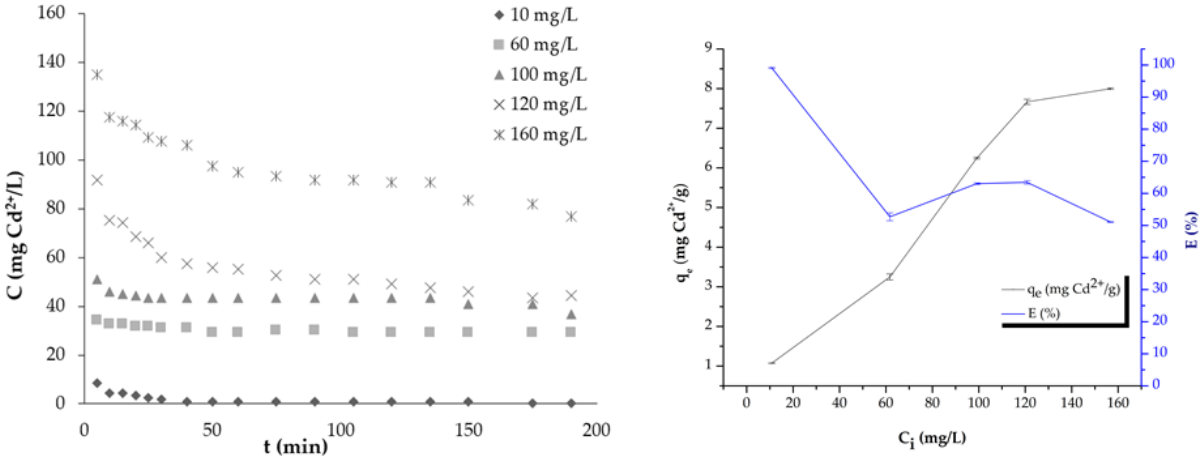

Figure 47. (a) Effect of contact time and (**b**) initial concentrations, where q is the adsorption capacity, quantity in equilibrium and E is the efficiency of the adsorption process on the removal of Cd^{2+} ions (C_i = 10–160 mg/L, 0.1 g/L ACC, pH = 7, T = 20 ± 1 °C).

The adsorption efficiency of Cd^{2+} ions on ACC were investigated at various initial concentrations between 10–160 mg/L via the batch adsorption method. In equilibrium, results showed (Figure 12) that the adsorption capacity (q) increased from 1.07 to 8 mg/g as the initial concentration increased from 10 to 160 mg/L. On the other hand, with the increase in concentration, the efficiency (E) decreased from 99 to 51%. This can happen because more cadmium ions were adsorbed at higher Cd^{2+} concentrations. However, as we have a fixed number of active sites available on the ACC surface, the efficiency decreases (Nagy et al., 2013b; Osasona et al., 2018; Tonk et al., 2017; Yusuff et al., 2019).

4.7.3. Adsorption Isotherms, Kinetic and Diffusion Models

Both the adsorbent (ACC) and the adsorptive material (Cd^{2+} ions) are influencing factors of the adsorption system. Isotherm models in equilibrium showed that the adsorptive (in our case, the Cd^{2+} ions) are distributed between the liquid (water) and solid (ACC) phase and the relationship, performance and interaction between these (Cd^{2+} + liquid phase, Cd^{2+} + clay surface) could also be defined (Çelebi et al., 2020; Es-sahbany et al., 2021). Langmuir, Freundlich, Temkin and Dubinin–Radushkevich linearized isotherm models were employed to investigate the interaction between the Cd^{2+} ions and clay using different initial concentrations of Cd^{2+} (10–160 mg/L), applying a constant temperature (20 °C) and adsorbent dosage (1 g). The results listed in Table 4 compared the regression correlation coefficients (R^2) of these models. Based on the results, we established the order of correspondence of the applied isotherm models: Langmuir II. (R^2 = 0.954) > Dubinin–Radushkevich (R^2 = 0.933) > Freundlich (R^2 = 0.885) > Temkin (R^2 = 0.859) > Langmuir I. (R^2 = 0.798) > Langmuir IV. (R^2 = 0.744) > Langmuir III. (R^2 = 0.605).

Table 10. Calculated parameters of different linear isotherm models.

Langmuir I.			**Langmuir II.**			**Langmuir III.**			**Langmuir IV.**		
Plotting: C_e vs. C_e/q_e			Plotting: $1/C_e$ vs. $1/q_e$			Plotting: q_e/C_e vs. q_e			Plotting: q_e vs. q_e/C_e		
K_L (l/mg)	**q_{max} (mg/g)**	**R^2**	**K_L (l/mg)**	**q_{max} (mg/g)**	**R^2**	**K_L (l/mg)**	**q_{max} (mg/g)**	**R^2**	**K_L (l/mg)**	**q_{max} (mg/g)**	**R^2**
0.01	12.03	0.798	2.39	5.59	0.954	2.05	6.36	0.605	0.02	4.30	0.744

Freundlich			**Dubinin–Radushkevich**			**Temkin**		
Plotting: $\ln C_e$ vs. $\ln q_e$			Plotting: ε^2 vs. $\ln q_e$			Plotting: $\ln C_e$ vs. q_e		
n	**K_f ($mg^{(1-1/n)}l^{1/n}$/g)**	**R^2**	**β ($mol^2\ kJ^2$)**	**E (kJ/mol)**	**R^2**	**A_T (l/g)**	**B (J/mol)**	**R^2**
2.44	2.31	0.885	5×10^{-8}	3.16	0.933	2.4	1×10^{-4}	0.859

As the regression correlation coefficient was highest in the case of Langmuir isotherm, the error functions, separation factor was calculated for this model (Çelebi et al., 2020; Rápó et al., 2020b; Subramani S.E. and Thinakaran N., 2017). According to the literature, the value of R_L can define the type and favorability properties of an isotherm model: $R_L = 0 \rightarrow$ irreversible and linear adsorption; $0 < R_L < 1 \rightarrow$ favorable adsorption; $R_L > 1 \rightarrow$ unfavorable adsorption.

R_L values calculated for Langmuir II. isotherm were in the range of 0.037–0.027; this result suggests that in our experimental conditions, the adsorption of Cd^{2+} ions was favorable but with a high tendency of irreversibility. According to the theoretical properties of Langmuir isotherm, the adsorption occurs on a homogenous surface, and only one layer is formed (monolayer adsorption) (Mustapha et al., 2019; Nagy et al., 2013b). The precisely calculated isotherm parameters tell us about the nature and type of the adsorption. In our experimental conditions, these constants (B-Temkin: 1×10^{-4} J/mol < 20 kJ/mol; E-Energy: 3.16 kJ/mol < 8 kJ/mol) indicated that the adsorption is a physical one, where weak van der Waals bonds are formed on the ACCs monolayer surface. Moreover, the binding sites on ACC surface are equivalent. In order to find the best adsorption equilibrium correlation, the isotherm models were also modelled in non-linear form using OriginPro 8.5 software. Based on the literature, nonlinear regression is the most feasible and accurate method for estimating the parameters of the isothermal models, as it uses the original equations rather than modified versions that may bias the results (Nagy et al., 2017). The parameters of the Langmuir, Freundlich and Temkin isotherms obtained after linear translation and non-linear fitting, we observed that the regression coefficient (R^2) was found to be higher for linear fitting. The values of $K_{L;F}$, q_{max}, n_F, A_T, and B also differ due to the bias in the fits (Table 11). Comparing the obtained linear regression coefficients (R^2 ; the larger the better) and Chi-squared (χ^2; the smaller the better), the degree of fit follows the following order: Liu (the best fit: $R^2 = 0.965$, $\chi^2 = 1.101$) > Toth > Khan > Langmuir > Freundlich > Temkin (Table 5).

Table 11. Calculated parameters of different non-linear isotherm models.

Two Parameter Non-Linear Isotherm Fitting					
Langmuir Isotherm		**Freundlich Isotherm**		**Temkin Isotherm**	
q_m (mg/g)	15.80	n_F	1.88	b_T	0.92
K_L (L/mg)	0.02	K_F ($mg^{(1-1/n)}l^{1/n}$/g)	0.84	K_T (L/mg)	23.76
R^2	0.831	R^2	0.824	R^2	0.705
χ^2	2.136	χ^2	1.944	χ^2	2.770
RMSE	1.419	RMSE	1.450	RMSE	1.875
HYBRID	23.220	HYBRID	15.027	HYBRID	−8.773
Three parameter non-linear isotherm fitting					
Toth isotherm		**Khan isotherm**		**Liu isotherm**	
q_m (mg/g)	23.74	q_m (mg/g)	4610.76	q_m (mg/g)	8.07
K_{TH} (L/mg)	0.00	K_K (L/mg)	4.71×10^{-5}	K_{Liu} (L/mg)	0.03
n_{TH}	4.47	n_K	191.33	n_{Liu}	0.14
R^2	0.980	R^2	0.842	R^2	0.965
χ^2	11.829	χ^2	2.103	χ^2	1.101
RMSE	4.861	RMSE	1.372	RMSE	0.647
HYBRID	−20.239	HYBRID	22.597	HYBRID	36.512

Under this isothermal model, which is considered optimal, the adsorption binding constant K_{Liu} = 0.03 L/mg and the maximum amount of cadmium bound q_{Liu} = 8.07 mg/g. Further study of the best-fit Liu isotherm parameters shows that q_{Liu} (8.07 mg/g) is almost the same as the q_{exp}. (8 mg/g) values for the 160 mg/L Cd^{2+} solution. Differences between the parameters calculated due to non-linear fitting of the isotherm models are observed. These differences are presumably due to the equations used, the accuracy of the fitting, the precision of the software used, the program package, the number of fitting iterations performed.

Kinetic models are used to determine the temporal effect of the adsorption process. They present information on the change in the experimental system over time, characterize the rate of adsorption uptake and binding at the solid-solution interface or during the sorption reaction (Giwa et al., 2013; Rao and Kashifuddin, 2014; Rongrong Zhang et al., 2020). In this study, pseudo-I-order (Lagergren) and pseudo-II-order (Ho and McKay) kinetic models were calculated when the initial concentration of Cd^{2+} was changed (between 10–160 mg/L). However, the temperature (20 °C) and adsorbent dosage (1 g) were constant. Table 6 contains the calculated results of kinetic models. Based on the obtained linear regression coefficient values, it can be observed that the adsorption system did not follow a pseudo-I-order model, as the value of R^2 was higher in the case of the pseudo-II-order model. The values of q_e(cal) also depicted a better fitness of the model since they were almost identical with the pseudo-II-order q_e(exp) values, this model was better obeyed.

Table 12. Calculated parameters of kinetic models.

		Pseudo-I-Order			Pseudo-II-Order		
C (mg/L)	**q_e (exp) (mg/g)**	**k_1 (1/min)**	**q_e (calc) (mg/g)**	**R^2**	**k_2 (g/mg × min)**	**q_e (calc) (mg/g)**	**R^2**
10.83	1.07	0.021	2.17	0.685	0.131	1.07	0.995
61.67	3.25	0.002	1.95	0.285	0.181	3.28	0.999
99.17	6.25	0.013	1.91	0.324	0.054	5.96	0.996
120.83	7.67	0.026	4.13	0.942	0.011	8.01	0.998
156.67	8.00	0.014	5.62	0.868	0.007	8.12	0.988

As shown above, one way to model kinetic data is to use pseudo-first-order and pseudo-second-order kinetic models. These models describe the interaction between the molecule or ion of the pollutant of interest (in our case Cd^{2+}) and the active binding sites on the surface of the adsorbent (ACC). However, diffusion models are also necessary, as the kinetics of the process can often be influenced by diffusion within the particles (Pholosi et al., 2020).

The diffusion model (intra-particle, liquid film) assumes that the rate is determined by the diffusion steps, since the interaction between the pollutant and the active sites on the sorbent surface is more immediate (Baraka, 2015). The literature records suggest that four main steps occur during the adsorption mechanism of heavy metals onto binding sites (Pholosi et al., 2020; Usman et al., 2020):

- From the water-Cd^{2+}-clay suspension, metal ions transport into the boundary layer of the clay adsorbent surface.
- The metal ions diffuse through the boundary layer on the surface of the adsorbent. This process is called liquid-film or external-film diffusion.
- Intraparticle surface diffusion, where the metal ions are diffused in the adsorbed state along the internal surface of a clay particle.
- Adsorption

The metal ions adsorbed on the active binding sites of the adsorbent by physical or chemical bonds. The physical and chemical properties of the adsorbent and the surface properties can influence the extent of each step. It can therefore be said that the intraparticle particle diffusion rate or the liquid film diffusion rate can control the sorption of Cd^{2+} ions on the surface of the ACC. In particular, the linear regression coefficients, the intersection points, the velocity values, and the particle diffusion coefficient (D) were calculated. The pore diffusion coefficients vary between 2.64×10^{-9} and 2.94×10^{-8} cm^2/s with changing concentration. Our results show that the linear plots of intra-particle and liquid film diffusion do not cross the origin, indicating that boundary layer diffusion was involved in the adsorption process. Intra-particle diffusion and liquid film diffusion are thus

not separate rate-determining steps. Thus, liquid film diffusion and intra-particle diffusion together control the adsorption process by which Cd^{2+} is removed from the aqueous solution by ACC (Oyelude et al., 2017; Tonk et al., 2017).

4.7.4. Potential Limitations of Clay Adsorbents

The first and most important task in adsorption studies is the selection of an adsorbent that meets a number of parameters (Rápó and Tonk, 2021). The comparison of individual sorbents is almost impossible due to the physical and chemical properties of the base materials of the adsorbents and the different impurities and processing conditions (Rápó et al., 2020b). A review article published in 2017 summarizes the advantages of different clay minerals, listing arguments for their use as adsorbents (Adeyemo et al., 2017). Their arguments include that clay minerals:

- Have strong sorption and complexing properties;
- Low cost;
- Are readily available;
- Have a high specific surface area compared to other sorbents;
- Non-toxic;
- And have ion exchange potential.

Based on sources, clays costs about $0.005 to $0.46/kg. Montmorillonite costs about $0.04 to $0.12/kg, which costs 20 times less than activated carbon (Srinivasan, 2011). In Romania 0.34 kg activated carbon for fish aquarium cleaning costs around $10. For this reason, many clay minerals are widely used for their adsorption-desorption properties of organic molecules (Adeyemo et al., 2017). Apart from the advantages, as with all adsorbents, the use of clay minerals has disadvantages and limitations. The barriers of adsorbents are summarized by Naef A. A. A. Qasem et al. in a recent review (Qasem et al., 2021). A major obstacle to water treatment is that the ability to simultaneously remove different types of ions has not been investigated in most cases. Most studies are laboratory based and only investigate the removal of single component contaminants. This may also mean that most of the adsorbents cannot be used on an industrial scale as detailed and optimized technology has not been developed. For industrial upgrading, high retention times, periodic cleaning or adsorbent regeneration or desorption, water after-treatment are also issues to be addressed. During the batch adsorption process, the sorbent may be further fragmented by agitation, and small particles or colloids may appear in the water, making sedimentation and sludge removal more difficult. Disposal and treatment of the resulting adsorbent waste, which can often be toxic, can be another obstacle.

5. CONCLUSIONS AND PERSPECTIVES

I. At the opening of my thesis, through a thorough review and presentation of the literature, we demonstrated that the development of an alternative bioremediation water purification method is an essential scientific task.

The scarcity of freshwater resources and the high levels of water pollution that we have at our disposal are the reasons for this conclusion. The dyes that threaten our waters and the brief history of dye use that led to the invention of synthetic dyes were presented. We classified the dyes, as each group has different chemical properties that can affect the way and effectiveness of removal. We also described possible sources of heavy metals and illustrated the problem of cadmium contamination in Romania through examples.

Several methods can be used to remove dyes and cadmium micropollutants, but by studying the general drinking water production process, we have identified adsorption as an established method. A wide range of scientific results have been obtained using adsorption, demonstrating its environmental and sustainable applicability. After describing the general characteristics of adsorption, the types of adsorption bonding and the possible adsorbents and their requirements, we selected the sorbents used during the research. In an effort to be economical and environmentally friendly, household and industrial waste, porous eggshells (in three forms), the *Saccharomyces cerevisiae* model organism most studied in biosorption research, and clay with proven high adsorption/absorption properties were used as adsorbents.

All, in all, even if there are several possible methods for water treatment have recently become available, adsorption is perhaps the most common commercial treatment.

II. By selecting the adsorption technology - an alternative remediation method - and the possible adsorbents, we fulfilled one of the objectives of this dissertation. We also aimed to determine the optimal use of this technique. The remediation process is influenced by several external parameters, the optimization of which is essential to ensure that the system can be applied with low costs, few by-products and high efficiency on a daily basis, even at low pollutant concentrations.

Looking at the effect of the *initial dye concentration,* it is observed that a wide range of adsorbents can be used, with efficiencies of more than 90% even at high concentration values. The investigated studies covered a concentration range from 3 to 1,000 mg/L. In the studies, the removal time ranged from 5 min. to 36 h. However, 100% efficiency was achieved in intervals of

up to 5–60 min. In most cases, the increase of the dye concentration negatively influenced the removal efficiency.

With the increase of initial indicator dye concentration in case of CR, BPB, MB and MG, the adsorption capacity also increased.

- $C_{10\ mg/L,\ CR}$: E=99.03%, q_{max}=0.33 mg/g; $C_{50\ mg/L,\ CR}$: E=93.42%, q_{max}=1.53 mg/g
- $C_{10\ mg/L,\ BPB}$: E=10.07%, q_{max}=0.04 mg/g; $C_{50\ mg/L,\ BPB}$: E=3.40%, q_{max}=0.06 mg/g
- $C_{10\ mg/L,\ MB}$: E=55.06%, q_{max}=0.2 mg/g; $C_{50\ mg/L,\ MB}$: E=62.98%, q_{max}=1.07 mg/g
- $C_{10\ mg/L,\ MG}$: E=88.3%, q_{max}=0.39 mg/g; $C_{50\ mg/L,\ MG}$: E=94.39%, q_{max}=1.59 mg/g

Similar trend ($C_i \uparrow \Rightarrow q_{max} \uparrow$) was observed in case of textile dye removals with powdered and calcined eggshell and yeast adsorbents, however, we could not clarify a specific trend between efficiency and variation of initial concentration.

The *pH* of the dye solution has been shown to significantly affect the adsorption process. We hypothesized that anionic dyes bind more efficiently in acidic media, whereas cationic dyes adsorb more efficiently in basic media. To this end, in our earliest published study, we investigated the removal of indicators used in laboratories from water at different pH. Four indicators were selected, two of which were anionic and two cationic. In our studies we confirmed our hypothesis, however, for the CR and MG dyes it was seen that pH was only slightly affected, this was attributed to the fact that the addition of the eggshell component ($CaCO_3$) to the solution imparted a basic character to the solution. The removal of fabric dyes was further considered, as their release from the textile industry poses a serious environmental risk. The Remazol family of dyes we have chosen, belong to the group of reactive dyes, which are anionic in nature. We were also interested in adsorption with other adsorbents.

Moreover, from literature data, the removal of 16 anionic and cationic dyes was demonstrated. Among the anionic dyes, direct dyes are the most frequently tested, while Methylene Blue is the model dye for cationic dyes. Most of the studies have investigated the removal of dyes between pH 2 and 10. Having examined the chemistry of the solution, it can be concluded that anionic and cationic dyes behave differently in acidic and basic media. When designing the adsorption process, it is important to keep in mind the ionic nature of the dye, thus reducing the time required for the optimization study.

The effect of *initial adsorbent dosage* was investigated for 5 different adsorbent-contaminant pairs: the RBV-5R dye with powder and calcined eggshell, the RB dye with calcined eggshell adsorption, and the RR dye with calcined eggshell and brewer's yeast.

In each research project, the effect of the amount of adsorbent between 0.5 and 2.5 g was studied. Our results show that quantity in equilibrium shows a decreasing trend as the amount of mass increases. On the opposite, the efficiency increases as the mass increases, this can be explained by the fact that the excess sorbent amount provides a larger active surface area and more active adsorption sites are available for the dye to bind. However, as the efficiencies change, it is observed that a saturation value is reached after which the efficiency is steady or slightly reduced.

- RBV-5R + powdered eggshell: 1.5 g, q_{max}= 1.27 mg/g, E= 95.07%
- RBV-5R + calcined eggshell: 1.5 g, q_{max}= 1.29 mg/g, E= 96.83%
- RB + calcined eggshell: 1.5 g, q_{max}= 1.35 mg/g, E= 98.83%
- RR+ calcined eggshell: 1.5 g, q_{max}= 1.96 mg/g, E= 97.83%

For the adsorption of yeast, almost identical values were obtained with increasing mass, with the highest efficiency obtained at 2.5 g (q_{max}= 0.13 mg/g, E= 63.33%).

Through numerous literature examples of adsorbents, it has been observed that even small amounts (as small as 0.05 g) have been found to remove dye with efficiencies greater than 85%. The conclusion of literature review and our experiments is that as the amount of adsorbent increases, the removal efficiency of dyes increases and the maximum amount of bound substances decreases.

The effect of *particle size* was only studied in case of powdered eggshell. Results showed that the 160 μm particle sized powder was the most effective, this is why in case of calcined eggshell the 160 μm particle sized powder was calcined at 1,000 ^{o}C for 4 hours. Bearing in mind that based on our result and the analyzed articles, the efficiency values varied from 8 to up to 99% by reducing the particle size, it can be said that particle size is a highly influential factor. Therefore, in future research, if possible and feasible, it is important to increase surface area and porosity by reducing particle size.

The effect of aqueous solution *temperature* was investigated between 20 and 40 ^{o}C. Both endothermic and exothermic adsorption processes were observed in our experiments in literature data. From a green chemistry point of view, the exothermic process is preferable, since no excess energy input is required by heating the system for optimal adsorption. Temperature, in addition to adsorption efficiency, affects the nature and mechanism of adsorption.

Studying powdered, calcined eggshells and eggshells embedded in alginate beads we concluded that calcined eggshell is the most effective, both in removal efficiency, highest quantity in equilibrium and time effectiveness.

In our study, the optimal parameters for the most efficient dye removal were (160 μm, 700 rpm):

- CR + powdered eggshell: C_i=10 mg/L, 3 g, pH=8.05±0.2, T=20±2 °C, where E=99.04%

- BPB + powdered eggshell: C_i=30 mg/L, 1.5 g, pH=2±0.2, T=20±2 °C, where E=57.65%
- MB + powdered eggshell: C_i=30 mg/L, 1.5 g, pH=10±0.2, T=20±2 °C, where E=75.10%
- MG + powdered eggshell: C_i=40 mg/L, 1.5 g, pH=2.76±0.2, T=20±2 °C, where E=96.59%
- RBV-5R + powdered eggshell: C_i=20 mg/L, 1.5 g, pH=6.0±0.2, T=20±2 °C, where E=95%
- RBV-5R + calcined eggshell: C_i=20 mg/L, 1.5 g, pH=5±0.2, T=20±2 °C, where E=97%
- RR + calcined eggshell: C_i=60 mg/L, 1.5 g, pH=7±0.2, T=20±2 °C, where E=98.44%
- RB + calcined eggshell: C_i=80 mg/L, 1.5 g, pH=7±0.2, T=20±2 °C, where E=99%
- RR + yeast: C_i=20 mg/L, 1.5 g, pH=3±0.2, T=20±2 °C, where E=88.5%.

III. In the second major part of the thesis, we have achieved another main objective. Adsorbents (eggshell, brewer's yeast, Aslavital cosmetic clay) and contaminants were characterized using known and commonly used analytical methods.

The thin section of eggshell was analyzed with various microscopes, where the well know layers of the shell were identified before and after RBV-5R dye adsorption. Therefore, we could see that the cuticle and membrane layer adsorbed the dye. This finding was further proven by EDS measurements for each layer and elemental maps. Moreover, after adsorption the Raman samples showed the presence of C–H, C–S and N=N functional groups that are specific of the dye.

For all adsorption studies with powdered and calcined eggshell, the SEM images showed that the porous, cross-linked structure of eggshell disappeared after dye adsorption. From EDS measurements it was obvious that powdered eggshell is mostly made of $CaCO_3$ while, calcined eggshell is composed of CaO. After adsorption, the characteristic components of the dyes were detectable. The amounts of nitrogen, sulphur, chromium, copper and bromine increased typically in samples containing each dye. Based on the peaks of control and dye adsorbed samples of FTIR and Raman spectra, functional groups and bonds specific to each component were found.

We have also shown that the decomposition of the eggshell occurs at 728.6 ºC. The total surface area of the powdered and calcined eggshell decreased after the adsorption of RBV-5R.

In case yeast morphology study, we saw the spindle and pointed egg-shaped forms, that after the adsorption process disappeared, we observed a cellular morphology difference. EDS results proved that after adsorption with RR dye, the amount of C and S increased in the samples.

IV. A key question in adsorption studies is what happens and what process takes place between the adsorbent and the pollutant. It is important to understand the mechanism of the phenomenon

in order to be able to optimize the process in practice. Analytical studies can be of great help in this respect, but mathematical models based on the concentration values obtained at equilibrium and the equilibrium data calculated from these can help to further understand the process. Isothermal, kinetic and diffusion models offer the possibility to determine different adsorption characteristics.

Among the studied isothermal models, the adsorption process was best characterized by the Langmuir isotherm, which assumes a single layer adsorption. Exceptions are MB, which follows the Dubinin-Radushkevich and MG, which follows the Freundlich model. However, it can be said that, based on the results of the Temkin constant and the E-energy, in all cases the primary bonds formed are physical in nature. The second order kinetic model is characteristic for all the adsorption processes. The results of the diffusion models proved that neither the intra-particle model nor the liquid film influences the rate of the adsorption process; only the adsorption is decisive. Thermodynamic measurements further confirmed the physical nature of adsorption, the spontaneity of the process, because as the temperature increases, the amount of adsorption decreased.

V. In the present work, ACC—ASLAVITAL commercial cosmetic clay—was morphologically and elementally analyzed; moreover, it was successfully used to remove Cd^{2+} from water.

It was observed that the initial concentration of contaminants decreased with time, as all investigated concentrations exhibited a rapid decrease rate in the first part of the experiment. Then the adsorption rates tended to be flat. Quantity in equilibrium increased from 1–8 mg/g with the increase in initial Cd^{2+} concentration. Our hypothesis proved that ACC is an excellent adsorbent as 99% Cd^{2+} removal efficiency was reached within 190 min.

Adsorption equilibrium results were further analyzed with linear (Langmuir, Freundlich, Temkin, Dubinin–Radushkevich) and non-linear (Langmuir, Freundlich, Temkin, Toth, Khan, Liu) isotherm models with OriginPro 8.5 software. The best fit in linear form was obtained for the Langmuir. II model, where $R^2 = 0.954$, while the R_L values ranged between 0.037–0.027. The B-Temkin constant was smaller than 20 kJ/mol and the E-Energy was smaller than 8 kJ/mol. Results indicated that physical bonds form during the favorable adsorption. For the non-linear fits, the Liu model proved to be the best $R^2 = 0.965$, $\chi^2 = 1.101$. Moreover, the investigations regarding the evaluation of linear regression coefficient values showed that the adsorption system had a higher linear regression coefficient ($R^2 = 0.988$–0.999) value in the case of the pseudo-II-order model.

The values of q_e(cal) also showed a better fit with the model since they were almost identical with the pseudo-II-order q_e(exp) values, (the differences ranged 0.03–0.34).

With the use of wide range of morpho-structural approaches, we studied the structure, texture, morphology and composition of the adsorbent. The morpho-structural investigations revealed that the clay mainly consists of kaolinite and illite in most considerable amounts. The elemental composition of the ACC contained Ca (20.65 ± 0.08%), Si (12.7 ± 1.9%), Al (8.3 ± 0.3%), Ti (0.34 ± 0.01%) and Fe (4.83 ± 0.02%). Using SEM investigations, it was observed that after adsorption, the surface is smoother, and some aggregates appeared on the clay surface.

The presence of clay-bound Cd^{2+} adsorbate was confirmed by analyzing the elemental contents (EDS) on the surface alongside spectral analysis (FTIR, Raman) and XRD. After adsorption, Wt(%) = 0.2 ± 0.01 Cd^{2+} was detected in the sample.

6. NOVEL SCIENTIFIC RESULTS

1. We have improved the adsorption process, an alternative bioremediation method. Novel, recycled, environmentally friendly industrial and household wastes were used as adsorbents for the treatment of wastewater from indicator-, textile dyes and Cd micropollutants.

2. During dye (Indicators: Congo Red (CR), Bromphenol Blue (BPB), Methylene Blue (MB) and Malachite Green (MG); Textile dyes: Remazol Brilliant Violet 5R (RBV-5R), Remazol Brilliant Red F3B (RR) and Remazol Brilliant Blue R (RB)) adsorption with powdered-, calcined eggshell and brewery's yeast, we observed that with the increase of initial dye concentration the adsorption capacity also increased.

3. The composition of the powder eggshell $CaCO_3$ and the calcined eggshell CaO provided a basic feature to the dye solutions, thus the adsorption of CR, MG powder with eggshell, RBV-5R, RR and RB textile dyes with calcined eggshell was not affected by the solution chemistry, and for all dye removals 90% efficiency was achieved.

In the case of MB and BPB dyes, the removal mode typical of anionic and cationic dyes was clearly distinguished, i.e. anionic dyes bind more efficiently in acidic media, whereas cationic dyes bind more efficiently in basic media.

The anionic RR textile dye on the surface of the brewer's yeast achieved maximum efficiency (E=88.5%) in acidic medium (pH=3), while the lowest efficiency was obtained at pH 11, E=46.5%.

4. The increase of adsorbent (powdered and calcined eggshell, brewer's yeast) dosage negatively affected the RBV-5R, RB and RR dye adsorption capacity. For example, qe decreased from 0.59 mg/g to 0.13 mg/g as the yeast mass increased in case of RR removal.

5. Studying powdered, calcined eggshells and eggshells embedded in alginate beads we concluded that calcined eggshell is the most effective, both in removal efficiency, highest quantity in equilibrium and time effectiveness.

6. In our study, the optimal parameters for the most efficient dye removal were (160 μm, 700 rpm):

- CR + powdered eggshell: C_i=10 mg/L, 3 g, pH=8.05±0.2, T=20±2 °C, where E=99.04%
- BPB + powdered eggshell: C_i=30 mg/L, 1.5 g, pH=2±0.2, T=20±2 °C, where E=57.65%
- MB + powdered eggshell: C_i=30 mg/L, 1.5 g, pH=10±0.2, T=20±2 °C, where E=75.10%
- MG + powdered eggshell: C_i=40 mg/L, 1.5 g, pH=2.76±0.2, T=20±2 °C, where E=96.59%
- RBV-5R + powdered eggshell: C_i=20 mg/L, 1.5 g, pH=6.0±0.2, T=20±2 °C, where E=95%
- RBV-5R + calcined eggshell: C_i=20 mg/L, 1.5 g, pH=5±0.2, T=20±2 °C, where E=97%
- RR + calcined eggshell: C_i=60 mg/L, 1.5 g, pH=7±0.2, T=20±2 °C, where E=98.44%

- RB + calcined eggshell: C_i=80 mg/L, 1.5 g, pH=7±0.2, T=20±2 °C, where E=99%
- RR + yeast: C_i=20 mg/L, 1.5 g, pH=3±0.2, T=20±2 °C, where E=88.5%.

7. Results of various microscopic studies, EDS and Raman spectra only the cuticle and membrane layer of chicken eggshell adsorbed the RBV-5R dye.

8. In case yeast morphology study, we saw the spindle and pointed egg-shaped forms, that after the adsorption process disappeared, we observed a cellular morphology difference. EDS results proved that after adsorption with RR dye, the amount of C and S increased in the samples.

9. Our hypothesis proved that ACC, that is mainly consists of kaolinite and illite, is an excellent adsorbent as 99% Cd^{2+} removal efficiency was reached within 190 min.

10. The presence of clay bound Cd^{2+} adsorbate was confirmed by analyzing the elemental contents (EDS) on the surface alongside spectral analysis (FTIR, Raman) and XRD. After adsorption, Wt(%) = 0.2 ± 0.01 Cd^{2+} was detected in the sample.

7. SUMMARY

To quote Albert Szent-Györgyi, without water there is no existence, as it is the essential source of everyday life. We all know that clean water, of a quality that meets standards, is a source of resources, and water is the end point of a wide range of pollutants that enter nature. Many industrial sectors (printing, textiles, mining, food processing) produce waste and wastewater.

The main focus of my thesis was the design and development of an alternative bioremediation method that could create opportunities for the recycling of industrial and domestic wastes in the field of water treatment. The aim was to purify artificially produced dye and Cd solutions using an adsorption process known from practical water treatment. Following optimized tests, the most favorable experimental parameters were determined and up to 99% efficiency was achieved in the dye removal process. In contrast, bromophenol blue was difficult to remove even under optimal conditions (E_{max}=57.65%). For Cd removal, we also achieved 99% efficiency within 190 min. In conclusion, we have succeeded in fulfilling our four main objectives, we have selected a remediation method that can solve the identified problem; we have optimized the chosen method, adsorption; we have characterized the adsorbents and the contaminants using the available techniques; we have studied the mechanism using mathematical models and analytical studies.

Our future plans include the publication of the results of our research already carried out with ostrich eggs and their comparison with the results obtained for chicken eggshell adsorbent. To study the similarities and differences between structure, morphology, elemental composition. We would also like to extend our experiments with brewer's yeast to indicators and RBV-5R, RB dyes (these studies have already been carried out, results evaluation is still to be done), in order to be able to formulate a general trend for yeast as an adsorbent. The adsorption process always raises the question of what happens to the resulting adsorbent waste. We would also like to study the disposal and reusability of this waste in the near future. We wish to optimize and develop a desorption process to recycle the adsorbent. Our more distant plans include the creation of a filter that can be refilled with household waste, which could even be used in our everyday life.

8. ÖSSZEFOGLALÁS

Szent-Györgyi Albert szavával élve, víz nélkül nincs élet, hiszen a mindennapi élet elengedhetetlen forrása. Mindannyian tudjuk, hogy a tiszta és a szabványoknak megfelelő minőségű víz egy erőforrás, amely a természetbe kijutott szennyeződések széles skálájának végállomása. Az ipar számos területe (nyomda- és textilipar, bányászat, élelmiszeripar) egyaránt termel hulladékokat és szennyvizet.

Kutatásom középpontjában alternatív bioremediációs módszer kidolgozása és fejlesztése állt, amely lehetőséget teremthet ipari és háztartásbeli hulladékok újrahasznosítására a víztisztítás területén. Mesterségesen előállított festék- és Cd oldat tisztítását tűztük ki célul használva a gyakorlati víztisztításból ismert adszorpciós eljárást. Az optimalizált vizsgálatokat követően meghatároztuk a legelőnyösebb kísérleti paramétereket és akár 99%-os hatékonyságot is elértünk a festékeltávolítás folyamán. Ezzel szemben a bromphenol kék még optimális körülmények között is nehezen volt eltávolítható (E_{max}=57.65%). A Cd eltávolításakor szintén 99%-os hatékonyságot értünk el 190 perc alatt. Összességében elmondható, hogy sikerült teljesítenünk a négy fő célunkat, kiválasztottunk egy remediációs módszert, amely a felismert problémát megoldhatja; a választott módszert, az adszorpciót optimalizáltuk; a rendelkezésünkre álló technikák segítségével jellemeztük az adszorbenseket és a szennyezőanyagokat; matematikai modellek és analitikai vizsgálatok segítségével tanulmányoztuk a mechanizmust.

Jövőbeli terveink között szerepel a strucctojással már elvégzett kutatási eredményeink publikálása és azok összehasonlítása a tyúktojás adszorbensre kapott eredményekkel. Tanulmányozni a szerkezet, morfológia, elemi összetétel közötti hasonlóságokat és különbségeket. A sörélesztővel végzett kísérleteinket is szeretnénk kiterjeszteni az indikátorokra és a RBV-5R, RB színezékekre (ezen kutatások is el vannak már végezve, az eredmények kiértékelése van hátra), annak érdekében, hogy egy általános tendenciát meg tudjunk fogalmazni az élesztőre, mint adszorbensre vonatkozóan is. Az adszorpciós eljárás következtében mindig felmerül a kérdés, hogy mi történik a keletkezett adszorbens hulladékkal. Ezen hulladék ártalmatlanítását és újra felhasználhatóságát is szeretnénk tanulmányozni a közeljövőben. Optimalizálnánk és kifejlesztenénk a deszorpciós eljárást, amellyel az adszorbens újrahasznosítható lenne. Távolabbi terveink között szerepel egy olyan háztartási hulladékkal utántöltős szűrő megalkotása, amelyet akár a mindennapjainkban alkalmazni tudnánk.

9. APPENDIX, SUPPLEMENTARY MATERIAL

A1. References

References were edited with Zotero program

© Society of Dyers and Colourists & AATCC, 2018. Definitions of a dye and a pigment | Colour Index. URL https://colour-index.com/definitions-of-a-dye-and-a-pigment (accessed 7.31.21).

© World Health Organization (WHO) and the United Nations Children's Fund (UNICEF) 2021, 2021. Progress on household drinking-water, sanitation and hygiene: Five years into the SDGs. Switzerland, Geneva.

Abbas, K., Znad, H., Awual, Md.R., 2018. A ligand anchored conjugate adsorbent for effective mercury(II) detection and removal from aqueous media. Chemical Engineering Journal 334, 432–443. https://doi.org/10.1016/j.cej.2017.10.054

Abdel-Aziz, M.H., El-Ashtoukhy, E.Z., Bassyouni, M., Al-Hossainy, A.F., Fawzy, E.M., Abdel-Hamid, S.M.S., Zoromba, M.S., 2020. DFT and experimental study on adsorption of dyes on activated carbon prepared from apple leaves. Carbon Letters 31, 863–878. https://doi.org/10.1007/s42823-020-00187-1

Abdel-Khalek, M.A., Abdel Rahman, M.K., Francis, A.A., 2017. Exploring the adsorption behavior of cationic and anionic dyes on industrial waste shells of egg. Journal of Environmental Chemical Engineering 5, 319–327. https://doi.org/10.1016/j.jece.2016.11.043

Abdulrahman, I., Tijani, H.I., Mohammed, B.A., Saidu, H., Yusuf, H., Ndejiko Jibrin, M., Mohammed, S., 2014. From Garbage to Biomaterials: An Overview on Egg Shell Based Hydroxyapatite. Journal of Materials 2014, 1–6. https://doi.org/10.1155/2014/802467

Abebe, B., Murthy, H.C.A., Amare, E., 2018. Summary on Adsorption and Photocatalysis for Pollutant Remediation: Mini Review. Journal of Encapsulation and Adsorption Sciences 8, 225–255. https://doi.org/10.4236/jeas.2018.84012

Abualnaja, K.M., Alprol, A.E., Abu-Saied, M.A., Ashour, M., Mansour, A.T., 2021. Removing of Anionic Dye from Aqueous Solutions by Adsorption Using of Multiwalled Carbon Nanotubes and Poly (Acrylonitrile-styrene) Impregnated with Activated Carbon. Sustainability 13, 7077. https://doi.org/10.3390/su13137077

Achala Amarasinghe, Dakshika Wanniarachchi, 2019. Eco-Friendly Photocatalyst Derived from Egg Shell Waste for Dye Degradation. Journal of Chemistry e8184732, 1–3. https://doi.org/10.1155/2019/8184732

Adeyemo, A.A., Adeoye, I.O., Bello, O.S., 2017. Adsorption of dyes using different types of clay: a review. Applied Water Science 7, 543–568. https://doi.org/10.1007/s13201-015-0322-y

Afroze, S., Sen, T.K., 2018. A Review on Heavy Metal Ions and Dye Adsorption from Water by Agricultural Solid Waste Adsorbents. Water Air Soil Pollut 229, 1–50. https://doi.org/10.1007/s11270-018-3869-z

Afsane Chavoshani, Majid Hashemi, Mohammad Mehdi Amin, Suresh C. Ameta, 2020. Micropollutants and Challenges. Elsevier. https://doi.org/10.1016/C2018-0-03939-0

Ahmed, M., Mashkoor, F., Nasar, A., 2020. Development, characterization, and utilization of magnetized orange peel waste as a novel adsorbent for the confiscation of crystal violet dye from aqueous solution. Groundwater for Sustainable Development 10, 100322. https://doi.org/10.1016/j.gsd.2019.100322

Aksu, Z., Dönmez, G., 2003. A comparative study on the biosorption characteristics of some yeasts for Remazol Blue reactive dye. Chemosphere 50, 1075–1083. https://doi.org/10.1016/S0045-6535(02)00623-9

Alghamdi, W.M., El Mannoubi, I., 2021. Investigation of Seeds and Peels of Citrullus colocynthis as Efficient Natural Adsorbent for Methylene Blue Dye. Processes 9, 1279. https://doi.org/10.3390/pr9081279

Al-Ghouti, M.A., Al-Absi, R.S., 2020. Mechanistic understanding of the adsorption and thermodynamic aspects of cationic methylene blue dye onto cellulosic olive stones biomass from wastewater. Sci Rep 10, 15928. https://doi.org/10.1038/s41598-020-72996-3

Al-Ghouti, M.A., Da'ana, D.A., 2020. Guidelines for the use and interpretation of adsorption isotherm models: A review. Journal of Hazardous Materials 393, 122383. https://doi.org/10.1016/j.jhazmat.2020.122383

Ali, F., Ali, N., Bibi, I., Said, A., Nawaz, S., Ali, Z., Salman, S.M., Iqbal, H.M.N., Bilal, M., 2020. Adsorption isotherm, kinetics and thermodynamic of acid blue and basic blue dyes onto activated charcoal. Case Studies in Chemical and Environmental Engineering 2, 100040. https://doi.org/10.1016/j.cscee.2020.100040

Alice Park, 2015. The World's Water Supply Could Dip Sharply in 15 Years [WWW Document]. Time. URL https://time.com/3753332/world-water-day-un-warning/ (accessed 1.27.22).

Aljeboree, A.M., Alshirifi, A.N., Alkaim, A.F., 2017. Kinetics and equilibrium study for the adsorption of textile dyes on coconut shell activated carbon. Arabian Journal of Chemistry 10, S3381–S3393. https://doi.org/10.1016/j.arabjc.2014.01.020

Arabhosseini, A., 2018. Application of eggshell wastes as valuable and utilizable products: A review. Research in Agricultural Engineering 64 (2018), 104–114. https://doi.org/10.17221/6/2017-RAE

Arabmofrad, S., Bagheri, M., Rajabi, H., Jafari, S.M., 2020. Nanoadsorbents and nanoporous materials for the food industry, in: Jafari, S.M. (Ed.), Handbook of Food Nanotechnology. Academic Press, pp. 107–159. https://doi.org/10.1016/B978-0-12-815866-1.00004-2

Aruna, Bagotia, N., Sharma, A.K., Kumar, S., 2021. A review on modified sugarcane bagasse biosorbent for removal of dyes. Chemosphere 268, 129309. https://doi.org/10.1016/j.chemosphere.2020.129309

Asif Tahir, M., Bhatti, H.N., Iqbal, M., 2016. Solar Red and Brittle Blue direct dyes adsorption onto Eucalyptus angophoroides bark: Equilibrium, kinetics and thermodynamic studies. Journal of Environmental Chemical Engineering 4, 2431–2439. https://doi.org/10.1016/j.jece.2016.04.020

Ayawei, N., Ebelegi, A.N., Wankasi, D., 2017. Modelling and Interpretation of Adsorption Isotherms. Journal of Chemistry 2017, 1–11. https://doi.org/10.1155/2017/3039817

Badawy, A.A., Ibrahim, S.M., Essawy, H.A., 2020. Enhancing the Textile Dye Removal from Aqueous Solution Using Cobalt Ferrite Nanoparticles Prepared in Presence of Fulvic Acid. J Inorg Organomet Polym 30, 1798–1813. https://doi.org/10.1007/s10904-019-01355-1

Balan, D.S.L., Monteiro, R.T.R., 2001. Decolorization of textile indigo dye by ligninolytic fungi. Journal of Biotechnology, Biotechnology in the Textile Industry - Perspectives for the New Millennium 89, 141–145. https://doi.org/10.1016/S0168-1656(01)00304-2

Baraka, A., 2015. Investigation of temperature effect on surface-interaction and diffusion of aqueous-solution/porous-solid adsorption systems using diffusion–binding model. Journal of Environmental Chemical Engineering 3, 129–139. https://doi.org/10.1016/j.jece.2014.11.001

Bashir, S., Zhu, J., Fu, Q., Hu, H., 2018. Comparing the adsorption mechanism of Cd by rice straw pristine and KOH-modified biochar. Environ Sci Pollut Res 25, 11875–11883. https://doi.org/10.1007/s11356-018-1292-z

Basu, M., Guha, A.K., Ray, L., 2017. Adsorption Behavior of Cadmium on Husk of Lentil. Process Safety and Environmental Protection 106, 11–22. https://doi.org/10.1016/j.psep.2016.11.025

Bayram, E., Ayranci, E., 2010. Investigation of changes in properties of activated carbon cloth upon polarization and of electrosorption of the dye basic blue-7. Carbon 48, 1718–1730. https://doi.org/10.1016/j.carbon.2010.01.013

Becking, J.H., 1975. The Ultrastructure of the Avian Eggshell. Ibis 117, 143–151. https://doi.org/10.1111/j.1474-919X.1975.tb04201.x

Bello, O.S., Ahmad, M.A., 2011. Removal of Remazol Brilliant Violet-5R dye using periwinkle shells. Chemistry and Ecology 27, 481–492. https://doi.org/10.1080/02757540.2011.600696

Benkhaya, B., Harfi, S.E., Harfi, A.E., 2017. Classifications, properties and applications of textile dyes: A review. Applied Journal of Environmental Engineering Science 3, 311–320. https://doi.org/10.48422/IMIST.PRSM/ajees-v3i3.9681

Benkhaya, S., M' rabet, S., El Harfi, A., 2020. A review on classifications, recent synthesis and applications of textile dyes. Inorganic Chemistry Communications 115, 107891. https://doi.org/10.1016/j.inoche.2020.107891

Benvenuti, J., Fisch, A., dos Santos, J.H.Z., Gutterres, M., 2019. Silica-based adsorbent material with grape bagasse encapsulated by the sol-gel method for the adsorption of Basic Blue 41 dye. Journal of Environmental Chemical Engineering 7, 103342. https://doi.org/10.1016/j.jece.2019.103342

Berkesi, M., Káldos, R., Park, M., Szabó, C., Váczi, T., Török, K., Németh, B., Czuppon, G., 2017. Detection of small amounts of N2 in CO2-rich high-density fluid inclusions from mantle xenoliths. European Journal of Mineralogy 29, 423–431. https://doi.org/10.1127/ejm/2017/0029-2615

Berradi, M., Hsissou, R., Khudhair, M., Assouag, M., Cherkaoui, O., El Bachiri, A., El Harfi, A., 2019. Textile finishing dyes and their impact on aquatic environs. Heliyon 5, e02711. https://doi.org/10.1016/j.heliyon.2019.e02711

Beulah, S.S., Muthukumaran, K., 2020. Methodologies of Removal of Dyes from Wastewater: A Review. International Research Journal of Pure and Applied Chemistry 68–78. https://doi.org/10.9734/irjpac/2020/v21i1130225

Bhardwaj, D., Bharadvaja, N., 2021. Phycoremediation of effluents containing dyes and its prospects for value-added products: A review of opportunities. Journal of Water Process Engineering 41, 102080. https://doi.org/10.1016/j.jwpe.2021.102080

Bhate, P.M., Devi, R.V., Dugane, R., Hande, P.R., Shaikh, L., Vaidya, S., Masand, S., 2017. A novel reactive dye system based on diazonium salts. Dyes and Pigments 145, 208–215. https://doi.org/10.1016/j.dyepig.2017.06.007

Bhatia, D., Sharma, N.R., Singh, J., Kanwar, R.S., 2017. Biological methods for textile dye removal from wastewater: A review. Critical Reviews in Environmental Science and Technology 47, 1836–1876. https://doi.org/10.1080/10643389.2017.1393263

Bontas, B.-I., Mirila, D.-C., Gritcu, G., Nistor, I.-D., Ureche, D., 2020. High Pollution with Heavy Metals NATURA 2000 Protected Area in Bacau County, Eastern Romania. Revista de Chimie 71, 154–169.

Bora, F.D., Bunea, C.I., Chira, R., Bunea, A., 2020. Assessment of the Quality of Polluted Areas in Northwest Romania Based on the Content of Elements in Different Organs of Grapevine (Vitis vinifera L.). Molecules 25, 750. https://doi.org/10.3390/molecules25030750

Bouabidi, Z.B., El-Naas, M.H., Cortes, D., McKay, G., 2018. Steel-Making dust as a potential adsorbent for the removal of lead (II) from an aqueous solution. Chemical Engineering Journal 334, 837–844. https://doi.org/10.1016/j.cej.2017.10.073

Božič, M., Kokol, V., 2008. Ecological alternatives to the reduction and oxidation processes in dyeing with vat and sulphur dyes. Dyes and Pigments 76, 299–309. https://doi.org/10.1016/j.dyepig.2006.05.041

Brião, G.V., Jahn, S.L., Foletto, E.L., Dotto, G.L., 2018. Highly efficient and reusable mesoporous zeolite synthetized from a biopolymer for cationic dyes adsorption. Colloids and Surfaces A: Physicochemical and Engineering Aspects 556, 43–50. https://doi.org/10.1016/j.colsurfa.2018.08.019

Brito, M.J.P., Veloso, C.M., Santos, L.S., Bonomo, R.C.F., Fontan, R. da C.I., 2018. Adsorption of the textile dye Dianix® royal blue CC onto carbons obtained from yellow mombin fruit stones and activated with KOH and H3PO4: kinetics, adsorption equilibrium and thermodynamic studies. Powder Technology 339, 334–343. https://doi.org/10.1016/j.powtec.2018.08.017

Bulgariu, L., Escudero, L.B., Bello, O.S., Iqbal, M., Nisar, J., Adegoke, K.A., Alakhras, F., Kornaros, M., Anastopoulos, I., 2019. The utilization of leaf-based adsorbents for dyes removal:

A review. Journal of Molecular Liquids 276, 728–747. https://doi.org/10.1016/j.molliq.2018.12.001
Bulut, Y., Aydın, H., 2006. A kinetics and thermodynamics study of methylene blue adsorption on wheat shells. Desalination 194, 259–267. https://doi.org/10.1016/j.desal.2005.10.032
Burkinshaw, S.M., 1995. Chemical Principles of Synthetic Fibre Dyeing. Springer Netherlands. https://doi.org/10.1007/978-94-011-0593-4
Burkinshaw, S.M., Salihu, G., 2019. The role of auxiliaries in the immersion dyeing of textile fibres: Part 6 analysis of conventional models that describe the manner by which inorganic electrolytes promote reactive dye uptake on cellulosic fibres. Dyes and Pigments 161, 595–604. https://doi.org/10.1016/j.dyepig.2017.09.028
Calmuc, V.A., Calmuc, M., Arseni, M., Topa, C.M., Timofti, M., Burada, A., Iticescu, C., Georgescu, L.P., 2021. Assessment of Heavy Metal Pollution Levels in Sediments and of Ecological Risk by Quality Indices, Applying a Case Study: The Lower Danube River, Romania. Water 13, 1801. https://doi.org/10.3390/w13131801
Castro, K.C. de, Cossolin, A.S., Reis, H.C.O. dos, Morais, E.B. de, Castro, K.C. de, Cossolin, A.S., Reis, H.C.O. dos, Morais, E.B. de, 2017. Biosorption of anionic textile dyes from aqueous solution by yeast slurry from brewery. Brazilian Archives of Biology and Technology 60. https://doi.org/10.1590/1678-4324-2017160101
Çelebi, H., Gök, G., Gök, O., 2020. Adsorption capability of brewed tea waste in waters containing toxic lead(II), cadmium (II), nickel (II), and zinc(II) heavy metal ions. Scientific Reports 10, 17570. https://doi.org/10.1038/s41598-020-74553-4
Chaari, I., Medhioub, M., Jamoussi, F., Hamzaoui, A.H., 2021. Acid-treated clay materials (Southwestern Tunisia) for removing sodium leuco-vat dye : Characterization, adsorption study and activation mechanism. Journal of Molecular Structure 1223, 128944. https://doi.org/10.1016/j.molstruc.2020.128944
Chakraborty, R., Asthana, A., Singh, A.K., Jain, B., Susan, A.B.H., 2020. Adsorption of heavy metal ions by various low-cost adsorbents: a review. International Journal of Environmental Analytical Chemistry 0, 1–38. https://doi.org/10.1080/03067319.2020.1722811
Chatterjee, Sandipan, Chatterjee, Sudipta, Chatterjee, B.P., Guha, A.K., 2007. Adsorptive removal of congo red, a carcinogenic textile dye by chitosan hydrobeads: Binding mechanism, equilibrium and kinetics. Colloids and Surfaces A: Physicochemical and Engineering Aspects 299, 146–152. https://doi.org/10.1016/j.colsurfa.2006.11.036
Chavan, R.B., 2011. 16 - Environmentally friendly dyes, in: Clark, M. (Ed.), Handbook of Textile and Industrial Dyeing, Woodhead Publishing Series in Textiles. Woodhead Publishing, United Kingdom, Sawaston, pp. 515–561. https://doi.org/10.1533/9780857093974.2.515
Chen, T., Da, T., Ma, Y., 2021. Reasonable calculation of the thermodynamic parameters from adsorption equilibrium constant. Journal of Molecular Liquids 322, 114980. https://doi.org/10.1016/j.molliq.2020.114980
Chen, X., Peng, S., Wang, J., 2014. Retention profile and kinetics characteristics of the radionuclide 90-Sr(II) onto kaolinite. Journal of Radioanalytical and Nuclear Chemistry 303, 509–519. https://doi.org/10.1007/s10967-014-3458-6
Chequer, F.M.D., Oliveira, G.A.R. de, Ferraz, E.R.A., Cardoso, J.C., Zanoni, M.V.B., Oliveira, D.P. de, 2013. Textile Dyes: Dyeing Process and Environmental Impact, Eco-Friendly Textile Dyeing and Finishing. IntechOpen, United Kingdom, London. https://doi.org/10.5772/53659
Chikri, R., Elhadiri, N., Benchanaa, M., El maguana, Y., 2020. Efficiency of Sawdust as Low-Cost Adsorbent for Dyes Removal. Journal of Chemistry 2020, e8813420. https://doi.org/10.1155/2020/8813420
Churchman, G.J., Gates, W.P., Theng, B.K.G., Yuan, G., 2006. Chapter 11.1 Clays and Clay Minerals for Pollution Control, in: Bergaya, F., Theng, Benny K. G., Lagaly, G. (Eds.), Developments in Clay Science, Handbook of Clay Science. Elsevier, pp. 625–675. https://doi.org/10.1016/S1572-4352(05)01020-2

Cie, C., 2015. 8 - Fixing ink jet printed textiles, in: Cie, C. (Ed.), Ink Jet Textile Printing, Woodhead Publishing Series in Textiles. Woodhead Publishing, United Kingdom, Sawaston, pp. 99–110. https://doi.org/10.1016/B978-0-85709-230-4.00008-X
Clark, M., 2011. Fundamental principles of dyeing. Woodhead Publishing, United Kingdom, Sawaston, pp. 3–27. https://doi.org/10.1533/9780857093974.1.1
Conway, J., 2020. Beer Industry - Statistics & Facts [WWW Document]. Statista. URL https://www.statista.com/topics/1654/beer-production-and-distribution/ (accessed 12.28.20).
Cornelia, M., Tfeil, H.O., Măicăneanu, A., Indolean (Afloroaei), L., Burcă, S., Tonk, S., Stanca, M., 2009. Fixed Bed Studies for Cd(II) Removal from Model Solutions Using immobilized Bentonite/Yeast Mixtures. Studia Universitatis Babes-Bolyai Chemia 153–161.
Costa, J.A.S., Paranhos, C.M., 2019. Evaluation of rice husk ash in adsorption of Remazol Red dye from aqueous media. SN Appl. Sci. 1, 397. https://doi.org/10.1007/s42452-019-0436-1
Crini, G., 2006. Non-conventional low-cost adsorbents for dye removal: A review. Bioresource Technology 97, 1061–1085. https://doi.org/10.1016/j.biortech.2005.05.001
Crini, G., Lichtfouse, E., Wilson, L.D., Morin-Crini, N., 2019. Conventional and non-conventional adsorbents for wastewater treatment. Environ Chem Lett 17, 195–213. https://doi.org/10.1007/s10311-018-0786-8
Crystal Quest© Water Filters, 2021. What Is Ultrafiltration? [WWW Document]. Crystal Quest Water Filters. URL https://crystalquest.com/pages/what-is-ultrafiltration (accessed 10.23.21).
Czamara, K., Majzner, K., Pacia, M.Z., Kochan, K., Kaczor, A., Baranska, M., 2015. Raman spectroscopy of lipids: a review. Journal of Raman Spectroscopy 46, 4–20. https://doi.org/10.1002/jrs.4607
Dai, L., Zhu, W., He, L., Tan, F., Zhu, N., Zhou, Q., He, M., Hu, G., 2018. Calcium-rich biochar from crab shell: An unexpected super adsorbent for dye removal. Bioresource Technology 267, 510–516. https://doi.org/10.1016/j.biortech.2018.07.090
D'Alba, L., Torres, R., Waterhouse, G.I.N., Eliason, C., Hauber, M.E., Shawkey, M.D., 2017. What Does the Eggshell Cuticle Do? A Functional Comparison of Avian Eggshell Cuticles. Physiol. Biochem. Zool. 90, 588–599. https://doi.org/10.1086/693434
Danouche, M., Arroussi, H.E., Bahafid, W., Ghachtouli, N.E., 2021. An overview of the biosorption mechanism for the bioremediation of synthetic dyes using yeast cells. Environmental Technology Reviews 10, 58–76. https://doi.org/10.1080/21622515.2020.1869839
Dauphin, Y., Cuif, J.-P., Salomé, M., Susini, J., Williams, C.T., 2006. Microstructure and chemical composition of giant avian eggshells. Anal Bioanal Chem 386, 1761. https://doi.org/10.1007/s00216-006-0784-8
De Angelis, G., Medeghini, L., Conte, A.M., Mignardi, S., 2017. Recycling of eggshell waste into low-cost adsorbent for Ni removal from wastewater. Journal of Cleaner Production 164, 1497–1506. https://doi.org/10.1016/j.jclepro.2017.07.085
De Gisi, S., Lofrano, G., Grassi, M., Notarnicola, M., 2016. Characteristics and adsorption capacities of low-cost sorbents for wastewater treatment: A review. Sustainable Materials and Technologies 9, 10–40. https://doi.org/10.1016/j.susmat.2016.06.002
de Oliveira, M., Frihling, B.E.F., Velasques, J., Filho, F.J.C.M., Cavalheri, P.S., Migliolo, L., 2020. Pharmaceuticals residues and xenobiotics contaminants: Occurrence, analytical techniques and sustainable alternatives for wastewater treatment. Science of The Total Environment 705, 135568. https://doi.org/10.1016/j.scitotenv.2019.135568
Dehghani, M.H., Salari, M., Karri, R.R., Hamidi, F., Bahadori, R., 2021. Process modeling of municipal solid waste compost ash for reactive red 198 dye adsorption from wastewater using data driven approaches. Sci Rep 11, 11613. https://doi.org/10.1038/s41598-021-90914-z
Demirbas, A., 2009. Agricultural based activated carbons for the removal of dyes from aqueous solutions: A review. Journal of Hazardous Materials 167, 1–9. https://doi.org/10.1016/j.jhazmat.2008.12.114

Doan, C.T., Tran, T.N., Wang, C.-L., Wang, S.-L., 2020. Microbial Conversion of Shrimp Heads to Proteases and Chitin as an Effective Dye Adsorbent. Polymers 12, 2228. https://doi.org/10.3390/polym12102228

Donkadokula, N.Y., Kola, A.K., Naz, I., Saroj, D., 2020. A review on advanced physico-chemical and biological textile dye wastewater treatment techniques. Rev Environ Sci Biotechnol 19, 543–560. https://doi.org/10.1007/s11157-020-09543-z

Druding, S.C., 1982. Dye History from 2600 BC to the 20th Century [WWW Document]. URL https://www.studypool.com/documents/116420/dye-history-from-2600-bc-to-the-20th-century

Dutta, S., Gupta, B., Kumar Srivastava, S., Kumar Gupta, A., 2021. Recent advances on the removal of dyes from wastewater using various adsorbents: a critical review. Materials Advances 2, 4497–4531. https://doi.org/10.1039/D1MA00354B

Easton, R., 1995. The dye maker's view in: P. Cooper (Ed.) Colour in dyehouse Effluents. The Aldren Press, England, Bradford, pp. 9–21.

Ejikeme, P.C.N., Ejikeme, E.M., Okonkwo, G.N., 2014. Equilibrium, kinetic and thermodynamic stuies on basic dye adsorption using composite activated carbon. International Journal of Technical Research and Applications 2, 96–103.

El Rasafi, T., Oukarroum, A., Haddioui, A., Song, H., Kwon, E.E., Bolan, N., Tack, F.M.G., Sebastian, A., Prasad, M.N.V., Rinklebe, J., 2020. Cadmium stress in plants: A critical review of the effects, mechanisms, and tolerance strategies. Critical Reviews in Environmental Science and Technology 0, 1–52. https://doi.org/10.1080/10643389.2020.1835435

El-Dars, F., M Ibrahim, H., A. B. Farag, H., Zakaria Abdelwahhab, M., Shalabi, M., 2015. Adsorption Kinetics of Bromophenol Blue and Eriochrome Black T using Bentonite Carbon Composite Material, International Journal of Scientific & Engineering Research, Volume 6, Issue 5, May-2015. International Journal of Scientific and Engineering Research.

El-Harby, N.F., Ibrahim, S.M.A., Mohamed, N.A., 2017. Adsorption of Congo red dye onto antimicrobial terephthaloyl thiourea cross-linked chitosan hydrogels. Water Science and Technology 76, 2719–2732. https://doi.org/10.2166/wst.2017.442

Elkady, M.F., Ibrahim, A.M., El-Latif, M.M.A., 2011. Assessment of the adsorption kinetics, equilibrium and thermodynamic for the potential removal of reactive red dye using eggshell biocomposite beads. Desalination 278, 412–423. https://doi.org/10.1016/j.desal.2011.05.063

El-Sikaily, A., Khaled, A., El Nemr, A., 2012. Textile Dyes Xenobiotic and Their Harmful Effect, in: Non-Conventional Textile Waste Water Treatment. Nova Science Publishers, USA, New York, pp. 31–64.

Emil Cardos, Cecilia Roman, Michaela Ponta, Tiberiu Frentiu, Radu Rautiu, 2007. Evaluation of Soil Pollution with Copper, Lead, Zinc and Cadmium in the Mining Area Baia Mare. Revista de Chimie 58, 1–5.

EMIS, 2020. Adsorption Techniques | EMIS [WWW Document]. URL https://emis.vito.be/en/bat/tools-overview/sheets/adsorption-techniques (accessed 7.28.21).

Esmaeili, H., Foroutan, R., Jafari, D., Aghil Rezaei, M., 2020. Effect of interfering ions on phosphate removal from aqueous media using magnesium oxide@ferric molybdate nanocomposite. Korean J. Chem. Eng. 37, 804–814. https://doi.org/10.1007/s11814-020-0493-6

Es-sahbany, H., El Hachimi, M.L., Hsissou, R., Belfaquir, M., Es-sahbany, K., Nkhili, S., Loutfi, M., Elyoubi, M.S., 2021. Adsorption of heavy metal (Cadmium) in synthetic wastewater by the natural clay as a potential adsorbent (Tangier-Tetouan-Al Hoceima – Morocco region). Materials Today: Proceedings. https://doi.org/10.1016/j.matpr.2020.12.1102

Farouk, R., Gaffer, H.E., 2013. Simultaneous dyeing and antibacterial finishing for cotton cellulose using a new reactive dye. Carbohydrate Polymers 97, 138–142. https://doi.org/10.1016/j.carbpol.2013.04.037

Fomina, M., Gadd, G.M., 2014. Biosorption: current perspectives on concept, definition and application. Bioresource Technology, Special Issue on Biosorption 160, 3–14. https://doi.org/10.1016/j.biortech.2013.12.102

Foo, K.Y., Hameed, B.H., 2010. Insights into the modeling of adsorption isotherm systems. Chemical Engineering Journal 156, 2–10. https://doi.org/10.1016/j.cej.2009.09.013
Forgács, E., Cserháti, T., Oros, G., 2004. Removal of synthetic dyes from wastewaters: a review. Environ Int 30, 953–971. https://doi.org/10.1016/j.envint.2004.02.001
Frost, R.L., Fredericks, P.M., Bartlett, J.R., 1993. Fourier transform Raman spectroscopy of kandite clays. Spectrochimica Acta Part A: Molecular Spectroscopy, Applications of fourier transform Raman spectroscopy\3-III 49, 667–674. https://doi.org/10.1016/0584-8539(93)80088-R
Frost, R.L., Gaast, S.J. van der, 1997. Kaolinite hydroxyls – a Raman microscopy study. Clay Minerals 32, 471–484. https://doi.org/10.1180/claymin.1997.032.3.09
Frost, R.L., Tran, T.H., Kristof, J., 1997. The structure of an intercalated ordered kaolinite — a Raman microscopy study. Clay Minerals 32, 587–596. https://doi.org/10.1180/claymin.1997.032.4.09
Frost, R.L., Vassallo, A.M., 1996. The Dehydroxylation of the Kaolinite Clay Minerals using Infrared Emission Spectroscopy. Clays Clay Miner. 44, 635–651. https://doi.org/10.1346/CCMN.1996.0440506
Gamoudi, S., Srasra, E., 2019. Adsorption of organic dyes by HDPy+-modified clay: Effect of molecular structure on the adsorption. Journal of Molecular Structure 1193, 522–531. https://doi.org/10.1016/j.molstruc.2019.05.055
Gao, X., Meng, X., 2021. Photocatalysis for Heavy Metal Treatment: A Review. Processes 9, 1729. https://doi.org/10.3390/pr9101729
Garg, D., Majumder, C.B., Kumar, S., Sarkar, B., 2019. Removal of Direct Blue-86 dye from aqueous solution using alginate encapsulated activated carbon (PnsAC-alginate) prepared from waste peanut shell. Journal of Environmental Chemical Engineering 7, 103365. https://doi.org/10.1016/j.jece.2019.103365
Ghorbel-Abid, I., Galai, K., Trabelsi-Ayadi, M., 2010. Retention of chromium (III) and cadmium (II) from aqueous solution by illitic clay as a low-cost adsorbent. Desalination 256, 190–195. https://doi.org/10.1016/j.desal.2009.06.079
Giwa, A.A., Bello, I.A., Oladipo, M.A., Adeoye, D.O., 2013. Removal of Cadmium from Waste-water by Adsorption Using the Husk of Melon (Citrullus lanatus) Seed. International Journal of Basic and Applied Science 02, 14.
Global Dyes & Pigments Market Size Report, 2021-2028 [WWW Document], 2021. URL https://www.grandviewresearch.com/industry-analysis/dyes-and-pigments-market (accessed 7.23.21).
Gomes, M.G., Pasquini, D., 2018. Utilization of eggshell waste as an adsorbent for the dry purification of biodiesel. Environmental Progress & Sustainable Energy 37, 2093–2099. https://doi.org/10.1002/ep.12870
González-López, M.E., Laureano-Anzaldo, C.M., Pérez-Fonseca, A.A., Arellano, M., Robledo-Ortíz, J.R., 2021. A Critical Overview of Adsorption Models Linearization: Methodological and Statistical Inconsistencies. Separation & Purification Reviews 0, 1–15. https://doi.org/10.1080/15422119.2021.1951757
Gul, I., Manzoor, M., Hashim, N., Shah, G.M., Waani, S.P.T., Shahid, M., Antoniadis, V., Rinklebe, J., Arshad, M., 2021. Challenges in microbially and chelate-assisted phytoextraction of cadmium and lead – A review. Environmental Pollution 287, 117667. https://doi.org/10.1016/j.envpol.2021.117667
Guo, X., Wang, J., 2019. A general kinetic model for adsorption: Theoretical analysis and modeling. Journal of Molecular Liquids 288, 111100. https://doi.org/10.1016/j.molliq.2019.111100
Gurdeep R. Chatwal, 2009. Synthetic Dyes. Himalaya Publishing House, Mumbai.
Gürses, A., Açıkyıldız, M., Güneş, K., Gürses, M.S., 2016. Dyes and Pigments, SpringerBriefs in Green Chemistry for Sustainability. Springer International Publishing, Switzerland, AG. https://doi.org/10.1007/978-3-319-33892-7

Guru, P.S., Dash, S., 2014. Sorption on eggshell waste--a review on ultrastructure, biomineralization and other applications. Adv Colloid Interface Sci 209, 49–67. https://doi.org/10.1016/j.cis.2013.12.013
Haider, F.U., Liqun, C., Coulter, J.A., Cheema, S.A., Wu, J., Zhang, R., Wenjun, M., Farooq, M., 2021. Cadmium toxicity in plants: Impacts and remediation strategies. Ecotoxicology and Environmental Safety 211, 111887. https://doi.org/10.1016/j.ecoenv.2020.111887
Hamid, Y., Tang, L., Hussain, B., Usman, M., Lin, Q., Rashid, M.S., He, Z., Yang, X., 2020. Organic soil additives for the remediation of cadmium contaminated soils and their impact on the soil-plant system: A review. Science of The Total Environment 707, 136121. https://doi.org/10.1016/j.scitotenv.2019.136121
Hamilton, R., 1986. The Microstructure of the Hen's Egg Shell - A Short Review. Food Structure 5.
Hamza, W., Dammak, N., Hadjltaief, H.B., Eloussaief, M., Benzina, M., 2018. Sono-assisted adsorption of Cristal Violet dye onto Tunisian Smectite Clay: Characterization, kinetics and adsorption isotherms. Ecotoxicology and Environmental Safety 163, 365–371. https://doi.org/10.1016/j.ecoenv.2018.07.021
Harrache, Z., Abbas, M., Aksil, T., Trari, M., 2019. Thermodynamic and kinetics studies on adsorption of Indigo Carmine from aqueous solution by activated carbon. Microchemical Journal 144, 180–189. https://doi.org/10.1016/j.microc.2018.09.004
Harripersadth, C., Musonge, P., Makarfi Isa, Y., Morales, M.G., Sayago, A., 2020. The application of eggshells and sugarcane bagasse as potential biomaterials in the removal of heavy metals from aqueous solutions. South African Journal of Chemical Engineering 34, 142–150. https://doi.org/10.1016/j.sajce.2020.08.002
Hassaan, M.A., El Nemr, A., Madkour, F.F., 2017. Testing the advanced oxidation processes on the degradation of Direct Blue 86 dye in wastewater. The Egyptian Journal of Aquatic Research 43, 11–19. https://doi.org/10.1016/j.ejar.2016.09.006
Hassani, A., Vafaei, F., Karaca, S., Khataee, A.R., 2014. Adsorption of a cationic dye from aqueous solution using Turkish lignite: Kinetic, isotherm, thermodynamic studies and neural network modeling. Journal of Industrial and Engineering Chemistry 20, 2615–2624. https://doi.org/10.1016/j.jiec.2013.10.049
He, Z., Ren, B., Hursthouse, A., Wang, Z., 2020. Efficient Removal of Cd(II) Using SiO2-Mg(OH)2 Nanocomposites Derived from Sepiolite. International Journal of Environmental Research and Public Health 17, 2223. https://doi.org/10.3390/ijerph17072223
Hessel, C., Allegre, C., Maisseu, M., Charbit, F., Moulin, P., 2007. Guidelines and legislation for dye house effluents. Journal of Environmental Management 83, 171–180. https://doi.org/10.1016/j.jenvman.2006.02.012
Hii, H.T., 2021. Adsorption Isotherm And Kinetic Models For Removal Of Methyl Orange And Remazol Brilliant Blue R By Coconut Shell Activated Carbon. Tropical Aquatic and Soil Pollution 1, 1–10. https://doi.org/10.53623/tasp.v1i1.4
Hincke, M., Nys, Y., Gautron, J., Mann, K., Rodriguez-Navarro, A., McKee, M., 2012. The eggshell: structure, composition and mineralization. Frontiers in Bioscience-Landmark 17. https://doi.org/10.2741/3985
Ho, Y.S., McKay, G., 1999. Pseudo-second order model for sorption processes. Process Biochemistry 34, 451–465. https://doi.org/10.1016/S0032-9592(98)00112-5
Homaeigohar, S., 2020. The Nanosized Dye Adsorbents for Water Treatment. Nanomaterials 10, 295. https://doi.org/10.3390/nano10020295
Hong, G.-B., Yu, T.-J., Lee, H.-C., Ma, C.-M., 2021. Using Rice Bran Hydrogel Beads to Remove Dye from Aqueous Solutions. Sustainability 13, 5640. https://doi.org/10.3390/su13105640
HORIBA, 2018. Raman Spectroscopy for Analysis and Monitoring [WWW Document]. URL http://www.horiba.com/fileadmin/uploads/Scientific/Documents/Raman/bands.pdf

Horng, J.Y., Huang, S.D., 1993. Removal of organic dye (direct blue) from synthetic wastewater by adsorptive bubble separation techniques. Environ. Sci. Technol. 27, 1169–1175. https://doi.org/10.1021/es00043a017

Hossain, M.D., Ngo, H., Guo, W., 2013. Introductory of Microsoft Excel SOLVER function-Spreadsheet method for isotherm and kinetics modelling of metals biosorption in water and wastewater. Journal of Water Sustainability 3, 223–237.

Hou, D., O'Connor, D., Igalavithana, A.D., Alessi, D.S., Luo, J., Tsang, D.C.W., Sparks, D.L., Yamauchi, Y., Rinklebe, J., Ok, Y.S., 2020. Metal contamination and bioremediation of agricultural soils for food safety and sustainability. Nat Rev Earth Environ 1, 366–381. https://doi.org/10.1038/s43017-020-0061-y

Hunger, K. (Ed.), 2002. Industrial Dyes: Chemistry, Properties, Applications, 1st ed. John Wiley & Sons, Germany, Weinheim. https://doi.org/10.1002/3527602011

Hynes, N.R.J., Kumar, J.S., Kamyab, H., Sujana, J.A.J., Al-Khashman, O.A., Kuslu, Y., Ene, A., Suresh Kumar, B., 2020. Modern enabling techniques and adsorbents based dye removal with sustainability concerns in textile industrial sector -A comprehensive review. Journal of Cleaner Production 272, 122636. https://doi.org/10.1016/j.jclepro.2020.122636

IARC Working Group on the Evaluation of Carcinogenic Risk to Humans, 2010. General introduction to the chemistry of dyes, Some Aromatic Amines, Organic Dyes, and Related Exposures. International Agency for Research on Cancer, France, Lyon.

Ihsanullah, I., Jamal, A., Ilyas, M., Zubair, M., Khan, G., Atieh, M.A., 2020. Bioremediation of dyes: Current status and prospects. Journal of Water Process Engineering 38, 101680. https://doi.org/10.1016/j.jwpe.2020.101680

Indolean, C., Măicăneanu, A., Cristea, V.-M., 2017. Prediction of Cu(II) biosorption performances on wild mushrooms Lactarius piperatus using Artificial Neural Networks (ANN) model. Can. J. Chem. Eng. 95, 615–622. https://doi.org/10.1002/cjce.22703

Intidhar Jabir Idan, Luqman Chuah Abdullah, Dalia Sadiq Mahdi, Maytham Kadhim Obaid, Siti Nurul Ain Binti Md. Jamil, 2017. Adsorption of Anionic Dye Using Cationic Surfactant-Modified Kenaf Core Fibers. Open Access Library Journal 04, 1. https://doi.org/10.4236/oalib.1103747

Iordache, M., Branzoi, I.V., Mandoc Popescu, L.R., Ioan, I., 2016. Evaluation of heavy metal pollution into a complex industrial area from Romania. Environmental Engineering and Management Journal 15, 389–394.

Iqbal, J., Wattoo, F.H., Wattoo, M.H.S., Malik, R., Tirmizi, S.A., Imran, M., Ghangro, A.B., 2011. Adsorption of acid yellow dye on flakes of chitosan prepared from fishery wastes. Arabian Journal of Chemistry 4, 389–395. https://doi.org/10.1016/j.arabjc.2010.07.007

Iqbal, M.J., Ashiq, M.N., 2010. Thermodynamics and kinetics of adsorption of dyes from aqueous media onto alumina. Journal of the Chemical Society of Pakistan 32, 419–428.

Irshad, S., Sultana, H., Usman, M., Saeed, M., Akram, N., Yusaf, A., Rehman, A., 2021. Solubilization of direct dyes in single and mixed surfactant system: A comparative study. Journal of Molecular Liquids 321, 114201. https://doi.org/10.1016/j.molliq.2020.114201

Ishak, S.A., Murshed, M.F., Md Akil, H., Ismail, N., Md Rasib, S.Z., Al-Gheethi, A.A.S., 2020. The Application of Modified Natural Polymers in Toxicant Dye Compounds Wastewater: A Review. Water 12, 2032. https://doi.org/10.3390/w12072032

Jadhav, A., Jadhav, N., 2021. Treatment of textile wastewater using adsorption and adsorbents, in: Sustainable Technologies for Textile Wastewater Treatments. Woodhead Publishing, Sawston, United Kingdom, pp. 235–273. https://doi.org/10.1016/B978-0-323-85829-8.00008-0

Jain, M., Garg, V.K., Kadirvelu, K., 2013. Cadmium(II) sorption and desorption in a fixed bed column using sunflower waste carbon calcium–alginate beads. Bioresource Technology 129, 242–248. https://doi.org/10.1016/j.biortech.2012.11.036

Johansson, U., Holmgren, A., Forsling, W., Frost, R., 1998. Isotopic exchange of kaolinite hydroxyl protons: a diffuse reflectance infrared Fourier transform spectroscopy study†. Analyst 123, 641–645. https://doi.org/10.1039/A707060H

José Eduardo Ferreira da Costa Gardolinski, 2005. Interlayer grafting and delamination of Kaolinite (Doctoral Thesis). Faculty of Mathematics and Natural Sciences of the Christian-Albrechts-University, Kiel, Germany.
Kamaya Parashar, 2015. Adsorption.
Kant, R., 2011. Textile dyeing industry an environmental hazard. Natural Science 4, 22–26. https://doi.org/10.4236/ns.2012.41004
Kanwal, A., Bhatti, H.N., Iqbal, M., Noreen, S., 2017. Basic Dye Adsorption onto Clay/MnFe2O4 Composite: A Mechanistic Study. Water Environment Research 89, 301–311. https://doi.org/10.2175/106143017X14839994522984
Kassinger, R., 2003. Dyes: From Sea Snails to Synthetics. Lerner Publishing Group: Twenty-First Century Books, USA, Minneapolis.
Katheresan, V., Kansedo, J., Lau, S.Y., 2018. Efficiency of various recent wastewater dye removal methods: A review. Journal of Environmental Chemical Engineering 6, 4676–4697. https://doi.org/10.1016/j.jece.2018.06.060
Kausar, A., Iqbal, M., Javed, A., Aftab, K., Nazli, Z.-H., Bhatti, H.N., Nouren, S., 2018. Dyes adsorption using clay and modified clay: A review. Journal of Molecular Liquids 256, 395–407. https://doi.org/10.1016/j.molliq.2018.02.034
Khalaf, I.H., Al-Sudani, F.T., AbdulRazak, A.A., Aldahri, T., Rohani, S., 2021. Optimization of Congo red dye adsorption from wastewater by a modified commercial zeolite catalyst using response surface modeling approach. Water Science and Technology 83, 1369–1383. https://doi.org/10.2166/wst.2021.078
Khamis, M.I., Ibrahim, T.H., Jumean, F.H., Sara, Z.A., Atallah, B.A., 2020. Cyclic Sequential Removal of Alizarin Red S Dye and Cr(VI) Ions Using Wool as a Low-Cost Adsorbent. Processes 8, 556. https://doi.org/10.3390/pr8050556
Khan, null, Ataullah, null, Al-Haddad, null, 1997. Equilibrium Adsorption Studies of Some Aromatic Pollutants from Dilute Aqueous Solutions on Activated Carbon at Different Temperatures. J Colloid Interface Sci 194, 154–165. https://doi.org/10.1006/jcis.1997.5041
Khasri, A., Jamir, M.R.M., Ahmad, A.A., Ahmad, M.A., 2021. Adsorption of Remazol Brilliant Violet 5R dye from aqueous solution onto melunak and rubberwood sawdust based activated carbon: interaction mechanism, isotherm, kinetic and thermodynamic properties. DWT 216, 401–411. https://doi.org/10.5004/dwt.2021.26852
Kőnigné Péter, A., 2012. Nehézfém adszorpció jellemzése különböző bioszorbenseken. Pécsi Tudományegyetem Kémia Doktori Iskola, Pécs.
Kostin, A.V., Mostalygina, L.V., Bukhtoyarov, O.I., 2015. The mechanism of adsorption of zinc and cadmium ions onto bentonite clay. Prot Met Phys Chem Surf 51, 773–778. https://doi.org/10.1134/S2070205115050172
Kumari, N., Mohan, C., 2021. Basics of Clay Minerals and Their Characteristic Properties. IntechOpen. https://doi.org/10.5772/intechopen.97672
Kyzas, G.Z., Bikiaris, D.N., Mitropoulos, A.C., 2017. Chitosan adsorbents for dye removal: a review. Polymer International 66, 1800–1811. https://doi.org/10.1002/pi.5467
Kyzas, G.Z., Deliyanni, E.A., Bikiaris, D.N., Mitropoulos, A.C., 2018. Graphene composites as dye adsorbents: Review. Chemical Engineering Research and Design 129, 75–88. https://doi.org/10.1016/j.cherd.2017.11.006
Kyzas, G.Z., Kostoglou, M., Lazaridis, N.K., Bikiaris, D.N., 2013. Decolorization of Dyeing Wastewater Using Polymeric Absorbents - An Overview, Eco-Friendly Textile Dyeing and Finishing. IntechOpen, United Kingdom, London. https://doi.org/10.5772/52817
Labanda, J., Sabaté, J., Llorens, J., 2009. Modeling of the dynamic adsorption of an anionic dye through ion-exchange membrane adsorber. Journal of Membrane Science 340, 234–240. https://doi.org/10.1016/j.memsci.2009.05.036
Lagergren S., 1898. About The Theory Of So-Called Adsorption Of Soluble Substances. Kungliga Svenska Vetenskapsakademiens Handlingar 24, 1–39.

Lai, K.C., Lee, L.Y., Hiew, B.Y.Z., Thangalazhy-Gopakumar, S., Gan, S., 2019. Environmental application of three-dimensional graphene materials as adsorbents for dyes and heavy metals: Review on ice-templating method and adsorption mechanisms. Journal of Environmental Sciences 79, 174–199. https://doi.org/10.1016/j.jes.2018.11.023

Lazaridis, N.K., Karapantsios, T.D., Georgantas, D., 2003. Kinetic analysis for the removal of a reactive dye from aqueous solution onto hydrotalcite by adsorption. Water Research 37, 3023–3033. https://doi.org/10.1016/S0043-1354(03)00121-0

Leach, R.M., 1982. Biochemistry of the Organic Matrix of the Eggshell. Poult Sci 61, 2040–2047. https://doi.org/10.3382/ps.0612040

Lei, T., Li, S.-J., Jiang, F., Ren, Z.-X., Wang, L.-L., Yang, X.-J., Tang, L.-H., Wang, S.-X., 2019. Adsorption of Cadmium Ions from an Aqueous Solution on a Highly Stable Dopamine-Modified Magnetic Nano-Adsorbent. Nanoscale Research Letters 14, 352. https://doi.org/10.1186/s11671-019-3154-0

Letha Malan Oelz, 2018. Textile dyeing: dyeing fabric… (Textiles – Dyeing Process) [WWW Document]. URL https://www.linkedin.com/pulse/textile-dyeing-fabric-textiles-process-letha-oelz/ (accessed 7.26.21).

Li, S., Zeng, Z., Xue, W., 2019. Kinetic and equilibrium study of the removal of reactive dye using modified walnut shell. Water Science and Technology 80, 874–883. https://doi.org/10.2166/wst.2019.324

Lipatova, I.M., Makarova, L.I., Yusova, A.A., 2018. Adsorption removal of anionic dyes from aqueous solutions by chitosan nanoparticles deposited on the fibrous carrier. Chemosphere 212, 1155–1162. https://doi.org/10.1016/j.chemosphere.2018.08.158

Liu, J., Wang, N., Zhang, H., Baeyens, J., 2019. Adsorption of Congo red dye on FexCo3-xO4 nanoparticles. Journal of Environmental Management 238, 473–483. https://doi.org/10.1016/j.jenvman.2019.03.009

Liu, W., 2001. Modeling description and spectroscopic evidence of surface acid–base properties of natural illites. Water Research 35, 4111–4125. https://doi.org/10.1016/S0043-1354(01)00156-7

Liu, Y., Xu, H., Yang, S.-F., Tay, J.-H., 2003. A general model for biosorption of Cd2+, Cu2+ and Zn2+ by aerobic granules. J Biotechnol 102, 233–239. https://doi.org/10.1016/s0168-1656(03)00030-0

Long, X., Chen, H., Huang, T., Zhang, Y., Lu, Y., Tan, J., Chen, R., 2021. Removal of Cd(II) from Micro-Polluted Water by Magnetic Core-Shell Fe3O4@Prussian Blue. Molecules 26, 2497. https://doi.org/10.3390/molecules26092497

López-Luna, J., Ramírez-Montes, L.E., Martinez-Vargas, S., Martínez, A.I., Mijangos-Ricardez, O.F., González-Chávez, M. del C.A., Carrillo-González, R., Solís-Domínguez, F.A., Cuevas-Díaz, M. del C., Vázquez-Hipólito, V., 2019. Linear and nonlinear kinetic and isotherm adsorption models for arsenic removal by manganese ferrite nanoparticles. SN Appl. Sci. 1, 950. https://doi.org/10.1007/s42452-019-0977-3

M, A.A., Choudhary, A., 2017. Removal of oil from seawater using charcoal and rice hull. IOP Conf. Ser.: Mater. Sci. Eng. 263, 032007. https://doi.org/10.1088/1757-899X/263/3/032007

Ma, C.M., Hong, G.B., Wang, Y.K., 2020. Performance Evaluation and Optimization of Dyes Removal using Rice Bran-Based Magnetic Composite Adsorbent. Materials (Basel) 13, 2764. https://doi.org/10.3390/ma13122764

Madhav, S., Ahamad, A., Singh, P., Mishra, P.K., 2018. A review of textile industry: Wet processing, environmental impacts, and effluent treatment methods. Environmental Quality Management 27, 31–41. https://doi.org/10.1002/tqem.21538

Mahapatra, N.N., 2016. Textile Dyes. Woodhead Publishing India PVT. Limited.

Mahmoud, M.S., 2016. Decolorization of certain reactive dye from aqueous solution using Baker's Yeast (Saccharomyces cerevisiae) strain. HBRC Journal 12, 88–98. https://doi.org/10.1016/j.hbrcj.2014.07.005

Maleš, L., Fakin, D., Bračič, M., Gorgieva, S., 2020. Efficiency of Differently Processed Membranes Based on Cellulose as Cationic Dye Adsorbents. Nanomaterials 10, 642. https://doi.org/10.3390/nano10040642

Mansour, H., 2013. Textile Dyeing: Environmental Friendly Osage Orange Extract on Protein Fabrics, in: Gunay, M. (Ed.), Eco-Friendly Textile Dyeing and Finishing. IntechOpen Limited, United Kingdom, London. https://doi.org/10.5772/54410

Mansouri, F.E., Farissi, H.E., Zerrouk, M.H., Cacciola, F., Bakkali, C., Brigui, J., Lovillo, M.P., Esteves da Silva, J.C.G., 2021. Dye Removal from Colored Textile Wastewater Using Seeds and Biochar of Barley (Hordeum vulgare L.). Applied Sciences 11, 5125. https://doi.org/10.3390/app11115125

Market Data Forecast ltd, 2021. Dyes Market | Size, Share & Trends | 2021 - 2026 [WWW Document]. Market Data Forecast. URL http://www.marketdataforecast.com/ (accessed 7.23.21).

Mashangwa, T.D., Tekere, M., Sibanda, T., 2017. Determination of the Efficacy of Eggshell as a Low-Cost Adsorbent for the Treatment of Metal Laden Effluents. Int J Environ Res 11, 175–188. https://doi.org/10.1007/s41742-017-0017-3

Mashkoor, F., Nasar, A., 2021. Environmental Application of Agro-waste Derived Materials for the Treatment of Dye-polluted Water: A Review. Current Analytical Chemistry 17, 904–916. https://doi.org/10.2174/1573411016666200102114854

Mazharul Islam Kiron, 2021. Difference between Dyes and Pigments [WWW Document]. Textile Learner. URL https://textilelearner.net/dyes-and-pigments/ (accessed 7.31.21).

Md. Imran Hossain, 2021. Sources and Applications of Natural Dyes [WWW Document]. Textile News, Views & Articles. URL https://textilefocus.com/sources-applications-natural-dyes/ (accessed 7.26.21).

Michaelian, K.H., 2011. The Raman spectrum of kaolinite #9 at 21°C. Canadian Journal of Chemistry. https://doi.org/10.1139/v86-048

Mikhailenko, A.V., Ruban, D.A., Ermolaev, V.A., van Loon, A.J. (Tom), 2020. Cadmium Pollution in the Tourism Environment: A Literature Review. Geosciences 10, 242. https://doi.org/10.3390/geosciences10060242

Miraboutalebi, S.M., Peydayesh, M., Bagheri, M., Mohammadi, T., 2020. Polyacrylonitrile/α-Fe2O3 Hybrid Photocatalytic Composite Adsorbents for Enhanced Dye Removal. Chemical Engineering & Technology 43, 1214–1223. https://doi.org/10.1002/ceat.202000140

Miranda-Trevino, J.C., Coles, C.A., 2003. Kaolinite properties, structure and influence of metal retention on pH. Applied Clay Science, Clay Microstructure. Proceedings of a Workshop held in Lund, Sweden, 15-17 October 2002 23, 133–139. https://doi.org/10.1016/S0169-1317(03)00095-4

Mohadi, R., Anggraini, K., Riyanti, F., Lesbani, A., 2016. Preparation Calcium Oxide From Chicken Eggshells. Sriwijaya Journal of Environment 1, 32–35. https://doi.org/10.22135/sje.2016.1.2.32-35

Mok, C.F., Ching, Y.C., Muhamad, F., Abu Osman, N.A., Hai, N.D., Che Hassan, C.R., 2020. Adsorption of Dyes Using Poly(vinyl alcohol) (PVA) and PVA-Based Polymer Composite Adsorbents: A Review. J Polym Environ 28, 775–793. https://doi.org/10.1007/s10924-020-01656-4

Mokhtari, N., Afshari, M., Dinari, M., 2020. Synthesis and characterization of a novel fluorene-based covalent triazine framework as a chemical adsorbent for highly efficient dye removal. Polymer 195, 122430. https://doi.org/10.1016/j.polymer.2020.122430

Moldoveanu, A.M., 2014. Assessment of Soil Pollution with Heavy Metals in Romania, Environmental Risk Assessment of Soil Contamination. IntechOpen. https://doi.org/10.5772/57595

Mondal, N.K., Kar, S., 2018. Potentiality of banana peel for removal of Congo red dye from aqueous solution: isotherm, kinetics and thermodynamics studies. Appl Water Sci 8, 157. https://doi.org/10.1007/s13201-018-0811-x

Morais da Silva, P.M., Camparotto, N.G., Grego Lira, K.T., Franco Picone, C.S., Prediger, P., 2020. Adsorptive removal of basic dye onto sustainable chitosan beads: Equilibrium, kinetics, stability, continuous-mode adsorption and mechanism. Sustainable Chemistry and Pharmacy 18, 100318. https://doi.org/10.1016/j.scp.2020.100318

Muinde, V., Onyari, J.M., Wamalwa, B.M., Wabomba, J., 2017. Adsorption Of Malachite Green From Aqueous Solutions Onto Rice Husks: Kinetic And Equilibrium Studies. Journal of Environmental Protection 8, 215–230.

Munagapati, V.S., Wen, J.-C., Pan, C.-L., Gutha, Y., Wen, J.-H., Reddy, G.M., 2020. Adsorptive removal of anionic dye (Reactive Black 5) from aqueous solution using chemically modified banana peel powder: kinetic, isotherm, thermodynamic, and reusability studies. International Journal of Phytoremediation 22, 267–278. https://doi.org/10.1080/15226514.2019.1658709

Murad, E., 1997. Identification of minor amounts of anatase in kaolins by Raman spectroscopy. American Mineralogist 82, 203–206. https://doi.org/10.2138/am-1997-1-222

Murcia-Salvador, A., Pellicer, J.A., Fortea, M.I., Gómez-López, V.M., Rodríguez-López, M.I., Núñez-Delicado, E., Gabaldón, J.A., 2019. Adsorption of Direct Blue 78 Using Chitosan and Cyclodextrins as Adsorbents. Polymers (Basel) 11, 1003. https://doi.org/10.3390/polym11061003

Mustapha, S., Shuaib, D.T., Ndamitso, M.M., Etsuyankpa, M.B., Sumaila, A., Mohammed, U.M., Nasirudeen, M.B., 2019. Adsorption isotherm, kinetic and thermodynamic studies for the removal of Pb(II), Cd(II), Zn(II) and Cu(II) ions from aqueous solutions using Albizia lebbeck pods. Appl Water Sci 9, 142. https://doi.org/10.1007/s13201-019-1021-x

N. Tangboriboon, R. Kunanuruksapong, A. Srivat, 2012. Meso-porosity and phase transformation of bird eggshells via pyrolysis. Journal of Ceramic Processing Research Journal of Ceramic Processing Research 13(4):413-419, 413–419.

Nagy, B., Maicaneanu, A., Indolean, C., Burca, S., Silaghi-Dumitrescu, L., Majdik, C., 2013a. Cadmium (II) ions removal from aqueous solutions using Romanian untreated fir tree sawdust–a green biosorbent. Acta Chimica Slovenica 60, 263–273.

Nagy, B., Mânzatu, C., Măicăneanu, A., Indolean, C., Barbu-Tudoran, L., Majdik, C., 2017. Linear and nonlinear regression analysis for heavy metals removal using Agaricus bisporus macrofungus. Arabian Journal of Chemistry 10, S3569–S3579. https://doi.org/10.1016/j.arabjc.2014.03.004

Nagy, B., Tonk, S., Indolean (Afloroaei), L., Andrada, M., Majdik, C., 2013b. Biosorption of Cadmium Ions by Unmodified, Microwave and Ultrasound Modified Brewery and Pure Strain Yeast Biomass. American Journal of Analytical Chemistry 04, 63–71. https://doi.org/10.4236/ajac.2013.47A009

Nasar, A., Mashkoor, F., 2019. Application of polyaniline-based adsorbents for dye removal from water and wastewater—a review. Environ Sci Pollut Res 26, 5333–5356. https://doi.org/10.1007/s11356-018-3990-y

Nawab, Y., Ashraf, M., Hussain, T., Rasheed, A., Shaker, K., Basit, A., Jabbar, M., Malik, Z., Fiaz, H., Shehzad, K., Umair, M., Ahmad, S., Maqsood, M., Ashraf, W., Baig, S., Hamdani, T., Zohaib, M., 2016. Textile Engineering. An Introduction. De Gruyter (Walter de Gruyter), Germany, Berlin, pp. 143–159.

Nayeri, D., Mousavi, S.A., 2020. Dye removal from water and wastewater by nanosized metal oxides - modified activated carbon: a review on recent researches. J Environ Health Sci Engineer 18, 1671–1689. https://doi.org/10.1007/s40201-020-00566-w

Neag, E., Moldovan, A., Băbălău-Fuss, V., Török, A., Cadar, O., Roman, C., 2019. Kinetic, Equilibrium and Phytotoxicity Studies for Dyes Removal by Low Cost Natural Activated Plant-Based Carbon. Acta Chimica Slovenica 66, 850–858. https://doi.org/10.17344/acsi.2018.4924

Nekhlaoui, S., Abdellaoui, H., Marya, R., Essabir, H., Rodrigue, D., Mohammed ouadi, B., Bouhfid, R., Qaiss, A., 2021. Assessment of thermo-mechanical, dye discoloration, and hygroscopic behavior of hybrid composites based on polypropylene/clay (illite)/TiO2. The

International Journal of Advanced Manufacturing Technology 113, 1–14. https://doi.org/10.1007/s00170-021-06765-5
Ngulube, T., Gumbo, J.R., Masindi, V., Maity, A., 2017. An update on synthetic dyes adsorption onto clay based minerals: A state-of-art review. Journal of Environmental Management 191, 35–57. https://doi.org/10.1016/j.jenvman.2016.12.031
Nikam, S., Mandal, D., 2020. Experimental Study of the Effect of Different Parameters on the Adsorption and Desorption of Trichloroethylene Vapor on Activated Carbon Particles. ACS Omega 5, 28080–28087. https://doi.org/10.1021/acsomega.0c03648
Niño, V., Bello, Y., Rios, C., Fiallo, L., 2013. Application of faujasite synthesized from illite to the removal of Cr3+ and Ni2+ from electroplating wastewater. Revista ION 26, 7–16.
Nitin Verma, Vivek Kumar, Mukesh C. Bansal, n.d. Utilization of Egg Shell Waste in Cellulase Production by Neurospora crassa under Wheat Bran-Based Solid State Fermentation. Pol. J. Environ. Stud. 21, 491–497.
Obaje, S.O., Omada, J.I., Dambatta, U.A., 2013. Clays and their Industrial Applications: Synoptic Review. International Journal of Science and Technology 3.
Osasona, I., Aiyedatiwa, K., Johnson, J., Faboya, O.L., 2018. Activated Carbon from Spent Brewery Barley Husks for Cadmium Ion Adsorption from Aqueous Solution. Indonesian Journal of Chemistry 18, 145–152. https://doi.org/10.22146/ijc.22422
Oyelude, E.O., Awudza, J.A.M., Twumasi, S.K., 2017. Equilibrium, Kinetic and Thermodynamic Study of Removal of Eosin Yellow from Aqueous Solution Using Teak Leaf Litter Powder. Sci Rep 7, 12198. https://doi.org/10.1038/s41598-017-12424-1
Pai, S., Kini, M.S., Selvaraj, R., 2021. A review on adsorptive removal of dyes from wastewater by hydroxyapatite nanocomposites. Environ Sci Pollut Res 28, 11835–11849. https://doi.org/10.1007/s11356-019-07319-9
Park, H.J., Jeong, S.W., Yang, J.K., Kim, B.G., Lee, S.M., 2007. Removal of heavy metals using waste eggshell. Journal of Environmental Sciences 19, 1436–1441. https://doi.org/10.1016/S1001-0742(07)60234-4
Parvin, S., Biswas, B.K., Rahman, M.A., Rahman, M.H., Anik, M.S., Uddin, M.R., 2019. Study on adsorption of Congo red onto chemically modified egg shell membrane. Chemosphere 236, 124326. https://doi.org/10.1016/j.chemosphere.2019.07.057
Patel, H., 2011. Equilibrium, kinetic and thermodynamic stuies on adsorption of reactive dyes onto activated guava leaf powder. Fresenius Environmental Bulletin 20.
Patil, S., Renukdas, S., Patel, N., 2011. Removal of methylene blue, a basic dye from aqueous solutions by adsorption using teak tree (Tectona grandis) bark powder. International Journal on Environmental Sciences.
Paul Rys, Heinrich Zollinger, 1989. Reactive dye-fibre systems, in: Theory of Coloration of Textiles. Dyers Company Publications Trust, England, Bradford, p. 564.
Pavithra, K.G., P., S.K., V., J., P., S.R., 2019. Removal of colorants from wastewater: A review on sources and treatment strategies. Journal of Industrial and Engineering Chemistry 75, 1–19. https://doi.org/10.1016/j.jiec.2019.02.011
Peck Kah Yeow, Sie Wei Wong, Tony Hadibarata, 2020. Removal of Azo and Anthraquinone Dye by Plant Biomass as Adsorbent – A Review. Biointerface Res Appl Chem 11, 8218–8232. https://doi.org/10.33263/BRIAC111.82188232
Pellicer, J., Rodriguez López, M.I., Fortea, M., Gabaldon, J., Lucas-Abellán, C., Mercader Ros, M., Serrano Martínez, A., Núñez-Delicado, E., Cosma, P., Fini, P., Franco, E., Garcia, R., Ferrándiz, M., Pérez, E., Ferrándiz, Miguel, 2017. Removing of Direct Red 83:1 using α- and HP-α-CDs polymerized with epichlorohydrin: Kinetic and equilibrium studies. Dyes and Pigments 149. https://doi.org/10.1016/j.dyepig.2017.11.032
Pellicer, J.A., Rodríguez-López, M.I., Fortea, M.I., Lucas-Abellán, C., Mercader-Ros, M.T., López-Miranda, S., Gómez-López, V.M., Semeraro, P., Cosma, P., Fini, P., Franco, E., Ferrándiz, Marcela, Pérez, E., Ferrándiz, Miguel, Núñez-Delicado, E., Gabaldón, J.A., 2019. Adsorption Properties of β- and Hydroxypropyl-β-Cyclodextrins Cross-Linked with

Epichlorohydrin in Aqueous Solution. A Sustainable Recycling Strategy in Textile Dyeing Process. Polymers 11, 252. https://doi.org/10.3390/polym11020252
Peng, Y., Li, Z., Yang, X., Yang, L., He, M., Zhang, H., Wei, X., Qin, J., Li, X., Lu, G., Zhang, L., Yang, Y., Zhang, Z., Zou, Y., 2020. Relation between cadmium body burden and cognitive function in older men: A cross-sectional study in China. Chemosphere 250, 126535. https://doi.org/10.1016/j.chemosphere.2020.126535
Pernyeszi, T., Farkas, R., Kovács, J., 2019. Methylene Blue Adsorption Study on Microcline Particles in the Function of Particle Size Range and Temperature. Minerals 9, 555. https://doi.org/10.3390/min9090555
Pham, T.D., Bui, V.P., Pham, T.N., Le, T.M.D., Nguyen, K.T., Bui, V.H., Nguyen, T.D., 2021. Adsorptive Removal of Anionic Azo Dye New Coccine Using Silica and Silica-gel with Surface Modification by Polycation. Polymers 13, 1536. https://doi.org/10.3390/polym13101536
Pholosi, A., Naidoo, E.B., Ofomaja, A.E., 2020. Intraparticle diffusion of Cr(VI) through biomass and magnetite coated biomass: A comparative kinetic and diffusion study. South African Journal of Chemical Engineering 32, 39–55. https://doi.org/10.1016/j.sajce.2020.01.005
Popa, S., Radulescu-Grad, M.E., Perdivara, A., Mosoarca, G., 2021. Aspects regarding colour fastness and adsorption studies of a new azo-stilbene dye for acrylic resins. Sci Rep 11, 5889. https://doi.org/10.1038/s41598-021-85452-7
Pourhakkak, P., Taghizadeh, A., Taghizadeh, M., Ghaedi, M., Haghdoust, S., 2021. Chapter 1 - Fundamentals of adsorption technology, in: Ghaedi, M. (Ed.), Interface Science and Technology, Adsorption: Fundamental Processes and Applications. Elsevier, United Kingdom, London, pp. 1–70. https://doi.org/10.1016/B978-0-12-818805-7.00001-1
Pradhan, P., Bajpai, A., 2020. Preparation and characterization of films from Chicken feathers for dye adsorption. Materials Today: Proceedings, International Conference on Advanced Functional Materials (Innovations in Chemical, Physical and Biological Sciences) 29, 1204–1212. https://doi.org/10.1016/j.matpr.2020.05.433
Prol, A.E.A., 2019. Study of Environmental Concerns of Dyes and Recent Textile Effluents Treatment Technology: A Review. Asian Journal of Fisheries and Aquatic Research 1–18. https://doi.org/10.9734/ajfar/2019/v3i230032
P. Vinayan, B., Zhao-Karger, Z., Diemant, T., Kiran Chakravadhanula, V.S., I. Schwarzburger, N., Ali Cambaz, M., Jürgen Behm, R., Kübel, C., Fichtner, M., 2016. Performance study of magnesium–sulfur battery using a graphene based sulfur composite cathode electrode and a non-nucleophilic Mg electrolyte. Nanoscale 8, 3296–3306. https://doi.org/10.1039/C5NR04383B
Qasem, N.A.A., Mohammed, R.H., Lawal, D.U., 2021. Removal of heavy metal ions from wastewater: a comprehensive and critical review. npj Clean Water 4, 1–15. https://doi.org/10.1038/s41545-021-00127-0
Qayyum, S., Nasir, A., Mian, A.H., Rehman, S., Qayum, S., Siddiqui, M.F., Kalsoom, U., 2020. Extraction of peroxidase enzyme from different vegetables for biodetoxification of vat dyes. Appl Nanosci 10, 5191–5199. https://doi.org/10.1007/s13204-020-01348-4
Qi, Y., Zhu, J., Fu, Q., Hu, H., Huang, Q., 2017. Sorption of Cu by humic acid from the decomposition of rice straw in the absence and presence of clay minerals. Journal of Environmental Management 200, 304–311. https://doi.org/10.1016/j.jenvman.2017.05.087
Qin, S., Liu, H., Nie, Z., Rengel, Z., Gao, W., Li, C., Zhao, P., 2020. Toxicity of cadmium and its competition with mineral nutrients for uptake by plants: A review. Pedosphere 30, 168–180. https://doi.org/10.1016/S1002-0160(20)60002-9
Qin, Y., Yuan, M., Hu, Y., Lu, Y., Lin, W., Ma, Y., Lin, X., Wang, T., 2020. Preparation and interaction mechanism of Nano disperse dye using hydroxypropyl sulfonated lignin. International Journal of Biological Macromolecules 152, 280–287. https://doi.org/10.1016/j.ijbiomac.2020.02.261
Rachakornkij, M., Sirawan, R., Sumate, T., 2004. Removal of reactive dyes from aqueous solution using bagasse fly ash. Songklanakarin Journal of Science and Technology 26.

Radke, C.J., Prausnitz, J.M., 1972. Adsorption of Organic Solutes from Dilute Aqueous Solution of Activated Carbon. Ind. Eng. Chem. Fund. 11, 445–451. https://doi.org/10.1021/i160044a003
Radu, L., Lacatusu, A.-R., 2008. Vegetable food quality within heavy metals polluted areas in Romania. Carpathian journal of earth and environmental sciences 3, 115–129.
Ramesh, G., Jayabalakrishnan, D., Rameshkumar, C., 2018. Mechanical and thermal characterization of heat/surface treated egg shell filler diffused natural rubber green composite. Journal of Optoelectronics and Biomedical Materials 10, 21–28.
Rao, R.A.K., Kashifuddin, M., 2016. Adsorption studies of Cd(II) on ball clay: Comparison with other natural clays. Arabian Journal of Chemistry 9, S1233–S1241. https://doi.org/10.1016/j.arabjc.2012.01.010
Rao, R.A.K., Kashifuddin, M., 2014. Kinetics and isotherm studies of Cd(II) adsorption from aqueous solution utilizing seeds of bottlebrush plant (Callistemon chisholmii). Appl Water Sci 4, 371–383. https://doi.org/10.1007/s13201-014-0153-2
Rápó, E., Aradi, L.E., Szabó, Á., Posta, K., Szép, R., Tonk, S., 2020a. Adsorption of Remazol Brilliant Violet-5R Textile Dye from Aqueous Solutions by Using Eggshell Waste Biosorbent. Sci Rep 10, 8385. https://doi.org/10.1038/s41598-020-65334-0
Rápó, E., Aradi, L.E., Szabó, Á., Posta, K., Szép, R., Tonk, S., 2020b. Adsorption of Remazol Brilliant Violet-5R Textile Dye from Aqueous Solutions by Using Eggshell Waste Biosorbent. Scientific Reports 10, 8385. https://doi.org/10.1038/s41598-020-65334-0
Rápó, E., Jakab, K., Posta, K., Suciu, M., Tonk, S., 2020c. A Comparative Study on the Adsorption of Two Remazol Dyes on Green Adsorbent. Rev. Chim. 71, 248–257. https://doi.org/10.37358/RC.20.4.8063
Rápó, E., Posta, K., Suciu, M., Szép, R., Tonk, S., 2019. Adsorptive Removal of Remazol Brilliant Violet-5R Dye from Aqueous Solutions using Calcined Eggshell as Biosorbent. Acta Chimica Slovenica 66, 648–658. https://doi.org/10.17344/acsi.2019.5079
Rápó, E., Szép, R., Keresztesi, Á., Suciu, M., Tonk, S., 2018. Adsorptive Removal of Cationic and Anionic Dyes from Aqueous Solutions by Using Eggshell Household Waste as Biosorbent. Acta Chimica Slovenica 65, 709–717. https://doi.org/10.17344/acsi.2018.4401
Rápó, E., Tonk, S., 2021. Factors Affecting Synthetic Dye Adsorption; Desorption Studies: A Review of Results from the Last Five Years (2017–2021). Molecules 26, 5419. https://doi.org/10.3390/molecules26175419
Raval, N.P., Shah, P.U., Shah, N.K., 2017. Malachite green “a cationic dye” and its removal from aqueous solution by adsorption. Appl Water Sci 7, 3407–3445. https://doi.org/10.1007/s13201-016-0512-2
Razi, M.A.M., Hishammudin, M.N.A.M., Hamdan, R., 2017. Factor Affecting Textile Dye Removal Using Adsorbent From Activated Carbon: A Review. MATEC Web Conf. 103, 06015. https://doi.org/10.1051/matecconf/201710306015
Redlich, O., Peterson, D.L., 1959. A Useful Adsorption Isotherm. J. Phys. Chem. 63, 1024–1024. https://doi.org/10.1021/j150576a611
Riaz, U., Aslam, A., Qamar uz Zaman, Javeid, S., Gul, R., Iqbal, S., Javid, S., Murtaza, G., Jamil, M., 2021. Cadmium Contamination, Bioavailability, Uptake Mechanism and Remediation Strategies in Soil-Plant-Environment System: a Critical Review. Current Analytical Chemistry 17, 49–60. https://doi.org/10.2174/1573411016999200817174311
Ribeiro, G.A.C., Silva, D.S.A., Santos, C.C. dos, Vieira, A.P., Bezerra, C.W.B., Tanaka, A.A., Santana, S.A.A., Ribeiro, G.A.C., Silva, D.S.A., Santos, C.C. dos, Vieira, A.P., Bezerra, C.W.B., Tanaka, A.A., Santana, S.A.A., 2017. Removal of Remazol brilliant violet textile dye by adsorption using rice hulls. Polímeros 27, 16–26. https://doi.org/10.1590/0104-1428.2386
Rios-Donato, N., Peña-Flores, A.M., Katime, I., Leyva-Ramos, R., Mendizábal, E., 2017. Kinetics and thermodynamics of adsorption of red dye 40 from acidic aqueous solutions onto a novel chitosan sulfate. Afinidad 74, 214–220.
Rodríguez-Arellano, G., Barajas-Fernández, J., García-Alamilla, R., Lagunes-Gálvez, L.M., Lara-Rivera, A.H., García-Alamilla, P., 2021. Evaluation of Cocoa Beans Shell Powder as a

Bioadsorbent of Congo Red Dye Aqueous Solutions. Materials 14, 2763. https://doi.org/10.3390/ma14112763
Rongrong Zhang, Daohao Li, Jin Sun, Yuqian Cui, Yuanyuan Sun, 2020. In situ synthesis of FeS/Carbon fibers for the effective removal of Cr(VI) in aqueous solution. Front. Environ. Sci. Eng. 14, 68. https://doi.org/10.1007/s11783-020-1247-8
Rosca, M., Cozma, P., Minut, M., Hlihor, R.-M., Bețianu, C., Diaconu, M., Gavrilescu, M., 2021. New Evidence of Model Crop Brassica napus L. in Soil Clean-Up: Comparison of Tolerance and Accumulation of Lead and Cadmium. Plants 10, 2051. https://doi.org/10.3390/plants10102051
Ruthven, D.M., 1984. Principles of Adsorption and Adsorption Processes. John Wiley & Sons, USA, New York.
Rygula, A., Majzner, K., Marzec, K.M., Kaczor, A., Pilarczyk, M., Baranska, M., 2013. Raman spectroscopy of proteins: a review. J. Raman Spectrosc. 44, 1061–1076. https://doi.org/10.1002/jrs.4335
Sachidhanandham, A., Periyasamy, A.P., 2020. Environmentally Friendly Wastewater Treatment Methods for the Textile Industry, in: Handbook of Nanomaterials and Nanocomposites for Energy and Environmental Applications. Springer, Switzerland, Cham, pp. 1–40. https://doi.org/10.1007/978-3-030-11155-7_54-1
Sahoo, T.R., Prelot, B., 2020. Chapter 7 - Adsorption processes for the removal of contaminants from wastewater: the perspective role of nanomaterials and nanotechnology, in: Bonelli, B., Freyria, F.S., Rossetti, I., Sethi, R. (Eds.), Nanomaterials for the Detection and Removal of Wastewater Pollutants, Micro and Nano Technologies. Elsevier, pp. 161–222. https://doi.org/10.1016/B978-0-12-818489-9.00007-4
Salahshour, R., Shanbedi, M., Esmaeili, H., 2021. Methylene Blue Dye Removal from Aqueous Media Using Activated Carbon Prepared by Lotus Leaves: Kinetic, Equilibrium and Thermodynamic Study. Acta Chimica Slovenica 68, 363–373. https://doi.org/10.17344/acsi.2020.6311
Salleh, M.A.M., Mahmoud, D.K., Karim, W.A.W.A., Idris, A., 2011. Cationic and anionic dye adsorption by agricultural solid wastes: A comprehensive review. Desalination 280, 1–13. https://doi.org/10.1016/j.desal.2011.07.019
Samad, A., Din, M.I., Ahmed, M., 2020. Studies on batch adsorptive removal of cadmium and nickel from synthetic waste water using silty clay originated from Balochistan–Pakistan. Chinese Journal of Chemical Engineering 28, 1171–1176. https://doi.org/10.1016/j.cjche.2019.12.016
Samsami, S., Mohamadizaniani, M., Sarrafzadeh, M.-H., Rene, E.R., Firoozbahr, M., 2020. Recent advances in the treatment of dye-containing wastewater from textile industries: Overview and perspectives. Process Safety and Environmental Protection 143, 138–163. https://doi.org/10.1016/j.psep.2020.05.034
Santhi, T., Manonmani, S., Smitha, T., Mahalakshmi, K., 2009. Adsorption of malachite green from aqueous solution onto a waste aqua cultural shell powders (prawn waste): Kinetic study. Rasayan Journal of Chemistry 2, 813–824.
Selvaraj, V., Swarna Karthika, T., Mansiya, C., Alagar, M., 2021. An over review on recently developed techniques, mechanisms and intermediate involved in the advanced azo dye degradation for industrial applications. Journal of Molecular Structure 1224, 129195. https://doi.org/10.1016/j.molstruc.2020.129195
Semeraro, P., Gabaldón, J.A., Fini, P., Núñez, E., Pellicer, J.A., Rizzi, V., Cosma, P., 2017. Removal of an Azo Textile Dye from Wastewater by Cyclodextrin-Epichlorohydrin Polymers, Cyclodextrin - A Versatile Ingredient. IntechOpen, United Kingdom, London. https://doi.org/10.5772/intechopen.72502
Şentürk, İ., Alzein, M., 2020. Adsorption of Acid Violet 17 Onto Acid-Activated Pistachio Shell: Isotherm, Kinetic and Thermodynamic Studies. Acta Chimica Slovenica 67, 55–69. https://doi.org/10.17344/acsi.2019.5195
Seow, T.W., Lim, C.K., 2016. Removal of Dye by Adsorption: A Review. International Journal of Applied Engineering Research 11, 2675–2679.

Shah, B., Jain, K., Jiyani, H., Mohan, V., Madamwar, D., 2016. Microaerophilic Symmetric Reductive Cleavage of Reactive Azo Dye-Remazole Brilliant Violet 5R by Consortium VIE6: Community Synergism. Appl Biochem Biotechnol 180, 1029–1042. https://doi.org/10.1007/s12010-016-2150-4

Shainberg, I., Levy, G.J., 2005. Flocculation and dispersion, in: Hillel, D. (Ed.), Encyclopedia of Soils in the Environment. Elsevier, Oxford, pp. 27–34. https://doi.org/10.1016/B0-12-348530-4/00363-5

Shamey, R., 2009. 12 - Improving the colouration/dyeability of polyolefin fibres, in: Ugbolue, S.C.O. (Ed.), Polyolefin Fibres, Woodhead Publishing Series in Textiles. Woodhead Publishing, United Kingdom, Sawaston, pp. 363–397. https://doi.org/10.1533/9781845695552.2.363

Sharma, K., Sharma, S., Sharma, Vipasha, Mishra, P.K., Ekielski, A., Sharma, Vishal, Kumar, V., 2021. Methylene Blue Dye Adsorption from Wastewater Using Hydroxyapatite/Gold Nanocomposite: Kinetic and Thermodynamics Studies. Nanomaterials 11, 1403. https://doi.org/10.3390/nano11061403

Sharma, S.K., 2007. New trends in telescopic remote Raman spectroscopic instrumentation. Spectrochimica Acta Part A: Molecular and Biomolecular Spectroscopy, Seventh International Conference on Raman Spectroscopy Applied to the Earth and Planetary Sciences 68, 1008–1022. https://doi.org/10.1016/j.saa.2007.06.047

Silva, C.E. de F., Gama, B.M.V. da, Gonçalves, A.H. da S., Medeiros, J.A., Abud, A.K. de S., 2020. Basic-dye adsorption in albedo residue: Effect of pH, contact time, temperature, dye concentration, biomass dosage, rotation and ionic strength. Journal of King Saud University - Engineering Sciences 32, 351–359. https://doi.org/10.1016/j.jksues.2019.04.006

Sims, R.A., Harmer, S.L., Quinton, J.S., 2019. The Role of Physisorption and Chemisorption in the Oscillatory Adsorption of Organosilanes on Aluminium Oxide. Polymers (Basel) 11, 410. https://doi.org/10.3390/polym11030410

Singh, P.K., Singh, R.L., 2017. Bio-removal of Azo Dyes: A Review. Int J Appl Sci Biotechnol 5, 108–126. https://doi.org/10.3126/ijasbt.v5i2.16881

Slama, H.B., Chenari Bouket, A., Pourhassan, Z., Alenezi, F.N., Silini, A., Cherif-Silini, H., Oszako, T., Luptakova, L., Golińska, P., Belbahri, L., 2021. Diversity of Synthetic Dyes from Textile Industries, Discharge Impacts and Treatment Methods. Applied Sciences 11, 6255. https://doi.org/10.3390/app11146255

Slimani, R., El Ouahabi, I., Abidi, F., El Haddad, M., Regti, A., Laamari, M.R., Antri, S.E., Lazar, S., 2014. Calcined eggshells as a new biosorbent to remove basic dye from aqueous solutions: Thermodynamics, kinetics, isotherms and error analysis. Journal of the Taiwan Institute of Chemical Engineers 45, 1578–1587. https://doi.org/10.1016/j.jtice.2013.10.009

Šljivić-Ivanović, M., Smičiklas, I., 2020. 23 - Utilization of C&D waste in radioactive waste treatment—Current knowledge and perspectives, in: Pacheco-Torgal, F., Ding, Y., Colangelo, F., Tuladhar, R., Koutamanis, A. (Eds.), Advances in Construction and Demolition Waste Recycling, Woodhead Publishing Series in Civil and Structural Engineering. Woodhead Publishing, United Kingdom, Sawaston, pp. 475–500. https://doi.org/10.1016/B978-0-12-819055-5.00023-1

smarter business, 2020. The Top 5 Industries That Consume the Most Water [WWW Document]. Smarter Business. URL https://smarterbusiness.co.uk/blogs/the-top-5-industries-that-consume-the-most-water/ (accessed 12.28.20).

Srinivasan, R., 2011. Advances in Application of Natural Clay and Its Composites in Removal of Biological, Organic, and Inorganic Contaminants from Drinking Water. Advances in Materials Science and Engineering 2011, e872531. https://doi.org/10.1155/2011/872531

Statista Research Department, 2019. Forecast: Industry revenue of »manufacture of dyes and pigments« in Romania 2011-2023 [WWW Document]. Statista. URL https://www.statista.com/forecasts/395518/manufacture-of-dyes-and-pigments-revenue-in-romania (accessed 7.23.21).

Stjepanović, M., Velić, N., Galić, A., Kosović, I., Jakovljević, T., Habuda-Stanić, M., 2021. From Waste to Biosorbent: Removal of Congo Red from Water by Waste Wood Biomass. Water 13, 279. https://doi.org/10.3390/w13030279

Subramani S.E., Thinakaran N., 2017. Isotherm, kinetic and thermodynamic studies on the adsorption behaviour of textile dyes onto chitosan. Process Safety and Environmental Protection 106, 1–10. https://doi.org/10.1016/j.psep.2016.11.024

Suwannahong, K., Wongcharee, S., Kreetachart, T., Sirilamduan, C., Rioyo, J., Wongphat, A., 2021. Evaluation of the Microsoft Excel Solver Spreadsheet-Based Program for Nonlinear Expressions of Adsorption Isotherm Models onto Magnetic Nanosorbent. Applied Sciences 11, 7432. https://doi.org/10.3390/app11167432

Ta Wee Seow, Chi Kim Lim, 2016. Removal of Dye by Adsorption: A Review. International Journal of Applied Engineering Research 11, 2675–2679.

Tan, I. a. W., Ahmad, A.L., Hameed, B.H., 2008. Adsorption of basic dye on high-surface-area activated carbon prepared from coconut husk: equilibrium, kinetic and thermodynamic studies. J. Hazard. Mater. 154, 337–346. https://doi.org/10.1016/j.jhazmat.2007.10.031

Tan, K.L., Hameed, B.H., 2017. Insight into the adsorption kinetics models for the removal of contaminants from aqueous solutions. Journal of the Taiwan Institute of Chemical Engineers 74, 25–48. https://doi.org/10.1016/j.jtice.2017.01.024

Tang, R., Dai, C., Li, C., Liu, W., Gao, S., Wang, C., 2017. Removal of Methylene Blue from Aqueous Solution Using Agricultural Residue Walnut Shell: Equilibrium, Kinetic, and Thermodynamic Studies [WWW Document]. Journal of Chemistry. https://doi.org/10.1155/2017/8404965

Tejada-Tovar, C., Villabona-Ortíz, Á., Gonzalez-Delgado, Á.D., 2021. Adsorption of Azo-Anionic Dyes in a Solution Using Modified Coconut (Cocos nucifera) Mesocarp: Kinetic and Equilibrium Study. Water 13, 1382. https://doi.org/10.3390/w13101382

Terangpi, P., Chakraborty, S., 2017. Adsorption kinetics and equilibrium studies for removal of acid azo dyes by aniline formaldehyde condensate. Appl Water Sci 7, 3661–3671. https://doi.org/10.1007/s13201-016-0510-4

Terry, P.A., Noble, R.D. (Eds.), 2004. Adsorption, in: Principles of Chemical Separations with Environmental Applications, Cambridge Series in Chemical Engineering. Cambridge University Press, Cambridge, pp. 182–213. https://doi.org/10.1017/CBO9780511616594.008

Thomas, D.B., Hauber, M.E., Hanley, D., Waterhouse, G.I.N., Fraser, S., Gordon, K.C., 2015. Analysing avian eggshell pigments with Raman spectroscopy. Journal of Experimental Biology 218, 2670–2674. https://doi.org/10.1242/jeb.124917

Tiwari, D.P., Singh, S.K., Sharma, N., 2015. Sorption of methylene blue on treated agricultural adsorbents: equilibrium and kinetic studies. Appl Water Sci 5, 81–88. https://doi.org/10.1007/s13201-014-0171-0

Tiyasha, Tung, T.M., Yaseen, Z.M., 2020. A survey on river water quality modelling using artificial intelligence models: 2000–2020. Journal of Hydrology 585, 124670. https://doi.org/10.1016/j.jhydrol.2020.124670

Tonk, S., Majdik, C., Robert, S., Suciu, M., Rápó, E., Nagy, B., Gabriela Niculae, A., 2017. Biosorption of Cd(II) Ions from Aqueous Solution Onto Eggshell Waste Kinetic and equilibrium isotherm studies. Revista de Chimie -Bucharest- Original Edition- 68, 1951–1958.

Tonk, S., Nagy, B., Török, A., Indolean (Afloroaei), L., Majdik, C., 2015. Cd(II), Zn(II) and Cu(II) Bioadsorption on Chemically Treated Waste Brewery Yeast Biomass: The Role of Functional Groups. Acta Chimica Slovenica 2015, 736–746. https://doi.org/10.17344/acsi.2014.1265

Tonk Szende, Rápó Eszter, 2020. Környezeti szennyezők, környezeti problémák, környezeti remediáció, 1st ed. EXIT Kiadó, Cluj Napoca, Romania.

Török, A., 2015. Phytoextraction studies using aquatic plants (PhD Thesis). Babes-Bolyai University Faculty of Chemistry and Chemical Engineering, Cluj Napoca, Romania.

Tóth, G., Hermann, T., Szatmári, G., Pásztor, L., 2016. Maps of heavy metals in the soils of the European Union and proposed priority areas for detailed assessment. Science of The Total Environment 565, 1054–1062. https://doi.org/10.1016/j.scitotenv.2016.05.115
Tóth, J., 1981. A uniform interpretation of gas/solid adsorption. Journal of Colloid and Interface Science 79, 85–95. https://doi.org/10.1016/0021-9797(81)90050-3
Tran, H.N., You, S.-J., Hosseini-Bandegharaei, A., Chao, H.-P., 2017. Mistakes and inconsistencies regarding adsorption of contaminants from aqueous solutions: A critical review. Water Research 120, 88–116. https://doi.org/10.1016/j.watres.2017.04.014
Tran, H.V., Hoang, L.T., Huynh, C.D., 2020. An investigation on kinetic and thermodynamic parameters of methylene blue adsorption onto graphene-based nanocomposite. Chemical Physics 535, 110793. https://doi.org/10.1016/j.chemphys.2020.110793
Triebskorn, R., Telcean, I., Casper, H., Farkas, A., Sandu, C., Stan, G., Colărescu, O., Dori, T., Köhler, H.-R., 2008. Monitoring pollution in River Mureş, Romania, part II: metal accumulation and histopathology in fish. Environ Monit Assess 141, 177–188. https://doi.org/10.1007/s10661-007-9886-9
Tsai, W.T., Yang, J.M., Lai, C.W., Cheng, Y.H., Lin, C.C., Yeh, C.W., 2006. Characterization and adsorption properties of eggshells and eggshell membrane. Bioresource Technology 97, 488–493. https://doi.org/10.1016/j.biortech.2005.02.050
Tyler, C., Geake, F.H., 1953. Studies on egg shells. III.—Some physical and chemical characteristics of the egg shells of domestic hens. J. Sci. Food Agric. 4, 587–596. https://doi.org/10.1002/jsfa.2740041205
Uddin, M.K., 2017. A review on the adsorption of heavy metals by clay minerals, with special focus on the past decade. Chemical Engineering Journal 308, 438–462. https://doi.org/10.1016/j.cej.2016.09.029
Ulas, B., Ergun, M., 2019. Biosorption of remazol orange RR from aqueous solution: kinetic, equilibrium and thermodynamic studies. Desalination and water treatment 163, 366–375. https://doi.org/10.5004/dwt.2019.24420
UNESCO, 2017. The United Nations World Water Development Report - Executive summary [WWW Document]. URL http://unesdoc.unesco.org/images/0024/002475/247552e.pdf
Usman, M., Zarebanadkouki, M., Waseem, M., Katsoyiannis, I.A., Ernst, M., 2020. Mathematical modeling of arsenic(V) adsorption onto iron oxyhydroxides in an adsorption-submerged membrane hybrid system. Journal of Hazardous Materials 400, 123221. https://doi.org/10.1016/j.jhazmat.2020.123221
Vahedi, S., Tavakoli, O., Khoobi, M., Ansari, A., Ali Faramarzi, M., 2017. Application of novel magnetic β-cyclodextrin-anhydride polymer nano-adsorbent in cationic dye removal from aqueous solution. Journal of the Taiwan Institute of Chemical Engineers 80, 452–463. https://doi.org/10.1016/j.jtice.2017.07.039
Velde, B., 1995. Composition and Mineralogy of Clay Minerals, in: Velde, Bruce (Ed.), Origin and Mineralogy of Clays: Clays and the Environment. Springer, Berlin, Heidelberg, pp. 8–42. https://doi.org/10.1007/978-3-662-12648-6_2
Vijayaraghavan, K., Won, S.W., Yun, Y.-S., 2009. Treatment of complex Remazol dye effluent using sawdust- and coal-based activated carbons. Journal of Hazardous Materials 167, 790–796. https://doi.org/10.1016/j.jhazmat.2009.01.055
Vikrant, K., Giri, B.S., Raza, N., Roy, K., Kim, K.-H., Rai, B.N., Singh, R.S., 2018. Recent advancements in bioremediation of dye: Current status and challenges. Bioresource Technology 253, 355–367. https://doi.org/10.1016/j.biortech.2018.01.029
Villar da Gama, B.M., Elisandra do Nascimento, G., Silva Sales, D.C., Rodríguez-Díaz, J.M., Bezerra de Menezes Barbosa, C.M., Menezes Bezerra Duarte, M.M., 2018. Mono and binary component adsorption of phenol and cadmium using adsorbent derived from peanut shells. Journal of Cleaner Production 201, 219–228. https://doi.org/10.1016/j.jclepro.2018.07.291
Wang, J., Chen, C., 2006. Biosorption of heavy metals by Saccharomyces cerevisiae: A review. Biotechnology Advances 24, 427–451. https://doi.org/10.1016/j.biotechadv.2006.03.001

Wang, J., Guo, X., 2020. Adsorption isotherm models: Classification, physical meaning, application and solving method. Chemosphere 258, 127279. https://doi.org/10.1016/j.chemosphere.2020.127279
Wang, Q., Wang, Y., Chen, L., 2019. A green composite hydrogel based on cellulose and clay as efficient absorbent of colored organic effluent. Carbohydrate Polymers 210, 314–321. https://doi.org/10.1016/j.carbpol.2019.01.080
Wang, Y.-B., Jehng, J.-M., 2011. Hydrotalcite-like compounds containing transition metals as solid base catalysts for transesterification. Chemical Engineering Journal 175, 548–554. https://doi.org/10.1016/j.cej.2011.09.126
Wiercigroch, E., Szafraniec, E., Czamara, K., Pacia, M.Z., Majzner, K., Kochan, K., Kaczor, A., Baranska, M., Malek, K., 2017. Raman and infrared spectroscopy of carbohydrates: A review. Spectrochim Acta A Mol Biomol Spectrosc 185, 317–335. https://doi.org/10.1016/j.saa.2017.05.045
Witoon, T., 2011. Characterization of calcium oxide derived from waste eggshell and its application as CO2 sorbent. Ceramics International 37, 3291–3298. https://doi.org/10.1016/j.ceramint.2011.05.125
World Health Organization, 2019. Preventing Disease through Healthy Environments - Exposure to Cadmium: A Major Public Health Concern.
Wu, J., Li, Q., Li, W., Li, Y., Wang, G., Li, A., Li, H., 2020. Efficient removal of acid dyes using permanent magnetic resin and its preliminary investigation for advanced treatment of dyeing effluents. Journal of Cleaner Production 251, 119694. https://doi.org/10.1016/j.jclepro.2019.119694
Yagub, M.T., Sen, T.K., Afroze, S., Ang, H.M., 2014. Dye and its removal from aqueous solution by adsorption: A review. Advances in Colloid and Interface Science 209, 172–184. https://doi.org/10.1016/j.cis.2014.04.002
Yao, L., Yang, J., Zhang, P., Deng, L., 2018. In situ surface decoration of Fe3C/Fe3O4/C nanosheets: Towards bi-functional activated carbons with supercapacitance and efficient dye adsorption. Bioresource Technology 256, 208–215. https://doi.org/10.1016/j.biortech.2018.02.027
Yaseen, D.A., Scholz, M., 2019. Textile dye wastewater characteristics and constituents of synthetic effluents: a critical review. Int. J. Environ. Sci. Technol. 16, 1193–1226. https://doi.org/10.1007/s13762-018-2130-z
Yildirim, A., 2021. Removal of the Anionic Dye Reactive Orange 16 by Chitosan/Tripolyphosphate/Mushroom. Chemical Engineering & Technology 44, 1371–1381. https://doi.org/10.1002/ceat.202100077
Yu, J., Zhang, X., Wang, D., Li, P., 2018. Adsorption of methyl orange dye onto biochar adsorbent prepared from chicken manure. Water Science and Technology 77, 1303–1312. https://doi.org/10.2166/wst.2018.003
Yusuff, A.S., Popoola, L.T., Babatunde, E.O., 2019. Adsorption of cadmium ion from aqueous solutions by copper-based metal organic framework: equilibrium modeling and kinetic studies. Appl Water Sci 9, 106. https://doi.org/10.1007/s13201-019-0991-z
Zadeh, B.S., Esmaeili, H., Foroutan, R., 2018. Cadmium(II) Removal from Aqueous Solution Using Microporous Eggshell: Kinetic and Equilibrium Studies. Indones. J. Chem. 18, 265–271. https://doi.org/10.22146/ijc.28789
Zaimee, M.Z.A., Sarjadi, M.S., Rahman, M.L., 2021. Heavy Metals Removal from Water by Efficient Adsorbents. Water 13, 2659. https://doi.org/10.3390/w13192659
ZDHC: Zero Discharge of Hazardous Chemicals, 2016. Textile Industry Wastewater Discharge Quality Standards [WWW Document]. URL https://wastewater.sustainabilityconsortium.org/downloads/textile-industry-wastewater-discharge-quality-standards/ (accessed 8.22.21).

Zeroual, Y., Kim, B.S., Kim, C.S., Blaghen, M., Lee, K.M., 2006. Biosorption of Bromophenol Blue from Aqueous Solutions by Rhizopus Stolonifer Biomass. Water Air Soil Pollut 177, 135–146. https://doi.org/10.1007/s11270-006-9112-3

Zhang, T., Fei, X., Wang, S., Zhou, C., 2000. Pigmentation of Vat Blue RS by ball milling in solvents. Dyes and Pigments 45, 15–21. https://doi.org/10.1016/S0143-7208(99)00098-4

Zhang, Y., Zhang, Yujie, Akakuru, O.U., Xu, X., Wu, A., 2021. Research progress and mechanism of nanomaterials-mediated in-situ remediation of cadmium-contaminated soil: A critical review. Journal of Environmental Sciences 104, 351–364. https://doi.org/10.1016/j.jes.2020.12.021

Zhang, Z., Wang, T., Zhang, H., Liu, Y., Xing, B., 2021. Adsorption of Pb(II) and Cd(II) by magnetic activated carbon and its mechanism. Science of The Total Environment 757, 143910. https://doi.org/10.1016/j.scitotenv.2020.143910

Zhao, M., Wang, S., Wang, H., Qin, P., Yang, D., Sun, Y., Kong, F., 2019. Application of sodium titanate nanofibers as constructed wetland fillers for efficient removal of heavy metal ions from wastewater. Environ Pollut 248, 938–946. https://doi.org/10.1016/j.envpol.2019.02.040

Zhao, X., Yu, X., Wang, X., Lai, S., Sun, Y., Yang, D., 2021. Recent advances in metal-organic frameworks for the removal of heavy metal oxoanions from water. Chemical Engineering Journal 407, 127221. https://doi.org/10.1016/j.cej.2020.127221

Zhao, Y., Deng, Q., Lin, Q., Zeng, C., Zhong, C., 2020. Cadmium source identification in soils and high-risk regions predicted by geographical detector method. Environmental Pollution 263, 114338. https://doi.org/10.1016/j.envpol.2020.114338

Zhao, Y., Wang, W., Yi, H., 2021. Mineral Adsorbents and Characteristics, in: Song, S., Li, B. (Eds.), Adsorption at Natural Minerals/Water Interfaces, Engineering Materials. Springer International Publishing, Cham, pp. 1–54. https://doi.org/10.1007/978-3-030-54451-5_1

Zhou, Q., Liu, Y., Li, T., Zhao, H., Alessi, D.S., Liu, W., Konhauser, K.O., 2020. Cadmium adsorption to clay-microbe aggregates: Implications for marine heavy metals cycling. Geochimica et Cosmochimica Acta 290, 124–136. https://doi.org/10.1016/j.gca.2020.09.002

Zhou, Yanbo, Lu, J., Zhou, Yi, Liu, Y., 2019. Recent advances for dyes removal using novel adsorbents: A review. Environmental Pollution 252, 352–365. https://doi.org/10.1016/j.envpol.2019.05.072

Zugravu, C., Parvu, M., Patrascu, D., Stoian, A., 2009. Correlations between Lead and Cadmium Pollution of Honey and Environmental Heavy Metal Presence in Two Romanian Counties. Bulletin UASVM Agriculture 66.

Zulfikar, M.A., Setiyanto, H., 2013. Study of the adsorption kinetics and thermodynamic for the removal of Congo Red from aqueous solution using powdered eggshell.

A2. Supplementary figures

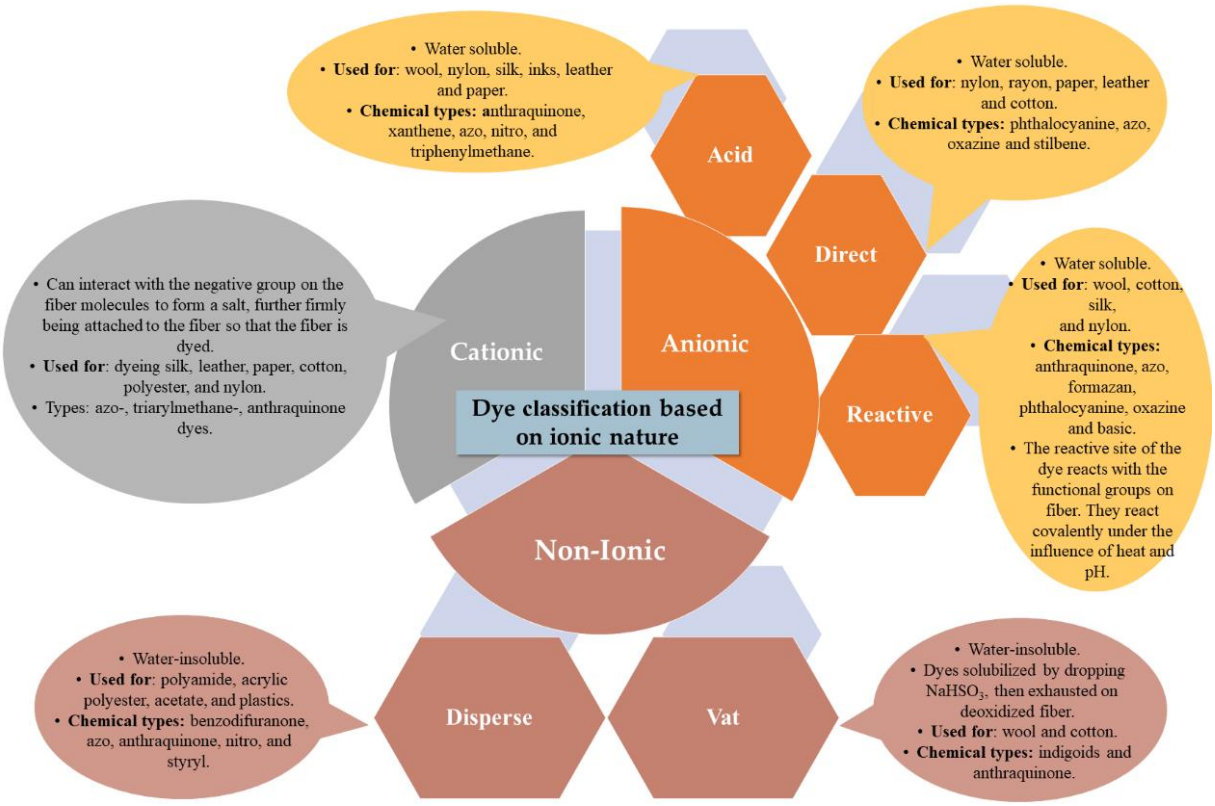

Figure S1. Dye classification based on ionic nature.

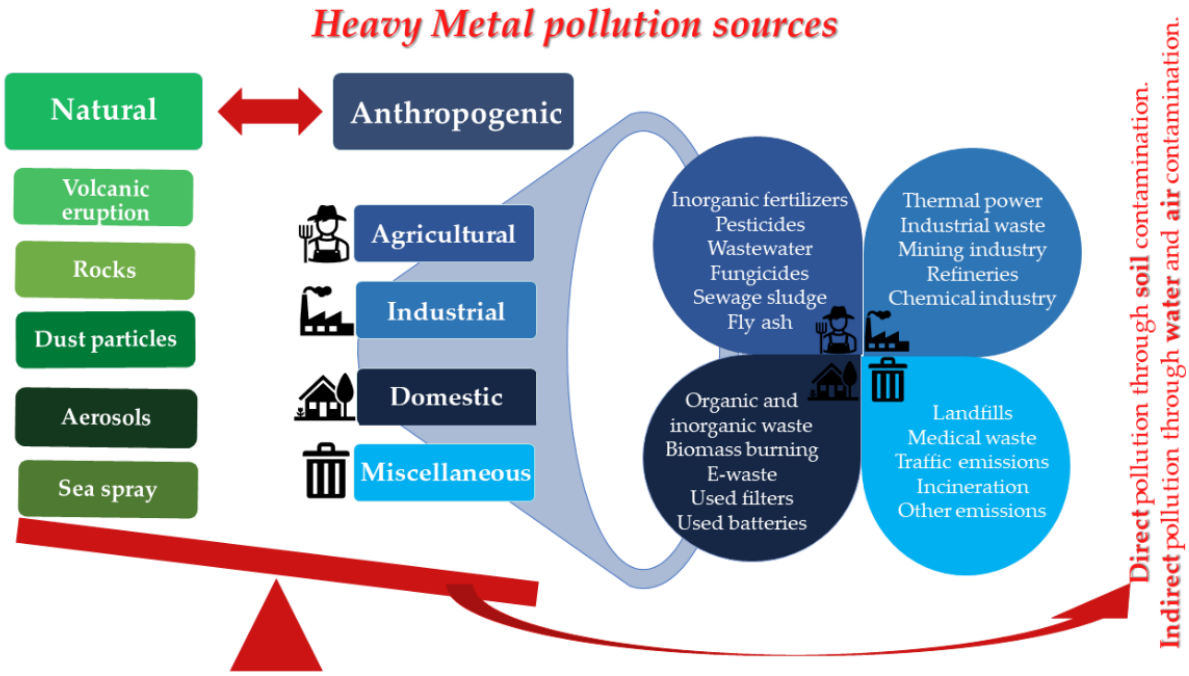

Figure S2. Main sources of Heavy Metal pollution (Edited and adapted based on (Rizvi et al., 2020)).

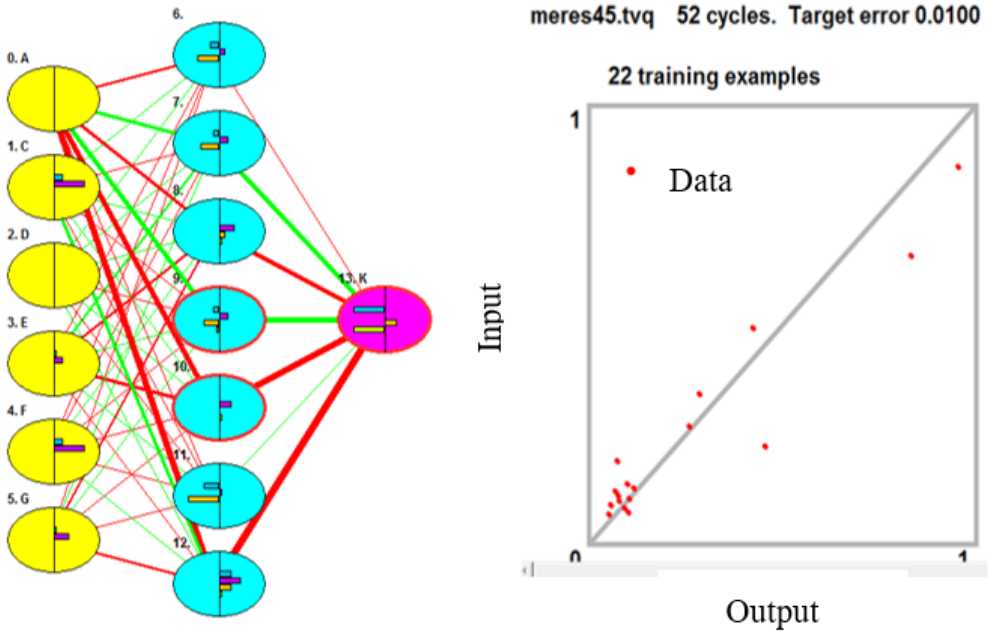

Figure S3. Topology and performance of ANN.

A3. Supplementary tables

Table S1. Results of various research regarding the effect of initial dye concentration.

Dyestuff	Adsorbent	Concentration (mg/L)	Reaction Time (min)	Efficiency Range (%)	Quantity in Equilibrium Range (q_e mg/g)	Reference
Methylene Blue	Algerian palygorskite	3–30	5	up to 97%	2.5–10	(Dali Youcef et al., 2019)
Methylene Blue	clinoptilolite	50–100	60	increased but no significant difference > 95%	-	(Mahmoudi et al., 2019)
Brilliant Green	activated carbon derived from medlar nucleus	110–200	60	-	100–180	(Abbas, 2020)
Methylene Blue	green olive stone	50–1000	24 h	fluctuating values, highest 65.9 at 50 ppm	-	(Al-Ghouti and Al-Absi, 2020)
Methylene Blue	black olive stone	50–1000	24 h	fluctuating values, highest 93.5 at 400 ppm	-	(Al-Ghouti and Al-Absi, 2020)
Acid Brown	*Haloxylon recurvum* plant	10–60	180	-	2.846–10.011	(Warda Hassan et al., 2020)
Congo Red	cocoa bean shells	40–120	4–36 h	negative linear effect		(Rodríguez-Arellano et al., 2021)
Methylene Blue	fava bean peels, utilizing ultrasonic-assisted (US) shaking	3.6–100	70	70–90	-	(Bayomie et al., 2020)
Methylene Blue	fava bean peels, conventional (CV) shaking	3.6–100	70	80–95	-	(Bayomie et al., 2020)
Reactive Blue 19	corn silk	10–500	60	-	2.0–71.6	(Değermenci et al., 2019)
Reactive Red 218	corn silk	10–500	60	-	2.0–63.3	(Değermenci et al., 2019)
Reactive Black 5	pent tea leaves	50–100	5–200	98.7–43.5	24.8 –6.7	(Wong et al., 2019)
Methyl Orange	pent tea leaves	50–100	5–200	88.7–32.7	22.2 –1.6	(Wong et al., 2019)
Methylene Blue	*Citrus limetta* peel	5–25	10–60	~100–97	0.06–1.62	(Singh et al., 2017)
Malachite Green	*Citrus limetta* peel	5–25	10–60	~97–95	0.17–4.70	(Singh et al., 2017)
Congo Red	*Citrus limetta* peel	5–25	10–60	~90–75	0.17–3.77	(Singh et al., 2017)
Crystal Violet	mango stone biocomposite	20–50	60	-	~25–352.79	(Shoukat et al., 2017)
Congo Red	chitosan	50–2000	30	-	increased to 0.2	(Ma et al., 2019)
Methylene Blue	chitosan	25–100	30	~100–50	increased to 1457.1	(Ma et al., 2019)
Rhodamine B	chitosan	25–100	30	~55–35	increased to 990	(Ma et al., 2019)
Reactive Red 120	*Moringa oleifera* seed	10–100	30	-	18.54–173.99	(Çelekli et al., 2019)
Crystal Violet	olive leaves powder	10–100	5–70	-	~5–45	(Elsherif et al., 2021)

Table S2. Results of various research regarding the effect of initial solution pH, where E is the efficiency of the adsorption process and E_{max} is the highest efficiency calculated in the specific article at a given condition.

Dyestuff	Adsorbent	Dyes Ionic Nature	pH	Observations: with the Increase (↑) of pH	Reference
Direct Red 5B	spent mushroom waste	anionic	2 to 10	E% ↓; $E_{max\_pH = 2}$ = 95%	(Alhujaily et al., 2020)
Direct Black 22		anionic	2 to 10	E% ↓; $E_{max\_pH = 2}$ = 98%	(Alhujaily et al., 2020)
Direct Black 71		anionic	2 to 10	E% ↓; $E_{max\_pH = 2}$ = 95%	(Alhujaily et al., 2020)
Reactive Black 5		anionic	2 to 10	E% ↓; $E_{max\_pH = 2}$ = 96%	(Alhujaily et al., 2020)
Congo Red	powdered activated carbon: rubber seed	anionic	4 to 11	E% ↓	(Nizam et al., 2021)
	powdered activated carbon: rubber seed shells		4 to 11	E% ↓	(Nizam et al., 2021)
Methylene Blue	powdered activated carbon: rubber seed	cationic	4 to 11	E% ↑	(Nizam et al., 2021)
	powdered activated carbon: rubber seed shells		4 to 11	E% ↑	(Nizam et al., 2021)
Eriochrome Black T	powdered vegetables wastes	anionic	2 to 10	E% ↓; 50.65 to 4.01%	(Aziz et al., 2018)
	calcined vegetables wastes		2 to 10	E% ↓; 68.87 to 31.23%	(Aziz et al., 2018)
Methyl Orange	natural olive stone	anionic	2 to 12	q (mg/g) ↓; 26.4 to 3.3 mg/g	(Al-Ghouti and Al-Absi, 2020)
	olive stone activated carbons		2 to 12	q (mg/g) ↓; 120 to 15 mg/g	(Al-Ghouti and Al-Absi, 2020)
Methylene Blue	natural olive stone	cationic	2 to 12	q (mg/g) ↑; 18 to 120 mg/g	(Al-Ghouti and Al-Absi, 2020)
	olive stone activated carbons		2 to 12	q (mg/g) ↑	(Al-Ghouti and Al-Absi, 2020)
Reactive Orange 16	carbon from *Phyllanthus reticulatus*	anionic	2 to 11	q (mg/g) ↓	(Kavitha et al., 2021)
Cationic Red X-5GN	ceramic	cationic	2 to 10	E% ↑	(Zhou et al., 2019)
Cationic Blue X-GRRL		cationic	2 to 10	E% ↑	(Zhou et al., 2019)
Methylene Blue	activated carbon/cellulose biocomposite films	cationic	3 to 11	q (mg/g) ↑; 50.54 to 60.48 mg/g	(Somsesta et al., 2020)
Eriochrome Black T	almond shell	anionic	2 to 11	q (mg/g) ↓	(Arfi et al., 2017)
Malachite Green		cationic	2 to 11	q (mg/g) ↑	(Arfi et al., 2017)
Basic Yellow 37	bast fibers: ramie	cationic	2 to 12	E% ↑; $E_{max\_pH = 12}$ = 91%	(Kyzas et al., 2018)
	bast fibers: flax	cationic	2 to 12	E% ↑; $E_{max\_pH = 12}$ = 88%	(Kyzas et al., 2018)
	bast fibers: kenaf	cationic	2 to 12	E% ↑; $E_{max\_pH = 12}$ = 78%	(Kyzas et al., 2018)
Remazol Brilliant Violet	*Trichoderma viride*	anionic	4 to 9	E% ↓; 79.05 to 50.25%	(Safitri et al., 2020)
Congo Red	eggshell powder	anionic	2 to 10	E% ↓; 98.71 to 93.17%	(Rápó et al., 2018)
Bromphenol Blue		anionic	2 to 10	E% ↓; 67.61 to 1.2%	(Rápó et al., 2018)
Methylene Blue		cationic	2 to 10	E% ↑; 14.8 to 75.1%	(Rápó et al., 2018)
Malachite Green		cationic	2 to 10	E% ↑; 89.95 to 97.92%	(Rápó et al., 2018)

Table 3. Results of various research regarding the effect of initial adsorbent dosage.

Adsorbent	Dyestuff	Adsorbent Dosage	Efficiency Range (%)	Quantity in Equilibrium Range (q_e mg/g)	Reference
walnut shell	Methylene Blue	0.5–2 g/L	-	178.93–47.51	(Miyah et al., 2018)
magnetic alginate/rice husk bio-composite	Methylene Blue	0.1–1 g	15–89	338–145	(Alver et al., 2020)
Tunisian smectite clay	Cristal Violet	0.05–0.3 g/L	10–100	-	(Hamza et al., 2018)
modified activated carbon (PABA@AC)	Malachite Green	10–50 mg	31.3–86.6	11.67–6.5	(Naushad et al., 2019)
commercial natural activated plant-based carbon (CNAC)	Methylene Blue	0.5–1.5 g	46–78	-	(Neag et al., 2019)
commercial natural activated plant-based carbon (CNAC)	Eosin Yellow	0.5–1.5 g	51–70	-	(Neag et al., 2019)
commercial natural activated plant-based carbon (CNAC)	Rhodamine B	0.5–1.5 g	52–60	-	(Neag et al., 2019)
calcined eggshell	Remazol Brilliant Violet-5R	0.5–2 g	89.83–96.3	3.59–0.96	(Rápó et al., 2019)
calcined eggshell	Remazol Red F3B	0.5–2 g	92–93.67	3.68–0.94	(Rápó et al., 2020b)
calcined eggshell	Remazol Blue RR	0.5–2 g	92–93.33	3.68–0.94	(Rápó et al., 2020b)
eggshell	Remazol Brilliant Violet-5R	0.5–2.5 g	74.67–93.85	2.96–0.75	(Rápó et al., 2020a)
activated carbon from lotus leaves	Methylene Blue	0.5–10 g/L	82.84–98.032	16.57–0.98	(Salahshour et al., 2021)
municipial solid waste compost ash	Reactive Red 198	0.5–2 g/L	79.25–92.92	-	(Dehghani et al., 2021, p. 198)
natural clayey composite	Basic Navy Blue 2RN	0.2–1.2 g/50 mL	78–97	-	(Márquez et al., 2021)
natural clayey composite	Drimaren Yellow CL-2R	0.2–1.2 g/50 mL	87–97	-	(Márquez et al., 2021)
geopolymer	Methylene Blue (10^{-5} M)	0.05–0.1 g	79.8–85.6	-	(Maleki et al., 2020)
mucilage of Salvia seeds	Cationic Blue 41	0.5–4 g/L	34.2–53.9	34.2–6.74	(Hamzezadeh et al., 2020)
raw petroleum coke	Congo Red	4–24 g/L	~10–60	-	(Raj et al., 2019)
activated petroleum coke	Congo Red	4–24 g/L	~15–70	-	(Raj et al., 2019)

Table 4. Results of various research regarding the effect of adsorbent particle size.

Dyestuff	Adsorbent	Particle Size (µm)	Efficiency Range (%)	Quantity in Equilibrium Range (q_e mg/g)	Reference
Congo Red	cabbage waste powder	150–300 to 360–4750	75.95–8.03	-	(Wekoye et al., 2020)
Reactive Black 5	macadamia seed husks	150–300 to 2360–4750	98.9–33.2	-	(Felista et al., 2020)
Maxilon Blue GRL	coconut shell activated carbon	50, 75, and 106	-	~27.5–22.5–17.5	(Aljeboree et al., 2017)
Direct Yellow DY 12	coconut shell activated carbon	50, 75, and 107	-	~5.5–4.5–3.5	(Aljeboree et al., 2017)
Methylene Blue	*Cucumis sativus* peel waste	80–150, 150–200, and > 200 BSS mesh	80.25–84.15–85.23	-	(Shakoor and Nasar, 2017)
Crystal Violet	coffee husks	0.15–0.3 to 2.36–4.75 mm	96.082–89.854	-	(Cheruiyot et al., 2019)
Methylene Blue	clay3	177–250 to 400–840	99–86.4	-	(Mahdavinia et al., 2014)

Table 5. Results of various research regarding the effect of temperature.

Dyestuff	Adsorbent	Temperature (K)	Efficiency Range (%)	Type of the Process	Quantity in Equilibrium Range (q_e mg/g)	Reference
Basic Orange 2	alkaline-modified nanoclay	288–308	80–100	endothermic	-	(Geroeeyan et al., 2021)
Congo Red	cross-linked TTU-chitosan	298, 308 and 328	-	endothermic	increased	(El-Harby et al., 2017)
Congo Red	modified Zeolite A	297–309	-	exothermic	decreased	(Khalaf et al., 2021)
Direct Sky Blue	ZnO	Beyond 313 K, the adsorption capacity was decreased, which is an indication of being endothermic up to 313 K, and exothermic beyond this temperature			highest: 40.94	(Noreen et al., 2020)
	MgO				highest: 46.25	(Noreen et al., 2020)
	FeO				highest: 42.86	(Noreen et al., 2020)
Methyl Orange	cationic polymer (Amberlite IRA 402)	293, 303, 328 and 348	-	endothermic	increased	(Santander et al., 2020)
Remazol Red	chitosan Schiff base	293, 303, and 313	-	endothermic	increased	(Ibrahim et al., 2020)
Reactive Red 120	activated carbon	The adsorption of RR-120 on activated carbon is of the physisorption type, as confirmed by the adsorbed energy values, and it is exothermic as verified by the internal energy				(Oueslati et al., 2020)
Methylene Blue	hydroxyapatite/gold nanocomposite	290–305	-	endothermic	increased	(Sharma et al., 2021)
		305–330	-	exothermic	decreased	(Sharma et al., 2021)
Methylene Blue	*Citrullus colocynthis* seed	293–333	93.58–98.00	endothermic	-	(Alghamdi and El Mannoubi, 2021)
	Citrullus colocynthis peel	294–333	91.43–82.52	exothermic	--	(Alghamdi and El Mannoubi, 2021)
Methylene Blue	magnetic carboxyl functional nanoporous polymer	298, 308 and 318	-	endothermic	52.16–52.58–53.75	(Su et al., 2018)

References for supplementary tables

Abbas, M., 2020. Removal of brilliant green (BG) by activated carbon derived from medlar nucleus (ACMN) – Kinetic, isotherms and thermodynamic aspects of adsorption. Adsorption Science & Technology 38, 464–482. https://doi.org/10.1177/0263617420957829

Alghamdi, W.M., El Mannoubi, I., 2021. Investigation of Seeds and Peels of Citrullus colocynthis as Efficient Natural Adsorbent for Methylene Blue Dye. Processes 9, 1279. https://doi.org/10.3390/pr9081279

Al-Ghouti, M.A., Al-Absi, R.S., 2020. Mechanistic understanding of the adsorption and thermodynamic aspects of cationic methylene blue dye onto cellulosic olive stones biomass from wastewater. Sci Rep 10, 15928. https://doi.org/10.1038/s41598-020-72996-3

Alhujaily, A., Yu, H., Zhang, X., Ma, F., 2020. Adsorptive removal of anionic dyes from aqueous solutions using spent mushroom waste. Appl Water Sci 10, 183. https://doi.org/10.1007/s13201-020-01268-2

Aljeboree, A.M., Alshirifi, A.N., Alkaim, A.F., 2017. Kinetics and equilibrium study for the adsorption of textile dyes on coconut shell activated carbon. Arabian Journal of Chemistry 10, S3381–S3393. https://doi.org/10.1016/j.arabjc.2014.01.020

Alver, E., Metin, A.Ü., Brouers, F., 2020. Methylene blue adsorption on magnetic alginate/rice husk bio-composite. International Journal of Biological Macromolecules 154, 104–113. https://doi.org/10.1016/j.ijbiomac.2020.02.330

Arfi, R.B., Karoui, S., Mougin, K., Ghorbal, A., 2017. Adsorptive removal of cationic and anionic dyes from aqueous solution by utilizing almond shell as bioadsorbent. Euro-Mediterr J Environ Integr 2, 20. https://doi.org/10.1007/s41207-017-0032-y

Aziz, E.K., Abdelmajid, R., Rachid, L.M., Mohammadine, E.H., 2018. Adsorptive removal of anionic dye from aqueous solutions using powdered and calcined vegetables wastes as low-cost adsorbent. Arab Journal of Basic and Applied Sciences 25, 93–102. https://doi.org/10.1080/25765299.2018.1517861

Bayomie, O.S., Kandeel, H., Shoeib, T., Yang, H., Youssef, N., El-Sayed, M.M.H., 2020. Novel approach for effective removal of methylene blue dye from water using fava bean peel waste. Sci Rep 10, 7824. https://doi.org/10.1038/s41598-020-64727-5

Çelekli, A., Al-Nuaimi, A.I., Bozkurt, H., 2019. Adsorption kinetic and isotherms of Reactive Red 120 on Moringa oleifera seed as an eco-friendly process. Journal of Molecular Structure 1195, 168–178. https://doi.org/10.1016/j.molstruc.2019.05.106

Cheruiyot, G.K., Wanyonyi, W.C., Kiplimo, J.J., Maina, E.N., 2019. Adsorption of toxic crystal violet dye using coffee husks: Equilibrium, kinetics and thermodynamics study. Scientific African 5, e00116. https://doi.org/10.1016/j.sciaf.2019.e00116

Dali Youcef, L., Belaroui, L.S., López-Galindo, A., 2019. Adsorption of a cationic methylene blue dye on an Algerian palygorskite. Applied Clay Science 179, 105145. https://doi.org/10.1016/j.clay.2019.105145

Değermenci, G.D., Değermenci, N., Ayvaoğlu, V., Durmaz, E., Çakır, D., Akan, E., 2019. Adsorption of reactive dyes on lignocellulosic waste; characterization, equilibrium, kinetic and thermodynamic studies. Journal of Cleaner Production 225, 1220–1229. https://doi.org/10.1016/j.jclepro.2019.03.260

Dehghani, M.H., Salari, M., Karri, R.R., Hamidi, F., Bahadori, R., 2021. Process modeling of municipal solid waste compost ash for reactive red 198 dye adsorption from wastewater using data driven approaches. Sci Rep 11, 11613. https://doi.org/10.1038/s41598-021-90914-z

El-Harby, N.F., Ibrahim, S.M.A., Mohamed, N.A., 2017. Adsorption of Congo red dye onto antimicrobial terephthaloyl thiourea cross-linked chitosan hydrogels. Water Science and Technology 76, 2719–2732. https://doi.org/10.2166/wst.2017.442

Elsherif, K., El-Dali, A., Alkarewi, A., Ewlad-Ahmed, A., Treban, A., 2021. Adsorption of Crystal Violet Dye Onto Olive Leaves Powder: Equilibrium and Kinetic Studies. Chemistry International 7, 79–89. https://doi.org/10.5281/zenodo.4441851

Felista, M.M., Wanyonyi, W.C., Ongera, G., 2020. Adsorption of anionic dye (Reactive black 5) using macadamia seed Husks: Kinetics and equilibrium studies. Scientific African 7, e00283. https://doi.org/10.1016/j.sciaf.2020.e00283

Geroeeyan, A., Niazi, A., Konoz, E., 2021. Removal of Basic Orange 2 dye and Ni2+ from aqueous solutions using alkaline-modified nanoclay. Water Science and Technology 83, 2271–2286. https://doi.org/10.2166/wst.2021.121

Hamza, W., Dammak, N., Hadjltaief, H.B., Eloussaief, M., Benzina, M., 2018. Sono-assisted adsorption of Cristal Violet dye onto Tunisian Smectite Clay: Characterization, kinetics and adsorption isotherms. Ecotoxicology and Environmental Safety 163, 365–371. https://doi.org/10.1016/j.ecoenv.2018.07.021

Hamzezadeh, A., Rashtbari, Y., Afshin, S., Morovati, M., Vosoughi, M., 2020. Application of low-cost material for adsorption of dye from aqueous solution. International Journal of Environmental Analytical Chemistry 0, 1–16. https://doi.org/10.1080/03067319.2020.1720011

Ibrahim, S.M., Hassanin, H.M., Abdelrazek, M.M., 2020. Synthesis, and characterization of chitosan bearing pyranoquinolinone moiety for textile dye adsorption from wastewater. Water Science and Technology 81, 421–435. https://doi.org/10.2166/wst.2020.097

Kavitha, G., Subhapriya, P., Dhanapal, V., Dineshkumar, G., Venkateswaran, V., 2021. Dye removal kinetics and adsorption studies of activated carbon derived from the stems of Phyllanthus reticulatus. Materials Today: Proceedings, 2nd International Conference on Materials, Manufacturing, and Machining for Industry 4.0 45, 7934–7938. https://doi.org/10.1016/j.matpr.2020.12.837

Khalaf, I.H., Al-Sudani, F.T., AbdulRazak, A.A., Aldahri, T., Rohani, S., 2021. Optimization of Congo red dye adsorption from wastewater by a modified commercial zeolite catalyst using response surface modeling approach. Water Science and Technology 83, 1369–1383. https://doi.org/10.2166/wst.2021.078

Kyzas, G.Z., Christodoulou, E., Bikiaris, D.N., 2018. Basic Dye Removal with Sorption onto Low-Cost Natural Textile Fibers. Processes 6, 166. https://doi.org/10.3390/pr6090166

Ma, H., Kong, A., Ji, Y., He, B., Song, Y., Li, J., 2019. Ultrahigh adsorption capacities for anionic and cationic dyes from wastewater using only chitosan. Journal of Cleaner Production 214, 89–94. https://doi.org/10.1016/j.jclepro.2018.12.217

Mahdavinia, G., Baghban, A., Zorofi, S., Massoudi, A., 2014. Kappa-Carrageenan Biopolymer-Based Nanocomposite Hydrogel and Adsorption of Methylene Blue Cationic Dye from Water. Journal of Materials and Environmental Science 5, 330–337.

Mahmoudi, M.M., Nadali, A., Arezoomand, H.R.S., Mahvi, A.H., 2019. Adsorption of cationic dye textile wastewater using Clinoptilolite: isotherm and kinetic study. The Journal of The Textile Institute 110, 74–80. https://doi.org/10.1080/00405000.2018.1465329

Maleki, A., Mohammad, M., Emdadi, Z., Asim, N., Azizi, M., Safaei, J., 2020. Adsorbent materials based on a geopolymer paste for dye removal from aqueous solutions. Arabian Journal of Chemistry 13, 3017–3025. https://doi.org/10.1016/j.arabjc.2018.08.011

Márquez, C.O., García, V.J., Guaypatin, J.R., Fernández-Martínez, F., Ríos, A.C., 2021. Cationic and Anionic Dye Adsorption on a Natural Clayey Composite. Applied Sciences 11, 5127. https://doi.org/10.3390/app11115127

Miyah, Y., Lahrichi, A., Idrissi, M., Khalil, A., Zerrouq, F., 2018. Adsorption of methylene blue dye from aqueous solutions onto walnut shells powder: Equilibrium and kinetic studies. Surfaces and Interfaces 11, 74–81. https://doi.org/10.1016/j.surfin.2018.03.006

Naushad, Mu., Alqadami, A.A., Al-Kahtani, A.A., Ahamad, T., Awual, Md.R., Tatarchuk, T., 2019. Adsorption of textile dye using para-aminobenzoic acid modified activated carbon: Kinetic and equilibrium studies. Journal of Molecular Liquids 296, 112075. https://doi.org/10.1016/j.molliq.2019.112075

Neag, E., Moldovan, A., Băbălău-Fuss, V., Török, A., Cadar, O., Roman, C., 2019. Kinetic, Equilibrium and Phytotoxicity Studies for Dyes Removal by Low Cost Natural Activated Plant-Based Carbon. Acta Chimica Slovenica 66, 850–858. https://doi.org/10.17344/acsi.2018.4924

Nizam, N.U.M., Hanafiah, M.M., Mahmoudi, E., Halim, A.A., Mohammad, A.W., 2021. The removal of anionic and cationic dyes from an aqueous solution using biomass-based activated carbon. Sci Rep 11, 8623. https://doi.org/10.1038/s41598-021-88084-z

Noreen, S., Khalid, U., Ibrahim, S.M., Javed, T., Ghani, A., Naz, S., Iqbal, M., 2020. ZnO, MgO and FeO adsorption efficiencies for direct sky Blue dye: equilibrium, kinetics and thermodynamics studies. Journal of Materials Research and Technology 9, 5881–5893. https://doi.org/10.1016/j.jmrt.2020.03.115

Oueslati, K., Lima, E.C., Ayachi, F., Cunha, M.R., Ben Lamine, A., 2020. Modeling the removal of Reactive Red 120 dye from aqueous effluents by activated carbon. Water Science and Technology 82, 651–662. https://doi.org/10.2166/wst.2020.347

Raj, R.A., Manimozhi, V., Saravanathamizhan, R., 2019. Adsorption studies on removal of Congo red dye from aqueous solution using petroleum coke. Petroleum Science and Technology 37, 913–924. https://doi.org/10.1080/10916466.2019.1575866

Rápó, E., Aradi, L.E., Szabó, Á., Posta, K., Szép, R., Tonk, S., 2020a. Adsorption of Remazol Brilliant Violet-5R Textile Dye from Aqueous Solutions by Using Eggshell Waste Biosorbent. Sci Rep 10, 8385. https://doi.org/10.1038/s41598-020-65334-0

Rápó, E., Jakab, K., Posta, K., Suciu, M., Tonk, S., 2020b. A Comparative Study on the Adsorption of Two Remazol Dyes on Green Adsorbent. Rev. Chim. 71, 248–257. https://doi.org/10.37358/RC.20.4.8063

Rápó, E., Posta, K., Suciu, M., Szép, R., Tonk, S., 2019. Adsorptive Removal of Remazol Brilliant Violet-5R Dye from Aqueous Solutions using Calcined Eggshell as Biosorbent. Acta Chimica Slovenica 66, 648–658. https://doi.org/10.17344/acsi.2019.5079

Rápó, E., Szép, R., Keresztesi, Á., Suciu, M., Tonk, S., 2018. Adsorptive Removal of Cationic and Anionic Dyes from Aqueous Solutions by Using Eggshell Household Waste as Biosorbent. Acta Chimica Slovenica 65, 709–717. https://doi.org/10.17344/acsi.2018.4401

Rodríguez-Arellano, G., Barajas-Fernández, J., García-Alamilla, R., Lagunes-Gálvez, L.M., Lara-Rivera, A.H., García-Alamilla, P., 2021. Evaluation of Cocoa Beans Shell Powder as a Bioadsorbent of Congo Red Dye Aqueous Solutions. Materials 14, 2763. https://doi.org/10.3390/ma14112763

Safitri, A., Febrianti, W.D., Rahmaniah, G., 2020. Effectiveness of Using Trichoderma viride as Biosorbent for Remazol Brilliant Purple in Batik Wastewater Treatment. JSMARTech: Journal of Smart Bioprospecting and Technology 1, 041–045. https://doi.org/10.21776/ub.jsmartech.2020.001.02.4

Salahshour, R., Shanbedi, M., Esmaeili, H., 2021. Methylene Blue Dye Removal from Aqueous Media Using Activated Carbon Prepared by Lotus Leaves: Kinetic, Equilibrium and Thermodynamic Study. Acta Chimica Slovenica 68, 363–373. https://doi.org/10.17344/acsi.2020.6311

Santander, P., Oyarce, E., Sánchez, J., 2020. New insights in the use of a strong cationic resin in dye adsorption. Water Science and Technology 81, 773–780. https://doi.org/10.2166/wst.2020.158

Shakoor, S., Nasar, A., 2017. Adsorptive treatment of hazardous methylene blue dye from artificially contaminated water using cucumis sativus peel waste as a low-cost adsorbent. Groundwater for Sustainable Development 5, 152–159. https://doi.org/10.1016/j.gsd.2017.06.005

Sharma, K., Sharma, S., Sharma, Vipasha, Mishra, P.K., Ekielski, A., Sharma, Vishal, Kumar, V., 2021. Methylene Blue Dye Adsorption from Wastewater Using Hydroxyapatite/Gold Nanocomposite: Kinetic and Thermodynamics Studies. Nanomaterials 11, 1403. https://doi.org/10.3390/nano11061403

Shoukat, S., Bhatti, H.N., Iqbal, M., Noreen, S., 2017. Mango stone biocomposite preparation and application for crystal violet adsorption: A mechanistic study. Microporous and Mesoporous Materials 239, 180–189. https://doi.org/10.1016/j.micromeso.2016.10.004

Singh, H., Chauhan, G., Jain, A.K., Sharma, S.K., 2017. Adsorptive potential of agricultural wastes for removal of dyes from aqueous solutions. Journal of Environmental Chemical Engineering 5, 122–135. https://doi.org/10.1016/j.jece.2016.11.030

Somsesta, N., Sricharoenchaikul, V., Aht-Ong, D., 2020. Adsorption removal of methylene blue onto activated carbon/cellulose biocomposite films: Equilibrium and kinetic studies. Materials Chemistry and Physics 240, 122221. https://doi.org/10.1016/j.matchemphys.2019.122221

Su, H., Li, W., Han, Y., Liu, N., 2018. Magnetic carboxyl functional nanoporous polymer: synthesis, characterization and its application for methylene blue adsorption. Sci Rep 8, 6506. https://doi.org/10.1038/s41598-018-24873-3

Warda Hassan, Sajida Noureen, Mujahid Mustaqeem, Tawfik A. Saleh, Shagufta Zafar, 2020. Efficient adsorbent derived from Haloxylon recurvum plant for the adsorption of acid brown dye: Kinetics, isotherm and thermodynamic optimization. Surfaces and Interfaces 20, 100510. https://doi.org/10.1016/j.surfin.2020.100510

Wekoye, J.N., Wanyonyi, W.C., Wangila, P.T., Tonui, M.K., 2020. Kinetic and equilibrium studies of Congo red dye adsorption on cabbage waste powder. Environmental Chemistry and Ecotoxicology 2, 24–31. https://doi.org/10.1016/j.enceco.2020.01.004

Wong, S., Tumari, H.H., Ngadi, N., Mohamed, N.B., Hassan, O., Mat, R., Saidina Amin, N.A., 2019. Adsorption of anionic dyes on spent tea leaves modified with polyethyleneimine (PEI-STL). Journal of Cleaner Production 206, 394–406. https://doi.org/10.1016/j.jclepro.2018.09.201

Zhou, L., Zhou, H., Hu, Y., Yan, S., Yang, J., 2019. Adsorption removal of cationic dyes from aqueous solutions using ceramic adsorbents prepared from industrial waste coal gangue. Journal of Environmental Management 234, 245–252. https://doi.org/10.1016/j.jenvman.2019.01.009

A4. List of publications

A4.1. Peer-reviewed scientific publications in foreign languages on the subject of the thesis

1. **Rápó E**, Szép R, Keresztesi Á, Suciu M, Tonk S. Adsorptive Removal of Cationic and Anionic Dyes from Aqueous Solutions by Using Eggshell Household Waste as Biosorbent. Acta Chimica Slovenica. 2018; 65(3):709–17. **IF: 1.076 Q3**
2. **Rápó E**, Posta K, Suciu M, Szép R, Tonk S. Adsorptive Removal of Remazol Brilliant Violet-5R Dye from Aqueous Solutions using Calcined Eggshell as Biosorbent. Acta Chimica Slovenica. 2019; 66(3):648–58. **IF: 1.263 Q3**
3. **Rápó E**, Aradi LE, Szabó Á, Posta K, Szép R, Tonk S. Adsorption of Remazol Brilliant Violet-5R Textile Dye from Aqueous Solutions by Using Eggshell Waste Biosorbent. Scientific Reports. 2020; 10(1):8385. **IF_{2020}: 4.379 Q1/D1**
4. **Rápó E**, Jakab K, Posta K, Suciu M, Tonk S. A Comparative Study on the Adsorption of Two Remazol Dyes on Green Adsorbent. Rev Chim. 2020; 71(4):248–57. **IF_{2020}: 1.755 Q3**
5. **Rápó E**, Tonk Sz. Factors Affecting Synthetic Dye Adsorption; Desorption Studies: A Review of Results from the Last Five Years (2017–2021). Molecules. 2021; 26(17): 5419. **IF_{2020}: 4.411 Q1**
6. Tonk, Sz., Aradi, L. E., Kovács, G., Turza, A., **Rápó, E***. Effectiveness and Characterization of Novel Mineral Clay in Cd^{2+} Adsorption Process: Linear and Non-Linear Isotherm Regression Analysis. Water. 2022; 14: 279. **IF_{2020}: 3.103 Q1**

A4.2. Peer-reviewed scientific publications in foreign languages not related to the subject of the thesis

1. Haddidi I, Duc NH, Tonk S, **Rápó E**, Posta K. Defence Enzymes in Mycorrhizal Tomato Plants Exposed to Combined Drought and Heat Stresses. Agronomy. 2020; 10(11):1657. **IF_{2020}: 3.417 Q1**
2. **Rápó E**, Posta K, Csavdári A, Vincze BÉ, Mara G, Kovács G, et al. Performance Comparison of *Eichhornia crassipes* and *Salvinia natans* on Azo-Dye (Eriochrome Black T) Phytoremediation. Crystals. 2020; 10(7):565. **IF_{2020}: 2.589 Q2**

A4.3. University lecture book

1. Tonk Szende Ágnes, **Rápó Eszter**, Környezeti szennyezők, környezeti problémák, környezeti remediáció. Editura Exit, Cluj-Napoca, 2020. 234 p., ISBN 978-606-9091-23-4

A4.4. Conference participations

1. 2022. April 10-12. Lisbon, Portugal, 7th International Conference on Environmental Pollution, Treatment and Protection (ICEPTP'22), **Rápó Eszter**, Tonk Sz., Adsorption of Remazol Brilliant Blue RR from aqueous solution with calcined ostrich eggshells
2. 2021. October 29. Cluj-Napoca, Romania, Hungarian Technical Scientific Society of Transylvania, XXVII. International Conference on Chemistry, **Rápó Eszter**, Tonk Sz., Ipari melléktermék lehetséges felhasználása a víztisztításban, reaktív festék adszorpciója
3. 2021. March 31. - april 2. Riga, Latvia, 12th Eastern European Young Water Professionals Conference - Water Research and Innovations in Digital Era, **Eszter Rápó**, Szende Tonk, Katalin Posta, Melinda Tamás, Maria Suciu, Brewery Waste By-Product Saccharomyces Cerevisiae as an Adsorbent for Remazol Dye Removal, ISBN: 978-9934-22-618-2
4. 2021. January 18-19. Rome, Italy, ICEPTT 2021: 23rd International Conference on Environmental Pollution and Treatment Technology, **Eszter Rápó**, Szende Tonk, Melinda Tamás, Maria Suciu, Irina Kacsó, Textile Dye Removal from Aqueous Solution by Brewery Waste Products from Romanian Manufactory

5. 2020. October 30. Cluj-Napoca, Romania, Hungarian Technical Scientific Society of Transylvania, XXVI. International Conference on Chemistry, **Rápó Eszter**, Szabó Á., Aradi L., Tonk Sz., A tojáshéj jellemzése és adszorpciós tulajdonságai reaktív festék példáján keresztül
6. 2020. April 26. - May 1. Wisła, Poland, 19th Alps-Adria Scientific Workshop, **Eszter Rápó**, Krisztina Jakab, Katalin Posta, Szende Tonk, Adsorptive Capacity of Brewery Yeast from Romanian Manufactory
7. 2019. October 24-27. Cluj-Napoca, Romania, Hungarian Technical Scientific Society of Transylvania, XXV. International Conference on Chemistry, **Rápó Eszter**, Jakab K., Posta K., Tonk Sz., Összehasonlító tanulmány Remazol textilfestékek kalcinált tojáshéjjal való adszorpciós tulajdonságairól
8. 2019. March 2. Cluj-Napoca, Romania, XXIX. Herman Ottó Kárpát-medencei Biológia Verseny (erdélyi forduló), **Rápó Eszter**, Előadás címe: Hogyan lehet hulladékkal vizet tisztítani?
9. 2019. May 31. Szeged, Hungary, Műszaki, technológiai és gazdasági kihívások a 21. században Konferencia, **Rápó Eszter**, Posta K., Keresztes R., Kovács G., Szabó Á., Aradi L., Tonk Sz., Ruhafesték adszorpciója vizes oldatból
10. 2019. April 3-6. Cluj-Napoca, Romania, XV. Kárpát-medencei Környezettudományi Konferencia, **Rápó Eszter**, Jakab Krisztina, Posta Katalin, Tonk Szende, Összehasonlító tanulmány Remazol textilfestékek kalcinált tojáshéjjal való adszorpciós tulajdonságairól
11. 2019. April 16-18. Debrecen, Hungary, XXXIV. Országos Tudományos Diákköri Konferencia, Agrártudományi szekció, Környezettechnológia tagozat, **Rápó Eszter**, témavezető: Dr. Tonk Szende, dolgozat címe: RBV-5R színezék eltávolítása vizes oldatból, háztartásból származó kalcinált és alginát gyöngyökbe ágyazott tojáshéj segítségével
12. 2018. October 28. Sfantu Gheorghe, Romania, XX. Székelyföldi Geológus Találkozó, Aradi László Előd, Berkesi Márta, Szabó Ábel, **Rápó Eszter**, Végvári Zsófia, Szabó Csaba, Raman mikroszkópia alkalmazásai a fold- és környezettudományokban

10. ACKNOWLEDGMENT

First of all, I would like to express my gratitude and appreciation to my thesis supervisor, Dr. Szende Tonk, not only for introducing me to the topic and making me passionate about it, but also for being a true mentor, whose help and support I could count on both professionally and personally.

I would like to thank my supervisor, Dr. Katalin Posta, for her help, for taking on my thesis supervision and for welcoming me into the Microbiology and Environmental Toxicology Group for her professional advice and friendship.

I am grateful to the board of Sapientia EMTE for giving me the opportunity to continue my research at the university.

During my doctoral studies, I was supported by the Sapientia Hungariae Foundation Collegium Talentum scholarship, and I would like to thank the employees of the Foundation for the useful professional meetings and support for attending conferences and professional trips. Moreover, special thank for Forerunner Federation Székely Előfutár Scholarship.

I would like to thank INCDTIM (Electron Microscopy Integrated Laboratory, National Institute for Research and Development of Isotopic and Molecular Technologies, Cluj-Napoca), the National Institute for Research and Development in Environmental Protection (Bucharest) and the staff of the ELTE Lithosphere Fluid Research Laboratory for their help with instrumental measurements.

Last but not least, I would like to thank my parents, family and friends from the bottom of my heart for their constant attention, support and for empowering me to do what I love.